Inaugural-Dissertation zur Erlangung der Doktorwürde
der Tierärztlichen Fakultät der Ludwig-Maximilians-Universität
München

Tuberculosis in Cattle (*M. caprae*) in the Years 2009-2014:
Pathomorphology and Histological Demonstration of Mycobacteria in
Bovine Tuberculosis

von Hazal Öztürk

aus Istanbul

München 2016

Aus dem Zentrum für Klinische Tiermedizin der Tierärztlichen Fakultät
der Ludwig-Maximilians-Universität München

Lehrstuhl für Allgemeine Pathologie und Pathologische Anatomie

Arbeit angefertigt unter der Leitung von:

Univ.-Prof. Dr. Walter Hermanns

Mitbetreuung durch: Dr. Miriam Leipig

Dekan: Univ.-Prof. Dr. Joachim Braun

Berichterstatter: Univ.-Prof. Dr. Walter Hermanns

Korreferent/en: Univ.-Prof. Dr. Gabriela Knubben-Schweizer

Tag der Promotion: 16.07.2016

For my family and Recep,

TABLE OF CONTENTS

ABBREVIATIONS

ABC	Avidin-biotin complex
Aqua dest.	Distilled water
BCG	Bacillus Calmette-Guérin
bTB	Bovine tuberculosis
˚C	Grad Celsius
DAB	3,3'-diaminobenzidine
DC	Dendritic cell
DNA	Deoxyribonucleic acid
DTH	Delayed type hypersensitivity
ELISA	Enzyme linked immune-sorbent assay
et al.	et alii (and others)
EU	European Union
FF	Fite-Faraco
Fig.	Figure
FISH	Fluorescence in situ hybridization
g	Gram
GMA	Glycol-methacrylate
h	Hour
H&E	Haematoxylin eosin
IFN-γ	Interferon gamma
Ig	Immunoglobulin
IHC	Immunohistochemistry
IL	Interluekin
IPO	Immunoperoxidase
ISH	In situ hybridization
l	Litre
LN	Lymph node
M	Molar
M.	*Mycobacterium*
mAG	Mycolylarabinogalactan
MHC	Major histocompatibility complex
min	Minute
ml	Millilitre
mm	Millimetre
mM	Millimolar
MNGC	Multinucleated giant cell
MT	Masson´s trichrome
MTBC	*Mycobacterium tuberculosis* complex
NF	Nuclear factor
NK	Natural killer
No.	Number
NOS	Nitric oxide synthase
OTF	Officially tuberculosis free
PCR	Polymerase chain reaction
PNA	Peptide nucleic acid
RNA	Ribonucleic acid
RNI	Reactive nitrogen intermediates
RT	Room temperature

sec	Second
subsp.	Subspecies
TBS	Tris buffer saline
TEM	Transmission electron microscopy
Th	T-helper
TLR(s)	Toll-like receptor(s)
TNF-α	Tumour necrosis alpha
UK	United Kingdom
W	Watt
WHO	World Health Organization
ZN	Ziehl-Neelsen
μm	Micrometre

1. INTRODUCTION

Bovine tuberculosis (bTB) is a chronic bacterial disease of cattle. Tuberculosis causes death in humans and animals world-wide. This disease still remains a major global health problem despite the control and prevention strategies and can cause severe economic losses. The etiologic causes of the disease are *Mycobacterium (M.) bovis* (KARLSON & LESSEL, 1970) and *M. caprae* (ARANAZ et al., 2003), which are members of *Mycobacterium tuberculosis* complex (MBTC).

An increasing number of bTB in cattle herds has been detected in some countries in Europe. Germany also plays a role by showing interval outbreaks in the recent years. Alpine countryside, especially the grazing pastures located at the border of Bavaria and western Austria have been reported to have bTB outbreaks caused by *M. caprae* among wild animals and domestic cattle herds in these regions (PRODINGER et al., 2002; KUBICA et al., 2003). However, through the eradication programs, the infection could be kept under control. Regular intra-dermal testing and removal of the infected and reactor animals by culling are the standard control programs of bTB in Bavaria (LGL, 2014).

In this study, some cattle flocks in Bavaria were screened through intra-dermal testing between 2009 and 2014. Subsequently, the positive reactors were culled in the regional rendering plant regarding the governmental regulations in Germany. Throughout the gross examination, tissue samples from 84 animals with macroscopic lesions of tuberculosis were collected for pathological and bacteriological investigations. The microbiological examination was performed by the 'Bayerisches Landesamt für Gesundheit und Lebensmittelsicherheit', Oberschleißheim and the results were positive for *M. caprae*.

Pathological investigations were performed at the Institute of Veterinary Pathology at the Center of Veterinary Medicine of the Ludwig-Maximilians-University, Munich. Histological investigations were performed using paraffin, plastic and epoxy resin tissue embedded materials. In addition to the routine staining methods (H&E, Giemsa), the tissue samples were also examined using special stainings and immune-labelling methods. Acid-fast staining according to modified Fite-Faraco (FF staining), immunohistochemistry (IHC) and in situ hybridization (ISH) were used to demonstrate the mycobacteria, mycobacterial antigen and

mycobacterial DNA, respectively. Transmission electron microscopy (TEM) was performed to detect intra- or extracellular mycobacteria within the ultra-thin sections.

It has been known for a long time that mycobacterium fights against the immune defence of the host. This bacillus can enable itself to evade from this immune response and pursue its own life in the host for a long time. However, little is known about the mechanism of tuberculosis. During the course of this work, it was aimed to determine the possible routes of infection; the pathomorphological alterations on the basis of both macroscopical and histological point of view; the developmental stages of the tuberculous inflammation and to demonstrate the mycobacteria within the affected organs.

With this purpose, this doctoral thesis was supported by the Bavarian State Ministry of Food, Agriculture and Forestry, research project "Bovine Tuberculosis im Allgäu" under the research number (A / 13/37). The processing of the acid-fast staining and the distribution of the acid-fast bacilli within the affected organs were performed in collaboration with Ms. Rieseberg (RIESEBERG, 2016).

2. LITERATURE OVERVIEW

2.1. Scientific Classification of Mycobacteria

Tubercle bacillus was first described by Robert Koch in 1882 as a causative agent of tuberculosis (KOCH, 1882). It was renamed as *Mycobacterium tuberculosis* and had its place under the new genus *Mycobacterium,* and was placed in the *Mycobacteriaceae* family (LEHMANN & NEUMANN, 1896).

The classification method is formed according to the features which all members of a group have. The genus of *Mycobacterium* is separated into two groups as "rapidly growing" and "slowly growing", depending on the time required of the visible colonies to appear on a solid medium. The appearance of colonies needs more than 7 days for slowly growing species and less than 7 days for rapidly growing species (WAYNE & KUBICA, 1986). Three minimal standards are defined for the genus of *Mycobacterium.* These are acid-alcohol fastness, having long-chain mycolic acids (containing between 60 and 90 atomic carbons), which are cleaved to C22 to C26 fatty acid methyl esters by pyrolysis, and the presence of a DNA guanine-plus cytosine (G+C) content (LEVY-FREBAULT & PORTAELS, 1992).

The *Mycobacterium* genus is further separated into 4 groups based on their pigmentation, growth rate, drug resistance, type of colonies and catalase activity properties (RUNYON, 1959);

- Photochromogens (Runyon group I)
- Scotochromogens (Runyon group II)
- Nonphotochromogens (Runyon group III)
- Rapid growers

2.1.1. *Mycobacterium tuberculosis* Complex

Mycobacterium tuberculosis complex (MBTC) is composed of slowly growing, nonphotochromogenic (Runyon group III) species (SHINNICK & GOOD, 1994). These members have close genetic relationship which has been demonstrated by several methods such as DNA-DNA hybridization, multilocus enzyme electrophoresis, sequencing of 16S

ribosomal rRNA gene and 16S-to-23S rDNA internal transcript spacer (KIRSCHNER et al., 1993; FROTHINGHAM et al., 1994; FEIZABADI et al., 1996). The polymerase chain reaction (PCR) has also been used as a diagnostic tool for mycobacteria detection through determining the 16S rRNA gene or a number of repetitive sequence elements. For instance, the insertion sequence IS*6110* is present only in species belonging to MBTC (BODDINGHAUS et al., 1990; THIERRY et al., 1990). The other specific genetic markers for the members of MBTC are determined as insertion sequences IS*1081* and the MPB70 genes (RADFORD et al., 1990; COLLINS & STEPHENS, 1991; COUSINS et al., 1991; LIEBANA et al., 1996). In spite of these common properties as mentioned above, they are separated from one another by having gene variations as follows; *M. tuberculosis, M. africanum, M. bovis, M. bovis BCG, M. canetti, M. microti, M. caprae* (BROSCH et al., 2002; MOSTOWY et al., 2002) and *M. pinniedii* (COUSINS et al., 2003).

2.1.2. The Taxonomy and Nomenclature of *M. caprae*

M. caprae was first isolated from goats and described as subspecies of *M. tuberculosis.* This new species has negative reaction for niacin accumulation and nitrate reduction and this differentiates it from *M. tuberculosis.* It shows no growth in the presence of thiophene-2-carboxylic acid hydrazide and this differentiates it from *M. africanum*. Having pyrazinamide susceptibility differentiates *M. caprae* from *M. bovis.* Showing negative reaction for niacin accumulation differentiates *M. caprae* from *M. microti*. In addition, this new species has its own genetic properties such as pncA, katG and gyrA gene polymorphism, which do not exist in any member of MBTC (ARANAZ et al., 1999). Restriction fragment length polymorphism (RFLP) with IS*6110*, polymorphic GC-rich repeat sequences (PGRS) (ROSS et al., 1992) and direct repeats (DR) (HERMANS et al., 1991) are shown to distinguish the caprine isolates from *M. bovis* (LIEBANA et al., 1997; ARANAZ et al., 1998). Spacer-oligotyping (spoligotyping) and DRs have been developed as a target for in-vitro DNA amplification to detect the presence or absence of spacer in the DR locus (KAMERBEEK et al., 1997). Spoligotyping is evaluated as a promising tool for typing *M. bovis* isolates from various animal sources isolates (ARANAZ et al., 1996). There is another technique which is based on *gyr-B* sequence. It works by using both PCR and PCR-RFLP methods. According to this, *M. caprae* can be distinguished from other MTBC strains by *gyr-B* sequence (KASAI et al., 2000; NIEMANN et al., 2000a).

M. caprae was first presented as *Mycobacterium tuberculosis* subsp. *caprae* (ARANAZ et al., 1999). Then it was considered as a subspecies of *M. bovis* and the name was changed to *Mycobacterium bovis* subsp. *caprae* (NIEMANN et al., 2002). But thereafter, in accordance with these various genetic and biochemical properties, this bacillus has been represented as *M. caprae* (ARANAZ et al., 2003).

Despite all of these differences between the two *M. caprae* and *M. bovis,* it is assumed that they cause tuberculosis in humans with no significant difference in age, gender or localisation among the patients (KUBICA et al., 2003). It is also concluded that *M. caprae* causes tuberculosis among the same animal species as *M. bovis* does (PRODINGER et al., 2005).

2.2. Morphology of Mycobacterium

The genus of mycobacterium is determined as lightly curved or as straight rods, 0.2 – 0.6 x 0.1 - 10 µm in length and width, less commonly branching; filamentous or mycelium-like growth may appear, but always become fragmented into rods or coccoid elements. Despite not being appropriate to staining with Gram's method, they are still named as Gram positive. They have no endospores, no capsules, no visible aerial hyphae (WAYNE & KUBICA, 1986).

Morphologically, *M. caprae* is described as an acid-alcohol-fast, non-spore forming, non-motile rod that grows slowly (dysgonic) at 36˚C and forms smooth and non-chromogenic colonies. In the case of the presence of pyruvate, visible growth can be recognized after 4-6 weeks of incubation at 36˚C (ARANAZ et al., 1999).

2.2.1. The Envelope of Mycobacterium

The envelope of mycobacteria consists of a plasma membrane and a cell wall (BRENNAN & NIKAIDO, 1995). The plasma membrane consists of phospholipids, which are derivatives of phosphatidic acid. The most common are phosphatidylglycerol, diphosphatidylglycerol, phosphatidylethanolamine, and phosphatidylinositol and its mannosides (PIMs). The PIMs are the major plasma membrane components and also participate in the formation of lipoarabinomannan and lipomannan, as described below (BRENNAN & NIKAIDO, 1995).

Peptidoglycan (murein) constitutes the basal unit of the mycobacterial cell wall structure. This unit covalently links to the mycolylarabinogalactan (mAG) via phosphodiester bonds and mAG layer is composed of α-branched, β-hydroxylated long chain fatty acids. Peptidoglycan-mAG structure also contains carbon atoms, which are covalently linked to arabinogalactan (AG). Mycolic acids are linked to this peptidoglycan-mAG structure at the carboxyl ends to D-arabinofuranose, and they are also linked to the AG polymer by the peptidoglycan-mAG (KANETSUNA, 1968; BARKSDALE & KIM, 1977; NIKAIDO et al., 1993; CHATTERJEE, 1997).

Peptidoglycan (mucopeptid or murein) is formed by a glycan and a peptide moiety. The peptide moiety has four aminoacids (GHUYSEN, 1968). The glycan substance consists of a repeating disaccharide unit linked to the peptide moiety. This disaccharide unit consists of N-glycolyl group, which is found in all mycobacteria species (AZUMA et al., 1970; LEDERER et al., 1975). Mycobacteria, nocardia and corynebacteria have the same deamidated tetrapeptide. The important adjuvant activity of the peptidogylcan is indicated as N-acyl muramyl L-Ala-D-isoglutamine (LEDERER et al., 1975).

Arabinogalactan (AG), glucan, mannan, and arabinomannan are determined as common constituents of mycobacterial polysaccharides and it is concluded that arabinomannan and AG are common immunologically active polysaccharide antigens in the mycobacteria (AZUMA et al., 1968). AG is composed of distinctive arabinan and galactan segments (DAFFE et al., 1990; BESRA et al., 1995).

The lipopolysaccharides of mycobacteria are lipoarabinomannan (LAM) and lipomannan (LM), within the bonds of AG, are anchored via phosphatidylinositol (HUNTER & BRENNAN, 1990). LAM and LM are based on the phosphatidylinositol mannosides (PIM) (CHATTERJEE et al., 1992a). ManLAM, which is also a derivative of LAM, is characterised by extensive mannose capping arabinan termini, which may affect the interaction of the mycobacteria with the host cell (CHATTERJEE et al., 1992b).

Mycolic acids are defined as high-molecular weight β-hydroxyl fatty acids with a long α-side chain (ASSELINEAU & LEDERER, 1950). These fatty acids are described as bound esters of AG and there they appear as tetramycolylpentaarabinosyl clusters and also extractable lipids, especially as α,α'-treholase dimycolate (Cord factor) (BRENNAN & NIKAIDO, 1995). The

other extractable glycolipids of the cell wall surface are lipooligosaccharides (LOSs), phenolic glycolipids (PGLs) and glycopeptidolipids (GPLs) (BRENNAN & NIKAIDO, 1995). *M. bovis* has 'Mycoside B' (MACLENNAN et al., 1961), which is a type of phenolic glycolipids characterised by a very large hydrophobic part (BRENNAN & NIKAIDO, 1995).

Waxes are another important antigenic cell wall component (AZUMA et al., 1968) and have the phenolic glycolipids in their core (BRENNAN & NIKAIDO, 1995).

2.3. Virulence Effect of Cell Wall Components

The cell wall components of the tubercle bacillus have crucial roles in the interaction of pathogenic species with their host (BRENNAN & NIKAIDO, 1995).

LAM suppresses immune responses and thereby contributes to the pathogenesis of mycobacterial infection (BRENNAN & NIKAIDO, 1995). This molecule inhibits the function of macrophages by scavenging toxic oxygen free radicals, inhibiting protein kinase C activity, and restricting transcriptional activation of the interferon-gamma (IFN-γ)-inducible genes (CHAN et al., 1991).

LM is responsible for apoptosis of macrophages via interaction with toll-like receptor (TLR) 2 on the surface of macrophages and also has an effect on interleukin (IL)-12 (DAO et al., 2004). However, ManLAM possesses an inhibitor effect on apoptosis mechanism of macrophages and on the IL-12 response (KEANE et al., 2000; ROJAS et al., 2000; HICKMAN et al., 2002). ManLAM also prevents the phagosome-lysosome fusion. The arrest of phagosome-lysosome maturation results and this could be defined as the most important factor in the pathogenesis of *M. tuberculosis* (FRATTI et al., 2001; FRATTI et al., 2003). PIMs, which are precursor molecules of LAM and LM, have an important role of maintaining granuloma formation by recruiting the natural killer (NK) cells (GILLERON et al., 2001).

Cord factor is another virulence factor for inducing immune response in the host. It has both leukotactic and leukotoxic properties. This effect inhibits leukocytic migration (BLOCH, 1950).

2.4. Transmission Pathways

The most important transmission route of bovine tuberculosis occurs by inhaled organisms via the respiratory route. The bacilli can spread via droplets, contact, dust or within droplet nuclei and is emanated from infected animals into the environment when they cough or sneeze. Aerosol droplet nuclei can exist in the air for a long time (LANGMUIR, 1961). Ambient air contains viable tubercle bacilli as a result of the exhalation by infected animal, so this condition can facilitate the transportation of organisms among indoor housing cattle (BURRELL, 1991). Other projects point out the transmission of mycobacterial infection from deer to cattle or from deer to deer by studying experimentally inoculated deer. It has been shown that these animals transmit the infection by shedding the bacilli through their saliva, nasal secretion, urine and faeces. In addition, the lesions have been found most commonly in respiratory tract instead of alimentary tract. It is supposed to be a result of inhalation of droplet nuclei on small fed particles during feeding (PALMER et al., 1999; PALMER et al., 2001; PALMER et al., 2004). On the other hand, it has been shown in cattle that the oral route plays an important role when the lesions are in the lymphoid organs of the head and the gastrointestinal tract (LIEBANA et al., 2008). In young calves, the consumption of infected raw milk from tuberculous udders may cause bovine tuberculosis via alimentary tract (NEILL et al., 1994). Animals also can be infected from contaminated pastures when they graze (MORRIS et al., 1994). Congenital transmission can rarely occur via umbilical vessels from infected cow (NEILL et al., 1994).

2.5. Source of Infection

Bovine tuberculosis has a wide range of sources that causes the infection among domestic and wildlife animals as well as humans. Both *M. bovis* and *M. caprae* can cause bovine tuberculosis and share the same resources and target populations (PRODINGER et al., 2005; PAVLIK, 2006). It is also indicated that infected purchased animals can be an important threat from an epizootiological aspect (PAVLIK, 2006).

Wild animal resources may also cause a disease threat and according to the report from United Kingdom (UK), moles (*Talpa europaea*), foxes (*Vulpes vulpes*), rats (*Rattus norvegicus*), wild deer (various species) and badgers play an important role in transmission of the disease to cattle (KREBS, 1997). It has been indicated that natural habitat of badgers is

placed just near the grazing land (TUYTTENS et al., 2000). Infected badgers can shed the acid-fast bacilli via their excretions of respiratory, urinary, digestive tract and also skin (GAVIER-WIDEN et al., 2001) and then, cattle may inhale the bacilli from contaminated pastures (HUTCHINGS & HARRIS, 1997). In a free-ranging area in Michigan, the white tailed deer has also been shown as a reservoir of mycobacterium (SCHMITT et al., 1997). Wild boar and red deer play an important role for the spread of bTB to the domestic livestock (GORTAZAR et al., 2005). It should not be forgotten that humans also constitute another source of bTB (GRANGE & YATES, 1994).

2.6. Survival of the Organism in the Environment

M. bovis is an facultative intracellular organism that survives for substantial periods in the environment under favourable conditions (MORRIS et al., 1994). In south of England, experimental studies with artificially infected faeces show that the tubercle bacilli can survive and remain virulent after exposure to pasture land for at least 5 months during winter, for 2 months during spring and for 4 months during autumn. There are no signs of live bacilli after 2 months of exposure in summer. The survival period of bacilli has been assumed to be approximately 4 months during summer when protected from sunlight. If the bacilli are protected from direct insolation, earthworms and insects, the survival period takes longer, about 6 months in autumn (WILLIAMS & HOY, 1930). Maddock recovered tubercle bacilli from the soil and dung after insolation of 178 days. Furthermore, in another study of MADDOCK (1933, 1934), the tubercle bacilli could be recovered under inappropriate drought and warm weather conditions after 152 days.

2.7. Epidemiology of Bovine Tuberculosis in European Countries

In 2012, Austria, Belgium, the Czech Republic, Denmark, Estonia, Finland, France, Germany, Latvia, Luxembourg, the Netherlands, Poland, Slovakia, Slovenia, Sweden, Norway and Switzerland have Officially Tuberculosis Free (OTF) status in accordance with European Union (EU) legislation (Decision 2012/204/EU29). Liechtenstein and Switzerland have the same status. The last epidemic of bovine tuberculosis occurred in 1959, in Iceland. But a special agreement concerning animal health status between this country and the EU does not exist. Furthermore, 5 Italian regions and 17 Italian provinces, Algarve in Portugal, Scotland in UK have obtained OTF status (EFSA, 2015).

Member states Bulgaria, Croatia, Cyprus, Greece, Hungary, Ireland, Italy, Lithuania, Malta, Portugal, Romania, Spain and the UK did not obtain country-level OTF status in 2013. Croatia, as a new member state, reported information for the first time in 2013 (EFSA, 2015).

In the EU OTF regions, out of the 1.384.692 existing cattle herds, 207 were positive for *M. bovis*. The ratio of herds with *M. bovis* was reported to be 0.015% in 2013, whereas out of the 1.362.234 existing cattle herds in the EU non-OTF regions, 18.256 herds were found to be infected with or positive for *M. bovis* in 2013. This group of infected/positive herds indicated 1.33% of the total number of herds in the EU non-OTF regions. Overall, in the EU OTF and non-OTF regions, the ratio of herds infected with *M. bovis* was 0.68% in 2013. The prevalence can range from nonexistence of positive animals in many OTF regions to a prevalence of 12.1% in the non-OTF regions of the United Kingdom (England, Northern-Ireland and Wales). Although there is a slight increase of positive herds between 2009 and 2012 (from 0.45% up to 0.68%), the ratio remains almost the same between 2012 and 2013 (0.67% - 0.68%). The number of herds infected with *M. bovis* decreased in France and increased in Belgium, Germany, Italy, and Poland in 2013 (EFSA, 2015).

Most of epidemiological studies of bTB are principally performed by spoligotyping and IS*6110* RFLP analyses (VANEMBDEN et al., 1993; KAMERBEEK et al., 1997). *M. caprae* has been shown to be widely distributed in Europe among humans and animals. Particularly, Austria, Italy, Spain, and Germany are the main countries (PRODINGER et al., 2005). Furthermore, the detection of *M. caprae* has also been presented, as following:

- Spain (GUTIERREZ et al., 1995; PRODINGER et al., 2005)
- France (HADDAD et al., 2001; PRODINGER et al., 2005)
- Czech Republic (PAVLIK et al., 2002b)
- Slovakia (PAVLIK et al., 2002a)
- Slovenia (ERLER et al., 2004)
- Croatia (CVETNIC et al., 2006)
- Austria (PRODINGER et al., 2002; PRODINGER et al., 2005)
- Italy (PRODINGER et al., 2005)
- Germany (KUBICA et al., 2003)

2.8. Bovine Tuberculosis in Germany

Germany obtained the status of "officially free of tuberculosis" on 1st July, 1996 (it was first declared according to EU Decision 97/76 / EC, then replaced by EU Decision 99/467/EC and then by EU Decision 2003/467/EC). EU definition is given as "the percentage of infected bovine herds has not been more than 0,01 % for six consecutive years and at least 99,9% of the herds have been declared officially tuberculosis free for 10 years" (Council Directive 97/12 / EC).

A systematic analyses of human patients was done between 1999 and 2001 by using spoligotyping and PCR-RFLP analysis. The regional propotion of *M. caprae* infections indicates that southern Germany has a large proportion (more than 80%) as compared with the northern parts of the country (less than 10%) (KUBICA et al., 2003). Between 2008/2009 and 2012/2013 bTB increased, especially in Bavaria, Allgäu (LGL, 2014). In Bavaria, in 2009 *M. caprae* was detected in cattle (LEIPIG et al., 2009) and in 2011, it was detected among red deer (GERSTMAIER, 2011). In 2012, 24 outbreaks of bTB were reported compared to 2011 with 5 outbreaks (FLI, 2012).

2.9. Tuberculosis Infection in Humans

TB still causes death in humans. The last report from the World Health Organization (WHO) indicates that in 2014, estimated 9.6 million developed TB and 1.5 million died from it (WHO, 2015).

Bovine tuberculosis (bTB) possesses a zoonotic risk to the public; especially to people who have close contact with infected animals (PATE et al., 2006). The isolation of *M. bovis* strains in humans shows that infected cattle constitute an important threat factor for the transmission of the disease from livestock to humans (GUTIERREZ et al., 1997). In the UK, agricultural workers have been detected to develop tuberculosis as a consequence of close contact with infected cattle (SMITH et al., 2004). In Spain, *M. caprae* has been isolated from hunters and wildlife managers (GORTAZAR et al., 2005).

The other important potential of transmission of bovine tuberculosis from animals to human occurs when consuming raw milk or non-pasteurized milk and milk products (CVETNIC et al., 2007).

Systematic analyses show the population structure of mostly human-origin *M. bovis* in Germany and indicate a high ratio of human tuberculosis (KUBICA et al., 2003). Moreover, another research in Germany verifies that *M. caprae* affects humans (NIEMANN et al., 2000b).

2.10. Control of Bovine Tuberculosis

In the European Community, member states regulated legislation to trade cattle, beef and products without risk of spreading the disease. Regulations in Council Directive 97/12 / EC states that no bovine animal over six weeks old can be introduced into a herd unless it has reacted negatively to an intradermal tuberculin test performed and assessed according to Annex B and carried out either in the 30 days prior to, or the 30 days after the date of its introduction into the herd. In Germany, the control of bTB is managed by "Regulations for Protection from Bovine Tuberculosis". According to these regulations, control is depended on the diagnosis of clinical symptoms, official meat inspection and post mortem examination by veterinary service laboratories and tuberculin testing in certain cases. In case of clinical suspicion or pathological tissue lesions, further diagnostic investigations including bacteriology, molecular biology, epidemiology, tuberculin testing of contact animals, gamma interferon test are initiated for clarification (TUBERKULOSE-VERORDNUNG, 2014).

In case of existence of the wild-life TB sources, the countries must develop their own strategies for prevention. Besides culling, applying the treatment regime and vaccination programs have been suggested to handle tuberculosis in wild-life animals (ARTOIS et al., 2011). It is emphasized that the vaccination strategies are applicable in the wild-life reservoir hosts (e.g. eurasian badgers in England, white-tail deer in the United States, wild boar and red deer in Spain) to limit the transmission of tuberculosis to cattle and also among wild-life populations (BUDDLE et al., 2011).

2.11. Vaccination

Bacillus Calmette Guérin (BCG) is an attenuated strain of *M. bovis*, which was developed by Calmette and Guérin. After a large scale of animal experiments, it was used in children to protect them from tuberculosis (CALMETTE, 1931). The efficacy of this vaccine has been seen in cattle and human. Low doses of BCG induce protection against tuberculosis (FINE, 1995; BUDDLE et al., 2002). This vaccine works via stimulation of the cellular immune response against the bacteria, which can replicate in the host macrophages. IFN-γ produced by T-cells helps to control the intracellular growth of mycobacteria in macrophages by activating these cells. T-cell immune responses occur in a higher amount in vaccinated cattle compared to non-vaccinated cattle (LIEBANA et al., 2000; VORDERMEIER et al., 2002). Besides this, some other vaccination methods have also been developed such as adjuvant subunits, virus-vectored or DNA vaccines, which are combined with BCG (BUDDLE et al., 2011). The combination of the adjuvant subunit vaccine with BCG maintains more effective protection than BCG used alone (WEDLOCK et al., 2005). The low doses of BCG have also been confirmed to be adequate in calves to initiate an immune response (BUDDLE et al., 1995).

According to the legistation in Germany vaccinations against tuberculosis in cattle and therapeutic trials are prohibited. The competent authority may permit exceptions to conduct scientific experiments, when issues of disease control do not preclude (TUBERKULOSE-VERORDNUNG, 2014).

2.12. Host Susceptibility

It is assumed that genetic predisposition plays an important role in the susceptibility of the bTB. In a study, the prevalence and the pathology of bTB among Holstein, Zebu and Zebu x Holstein cross bred cattle have been compared. High differences in prevalence and severity of the pathology among these breeds have been demonstrated. Holstein (Bos taurus) cattle have been found to be more susceptible than crosses or Zebu (Bos incidus) cattle (AMENI et al., 2007).

It is suggested that susceptibility to tuberculosis infection may increase as a consequence of being persistently infected with immunosuppressive viruses such as bovine viral diarrhoea virus or bovine immunodeficiency virus (MENZIES & NEILL, 2000). Besides this, poor

nutrition can be demonstrated as a predisposing factor for tuberculosis (DOHERTY et al., 1996). Furthermore, grazing in an area of poor quality soil with deficient mineral content can cause an increased risk of having severe course of tuberculosis, if the animals are not supported with mineral supplements (GRIFFIN et al., 1993). In winter time, cattle are housed in most countries, which is thought to be a reason for an increased incidence of bTB, so-called seasonal effect (MENZIES & NEILL, 2000). Moreover, it is emphasized that housed cattle, even if better fed, show a higher incidence of tuberculosis than cattle which are exposed to the rigors of life in the open (FRANCIS, 1971).

2.13. Immune Response

The immune reaction is considered to be an interplay between the cell mediated immunity and delayed type hypersensitivity (DTH) throughout the course of the infection (DANNENBERG, 1993). It can be concluded from the previous studies that bovine tuberculosis shows a spectrum of immune responses, in which cell mediated immune response dominates the infection (RITACCO et al., 1991; NEILL et al., 2001).

2.13.1. Initiate and Cellular Immune Response

Initiate immunity is developed by non-specific mechanisms, in which neutrophils and macrophages manage the rate of the inflammation (SILVA et al., 1989; TURNER et al., 2003). It is mainly characterised by imigration of monocytes and occasional immature macrophages. In seven days, these monocytes evolve into mature macrophages and then into much larger epithelioid cells (ADAM, 1975). On the other hand, *M. bovis* has regulatory effects on neutrophils, which accumulate rapidly to the sites of infection to eliminate the bacilli (WANG et al., 2013). IL-17 induces this recruitment and the T-helper (Th) 1 type acquired immunity. This cytokine is produced mainly by TCR γδ T cells and is stimulated mainly by IL-23 (UMEMURA et al., 2007). Stimulated neutrophils can generate a respiratory burst and up-regulate the microbicidal activity and the expression of some cell surface receptors. The infection of neutrophils with *M. bovis* results in the increase of tumour necrosis factor alpha (TNF-α) and IL-10 secretion and an up-regulation of early apoptosis rate, late necrosis, and autophagy (WANG et al., 2013). In addition, neutrophils also have an effect on the development of CD4+ T cells, which facilitates dendritic cell (DC) migration and antigen presentation (BLOMGRAN & ERNST, 2011).

Toll-like receptors (TLRs) recognize the mycobacterium as a pathogen (KOPP & MEDZHITOV, 2003). Macrophages recognize the mycobacterial cell wall component via TLR2 and become stimulated to produce TNF-α (UNDERHILL et al., 1999). It was confirmed that TLR2 possesses an important function on the progression of the inflammation. After the recognition of microbial lipoproteins, monocyte-derived DCs become activate and express TLR2. Monocytes and DCs participate in the production of IL-12 and IL-10, but DCs have little effect on the IL-10 production (THOMA-USZYNSKI et al., 2000).

Interleukin (IL)-12 triggers NK and Th1 cells to release IFN-γ (TRINCHIERI, 1993), while IL-10 has an antagonistic effect by inhibiting both the release and the function of IL-12 (BUELENS et al., 1997; DESMEDT et al., 1997). IFN-γ activates macrophages via the nitric oxide synthase (NOS)-dependent way and allows the production of reactive nitrogen intermediates (RNI). IFN-γ also has an effect on macrophages to express more major histocompatibility complex (MHC) class II molecules (DALTON et al., 1993; FLYNN et al., 1993).

Dendritic cells (DCs) are induced to become antigen presenting cells (APCs) (DEMANGEL et al., 1999), which have MHC class II molecules on their surface (BANCHEREAU & STEINMAN, 1998). Lipopolysaccharides induce nuclear translocation of nuclear factor (NF)-κB, which stimulates the maturation of DCs to up-regulate MHC and co-stimulatory molecules (RESCIGNO et al., 1998). They also up-regulate some important cytokines: IL-1, IL-6, IL-12, IL-10 and TNF-α (HENDERSON et al., 1997; THOMA-USZYNSKI et al., 2000; DEMANGEL et al., 2002). Mycobacteria-infected DCs migrate to the draining lymph nodes, where they initiate the development of native T cells into the Th1-polarized CD+4 T cells (HICKMAN et al., 2002) and CD8+ cells (PETERS & ERNST, 2003). This process starts after the interaction between T lymphocytes and MHC molecules of APCs via their T cell antigen receptors (TCRs). MHC Class I and MHC Class II stimulate cytotoxic CD8+ T cells and CD4 helper T cells, respectively (BANCHEREAU & STEINMAN, 1998). After the activation of naïve T cells, they migrate via the bloodstream to the site of inflammation (PETERS & ERNST, 2003).

T cell subpopulations have a role in response to mycobacterial infection in the host. At the initial phase of infection, WCI γδ T cells become predominant (POLLOCK et al., 1996; CASSIDY et al., 2001). CD8+ T lymphocytes mediate the lysis of host cells infected with

mycobacteria (KAUFMANN, 1988). An experimental study indicates that the major role of CD4+ T lymphocytes is to participate in early immune response against mycobacteria, to establish the granuloma formation by producing IFN-γ and also to stimulate NOS expression. In addition, this study also shows the occurrence of IFN-γ response from CD8+ T lymphocytes after two weeks of infection (CARUSO et al., 1999).

2.13.2. Delayed Type Hypersensitivity

The delayed type hypersensitivity is principally mediated by the T cell response and corresponding sets of cytokines. In an experimental study with *M. bovis* purified protein derivative (PPDb) injected cattle, these animals show an accumulation of T cells, especially γδ T cells and a CD4+ T cell proliferation, and an increased IFN-γ production (WATERS et al., 2000). This cytokine amplifies the release of TNF-α from macrophages. Moreover, local tissue cells and leukocytes also participate in this reaction by producing chemokines to recruit monocytes and macrophages from the blood into the infected area. Subsequently, TNF-α up-regulates the release of chemokines to recruit blood-borne monocytes to the infected area. Thus, the believed theory of 'walling off' is developed to prevent the dissemination of bacteria (ORME & COOPER, 1999).

2.13.3. Humoral Immune Response

Experimental studies conducted with *M. bovis* infected cattle have determined varying amounts of antigen recognition (FIFIS et al., 1994; LYASHCHENKO et al., 1998). The antibody levels increase in the late stages of the infection (HARBOE et al., 1990; FIFIS et al., 1994). The relationship between cell mediated immune response and humoral immune response has been investigated. The observation of the late stage of infection shows a high amount of IL-10, a decreased amount of cellular response and IFN-γ. Moreover, a positive correlation has been seen between the severity of infection and the amount of immunoglobulin G (IgG) (WELSH et al., 2005). The role of B cells has been studied in mice and it has been seen that these lymphocytes have striking role in managing the granuloma development by producing chemokines and cytokines. They also participate in the protective immunity by producing IgG and IgM (MAGLIONE et al., 2007).

2.14. Pathogenesis

In animals and humans, tuberculosis infection can be divided into two different periods. These are the primary infection period and the super infection or re-infection period. Principally, the exudative or the productive type of granulomatous inflammation can be predominant during the infection (NIEBERLE, 1938; PALLASKE, 1961).

The productive type starts with an accumulation of macrophages, which phagocytise the bacilli. The bacilli are killed within the macrophages, if the immune response of the host is adequate. Otherwise, the balance turns the other way and ingested bacilli in the macrophages proliferate and are released from the killed macrophages. In the meantime, cellular and hypersensitivity immune responses develop against the mycobacteria (JUBB & KENNEDY, 1963). Inflammatory cell infiltration mainly consists of mononuclear cells and their derivatives, epithelioid and Langhans-type multinucleated giant cells. The admixture of epithelioid and multinucleated giant cells forms the centre of the young granulomas. The periphery is surrounded by a narrow zone of lymphocytes. Subsequently, fibrous encapsulation develops in the periphery and caseous necrosis in the centre, if the lesion progresses. Caseous necrosis is assumed to be a result of hypersensitivity reaction and may liquefy or calcify in time (JUBB & KENNEDY, 1963).

Exudative granuloma formation occurs acutely and results in caseation necrosis, too. The exudative form consists of an accumulation of fibrin and neutrophils as well as monocytes. There are many factors that cause exudative tuberculosis. The main factor is stated to be a high degree of altered reactivity. A high burden of bacteria, bacilli of high virulence, and a susceptible host are other factors for the development of the exudative granuloma type (JUBB & KENNEDY, 1963).

2.14.1. Primary Infection and Early Generalisation

The beginning of the tuberculosis is characterised by a development of a primary focus. This primary focus can develop in any organ depending on the transmission pathways. The tubercle bacilli can enter the host via alimentary, respiratory or congenitally ways and create the primary focus at the portal of entry. Subsequently, the bacteria reach the regional lymph

nodes via lymphatic vessels (NIEBERLE, 1938). Both affected organ and associated lymph nodes together form a primary complex (JUBB & KENNEDY, 1963).

The characteristic feature of the primary infection and early generalisation are concurrent lesions in an organ and in the regional lymph nodes with a tendency to calcification (NIEBERLE, 1938). In cattle, depending on the transmission pathway, primary foci are observed mostly (90%) in the lungs. They occur in the best ventilated portion of the lung, just beneath the pleura, in the main lobe or in the lower parts of the lung. Extensive alterations are also seen in the regional lymph nodes (NIEBERLE, 1938; PALLASKE, 1961). The primary foci in alimentary tract can initially occur in the tonsils, and also in retropharyngeal lymph nodes (NIEBERLE, 1938). But if the primary focus is seen only in retropharyngeal lymph nodes, this can be associated with both the respiratory and alimentary ways (STAMP, 1944). Primary focus in the alimentary tract is found in the posterior part of the intestine and especially associated with individual or multiple lymph nodes alterations. However, it is indicated for both alimentary and respiratory infection that bacteria can only affect the regional lymph nodes without alterations in the organ. This situation is named as incomplete primary complex (NIEBERLE, 1938).

Primary infections can also develop by congenital pathway. The congenital tuberculosis is pointed out as the most common (39%) transmission pathway in calves (NIEBERLE, 1938). The infection spreads via umbilical cord to the fetus, thus the lesions arise in the liver and portal lymph nodes. Congenital tuberculosis in calves progresses rapidly and causes death in a few weeks or months, usually due to a generalisation with lesions in spleen, lung, and occasionally in heart muscle (STAMP, 1944).

The inflammatory process of the primary complex might stop and heal, or might progress to an early generalisation. In the healing process, the primary focus calcifies progressively and is surrounded by fibrous tissue. This encapsulated focus can remain stable lifelong in this form (NIEBERLE, 1938; PALLASKE, 1961). The early generalisation occurs when the bacteria are released into the blood stream, and spread out to the different organs. Other forms of spreading besides haematogenous occur via contact growth, lymphogenous, or intracanalicular ways (NIEBERLE, 1938). In the initial phase, the occurrence of small cavities allows a local dissemination of the bacteria via intracanalicular ways (JUBB & KENNEDY, 1963). The course of the disease depends on the burden of bacilli in the blood

and the defence mechanisms of the host. Multiple metastatic foci can arise in different organs such as lung, liver, kidney, spleen and also bone marrow through the haematogenous or lymphogenous spread. Lesions occur in different forms; a) acute miliary tuberculosis, b) protracted generalisation (NIEBERLE, 1938).

2.14.2. Re-infection

Observations of pulmonary tuberculosis in men reveal that primary infection and early generalisation commonly occur in children. However, the chronic tuberculosis occurs in adults. Primary infection may persist for a long time without any clinical signs and it can arise again following puberty. In this case, clinical signs become indicative and re-infection period starts (NIEBERLE, 1938). The outcome of re-infection may develop by either endogenous way, as a result of reactivation of an old primary focus, or exogenous way (NIEBERLE, 1938; AUERBACH, 1959). In animals, this form is generally seen in cattle (NIEBERLE, 1938).

2.14.2.1. Chronic tuberculosis (Organ Tuberculosis)

Chronic organ tuberculosis in cattle progresses slowly in time and causes distinctive emaciation. The pathological alterations in chronic organ tuberculosis are especially seen in a particular organ, which is generally the lung with acinar tuberculosis (NIEBERLE, 1938). The progression may result in either fibrous encapsulation and eventually heals or progresses through large confluent acinar nodular foci. These foci can dissolve and cause cavities as a result of liquefaction necrosis (NIEBERLE, 1938; PALLASKE, 1961).

The distinctive feature of the chronic organ tuberculosis is a lack of alterations in lymph nodes and lack of haematogenous spreading. Only canalicular spread can occur within the affected organ (NIEBERLE, 1938). This canalicular spread causes bronchiolitis, caseation and ulcers in bronchia, trachea and larynx. Caseating bronchiolitis causes destruction on the bronchial muscles and elastic walls, thus bronchioectatic tuberculous cavities develop after destruction of the bronchial walls (PALLASKE, 1961). Besides the lung, the organ tuberculosis can also be seen in the udder. Three different forms of mammary tuberculosis are described by Nieberle. These are the miliary tuberculosis, the lobular infiltrative or chronic mammary tuberculosis and the mastitis caseosa. The most common form is the chronic

infiltrative lobular tuberculosis, which is seen approximately in 80-90% of mammary tuberculosis cases (NIEBERLE, 1938).

2.14.2.2. Late Generalisation

In the late generalisation, it is assumed that the immune response of the host has been broken down, which permits the bacteria to spread via haematogenous or lymphogenous ways. Haematogenous metastases can arise in most of the major organs, and also in the regional lymph nodes, serous membranes, including the peritoneum, pericardium, and menings and skeleton (JUBB & KENNEDY, 1963). This phase of disease is dominated by an acute exudative and caseating process. Regional lymph node alterations are common, as described in the primary infection (PALLASKE, 1961). Late generalisation can occur in different types, which are miliary tuberculosis, multiple lobular caseating pneumonia and galloping acinar pneumonia (NIEBERLE, 1938).

2.14.2.2.1. Acute Miliary Tuberculosis

Miliary tuberculosis in cattle can be lethal or lesions can be found during the slaughter as an incidental finding. In case of the weakening of the immune response, the bacteria can largely increase and spread out to the other organs (generalisation). The distinctive alterations seen in lung consist of miliary foci and there are not any alterations in the regional lymph nodes (NIEBERLE, 1938).

2.14.2.2.2. Lobular Caseating Pneumonia

Mostly, the massive destruction of tissue is a finding of lobular caseating pneumonia. It spreads over the entire cross section of the lung lobes. In addition to that, miliary foci can also be observed in the lung following lympho-haematogenous spread (PALLASKE, 1961).

2.14.2.2.3. Galloping Acinar Pulmonary Tuberculosis

The galloping acinar pulmonary tuberculosis is restricted in the bronchial tree branches in the form of a caseating bronchitis. Acinar pulmonary tuberculosis develops in large part of the lung, and the regional lymph nodes are affected, too (NIEBERLE, 1938).

2.15. Pathology

2.15.1. Macroscopic Findings

2.15.1.1. Lung and Regional Lymph Nodes

2.15.1.1.1. Initial Phase and Early Generalisation

In lung and mediastinal lymph nodes, the tuberculous lesions are found in the initial phase of the infection as complete primary complexes (STAMP, 1944). Tubercles can be found sub-pleurally in any lobe of the lung. They are caseated and calcified approximately from hazelnut size to fist size and are encapsulated by granulation tissue (NIEBERLE, 1938; PALLASKE, 1961). Lesions in regional lymph nodes have the same appearances as seen in the lung (PALLASKE, 1961).

Lesions in cases of early generalisation are divided into different groups, as mentioned above (see in chapter 2.14.1. primary infection and early generalisation) (NIEBERLE, 1938). Lesions in the acute miliary tuberculosis appear as glassy and translucent fine submiliar foci at first. Later, they are greyer and yellowish. The regional lymph nodes are also affected and appear swollen, necrotic and calcified. In calves, this process is associated with translucent tubercles in the lung (NIEBERLE, 1938). The protracted generalisation is characterised by presence of caseated and calcified tubercles, which are in different sizes (NIEBERLE, 1938). Another form is the lobular infiltrative tuberculosis, which shows whitish, rough and greasy foci in the emphysematous lung lobes. The lymph nodes are severely enlarged and calcified (NIEBERLE, 1938). The galloping acinar and lobular caseating pneumonia is another lesion pattern in calves and young cattle. This form is characterised by multiple, greasy, partly calcified foci of variable size in the lung lobes. Mediastinal lymph nodes are found enlarged and in association with the alterations in the lung (NIEBERLE, 1938).

2.15.1.1.2. Chronic Tuberculosis (Organ Tuberculosis)

The pathological alterations in chronic organ tuberculosis of lung are described as acinar and acinar-nodular foci, cavities, and ulcerations in bronchia and trachea. The acinar foci are generally found in the main lobes, but can also be seen in cranial lobes. The affected lobe or

lobes are found in purple-red colour with compact, smooth and moist cut surface. These lobes consist of millet seed to lentil-sized foci, which form small groups and appear as a shamrock. Intra- and inter-lobular bronchia are characterised by a thickened bronchial wall. As a result of a liquefaction of acinar-nodular foci they have purulent cheesy masses in their lumens. The cavities in the organ tuberculosis appear either as melting cavities or bronchioectatic tuberculous cavities. But bronchioectatic cavities are pathognomonic for bovine chronic lung tuberculosis (NIEBERLE, 1938).

2.15.1.1.3. Late Generalisation

Three different pathological reaction patterns can be found in the case of the late generalisation (NIEBERLE, 1938; PALLASKE, 1961). The first one is the miliary tuberculosis and is characterised by a voluminous lung, which shows partly emphysematous, partly oedematous alterations and also small, irregularly scattered foci (miliary pneumonia). The regional lymph nodes are mildly enlarged (NIEBERLE, 1938). The second one is the acute multiple, lobular caseating pneumonia. It is mainly characterised by an exudative process. The main macroscopic picture is a composition of caseous foci, which are irregular in size and shape within the lobules, either only in some parts of a lobule or the entire lobule. The cut surface is moist, cheesy and yellow, commonly accompanied by fine blood spots and disintegration, possibly with cavity formation. The lymph nodes appear oedematous and enlarged (NIEBERLE, 1938). The third reaction pattern is the galloping acinar pulmonary tuberculosis. It is characterised by acinar tubercles scattered throughout the emphysematous lung. The regional lymph nodes are enlarged, oedematous and caseated (NIEBERLE, 1938; PALLASKE, 1961).

2.15.1.2. Intestine and Regional Lymph Nodes

Intestinal alterations are generally seen in the posterior part of the intestinal tract. Frequently, they are only found in mesenterial lymph nodes without alterations in intestine, as incomplete primary complex form. Affected mesenterial lymph nodes are either mildly or severely swollen. The cut surface shows tubercles with caseation and/or calcification, and fibrous demarcation. On the other hand, lesions in intestine are occasionally seen in calves and young cattle, as complete primary complex form. In calves, they also show lentil-sized ulcerations (PALLASKE, 1961).

2.15.1.3. Liver and Regional Lymph Node

In the liver, the lesions appear as nodular, capsulated, centrally caseous, calcified foci in pea-size (NIEBERLE, 1938). The portal lymph nodes are also affected and generally swollen, caseated and calcified (PALLASKE, 1961). The nodules tend to be rounded and often appear hemispherically above the surface. A thick capsule and the pale, yellow and caseous content can be seen on the cut surface. The caseous exudate may be dense and calcified, but occasionally it is liquefied like pus (JUBB & KENNEDY, 1963).

2.15.1.4. Kidney

In the kidneys, tuberculous lesions can be found in form of few encapsulated nodules or as large destructive caseous lesions (STAMP, 1944). Most kidney lesions are seen in the renal cortex at the phase of acute miliary tuberculosis (NIEBERLE, 1938).

2.15.1.5. Pearl Disease

An involvement of the serosal surfaces can also be seen, especially the pericardium, pleura or peritoneum, during generalisation (DOMINGO et al., 2014). Pleural tuberculosis is characterised by nodular lesions, which have a tendency to calcify and to occur in clusters. These lesions can also appear pedunculated, and can coalesce to form cauliflower-like masses. The severe calcification gives the name of the term as 'pearl disease'. Caseous tuberculous pleuritis is characterised by large plaques of caseous exudates and a thickened pleura. The peritoneal lesions are softer, more diffuse and have tubercles embedded in extensive granulation tissue. Although these lesions are found similar as those of the pleura, they are not exactly nodular or 'pearly' (JUBB & KENNEDY, 1963).

2.15.1.6. Skeleton, Brain and Meninges

Tuberculous lesions in the skeleton occur due to haematogenous dissemination during early generalisation and result in osteomyelitis characterised by large granulomas with extensive caseation (JUBB & KENNEDY, 1963).

The lesions in the brain are found after the primary infection and/or during the early generalisation phase of the mycobacterial infection and are characterised by the presence of focal, caseated, calcified tubercles with fibrous encapsulation in walnut size. The meningeal lesions are seen in the acute miliary tuberculosis, most frequently affecting the leptomeninges (PALLASKE, 1961).

2.15.1.7. Spleen, Muscles, Pancreas and Salivary Glands

Tuberculous lesions occur rarely in salivary glands and muscles, including myocardium, and spleen following haematogenous dissemination in postnatal infection (JUBB & KENNEDY, 1963).

2.15.1.8. Genital Organs

Genital tuberculosis can be seen both in male and female sexual organs. In females, uterus is the most encountered organ. In males, caseated, calcified tubercles occur at the penis and the prepuce as primary infection or more frequently in testicles and the epididymis following haematogenous dissemination (PALLASKE, 1961).

2.15.1.9. Mammary and Supramammary Lymph Nodes

Mammary lesions can be divided into three groups by Nieberle; the first form is the miliary tuberculosis, which occurs in context of an early generalisation in form of miliar or large foci with central caseation and calcification. The mammary lymph nodes are also affected. The second form is a chronic infiltrative lobular tuberculosis form with the usually caseified tubercles. They are enlarged, dry, compact and grey-reddish with a greasy transparent appearance on the cut surface. Mammary lymph nodes are generally not affected. The last form is described as mastitis caseosa, which display an exudative inflammatory process (NIEBERLE, 1938). Supramammary lymph nodes are barely found swollen and are mostly without any tubercle (PALLASKE, 1961).

2.15.2. Histological Findings

Histologically, tuberculous inflammation can be divided into a productive type and an exudative type, as mentioned above (see in 2.14. Pathogenesis). Classical productive granuloma formation is predominantly characterised by a proliferation of epithelioid and Langhans-type multinucleated giant cells (NIEBERLE, 1938; PALLASKE, 1961). The epithelioid cells stain palely and have large vesicular nuclei, and broad, pale cytoplasma with uncertain cell borders. Langhans-type multinucleated giant cells have extensive cytoplasma and several nuclei. Intracytoplasmic ingested bacilli can be seen in these cells (JUBB & KENNEDY, 1963). A narrow zone of lymphocytes, plasma cells and macrophages surrounds this epithelioid cell proliferation. The central necrosis has caseous character and appears as amorphous eosinophilic material with necrotic debris and central calcification. Small numbers of bacilli are present within the necrotic mass. The granuloma is encapsulated by an outer layer of fibrous connective tissue (NEILL et al., 2001). However, the fibroplasia and the central necrosis are related to the progressive proliferative granulomas. They are not seen in all granulomas (JUBB & KENNEDY, 1963).

Exudative inflammation is predominantly composed of plasma cells, lymphocytes and neutrophil granulocytes; unlike an accumulation of the "specific" cells (epithelioid and Langhans-type giant cells). In pulmonary tuberculosis, a caseation necrosis is often surrounded by a perifocal zone of inflammation consisting of alveolar and bronchiolar inflammation with capillary hyperaemia, exudation of fibrin, and desquamation of alveolar epithelium, and neutrophil infiltration. In addition there are no specific cells and no bacteria can be found in this inflammation zone (PALLASKE, 1961).

2.16. Differential diagnosis

2.16.1. Paratuberculosis

In cattle, paratuberculosis is clinically presented with watery diarrhoea, chronic weight loss despite normal appetite, and decreased milk production (WHITLOCK & BUERGELT, 1996). Macroscopically, lesions can be found segmental or diffuse throughout the intestine and the mesenterial lymph nodes. The lesions can be found from duodenum to rectum throughout the intestine. The ileocecal valve is affected most commonly (BUERGELT, 1978). The intestinal

wall is mostly thickened, oedematous and has transversal folds of the mucosa. Lymphatic vessels are dilated and prominent. Mesenterial lymph node enlargement is also seen predominantly. Histologically, there is a multifocal to diffuse granulomatous inflammation in the intestine, the mesenterial lymph nodes and the liver without necrosis or calcification (BUERGELT, 1978).

2.16.2. Parasitic Granulomas

Parasite larvae (trematodes) in cattle form nodules within the mesenterial lymph nodes, where they die. First, the nodules have pus-like consistence, then they dry and calcify. Histological examination serves for the differentiation from tuberculosis through the detection of remnants of the trematodes and infiltration with eosinophils (PALLASKE, 1961).

2.16.3. Rhodococcosis

Rhodococcus (R.) equi causes bacterial disease in foals, which is characterised by a pyogranulomatous pneumonia, granulomatous lymphadenitis and enteritis (PRESCOTT, 1991). In a study, the bacteria are also found in the lymph nodes with similar macroscopic alterations as seen in tuberculosis. In the histology, infected cattle show severe accumulation of neutrophil granulocytes nearby the caseous necrosis. But the definitive diagnosis should be done by Gram staining or culture media (MCKENZIE & DONALD, 1979).

2.16.4. Actinomycosis

Actinomycosis affects submaxillar, submandibular, and retropharyngeal lymph nodes in cattle and causes gray-yellowish granulation tissue, which is associated with purulente clot material, but without calcification. The differentiation is possible by histological examination. Typically single or multiple inflammatory foci are found in the tongue with a plate-like expansions originating from the superficial mucosa without calcification. This finding helps to macroscopically differentiate actinomycosis from tuberculosis. Lip lesions are characterised by the presence of nodules, ulcers or a diffuse thickening. In the nasal cavity, nodules, ulcers or flat growths of granulation tissue can be observed. Scattered metastatic focal lung lesions consist of grey-yellowish soft granulation tissue with purulen clot material.

Liver lesions consist of either isolated or metastatic foci in connection with actinomycosis of the maxilla (PALLASKE, 1961).

2.17. Diagnosis of Tuberculosis

2.17.1. Intra-dermal Testing

The tuberculin test has been developed for the detection of tuberculosis and has been used over years based on the immune response against the intra-dermal injection of tuberculin. This test technique has facilitated the eradication of the disease in cattle. The basic principle is a delayed-type hypersensitivity response. There are two types of tuberculin tests currently in use; single intra-dermal test (SIT), consisting of bovine tuberculin, and the single intra-dermal comparative tuberculin test, including both bovine and avian tuberculin (SICTT) (MONAGHAN et al., 1994). In Germany tuberculin testing is regulated as indicated in Commission Regulation (EC) No 1226/2002 of 8 July 2002 amending Annex B to Council Directive 64/432/EEC. On the other hand, a recent survey study shows that many practitioners do not follow the requirements of the Council Directive 64/432/EEC when evaluating the results of intradermal test. The same study also guides the farm animal practitioners to improve the performance of the intradermal test (PUCKEN et al., 2015). According to Council Directive 64/432/EEC, the injection site for tuberculin should be in the transition region between the first and middle thirds of the neck (in cranio-caudal direction). The injection side of avian tuberculin shall be about 10 cm from the crest of the neck and the site of injection of bovine tuberculin about 12,5 cm lower on a line roughly parallel with the line of the shoulder or on different sides of the neck. The interpretation can be done 72 hours after the injection based on the clinical findings at the site of injection as following;

1. Negative reaction: if there is only limited swelling lesser than 2 mm in the thickness and no clinical signs such as diffuse or extensive oedema, exudation, necrosis, pain or inflammation of the lymphatic ducts in that region or of the lymph nodes.
2. Inconclusive reaction: if no clinical signs are observed (as mentioned 1.) and if the increase of the skin-fold thickness is found more than 2 mm and less than 4 mm.
3. Positive reaction: if clinical signs (as mentioned 1.) are found or there is an increase of 4 mm or more in the thickness of the fold of skin at the injection site.

2.17.2. *In vitro* Immunodiagnostic Assays

Interferon gamma (IFN-γ) is a cytokine released by T lymphocytes after the infection of tuberculosis and plays an improtant role in the immune response process. IFN-γ test is used to detect cellular immune response of the host against bTB (WOOD et al., 1991, POLLOCK et al., 2005). Regulations in Germany indicate that IFN-γ test (for example; Bovigam®) can be used as an altenative diagnostic tool to intra-dermal skin test (TUBERKULOSE-VERORDNUNG, 2014). The estimated sensitivitiy of IFN-γ test in international studies ranges between 73.0 and 100%, with a median value 87.6%. Its median specificity is 96.6%, with a range of 85.0 to 99.6% (DE LA RUA-DOMENECH et al., 2006).

2.17.3. Serological Diagnosis

Enzyme-linked immunosorbent assay (ELISA) has been used as a diagnostic tool for the diseases with the high rate of sensitivity and specificity (RITACCO et al., 1987), but also with a low sensitivity (RITACCO et al., 1990). Extensive antigenic cross-reactivity between the strains of mycobacterium occurs as a problem for the sensitivity of this method (WOOD & ROTHEL, 1994). In another study, *M. bovis*-specific protein (MPB70), a purified component of main antigen of *M. bovis,* has been shown to improve the specificity of an ELISA (FIFIS et al., 1991).

2.17.4. Necropsy

Necropsy is a procedure to examine the suspected cattle after a positive tuberculin test. The first step is the macroscopical examination of the organs, followed by the collection of the tissue specimens for bacteriological and histological examinations. The gross examination must be done thoroughly. All organs should be examined, because sometimes lesions cannot be visible, but can be detected by bacteriological examinations (CORNER, 1994; WHIPPLE et al., 1996).

The sensitivity of gross necropsy as a diagnostic tool has been investigated and the proportion has been assessed as high as caudal fold or cervical intradermal skin tests (NORBY et al., 2004).

2.17.5. Microbiological Examination

Microbiological cultivation is an effective traditional diagnostic tool for the identification of mycobacterium. Two basic media are used for the cultivation of *M. bovis*. They are agar and egg based. B-83 Agar (COUSINS et al., 1989) and Middlebrook 7H11 (GALLAGHER & HORWILL, 1977) are used as an agar medium. Stonebrink (LESSLIE, 1959) and Lowenstein-Jensen mediums are used as an egg medium. The growth and appearance of bacteria on these media take several weeks. For instance, the first appearance occurs after 3 weeks of incubation in use of B-83 blood agar medium. However the incubation period should be at least 8 weeks in order to obtain high number of bacilli (COUSINS et al., 1989). The first appearance is obtained in 28 days of incubation with Middlebrook 7H11 (GALLAGHER & HORWILL, 1977).

Lowenstein-Jensen medium is utilised to cultivate *M. caprae* and the first appearance of the colonies occurs after 4-6 weeks of incubation (as indicated in 2.2 Morphology of Mycobacterium) (ARANAZ et al., 1999).

2.17.6. PCR Analysis

Polymerase Chain Reaction (PCR) is described as a practical technique and can be used in most fields of science for biological investigations that require the demonstration of DNA (EISENSTEIN, 1990). This method permits detecting and identifying the mycobacteria in animals and humans as an alternative choice, besides other traditional diagnostic tests. PCR analyses can be performed on biological samples, such as milk, nasal swab, lymph node aspirates, which are taken from the suspected animals. The detection of tuberculosis depends on their remarkable nucleotide sequences. It is considered that PCR method enables a rapid and accurate differentiation of members of MTBC by amplifying different specific DNA regions (VITALE et al., 1998; HUARD et al., 2003; WARREN et al., 2006). The sensitivity of the sequence-capture PCR technique is confirmed by detecting the mycobacterial DNA in the culture-negative pleural fluid samples from patients with tuberculosis (MANGIAPAN et al., 1996).

2.17.7. Histopathological Diagnostic Methods

Histopathological techniques are utilised to detect tuberculosis in cattle by their classical histomorphologic appearance. These techniques serve as rapid diagnostic tools after post-mortem examination (VARELLO et al., 2008). In the light microscope, the basic architecture of tubercles can be examined by H&E staining (PALMER et al., 2007; LIEBANA et al., 2008) as also described above (see pathology 2.15.2.).

Giemsa staining is used to demonstrate estimated amount of neutrophils, which migrated to the granulomatous inflammation site (ERUSLANOV et al., 2005).
Masson's trichrome staining is applied on the tissue sections for the demonstration of fibrous connective tissue in the granulomatous inflammation. The collagen appears blue following the staining. The aim is to classify the granuloma formation into the developmental stages by evaluating of the thickness of the surrounding fibrous tissue. Von Kossa staining is also used concurrently for the detection of mineralization (RHOADES et al., 1997; PALMER et al., 2007). The stages of granuloma development can also be demonstrated by using immunohistochemical staining methods against T and B cell lymphocytes and also pro-collagen I, which is a precursor of new collagen synthesis (WANGOO et al., 2005).

2.17.7.1. Auramine O/rhodamine B Staining

By using auramine O/rhodamine B staining and fluorescence microscopy, bacilli are recognized as yellow against the dark background staining at higher magnification. The sensibility is considered to be between immunohistochemistry and Ziehl-Neelsen staining (WATRELOT-VIRIEUX et al., 2006). Prior to that, auramine O and acridine orange staining has been used to identify Runyon Group III mycobacterium species (MOTE et al., 1975).

2.17.7.2. Ziehl-Neelsen (ZN) Staining

The first attempt to demonstrate the mycobacterium by light microscopy was achieved by Robert Koch, and so the first rod-like structure became visible after 24 h of incubation with a solution consisted of distilled water, methylene-blue and potassium hydroxide, (KOCH, 1882). Subsequently, the staining method was developed by using aniline oil and fuchsine that helped to reduce the time from 24 h to 1 h (EHRLICH, 1882). In Ziehl`s studies, aniline oil

solution was used in combination with carbolic acid (ZIEHL, 1882). Thereafter, Neelsen combined Ziehl`s carbolic acid with Ehrlich`s red stain fuchsin. In this way, the "Ziehl-Neelsen Staining" was born (MADKOUR, et al. 2004).

Studies show that the acid-fast bacilli can be recognized in the cytoplasm of epithelioid cells, macrophages, multinucleated giant cells and also free in the caseous debris. According to comparative studies between ZN and immunohistochemistry, ZN staining method is confirmed to have high specificity but lack sensibility (CANCELA & MARIN, 1993; WATRELOT-VIRIEUX et al., 2006; VARELLO et al., 2008), thus it is deemed that this technique can detect only perfect (complete) organisms (CANCELA & MARIN, 1993).

2.17.7.3. Immunohistochemistry (IHC)

IHC has been used for the detection of mycobacterial antigen. Whole organisms or fragments of those can be determined both in the intracellular and extracellular localisations (ULRICHS et al., 2005; WATRELOT-VIRIEUX et al., 2006). Moreover, it allows us to investigate the development of granulomatous lesion in tissue samples with tuberculosis by simultaneously immunolabelling of the cell subsets and nitrite oxide synthase at the side of inflammation (PALMER et al., 2007).

Monoclonal and polyclonal antibodies have been developed against the antigens of mycobacterium (CORNER et al., 1988; BARBOLINI et al., 1989; BONENBERGER et al., 2001; MUSTAFA et al., 2006).

Although the sensitivity is found high, the specificity of IHC interpreted different. While some authors see this method with a good specificity (HUMPHREY & WEINER, 1987; CORNER et al., 1988; PUROHIT et al., 2007), some authors think the opposite (CASSIDY et al., 1999; WATRELOT-VIRIEUX et al., 2006).

2.17.7.4. In Situ Hybridization

In situ hybridization is considered to be a diagnostic tool with high specificity and sensitivity. This method detects the distribution of the tuberculous bacilli in the granulomatous lesion (STENDER et al., 1999b; FENHALLS et al., 2002a and b). Mycobacterial DNA probes allow

the observation of the spatial arrangement between the host cells and the bacilli, while mRNA probes provide us to see whether the bacilli are alive or not (FENHALLS et al., 2002b). Peptide nucleic acid (PNA) probes distinguish the bacilli, which belong to MTBC, from non-tuberculosis mycobacterium species by using fluorescence in situ hybridization (FISH) method (STENDER et al., 1999a).

This method has also been used to simultaneously detect type I pro-collagen, and so to evaluate the thickness of the fibrous capsule around the granulomas and thereby makes it possible to divide the granulomatous inflammation into the developmental stages (WANGOO et al., 2005).

2.17.8. Electron Microscopy

Electron microscopy methods demonstrate the ultra-structure of the mycobacterial cell wall components, and their roles in mycobacterial biogenesis (BARKSDALE & KIM, 1977).

In addition, the progression of epithelioid granulomatous inflammation is demonstrated with the ultra-structural differentiation of monocytes into macrophages, and then into well-developed epithelioid cells by electron microscopy (ADAM, 1974, 1975).

3. MATERIALS AND METHODS

3.1. Materials and Sampling Period

The examined cattle in this study derived from different herds located in Allgäu, Germany, suffering from bovine tuberculosis (bTB) outbreaks from 2009 to 2014. The herds included tuberculin positive reactor animals. The animals were submitted to the flaying house. During necropsy, tissue samples were collected for histopathological and bacteriological investigations. Further processes for histopathological investigations were carried out at the Institute of Veterinary Pathology at the Center of Veterinary Medicine of the Ludwig-Maximilians-University in Munich.

3.1.1. Preparation of Tissue Samples

The collected tissue samples included retropharyngeal lymph node, lung, mediastinal lymph node, liver, portal lymph node, small intestine and mesenterial lymph node. The tissue samples were fixed in 4% buffered formaldehyde (Appendix 9.2.1.) for 24 to 48 h. Subsequently, tissue pieces of approximately 3 mm thickness were cut from the tissue samples, placed in the tissue-embedding capsules and then embedded in the paraffin, glycol-methacrylate (GMA) resin or epoxy resin. Blocks were cut using different types of microtomes. Sections were stained with H&E and the Giemsa stain for light microscopy. For further analyses special stainings including a modified acid-fast staining according to Fite-Faraco (FF), immunohistochemistry, in situ hybridization as well as electron microscopy were performed.

3.1.2. Preparation of Positive Control Materials

Positive control specimens were prepared in collaboration with the Institute for Infectious Diseases and Zoonoses (Head Prof. Dr. R. Straubinger) of the Veterinary Faculty, Ludwig-Maximilians University in Munich. *M. kansasii* and *M. bovis* BCG subtype were cultured in Loewenstein-Jensen medium and embedded as mentioned above. In the course of this study, sections from these specimens served as positive controls for immunohistochemistry and in situ hybridization.

3.2. Methods

3.2.1. Methods for Tissue Samples

3.2.1.1. Embedding, Sectioning, and Staining Procedures for Paraffin Wax Technique

Dehydration of the tissue samples was done in a tissue processor (Gewebeeinbettungsautomat Histomaster Modell 2050/DI, Bavimed, Birkenau):

- 30 min washing with aqua dest.
- 2 x 1.5 h 70% ethanol
- 2 x 1.5 h 96% ethanol
- 2 x 1.5 h 100% ethanol
- 2 x 30 min xylene (SAV Liquid Production, Flintsbach, No. XTR-5000-97-1)
- 1.5 h xylene
- 2 h paraffin 60˚C (SAV Liquid Production, Flintsbach, No. PFNP-5-5658-1)
- 3 h paraffin 60˚C

After this process, tissue samples were embedded in paraffin (Unilink-embedding cassette, No. 17985k, light blue and No. 17980, green, Langenbrinck, Emmendingen) using an embedding device (TBS 88 Paraffin Embedding System, Medite Medizintechnik, Burgdorf). Sections of 4 μm thickness were cut from each tissue block with a rotary microtome (HM 315, Microm, Walldorf) and were mounted on object slides (Engelbrecht, Edermünde, No. 1110022 or No. 11250 Star Frost). A decalcification process was applied for severely calcified tissues before the cutting process using a decalcification solution (VWR, International GmbH, Darmstadt, No. 11028304.P). The cut sections were stored at 40˚C for 24 h before further use.

Each sample was stained using H&E, according to Giemsa, and the modified acid-fast staining according to Fite-Faraco (FF). In some cases, Masson´s trichrome (MT) staining for connective tissues was applied.

Except for FF staining, the tissue slides were deparaffinised by a 10 min incubation in xylene. The rehydration was done using a descending ethanol-series and finally distilled water. Paraffin oil was used for the deparaffinisation for the FF staining method.

3.2.1.1.1. Haematoxylin Eosin (H&E) Staining

- 5 min Mayer`s haemalaun (Appendix 9.3.1.1.)
- 4 min rinsing in running warm tap-water
- 5x immersion in 0.5% HCl acid alcohol (Appendix 9.3.1.3.)
- 4 min rinsing in running warm tap-water
- 2 min eosin (Appendix 9.3.1.4.)
- Rinsing in aqua dest.
- Dehydration with an ascending ethanol-series (70%, 96%, 100% ethanol)
- Clearing in xylene
- Mounting with cover slips (Engelbrecht, Edermünde, No. k 12440) and a mounting medium (K. Hecht, Sondheim, Histokitt, No. 1025/500)

3.2.1.1.2. Giemsa Staining

- 1 h in Giemsa solution (Appendix 9.3.2.2.) at 65°C
- Rinsing in aqua dest.
- 1 sec differentiation using 0.5% acetic acid (until the colour changes from blue to red!) (Appendix 9.3.2.3.)
- 5x immersion in 96% ethanol
- 5x immersion in 100% ethanol
- Clearing in xylene
  Mounting with cover slips (Engelbrecht, Edermünde, No. k 12440) and a mounting medium (K. Hecht, Sondheim, Histokitt, No. 1025/500)

3.2.1.1.3. Masson´s Trichrome (MT) Staining

- 5 min Weigert's iron-haematoxylin (Appendix 9.3.3.1.)
- 5 min rinsing running warm tap-water

- Differentiation with 0.5% HCl acid alcohol (Appendix 9.3.1.3.)

- 5 min rinsing in running warm tap-water

- 5 min red-colour solution (Appendix 9.3.3.4.)

- Rinsing in 0.5% acetic acid (Appendix 9.3.2.3.)

- 3 min phosphotungstic acid-orange G (connective tissue must be decolorized!) (Appendix 9.3.3.5.)

- Rinsing in 0.5% acetic acid (Appendix 9.3.2.3.)

- 5 min aniline blue (Appendix 9.3.3.6.)

- Short rinsing in 0.5% acetic acid (Appendix 9.3.2.3.)

- Dehydration in an ascending ethanol-series (96%, 100% ethanol)

- Clearing in xylene

- Mounting with cover slips (Engelbrecht, Edermünde, No. k 12440) and a mounting medium (K. Hecht, Sondheim, Histokitt, No. 1025/500)

3.2.1.1.4. Acid-Fast Staining Modified According to Fite-Faraco

- 2x 10 min deparaffinisation in paraffin oil (Appendix 9.3.4.1.)

- 30 min Ziehl-Neelsen carbolfuchsin (VWR, International GmbH, Darmstadt, No. 1.092152500)

- 10 min rinsing in running cold tap-water

- Decolorisation with 1% HCl acid alcohol (until light pink and colour stops running out) (Appendix 9.3.4.2.)

- 5 min rinsing in cold tap-water

- 3x immersion in methylene blue

- 5 min rinsing in running cold tap-water

- Dehydration in 100% ethanol

- Clearing in xylene

- Mounting with cover slips (Engelbrecht, Edermünde, No. k 12440) and a mounting medium (K. Hecht, Sondheim, Histokitt, No. 1025/500)

3.2.1.1.5. Immunohistochemistry on Paraffin Sections

Immunohistochemistry was performed for all tissue samples against mycobacterial antigens using the polyclonal primary antibodies rabbit anti-*M. tuberculosis* complex (Rb x tbc) and rabbit anti-*M. bovis,* to determine the localisation of mycobacterial antigens within the granulomatous inflammation. Furthermore, antibodies against CD3, CD20, CD79a, calprotectin (MAC387), and lysozyme were used to specify inflammatory cells in selected cases.

The standard protocol for the avidin-biotin complex (ABC) method was used for the antibodies against CD3, CD20, CD79a, and *M. bovis.* The standard protocol for the indirect immunoperoxidase method was used for antibodies against calprotectin (MAC387), lysozyme, and *M. tuberculosis* complex. The used antigen retrieval methods including used buffer solutions, the normal serums and the antibodies for each procedure are outlined in Table 1.

Antigen retrieval procedures were performed following deparaffinisation. For the heat induced antigen retrieval method, two different buffer solutions were used: citrate buffer (Appendix 9.7.5.) and tris/EDTA buffer (Appendix 9.7.2.). Sections were incubated in these solutions in the microwave oven at 800 W for 2x 10 minutes followed by a cool down period of approximately 20 minutes. Enzymatic antigen retrieval process was performed using proteinase K (Dako, Hamburg, No. S3020) at room temperature (RT).

3.2.1.1.5.1. Standard Protocol for ABC-Method

- Deparaffinisation for 20 min in xylene (SAV Liquid Production, Flintsbach No. XTR-5000-97-1)
- Rehydration in a descending ethanol-series (2x 100%, 2x 96%, 1x 70% ethanol) and aqua dest.
- Antigen retrieval procedure (Table 1)
- Blocking the endogenous peroxidase activity by incubation in 1% hydrogen peroxide (Appendix 9.7.6.) for 15 min at RT
- 5 min washing in TBS (Appendix 9.7.1.)

- Reduction of non-specific binding sites by incubation with normal serum for 30 min (diluted in TBS, Table 1)

- Incubation for 1 h with the primary antibody (diluted in TBS, Table 1) at RT

- 5 min washing in TBS

- Incubation for 1 h with the secondary antibody (diluted in TBS, Table 1) at RT

- 5 min rinsing in TBS

- 30 min incubation with ABC (diluted 1:100 in TBS) (Appendix 9.7.8.) at RT

- 5 min rinsing in TBS

- 3 min incubation with substrate and chromogen (Appendix 9.7.7.) at RT

- 5 min rinsing in running cold tap-water

- 20 sec counterstaining with 10% haemalaun (Appendix 9.3.1.1.)

- 5 min rinsing in running cold tap-water

- Dehydration in an ascending ethanol-series (70 %, 96 %, 100 % ethanol)

- Clearing in xylene

- Mounting with cover slips (Engelbrecht, Edermünde, No. k 12440) and a mounting medium (K. Hecht, Sondheim, Histokitt, No. 1025/500)

Table 1. IHC using the ABC-method.

	Dilution
CD3	
Antigen retrieval: tris/EDTA buffer (Appendix 9.7.2.)	
Normal serum: goat (MP Biomedicals, Eschwege, No. 092939149)	1:10
Primary antibody: polyclonal rabbit anti-CD3 (Dako, Hamburg, No. 0452)	1:100
Secondary antibody: monoclonal biotinylated goat anti-rabbit IgG (Vector Laboratories, Burlingame, No. 41228)	1:200
CD20	
Antigen retrieval: -	
Normal serum: goat (MP Biomedicals, Eschwege, No. 092939149)	1:10
Primary antibody: polyclonal rabbit anti-CD20 (Thermo Scientific, Waltham, No. RB-9013R7)	1:400
Secondary antibody: polyclonal biotinylated goat anti-rabbit IgG1 (Vector Laboratories, Burlingame, No. BA-1000)	1:200

CD79a

Antigen retrieval: tris/EDTA buffer (Appendix 9.7.2.)

Normal serum: goat (MP Biomedicals, Eschwege, No. 092939149) 1:10

Primary antibody: monoclonal mouse anti-CD79a (Linaris, Dossenheim, No. MAK 2538) 1:100

Secondary antibody: polyclonal biotinylated goat anti-mouse 1:200

(Dako, Hamburg, No. E0433)

M. bovis

Antigen retrieval: citrate buffer (Appendix 9.7.5.)

Normal serum: goat (MP Biomedicals, Eschwege, No. 092939149) 1:10

Primary antibody: polyclonal rabbit anti-*M. bovis* (Biorbyt, California, No. orb100411) 1:50

Secondary antibody: goat anti-rabbit IgPO (Dako, Hamburg, No. 20003813) 1:100

3.2.1.1.5.2. Standard Protocol for the Indirect Immunoperoxidase Method

- Deparaffinisation for 20 min in xylene (SAV Liquid Production, Flintsbach, No. XTR-5000-97-1)
- Rehydration in a descending ethanol-series (2x 100%, 2x 96%, 1x 70% ethanol) and aqua dest.
- Antigen retrieval procedure (Table 2)
- Blocking the endogenous peroxidase by incubation in 1% hydrogen peroxide (Appendix 9.7.6.) for 15 min at RT
- 5 min washing in TBS (Appendix 9.7.1.)
- Reduction of non-specific binding sites by incubation with normal serum for 30 min (diluted in TBS, Table 2)
- Incubation for 1 h with the primary antibody (diluted in TBS, Table 2) at RT
- 5 min washing in TBS
- Incubation for 1 h with the secondary antibody (diluted in TBS, Table 2) at RT
- 5 min rinsing in TBS
- 3 min incubation with substrate and chromogen (Appendix 9.7.7.) at RT
- 5 min rinsing in running cold tap-water
- 20 sec counterstaining with 10% haemalaun (Appendix 9.3.1.1.)
- 5 min rinsing in running cold tap-water
- Dehydration in an ascending ethanol-series (70%, 96%, 100% ethanol)

- Clearing in xylene (SAV Liquid Production, Flintsbach No. XTR-5000-97-1)
- Mounting with cover slips (Engelbrecht, Edermünde, No. k 12440) and a mounting medium (K. Hecht, Sondheim, Histokitt, No. 1025/500)

Table 2. IHC using the indirect IPO-method.

	Dilution
MAC387	
Antigen retrieval: proteinase K (Dako, Hamburg, No. S3020)	
Normal serum: rabbit (MP, Biomedicals, Eschwege, No. 092941149)	1:10
Primary antibody: monoclonal mouse anti-MAC387 (Dako, Hamburg, No. M0747)	1:300
Secondary antibody: polyclonal rabbit anti-mouse IgPO (Dako, Hamburg, No. P0161)	1:100
Lysozyme	
Antigen retrieval: proteinase K (Dako, Hamburg, No. S3020)	
Normal serum: porcine (MP, Biomedicals, Eschwege, No. 092924149)	1:10
Primary antibody: polyclonal rabbit anti-lysozyme (Dako, Hamburg, No. A 0099)	1:50
Secondary antibody: polyclonal swine anti-rabbit IgPO (Dako, Hamburg, No. P0217)	1:100
M. tuberculosis complex	
Antigen retrieval: citrate buffer (Appendix 9.7.5.)	
Normal serum: goat (MP Biomedicals, Eschwege, No. 092939149)	1:10
Primary antibody: polyclonal rabbit anti-*M. tuberculosis* complex (Bio-Rad, Munich, No. 220713)	1:100
Secondary antibody: polyclonal goat anti-rabbit IgPO (Dako, Hamburg, No. 20003813)	1:10

3.2.1.1.6. In situ Hybridization

Non-radioactive hybridization method was performed to determine the localisation of mycobacteria. Previously described *M. tuberculosis*-oligonucteotide DNA probes were used as a cocktail for hybridization (AMAND et al., 2005). EU bacteria DNA probe (AMAND et al., 2005) was separately performed on some positive slides as control. The used probes and their sequences are given in Table 3.

Table 3. The sequences of ISH probes against mycobacterial genes.

Probe	Sequence
MTB770	(5- CACTATTCACACGCGCGT-3)
MTB226	(5- CCACACCGCTAAAG-3)
MTB187	(5- TGCATCCCGTGGTCCTATCC-3)
EUB338	(5- GCT GCC TCC CGT AGG AGT -3)

Besides the standard protocol (see 3.2.1.1.6.1.), numerous variations of the protocol were performed to obtain a positive reaction. Citrate buffer, different enzyme types and their combinations were used for the pre-treatment step. Instead of proteinase K, achromopeptidase and lysozyme were used as alternative enzyme types. Red substrate kit (Vector Laboratories, Burlingame, No. SK-5100), in the colour reaction step, and levamisole (Applichem, Darmstadt, No. A4341) pre-treatment against endogenous alkaline phosphatase activity were tested. Furthermore, different incubation times and temperatures were applied. Alternative applications in some steps of the standard protocol are listed (in Chapter 3.2.1.1.6.2.).

3.2.1.1.6.1. Standard Protocol of ISH

- Deparaffinisation of paraffin slides for 5 min in xylene
- Rehydration in a descending ethanol-series (100%, 96%, 70% ethanol, and aqua dest.) 5 min each
- 15 min incubation in proteinase K buffer (Appendix 9.8.9.) at 37°C in the water bath
- Deactivation of proteinase K: 2x aqua dest., 1x 96% ethanol, 5 min 100% absolute ethanol
- Air-drying of the Slides
- Hybridization:
  - Mix of solution I (Appendix 9.8.10.) and solution II (Appendix 9.8.11.), applying the mixed solutions on the slides and heating at 95°C for 6 min.
  - Incubation overnight at 40°C
- Post-hybridization Washes:
  - 10 min immersion in SSC (2x) (Appendix 9.8.3.)
  - 10 min immersion in SSC (1x) (Appendix 9.8.4.)
  - 10 min immersion in SSC (0.1x) (Appendix 9.8.5.)

- Immunochemical Detection:
  - 30 min equilibration buffer (Appendix 9.8.14.)
  - 60 min anti-digoxigenin antibody solution (Appendix 9.8.15.)
- Rinsing with
  - 15min buffer I (1x) (Appendix 9.8.12.2.)
  - 15 min buffer I (1x) (Appendix 9.8.12.2.)
  - Immersion in buffer III (Appendix 9.8.13.)
- Colour Reaction:
  - 1 h incubation with NTB-BCIP solution (Appendix 9.8.16.), in a dark place
- Stopping the Colour Reaction:
  - TE-buffer (1x) (Appendix 9.8.17.1.) pH 8.0 10 min
  - Aqua dest.
- Counterstaining:
  - Immersion once in haemalaun solution (VWR, International GmbH, Darmstadt, No. 1.092492500)
  - Rinsing in aqua dest.
- Mounting with cover slips (Engelbrecht, Edermünde, No. k 12440), using aqua dest.

3.2.1.1.6.2. Alternative Applications for ISH

ISH-*M. tuberculosis* complex-oligonucleotide DNA probes

- Pre-treatment with proteinase K for 1 hour

- Pre-treatment with higher concentration of proteinase K (Appendix 9.8.26.)

- Decreased hybridization temperature: 37˚C

- Pre-treatment with 1 and 10 mM citrate buffer for 2x 5 min in the microwave oven at 800 W

-
  - Incubation of proteinase K for 30 min,

- o Pre-treatment with 1 mM citrate buffer for 2x 5 min in the microwave oven at 800 W

- •

  - o Pre-treatment with 1 mM citrate buffer for 2x 5 min in the microwave oven at 800 W
  - o Hybridization of tissue sections at 37˚C

- •

  - o Pre-treatment with 1 mM citrate buffer for 2x 5 min in the microwave oven at 800 W
  - o Overnight incubation with the anti-digoxigenin antibody

- •

  - o Pre-treatment with 1 mM citrate buffer for 2x 5 min in the microwave oven at 800 W
  - o Using red substrate kit for the colour reaction

- •

  - o Pre-treatment with 1 mM citrate buffer for 2x 5 min in the microwave oven at 800 W
  - o Incubation of tissue sections in saline sodium citrate (SSC) (2x/1x/0.1x) (Appendix 9.8.3.4.5.) rinse solutions, 20 min each

- •

  - o Pre-treatment with 1 mM citrate buffer for 2x 5 min in the microwave oven at 800 W
  - o Pre-treatment with levamisole before the colour reaction

- •

  - o Pre-treatment with 1 mM citrate buffer for 2x 5 min in the microwave oven at 800 W

- o Incubation of tissue sections in SSC (2x/1x/0.1x) rinse solutions at 40˚C, 20 min each

-
  - o Pre-treatment with 1 mM citrate buffer for 2x 5 min in the microwave oven at 800 W
  - o Incubation of tissue sections in SSC (2x/1x/0.1x) rinse solutions at 40˚C, 20 min each
  - o Pre-treatment with levamisole (Appendix 9.8.27.) at 40˚C before the colour reaction

-
  - o Pre-treatment with 1 mM citrate buffer for 2x 5 min in the microwave oven at 800 W
  - o Incubation of tissue sections in SSC (2x/1x/0.1x) rinse solutions at 37˚C, 20 min each,
  - o Pre-treatment with levamisole at 37˚C before the colour reaction

-
  - o Pre-treatment with 1 mM citrate buffer for 2x 5 min in the microwave oven at 800 W
  - o Hybridization at 37˚C and incubation in SSC (2x/1x/0.1x) rinse solutions at 37˚C, 20 min each

-
  - o Pre-treatment with achromopeptidase (60 U/ml) solution (Appendix 9.8.22.) for 30 min at 37˚C
  - o Incubation in lysozyme (10 mg/ml) solution (Appendix 9.8.23.) for 1 h
  - o Stopping of the enzyme treatment by incubation in 0.01 M HCl solution (Appendix 9.8.25.) for 5 min
  - o Incubation of tissue sections in SSC (2x/1x/0.1x) rinse solutions at 40˚C, 20 min each

-

- o Pre-treatment with achromopeptidase (30 U/ml) and lysozyme (10 mg/ml) solution (Appendix 9.8.24.) for 25 min at 37˚C

- o Stopping of the enzyme treatment by incubation in 10 M tris solution (Appendix 9.8.20.3.) for 5 min

- o Incubation of tissue sections in SSC (2x/1x/0.1x) rinse solutions at 40˚C, 20 min each

- •

  - o Pre-treatment with 1 mM citrate buffer for 2x 5 min in the microwave oven at 800 W

  - o Incubation with achromopeptidase (30 U/ml) and lysozyme (10 mg/ml) solution (Appendix 9.8.24.) for 25 min at 37˚C

  - o Stopping of the enzyme treatment by incubation in 10 M tris solution (Appendix 9.8.20.3.) for 5 min

  - o Incubation of tissue sections in SSC (2x/1x/0.1x) rinse solutions at 40˚C, 20 min each

- •

  - o Pre-treatment with 1 mM citrate buffer for 2x 5 min in the microwave oven at 800 W, then proteinase K at 37˚C

  - o Incubation with achromopeptidase (30 U/ml) and lysozyme (10 mg/ml) solution (Appendix 9.8.24.) for 25 min

  - o Stopping of the enzyme treatment by incubation in 10 M tris solution (Appendix 9.8.20.3.) for 5 min

  - o Incubation of tissue sections in SSC (2x/1x/0.1x) rinse solutions at 40˚C, 20 min each

- •

  - o Incubation with proteinase K at 37˚C, and then microwaving in 1 mM citrate buffer 2x 5 min at 800 W

  - o Pre-treatment of tissue sections with achromopeptidase (30 U/ml) and lysozyme (10 mg/ml) solution (Appendix 9.8.24.) for 25 min

  o Stopping of the enzyme treatment by incubation in 10 M tris solution (Appendix 9.8.20.3.) for 5 min

  o Incubation of tissue sections in SSC (2x/1x/0.1x) rinse solutions at 40˚C, 20 min each

3.2.1.2. Embedding, Sectioning and Staining Procedure for GMA Embedded Tissues

The tissue samples were incubated in a rinsing solution (Appendix 9.4.1.) in a tissue processor (Citadel 1000, Shandon GmbH, Schwerte) for 3 h followed by an ascending ethanol-series (2x 1 h 30%, 2x 1 h 50%, 2x 2 h 70%, 2x 2 h 96 %, 2 x 3 h 96% ethanol).

The tissue samples were put into the 1:1 plastic monomer mixture of glycol methacrylate (GMA, Merck, Darmstadt, No. 8.00588.0250) and methyl methacrylate (MMA, Merck, Darmstadt, No. 8.00590.1000) for 24 h at 4˚C on a shaking device.

Afterwards tissue samples were incubated in solution A of the embedding medium (Appendix 9.4.2.) for at least 2 hours at 4˚C on a shaking device. Thereafter samples were placed in air-tight plastic tubes containing solution B of the embedding medium (Appendix 9.4.3.) with benzoyl peroxide as starter of the polymerization process and N,N-dimethylaniline (Merck, Darmstadt, No. 803060) as accelerator. Polymerisation took place in a water bathtub in the fridge at 4˚C, to reduce polymerisation heat, for 24 h. After removing the polymerised plastic blocks from the plastic tubes, 0.5 µm sections were cut using a heavy duty rotary microtome (HM 360, Microm, Walldorf) with special tungsten carbide knifes with profile d. After mounting on object slides, sections were stained with haematoxylin eosin-phloxine or Giemsa staining. In addition, a silver staining was performed on selected tissue samples.

3.2.1.2.1 Haematoxylin Eosin-Phloxine Staining

- 5 min acidic haemalaun, after Mayer (Appendix 9.3.1.1.)
- 10 min rinsing in running tap-water
- 2 sec differentiation in 1% HCl alcohol (Appendix 9.5.1.1.)
- 10 min rinsing in running tap-water

- 2 min air dry, first between two blotting papers, then on a heating plate (OTS 40, Medite Medizintechnik, Burgdorf) at 60˚C

- 20 min eosin-phloxine ready to use solution (Appendix 9.5.1.3.)

- 2 x 2 min rinsing in aqua dest.

- 2 min air dry, first between two blotting papers, then on a heating plate at 60˚C

- 2 sec xylene

- Mounting with cover slips (Engelbrecht, Edermünde, No. k 12440) and a mounting medium (K. Hecht, Sondheim, Histokitt, No. 1025/500)

3.2.1.2.2 Giemsa Staining

- 1.5 h incubation in the Giemsa ready to use solution (Appendix 9.5.2.2.) in a water bathtub at 65˚C

- 2 sec phosphate-buffer (Appendix 9.5.2.1.)

- 2 x 2 sec differentiation in 0.5% acetic-acid (Appendix 9.5.2.3.)

- 2 sec rinsing in aqua dest.

- 2 min air dry, first between two blotting papers, then on a heating plate at 60˚C

- 2 sec xylene

- Mounting with cover slips (Engelbrecht, Edermünde, No. k 12440) and a mounting medium (K. Hecht, Sondheim, Histokitt, No. 1025/500)

3.2.1.2.3. Silver Staining

- 15 min incubation in 1% periodic acid (Appendix 9.5.3.5.)

- Rinsing in aqua dest.

- 25 min incubation in the silver nitrate solution at 65˚C (Appendix 9.5.3.3.)

- Rinsing in aqua dest.

- 10-20 sec toning in 0.1% gold chloride (Appendix 9.5.3.4.2.)

- Rinsing in aqua dest.

- 1 min incubation in 2% sodium thiosulphate (Appendix 9.5.3.6.)

- Rinsing in aqua dest.

- Air-drying

- 2 sec xylene

- Mounting with cover slips (Engelbrecht, Edermünde, No. k 12440) and a mounting medium (K. Hecht, Sondheim, Histokitt, No. 1025/500)

3.2.1.3. Tissue Preparations for Transmission Electron Microscopy (TEM)

The tissue samples were cut into small pieces approximately 1 mm³, fixed in 6.25% buffered glutardialdehyde (Appendix 9.6.1.2.) and then embedded in epoxy resin. The epoxy resin blocks were cut in semi-thin sections of approximately 0.5 µm thickness using an ultramicrotome (Ultracut E, Reichert und Jung, Vienna, Austria) with a histo-diamond knife (Diatome, Bienne, Switzerland). Staining with toluidine blue-safranin and postembedding immunohistochemistry with the antibody against *Mycobacterium tuberculosis* (Rb x tbc) were performed on selected cases.

Similarly, ultra-thin section examination on the transmission electron microscope was carried out on selected cases, cases which showed a good positive reaction in IHC against mycobacterial antigen on semi-thin sections (especially intracellular positivity was taken into account). The ultra-thin sections were examined at an electron microscope (EM 10, Zeiss, Oberkochen) and were photographed on flat films (ES206, Maco Photo Products, Stapelfeld).

3.2.1.3.1. Embedding Procedure

- Washing with rinse solution (Appendix 9.6.1.3.)
- Incubation in 1% osmium(VIII)oxide solution (Appendix 9.6.1.5.) 2 h in the fridge, part of the tissue blocks was not postfixed with osmium to avoid cross reactions between osmium and the IHC
- Washing 3x in washing buffer, then storage in the fridge for 24 h
- Rinsing 3x in 50% acetone (Roth, Karlsruhe, No. CP40.4)
- 2x 10 min immersion in 70% acetone in the fridge
- 2x 10 min immersion in 90% acetone in the fridge
- 2x 20 min immersion in 100% acetone in the fridge
- 1x 20 min immersion in 100% acetone (RT)
- 1 h immersion in 100% acetone/epon
- 2x 30 min immersion in epon (Appendix 9.6.1.6.)

- Embedding the tissue samples in fresh epon and storage at 60˚C for 48 h

- Cutting process of the resin blocks

- Drying of sections at 60˚C before the next staining procedures

3.2.1.3.2. Toluidine Blue-Safranin Staining of Semi-thin Sections

- Short fixation of the air-dried tissue sections over a flame

- Staining with toluidine blue for 45 sec (Appendix 9.6.2.1.)

- Rinsing with aqua dest.

- Counterstaining with safranin (Appendix 9.6.2.2.)

- Air-drying

3.2.1.3.3. Postembedding Immunohistochemistry on Semi-thin Sections

- 2-3 min keep of sections at 80˚C, then storage overnight at 60˚C

- 1 h incubation in sodium ethylate solution to remove the epon (Appendix 9.7.9.)

- Immersion 3x in 100% ethanol

- Rehydration in a descending ethanol-series (2x 2 min in 100% l, 2x 2 min in 96%, 1x 2 min 70% ethanol)

- Immersion in aqua dest.

- 10 min incubation in 1% H_2O_2 (only used for samples treated with osmium to remove the osmium) (Appendix 9.7.6.)

- 5 min rinsing in TBS (Appendix 9.7.1.)

- 30 min incubation with normal goat serum, diluted 1:10

- 1 h incubation with the primary antibody (polyclonal rabbit anti-*Mycobacterium tuberculosis* complex antibody, Bio-Rad, Munich, 220713), dilution 1:100

- 5 min rinsing in TBS (Appendix 9.7.1.)

- 1 h incubation with secondary antibody (polyclonal goat anti-rabbit IgPO, Dako, Hamburg, No. 20003813) dilution 1:100

- 5 min rinsing in TBS (Appendix 9.7.1.)

- 30 min incubation with avidin-biotin complex 1:100 (ABC) (Appendix 9.7.8.)

- 5 min rinsing in TBS (Appendix 9.7.1.)

- 3 min incubation with H_2O_2 and 3,3`-diaminobenzidine tetrahydrochloride (Appendix 9.7.7.)

- 5 min rinsing in running tap-water

- 30 sec immersion in 10% haemalaun (Appendix 9.3.1.1.)

- 5 min rinsing in running tap-water

- Dehydration with ascending ethanol-series (70%, 96%, 100% ethanol)

- Clearing in xylene

- Mounting with cover slips (Engelbrecht, Edermünde, No. k 12440) and a mounting medium (K. Hecht, Sondheim, Histokitt, No. 1025/500)

3.2.1.3.4. Preparation and Contrasting of Ultra-thin Sections

- The ultra-sections of approximately 70 nm thickness were cut from the resin blocks of preselected tissue samples

- Mounting the ultra-sections on formvar film-coated cooper grids

- 30 min contrasting with uranyl acetate (Appendix 9.6.3.1.)

- Rinsing in aqua dest.

- Air-drying the sections

- Contrasting with lead citrate (Appendix 9.6.3.2.)

- Rinsing in aqua dest.

- Air-drying

3.2.2. Methods for Positive Control Materials

To prepare positive control blocks, the bacteria *M. kansasii* and *M. bovis* BCG subtype were cultured in Loewenstein-Jensen medium in glass tubes at the Institute of Microbiology. After the colonies were recognizable, 4% buffered formalin (Appendix 9.2.1.) was added in the tubes and fixed for 2 days. After the fixation process, the bacteria were placed in the tissue embedding capsules. Two different embedding methods were used to embed the mycobacteria: first method was done using agar (see 3.2.2.1.) and the second method was done without agar (see 3.2.2.2.).

3.2.2.1. Method with Agar

- Mix aqua dest. and agar powder (Agar-Agar, Kobe I, Roth, Karlsruhe, No. 5210.3)

- Heat the agar-aqua dest.-mix in the microwave oven at 800 W

- Draining formalin from the tube

- Filling up the metal embedding tubes with the agar

- Taking little pieces from culture consisting of bacteria, using a spatula

- Embedding bacteria into the agar

- Embedding in paraffin, GMA or epoxy

- Further staining procedures (including H&E, Giemsa and FF staining), immunohistochemical investigations and examination using the TEM were performed as described above for the tissue sections.

3.2.2.2. Method without Agar

- Take out the bacteria from the culture by a spatula

- Put into a piece of blotting paper to prevent slipping of the material

- Embedding in paraffin, GMA or epoxy

- Further staining procedures (including H&E, Giemsa and FF staining), immunohistochemical investigations and examination using the transmission electron microscope were performed as described above for the tissue sections.

The same procedures as applied to materials from the diseased cattle were performed on the positive control material.

3.2.5. Measuring of the Mean Diameter of the Granulomas and Statistical T-Test

A total of 668 granulomas were measured, 251 and 417 granulomas presented pattern I and pattern II, respectively. The mean diameters of the granulomas were analysed using Ferret's diameter methods (Videoplan® image analysis system, Zeiss-Kontron, Erding) using colour prints of macroscopic pictures of affected organs. The mean diameter values were compared using T-test program of the Microsoft Office Excel 2007 program.

4. RESULTS

4.1. Materials

4.1.1. Numbers of Investigated Animals

Post-mortem investigations were performed on 241 cattle with suspected bovine tuberculosis (bTB), on the basis of a positive dermal tuberculin test. They were examined for the presence of macroscopic lesions compatible with bTB. Tissue samples were collected from the cattle with tuberculous lesions for detailed histological and bacteriological investigations.

4.1.2. Cattle Diagnosed with Bovine Tuberculosis

Eighty-four out of 241 necropsied animals showed macroscopic lesions, which were compatible with tuberculosis. The collected tissue samples for bacteriological investigation were submitted to the 'Bayerisches Landesamt für Gesundheit und Lebensmittelsicherheit' in Oberschleissheim. Bovine tuberculosis was confirmed by the bacteriological detection of *M. caprae* in the investigated herds.

4.1.3. Distribution and Quantification of Macroscopic Lesions in the Examined Organs

Collected tissue samples consisted of lung, liver, small intestine, their regional lymph nodes and the retropharyngeal lymph nodes. The quantity of the affected organs is demonstrated in Table 4.

In lungs, the lesions occurred in different lobes. There was only one lobe in which the pleura was also affected.

Similarly affected livers showed lesions in their different lobes and in one case the peritoneum was affected, too. The small intestine showed a focal lesion in the ileum on the edge of a Peyer's patch. In lymph nodes, lesions were observed both in the cortical and medullary zones.

Table 4. Number of affected organs in 84 animals.

Lung	11
Mediastinal lymph node	20
Small intestine	1
Mesenterial lymph node	63
Liver	5
Portal lymph node	11
Retropharyngeal lymph node	6

4.2. Investigations on Positive Control Material

The positive control slides were prepared using cultivated *M. bovis* BCG and *M. kansasii* provided by the Institute for Infectious Diseases and Zoonoses. The main purpose for the positive control material was to demonstrate that the immunohistochemistry against mycobacterial antigen works reliably.

4.2.1. Paraffin Sections

All paraffin sections of the positive control material were stained with H&E, Giemsa, and the acid-fast staining according to Fite-Faraco (FF staining). Mycobacteria were detected on the top surface and slightly in the inner side of the agar medium. Acid-fast rods appeared as pink-reddish, purple and red in H&E, Giemsa and FF staining, respectively. The positive immunohistochemical reaction presented as dense brown spots in the same localisation as seen in other staining methods (Fig. 1). The bacteria were displayed light purple by ISH, but the reaction was only weakly positive.
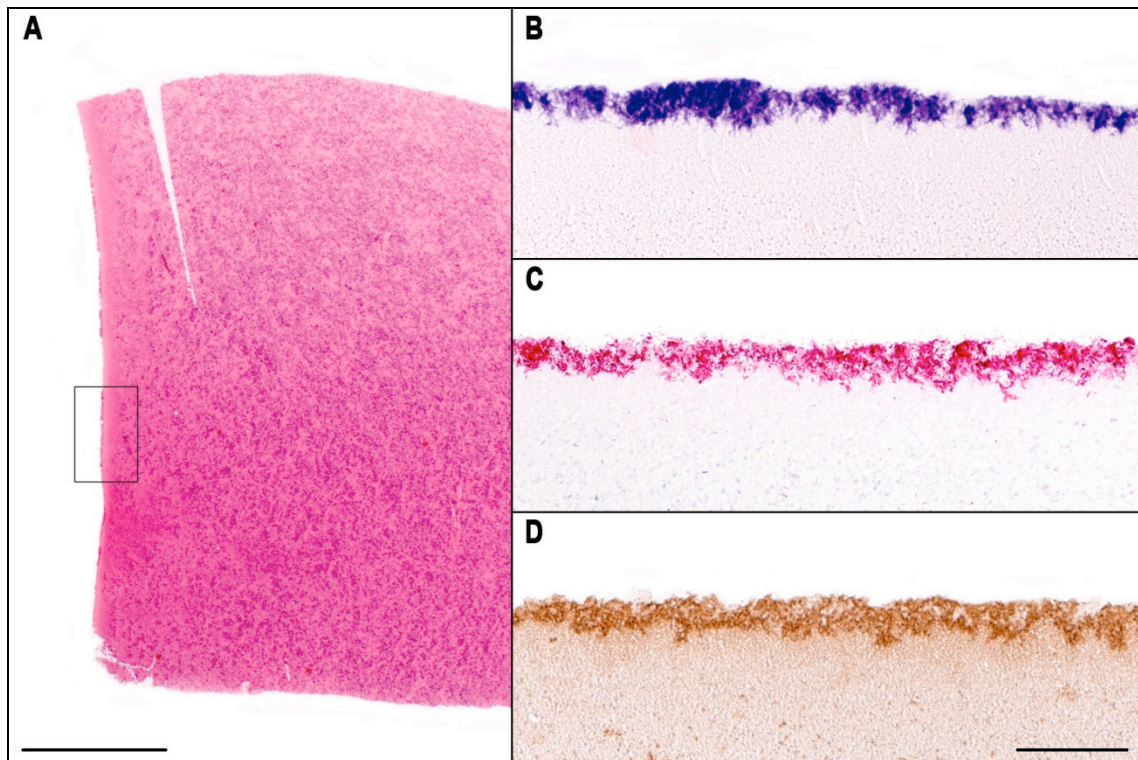
Figure 1. *M. bovis* positive control. Paraffin section:
A: Overview of H&E staining. Right: Higher magnification of the square, bacilli can be recognized (B) in Giemsa staining (purple), (C) in FF staining (red), (D) in immunohistochemistry for mycobacterial antigen (dark brown reaction); E 2245/14; bars in A = 1 mm, B, C and D = 50 µm.

4.2.2. Plastic (GMA) Sections

H&E and Giemsa staining were performed for plastic (GMA) sections and the bacilli were detected in red and purple colours on the top surface and slightly on the inner side of the agar medium (Fig. 2).
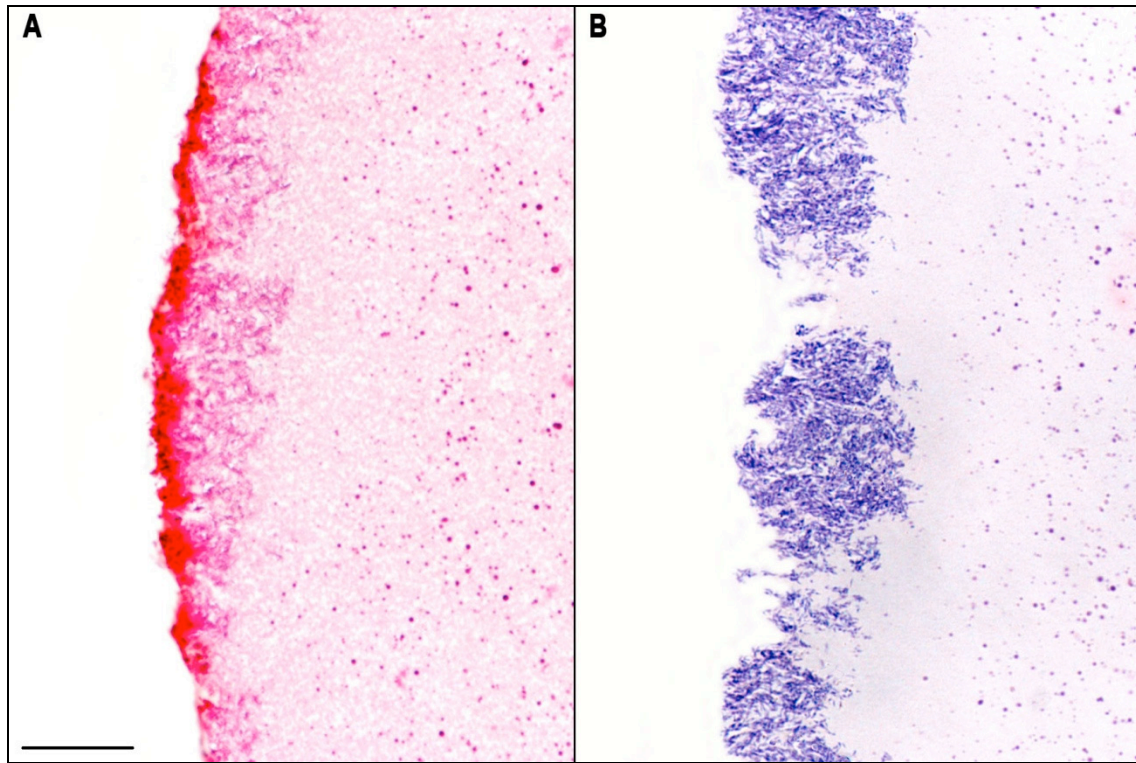
Figure 2. *M. bovis* positive control. GMA section:
A: H&E staining, bacilli can be seen. B: Giemsa staining, bacilli can be seen purple in the same area;
E 2245/14; bars in A and B = 25 µm.

4.2.3. Semi-thin Sections

On the semi-thin sections, toluidine blue-safranin staining and IHC against mycobacterial antigen were performed. The rod-shaped bacteria appeared in red colour. They were found scattered within the agar medium. The mycobacterial antigen was demonstrated as compact, dark brown spots at the same localisation as in the toluidine blue-safranin staining (Fig. 3).

4.2.4. Transmission Electron Microscopy (TEM)

The ultra-sections of the acid-fast bacilli were investigated using TEM. Longitudinal and cross sections of bacteria are demonstrated in the Figure 4.
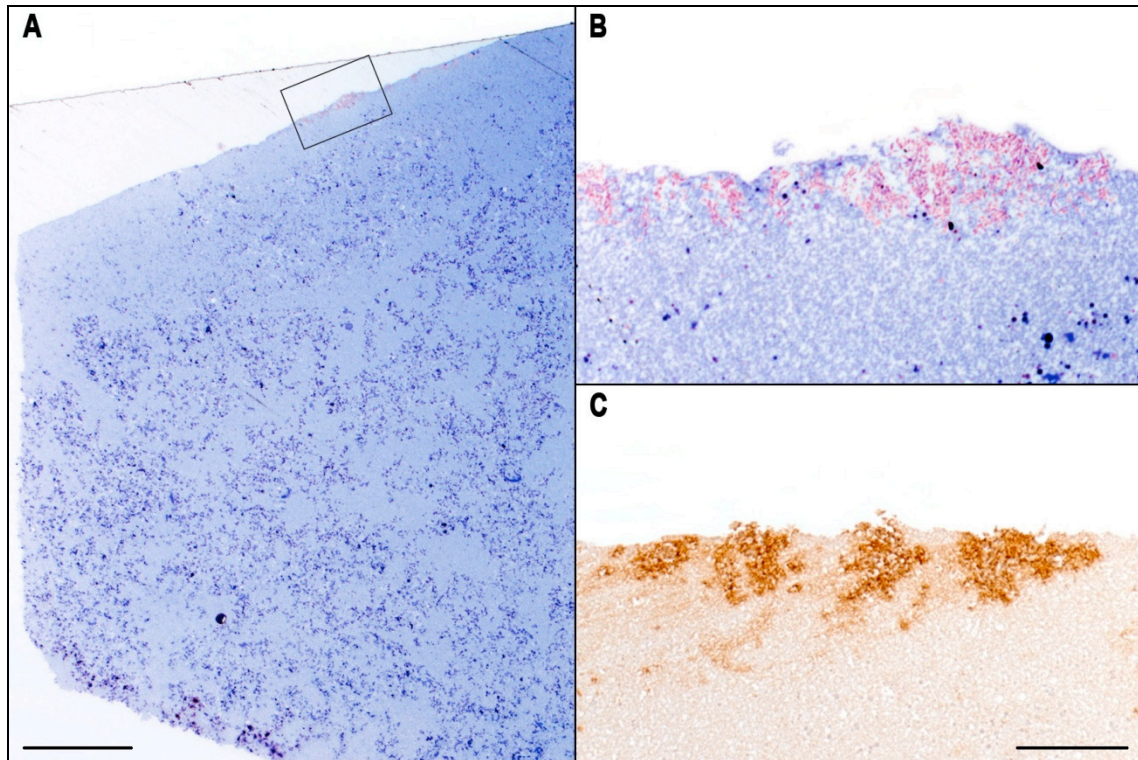
Figure 3. *M. bovis* positive control. Semi-thin section:
A and B: Toluidine blue-safranin staining. C: Bacilli can be recognized in anti-mycobacterium immunohistochemistry (dark-brown positive reaction); E 1588/14; bars in A = 200 µm, B and C = 25 µm.
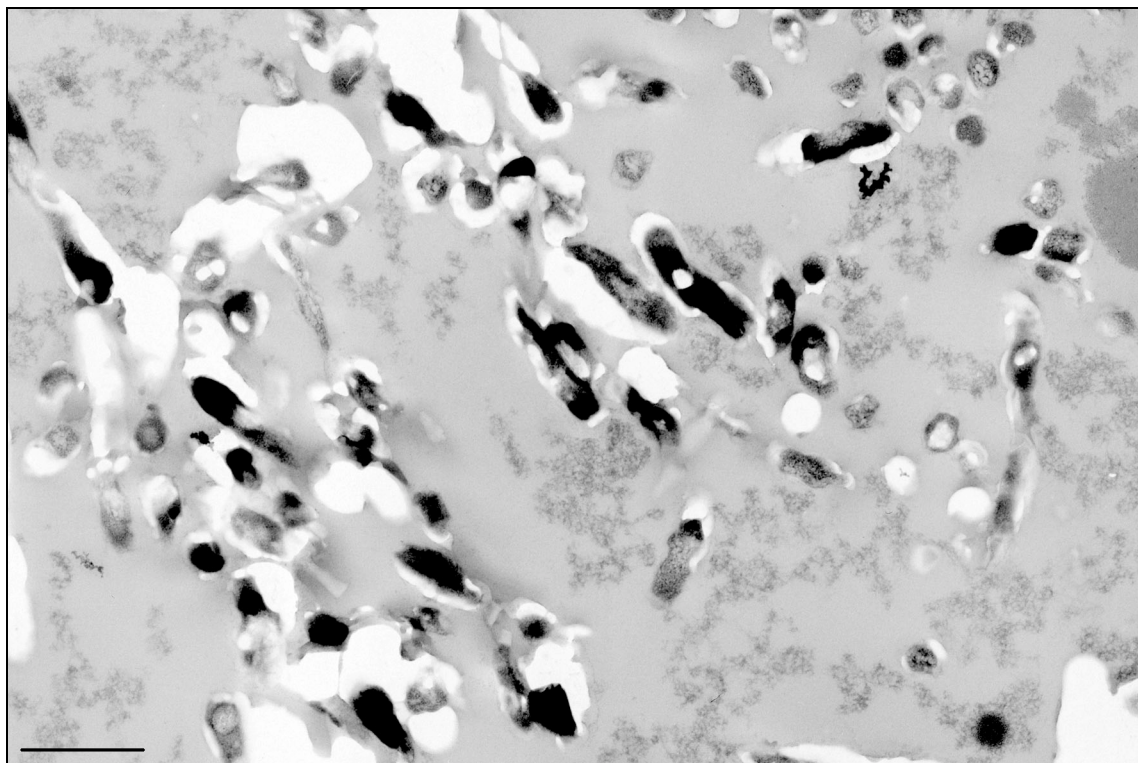
Figure 4. Longitudinal and cross sections of *M. bovis* BCG in TEM.

4.3. Investigations on Material of Cattle with Bovine Tuberculosis

4.3.1. Macroscopic Findings of Bovine Tuberculosis

The macroscopic appearance of the tuberculous lesions could be classified into five patterns according to three measurements, i. the macroscopically visible components of the inflammation (yellowish caseous necrosis with or without calcification, light brown areas of inflammation, greyish fibrous tissue), ii. the arrangement of these components (concentric layering of the three components or an unordered arrangement within the affected organ), and iii. the number and size of the tuberculous foci. The lungs showed additional macroscopic features (liquefying necrosis and cavitating tuberculosis), which were described separately. The study of RIESEBERG (2016) has also described macroscopic patterns; these patterns were revised and additionally compared with the histologic alterations in this study.

4.3.1.1. Patterns of Macroscopic Alterations

4.3.1.1.1. Pattern I

This pattern occurred as solitary or rarely multiple roundish foci measuring between 0.5 and 2.4 cm in diameter (Fig. 5 and 6). These foci were characterised by the presence of three concentric layers on the cut section. The two outer layers were the most prominent in large lesions. The centre was yellowish, dry, eventually greasy and showed white-yellowish irregular foci, which crepitated during cutting. Adjacent, there was a narrow light brown zone with scattered small pale foci, surrounded by the outer large whitish-grey zone.

In addition to the macroscopic view the histological overview showed that the centre consisted of caseous necrosis with irregular calcified foci; followed by a middle layer of inflammatory cell infiltration, and an outer fibrous capsule.
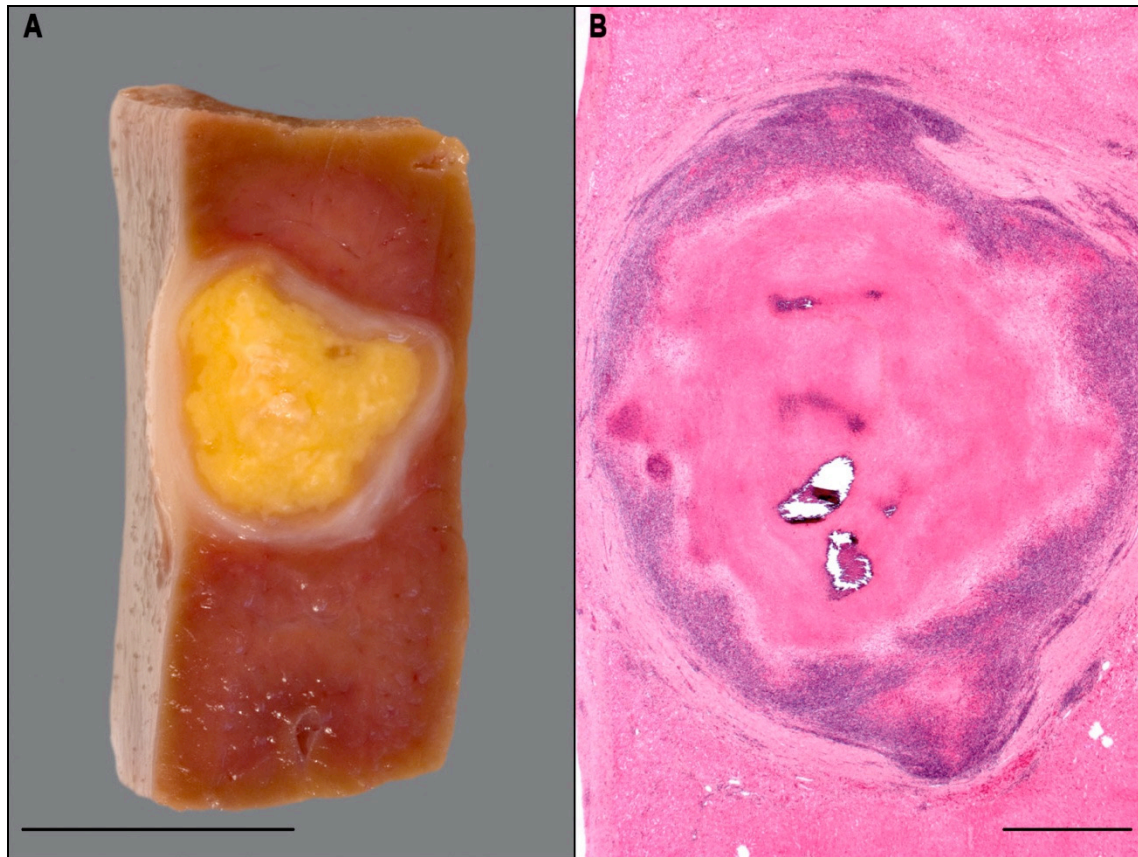
Figure 5. Macroscopic pattern I of bovine tuberculosis:
A: Macroscopy; focal, roundish, tuberculous granuloma (tubercle) with a yellow, dry centre with yellowish to white irregular foci, surrounded by a narrow light brown zone, and an outer large, whitish-grey zone (the organ was fixed in Klotz´s solution). B: Histology; central necrosis with calcification, surrounded by inflammatory cells and a capsule of fibrous connective tissue; liver, E 110/09, H&E (GMA); bars in A = 1cm, B = 1 mm.
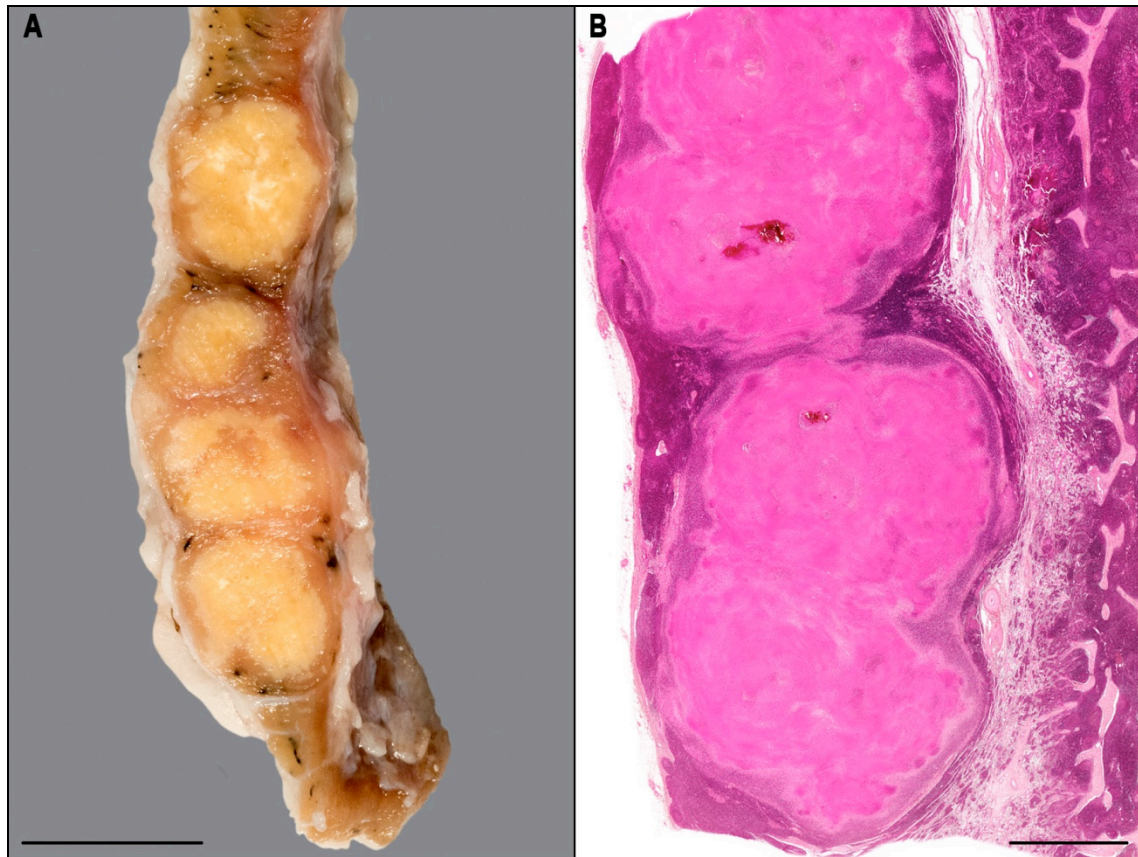
Figure 6. Macroscopic pattern I of bovine tuberculosis:
A: Macroscopy; multifocal, roundish tuberculous granulomas (tubercles) with a yellow, dry centre with yellowish to white irregular foci, surrounded by a narrow light brown zone and an outer whitish-grey zone (the organ was fixed in Klotz´s solution). B: Histology; central necrosis with calcification, surrounded by inflammatory cells and a capsule of fibrous connective tissue; mediastinal lymph node, E 110/09, H&E (Paraffin); bars in A = 1 cm, B = 2 mm.

4.3.1.1.2. Pattern II

The form and organisation of the foci in pattern II was similar to the foci in Pattern I. In contrary to pattern I, they occurred generally multifocal (on the sectional surface up to 124 foci) and the foci were smaller than the foci of pattern I with up to 0.5 cm in diameter (Fig. 7). Histologically, the same layering was visible as seen in pattern I. Pattern I and II could be distinguished only by the size and number of foci. This was confirmed by measuring large number of foci in cases from both patterns (see 4.3.4).
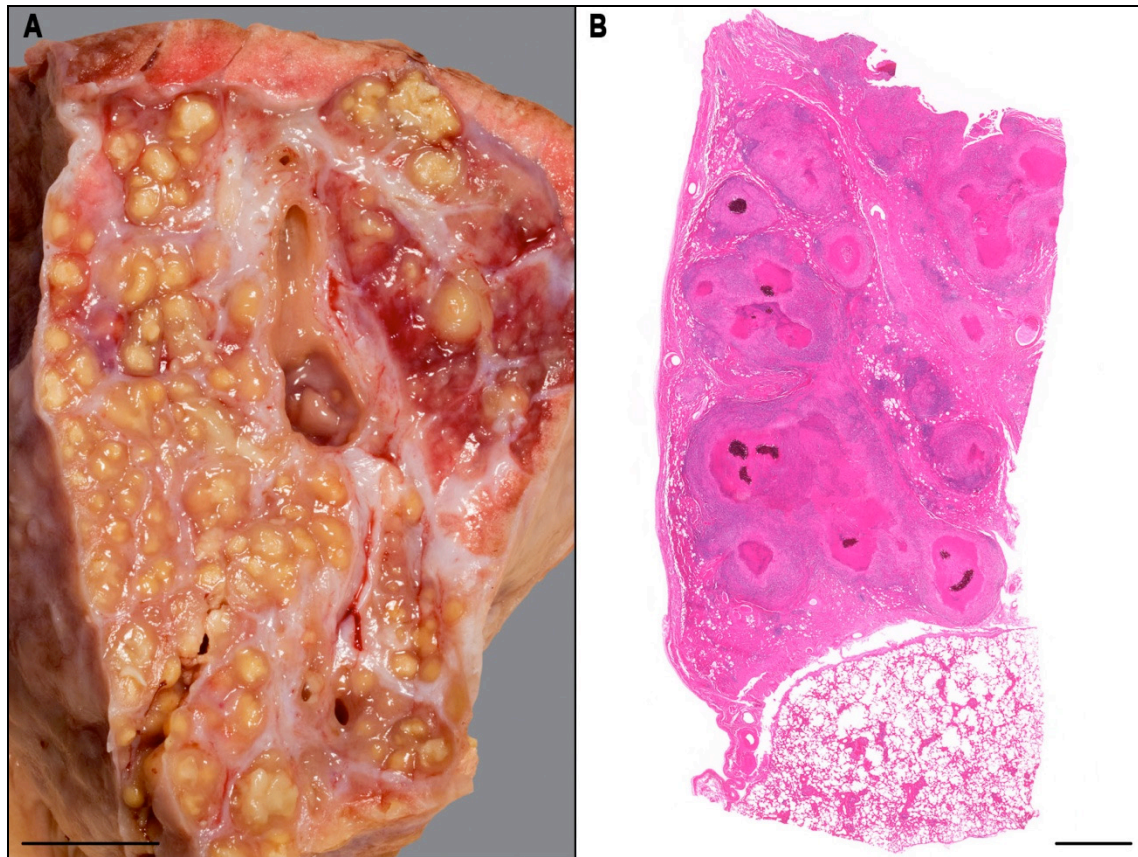
Figure 7. Macroscopic pattern II of bovine tuberculosis:
A: Macroscopy; small, multifocal yellowish circumscribed granulomas (tubercles) (the organ was fixed in Klotz´s solution). B: Histology; regular layers of multiple typical tubercles; lung, S 605/13, H&E (Paraffin); bars in A = 1 cm, B = 2 mm.

4.3.1.1.3. Pattern III

Macroscopic lesions classified under this pattern had not a clearly layering structure in comparison with patterns I and II. Frequently, large areas of the organ (lung) or the complete cut surface (lymph nodes) were altered. The lesions consisted of irregularly formed pale foci (Fig. 8) or the cut surface was completely greasy-yellow with intercalated pale, not well distinguishable foci (Fig. 9). Histologically, there was a disorderly coexistence of caseous necrosis, lymphocyte aggregates, and an irregularly formed fibrosis.
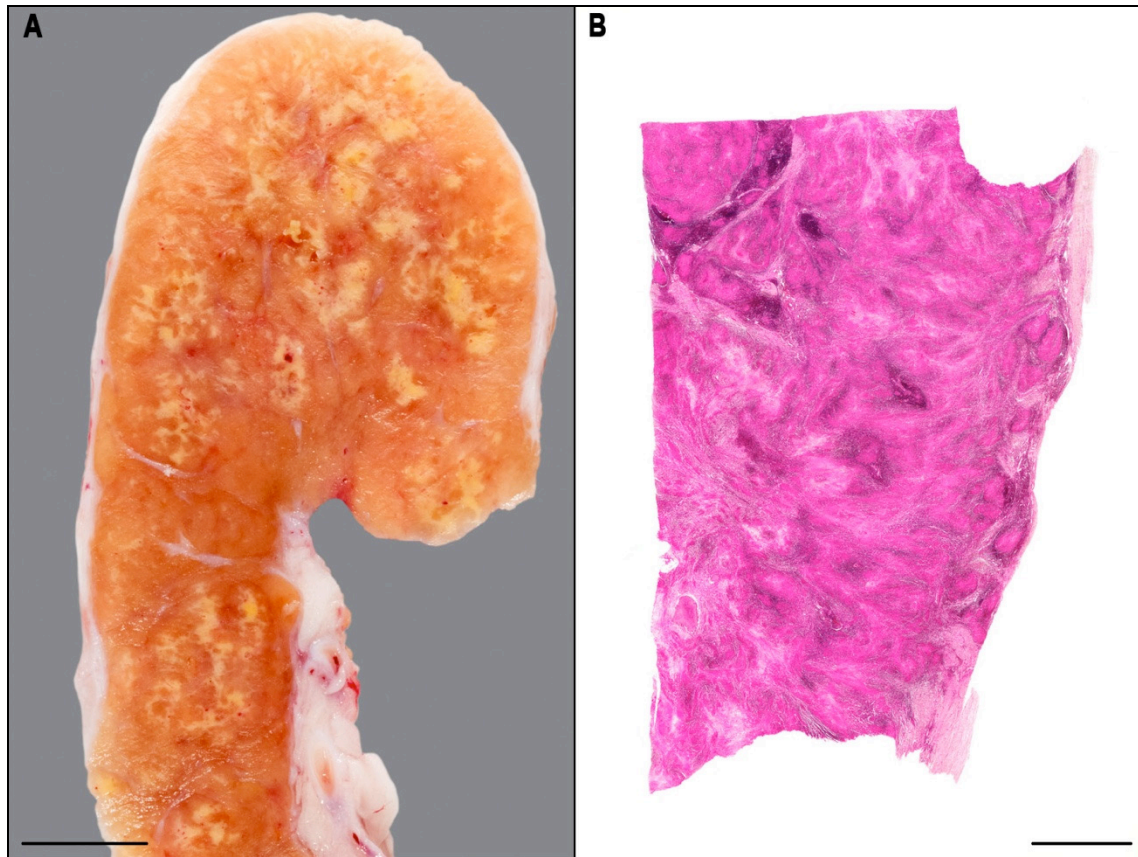
Figure 8. Macroscopic pattern III of bovine tuberculosis:
A: Macroscopy; greasy-yellowish cut surface with multiple irregularly formed, yellow foci (the organ was fixed in Klotz´s solution). B: Histology; necrosis, inflammatory infiltrates and fibrous tissue irregularly intermingled without a regular layering; mediastinal lymph node, E 108/09, H&E (Paraffin); bars in A = 1 cm, B = 2 mm.
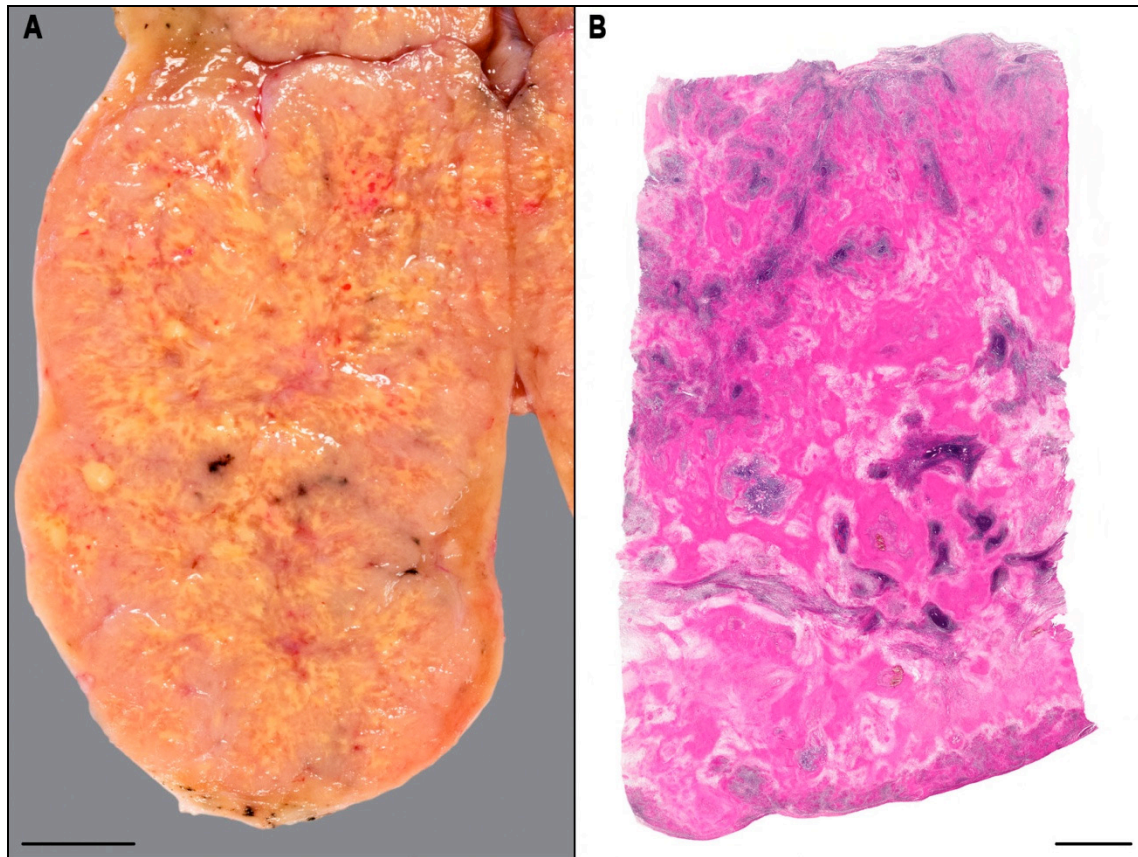
Figure 9. Macroscopic pattern III of bovine tuberculosis:
A: Macroscopy; the whole cut surface consisted of irregular yellow and light-grey foci (the organ was fixed in Klotz´s solution). B: Histology; unregular accumulations of necrosis, inflammatory cells and fibrous tissue; mediastinal lymph node, E 322/09, H&E (Paraffin); bars in A = 1 cm, B = 2 mm.

4.3.1.1.4. Pattern IV

Pattern IV was characterised by the extent of the lesion. Frequently, the entire cut surface of the lymph node was altered (Fig. 10). The lesion consisted predominantly of the caseation. The middle and the outer layers of the typical tubercles were clearly smaller than in pattern I or not discernible.
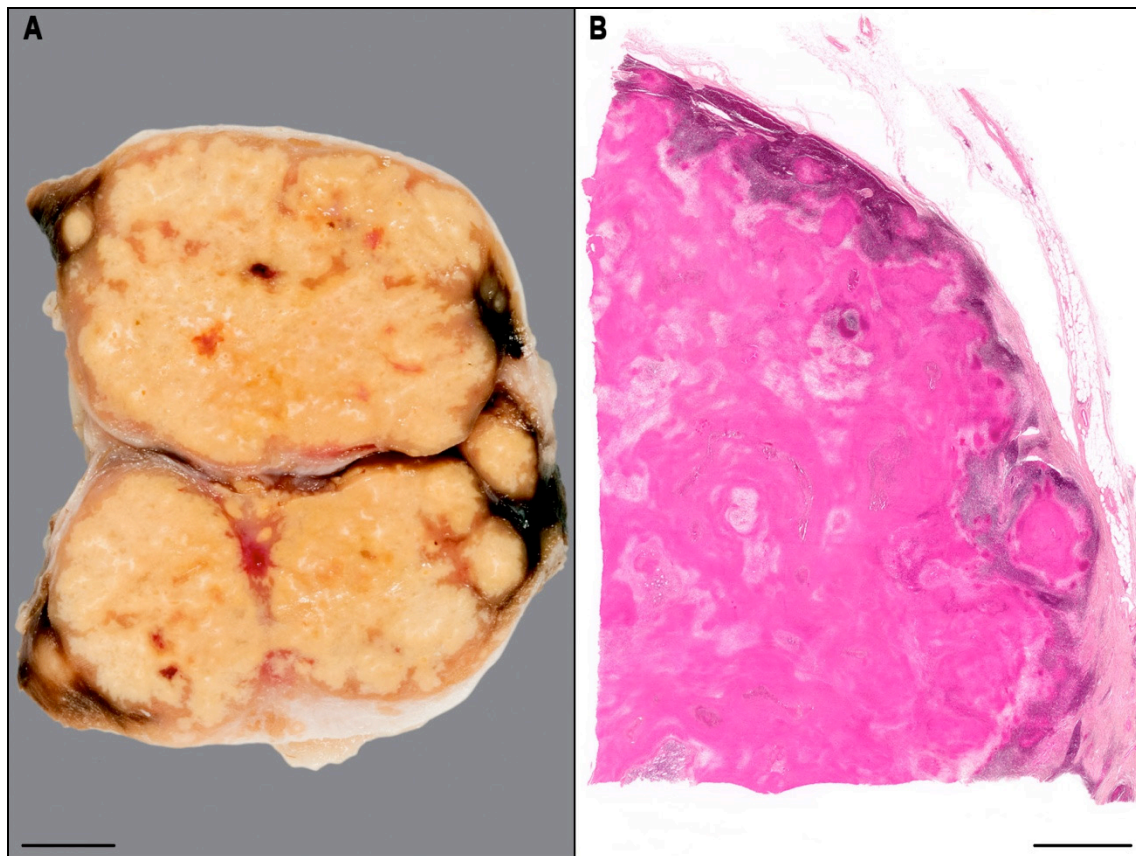
Figure 10. Macroscopic pattern IV of bovine tuberculosis:
A: Macroscopy; yellow, well-circumscribed foci of caseating necrosis with a thin capsule of light brown tissue. B: Histology; predominant necrosis, surrounded by a small layer of inflammatory cells and fibrous tissue; mesenterial lymph node, E 110/09, H&E (Paraffin); bars in A= 1 cm, B = 2 mm.

4.3.1.1.5. Pattern V

This pattern occurred generally in combination with pattern I. Main feature of this pattern was the formation of cavities caused by liquefaction of the caseated tissue (cavitating tuberculosis) (Fig. 11). The histological overview showed remnants of caseous necrosis adjacent to a central cavity surrounded by an extensive accumulation of inflammatory cells consisting predominantly of neutrophilic granulocytes. Discrete infiltrates of other inflammatory cells were visible in the lesion periphery (Fig. 11).
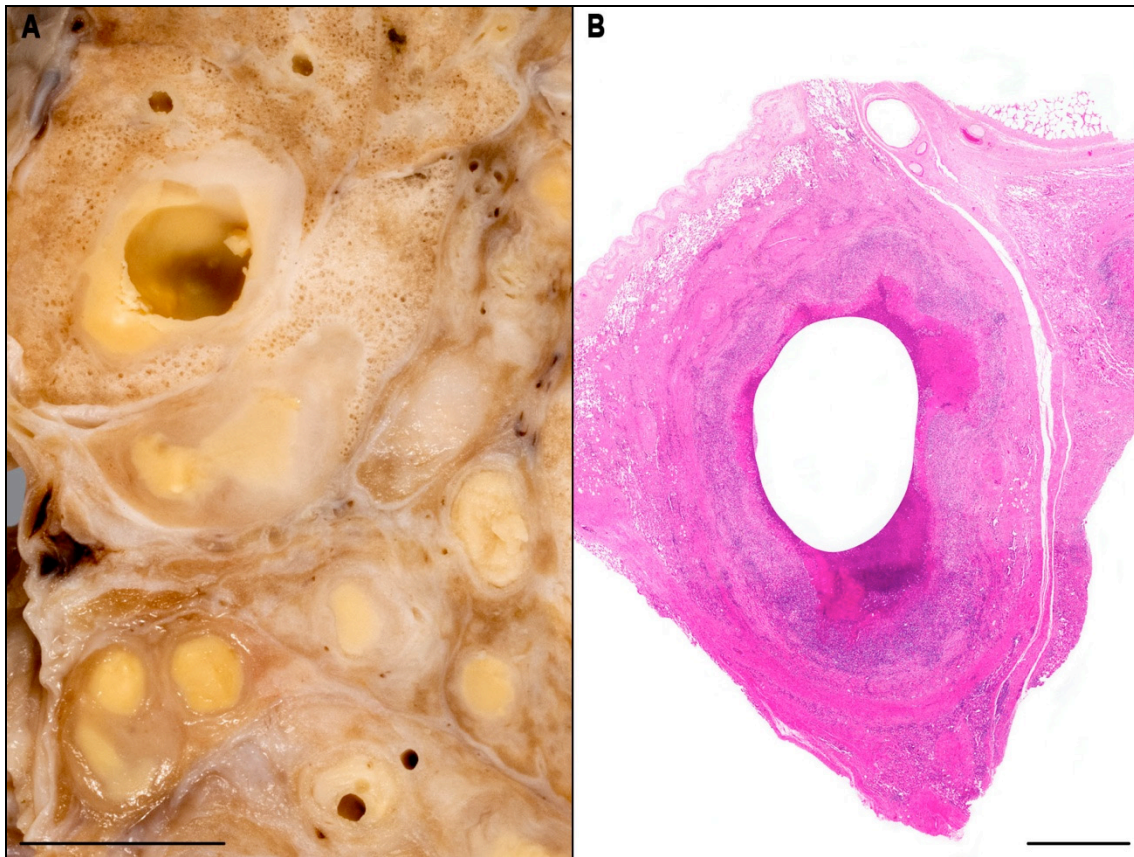
Figure 11. Macroscopic pattern V of bovine tuberculosis:
A: Macroscopy; multiple, roundish, yellowish tubercles, some of them with cavities. B: Histology; a central cavity surrounded by caseous necrosis, inflammatory cell infiltrations and fibrous tissue with layer formation; lung, S 770/13, H&E (GMA); bars in A = 1 cm, B = 1 mm.

4.3.1.1.6. Lung – Additional Macroscopic Alterations (Macroscopic pattern VI)

In the lung, a further pattern of alterations could be found in addition to the five macroscopic patterns described above (Fig. 12). Individual lung lobules or parts of lung lobules were showing a brown discoloration with irregular yellowish foci. The surface was moister than the surrounding lung area. Severe alveolar oedema with focal acute degeneration of lung parenchyma was obvious in the histological overview.
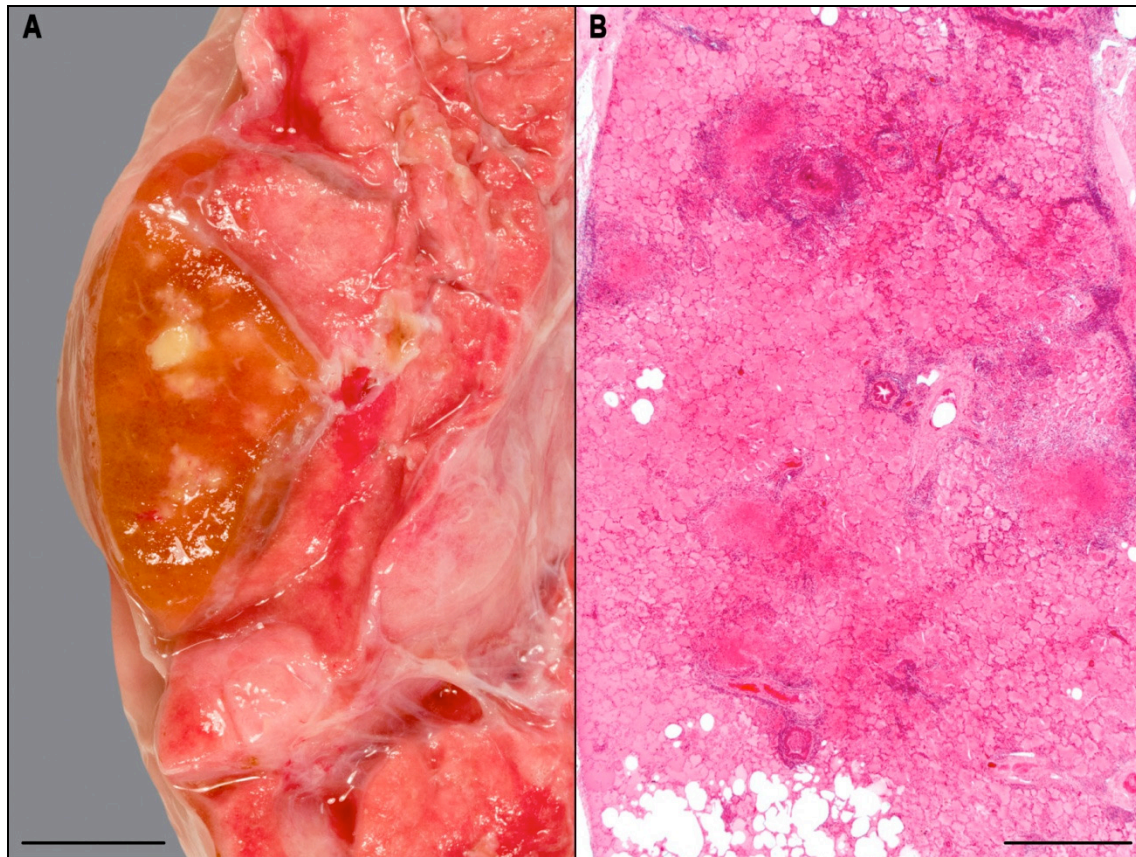
Figure 12. Macroscopic pattern VI of bovine tuberculosis:
A: Macroscopy; individual lobule with brownish discoloration and small yellow, irregular formed foci (the organ was fixed in Klotz´s solution); E323/09. B: Histology; severe alveolar oedema, oligofocal inflammatory cell infiltrates and necrotic areas; lung, E 322/09, H&E (GMA); bars in A = 1 cm, B = 1 mm.

4.3.1.2. The Differentiation of Macroscopic Pattern I and II

Although there was a striking difference in the size of the foci between macro-patterns I and II at the macroscopic point of view, this distinction could not be well determined in the histological investigations. For that reason, this question was analysed using t-test method in Excel-07. The null hypothesis was 'pattern I is equal in diameter to pattern II'. The mean diameter values of each tuberculous granuloma of both patterns were measured. These mean diameter values were listed under pattern I and II in Excel-07. The calculated t-value showed that the probability of the null hypothesis was extremely low. Thus, it could be proved that there was a significant difference in diameter between patterns I and II.

4.3.1.3. Quantification of the Macroscopic Patterns

The macroscopic lesions from 76/84 animals were evaluated previously, as seen in the study of Rieseberg (RIESEBERG, 2016).

In the present study, the macroscopic lesions were revaluated and two of them were re-classified. The total numbers of macroscopic patterns are demonstrated in Table 5.

Table 5. The total numbers of macroscopic patterns seen in the organs affected by tuberculosis.

Pattern I	23
Pattern II	14
Pattern III	42
Pattern IV	4
Pattern V	7

4.3.1.4. Organ Distribution of the Macroscopic Patterns

The numbers of patterns detected in each organ are summarized in Table 6. The macroscopic lesions of the lungs and the lymph nodes showed different patterns. All liver samples and the intestinal sample were compatible with pattern I.

Table 6. The distribution of the five macroscopic patterns in the individual organs.

Organ	Pattern I	Pattern II	Pattern III	Pattern IV	Pattern V
Lung	4	2	1	-	3
Mediastinal lymph node	3	4	7	-	1
Small intestine	1	-	-	-	-
Mesenterial lymph node	9	5	33	4	2
Liver	2	-	-	-	-
Portal lymph node	2	-	2	-	-
Retropharyngeal lymph node	2	2	-	-	1

4.3.1.5. Possible Routes of Infection

On the basis of the distribution of the lesions in the different organ systems, possible routes of transmission (portal of entrance) were determined. Lesions restricted to the gastrointestinal tract including intestine, mesenterial lymph nodes, liver and portal lymph nodes were defined

to the originate from the alimentary infection route. Lesions restricted to the respiratory tract including lung and mediastinal lymph nodes were defined to reflect an aerogen transmission type. All combinations of lesions in the gastrointestinal tract, the respiratory tract and other organs were defined to display combination of the aerogen and alimentary transmission route.

A total of 68%, 19% and 13% of animals acquired tuberculosis via alimentary, aerogen, and via both transmission ways, respectively.

4.3.2. Histological Findings of Bovine Tuberculosis

4.3.2.1. Components of Tuberculous Granulomatous Inflammation

All tissue samples showing macroscopic lesions were examined for histopathological diagnosis (in a pre-study tissue samples from macroscopically unaltered organs were examined histologically, no lesions pointing to an infection could be found). The diagnostic inclusion criterion was the presence of a granulomatous inflammation, as a possible sign for bovine tuberculosis. Histological diagnoses were evaluated through H&E, Giemsa, Masson´s trichrome, and Silver staining methods. In addition, immunohistochemical methods were utilized to determine the type of cells and their localisation within the lesions.

The granulomatous inflammation seen in the tissue sections was principally composed of macrophages (epithelioid cells), commonly accompanied by multinucleated giant cells (MNGC) of the so-called Langhans-type. The other components of a tuberculous inflammation consisted of a caseous necrosis with or without amorphous multiple calcified foci, infiltration of neutrophilic polymorphonuclear granulocytes, lymphocytes, plasma cells, and fibrous tissue proliferation. These components were found mostly together within a granuloma, but sometimes epithelioid cells and/or MNGCs were the only participants.

Tuberculous granulomatous inflammation showed distinct histological appearances, similarly as seen macroscopically (see 4.3.1.1.). Histological lesions were characterised by two main types epithelioid cell granulomatous inflammation and tubercles containing the cytological components described above. Granulomas (tubercles) occurred as solitary, multiple or coalescent foci.

Epithelioid cell granulomatous inflammations were seen as small or large clusters of epithelioid cells and commonly MNGCs. Epithelioid cell granulomatous inflammations could also be associated with an encapsulation by thin fibrous connective tissue or a small central necrotic area often associated with a small number of neutrophils.

The components of the tuberculous inflammation appeared mainly either in a concentric layering or in an irregular arrangement. In the first type central caseous necrosis with calcification was surrounded by neutrophils, epithelioid cells, and MNGCs as the first zone of the inflammatory reaction, which was then followed by lymphocytes and smaller numbers of plasma cells. The outer layer was characterised by an encapsulation with fibrous connective tissue. In the second histological type, the components are arranged in a totally unordered manner.

The characteristic features and localisations of the components within a tubercle structure were described in the following:

4.3.2.1.1. Caseous Necrosis and Calcification

Caseation was a special form of coagulation necrosis typical for tuberculosis. The characteristic feature for caseation should be its relatively high lipid content. Macroscopically, the caseation was a pale, yellowish, solid elastic, dry material with fatty gloss. Histologically, the caseation represented as almost amorphous, distinct eosinophilic mass. A caseation could occur in various types of the tuberculous inflammation: in the epithelioid cell granulomatous inflammation, in the classical tubercle, with in fibrous foci, and in the acute tuberculous inflammation of the lung.

In the epithelioid cell granulomatous inflammation, caseation could occur in the centre of the foci (Fig. 13). It could not be determined, whether the occurrence of the caseation depended on a particular size of the foci, because no serial sections were prepared. Thus, in areas with numerous foci caseation could be found in individual tubercles only (Fig. 13 A), while others were found as solid cell accumulations. The size of the caseation could only be estimated in relation to the size of the entire focus (Fig. 13 B and C). A pale border around a caseation in H&E stainings pointed commonly to a fatty degeneration of the epithelioid cells (Fig. 13 B and C). But a sudden change of intact cells to caseation occurred, too (Fig. 13 D).
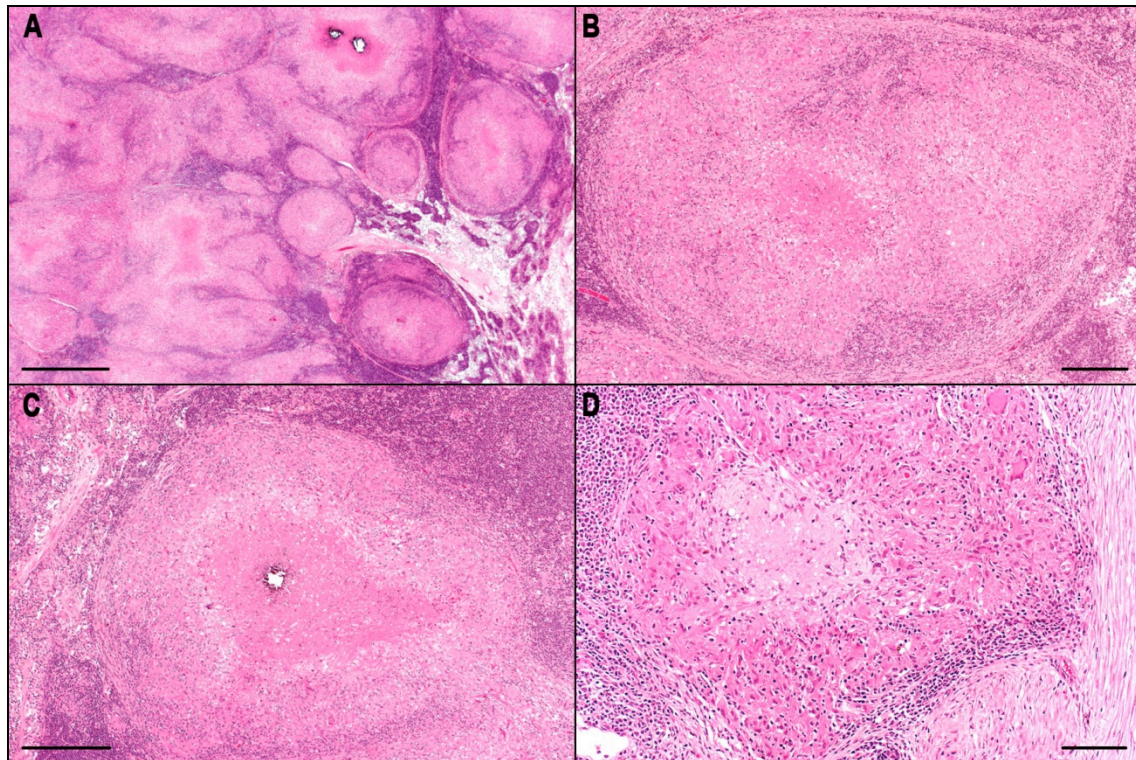
Figure 13. Caseation and calcification in bovine tuberculosis:
A: Numerous foci with epithelioid cell granulomatous inflammation; central caseation is found in several foci, the other foci consist only of intact cells; mesenterial lymph node, S 413/14, H&E (GMA). B: Focal epithelioid cell granulomatous inflammation with central caseation; a pale rim of fatty degenerated epithelioid cells surround immediately the caseation; mesenterial lymph node, S 413/14, H&E (GMA). C: Focal epithelioid cell granulomatous inflammation with extensive central caseation and a beginning calcification; again with a pale rim of fatty degenerated epithelioid cells; mesenterial lymph node, S 413/14, H&E (GMA). D: Focal epithelioid cell granulomatous inflammation, the border between the caseation and the intact epithelioid cells is clearly demarcated, there is no indication of fatty degeneration; mesenterial lymph node, E 97/09, H&E (GMA); bars in A = 1 mm, B and C = 200 μm, D = 100 μm.

The central caseation was the main component in large classic tubercles (Fig. 14 A). Mostly, the outer line of the caseation was not completely round; the cause is explained below (see 4.3.2.2.). Foci of calcification could occur in the caseation (see below and Fig. 14 A). Commonly, fatty degenerated epithelioid cells were found adjacent to the caseation (Fig. 14 B and C). Despite the apparent amorphousness of the caseation in the H&E section, different amounts of fiber remnants could often be detected in the Silver staining (Fig. 14 D), which could point to a previously existing fibrous capsule.
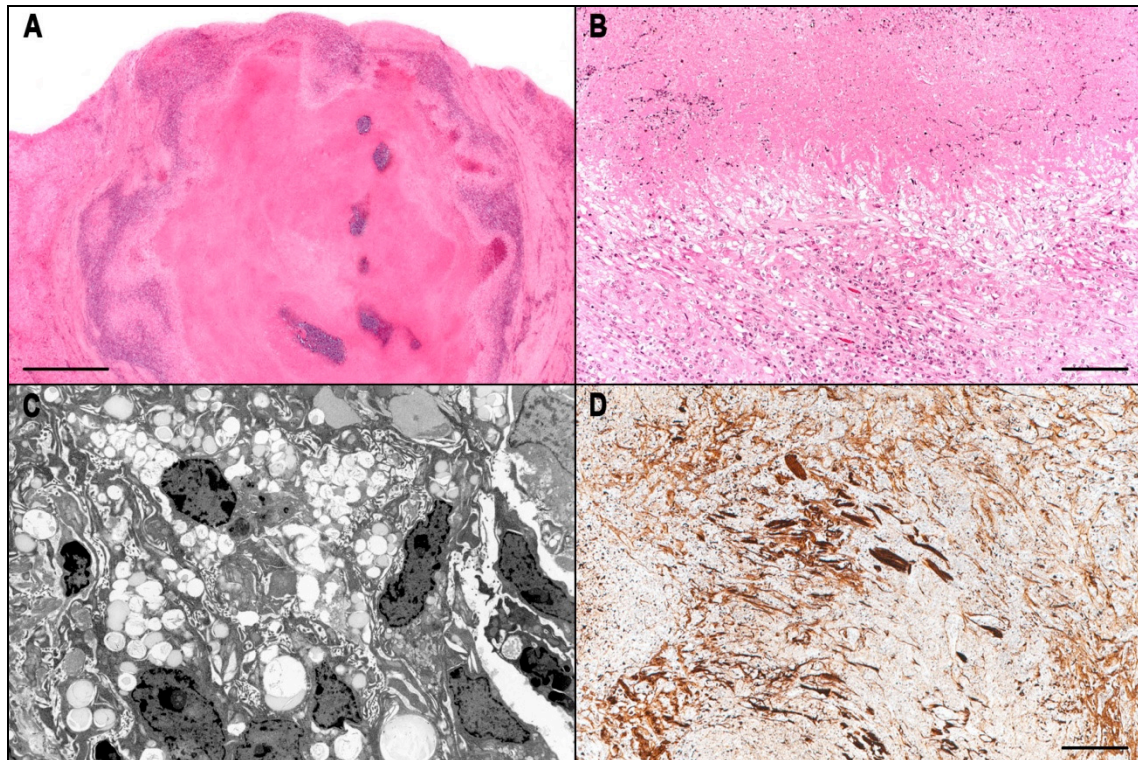
Figure 14. Caseation and calcification in bovine tuberculosis:
A: Typical tubercle with extensive central caseation and multiple foci of calcification; the outer line of the caseation is irregularly formed; a pale rim of fatty degenerated epithelioid cells immediately around the caseation; liver, E 110/09, H&E (GMA). B: Band of fatty degenerated epithelioid cells between the central caseation (above) and intact epithelioid cells and lymphocytes (below); mesenterial lymph node, S 413/14, H&E (GMA). C: Ultrastructure of epithelioid cells with marked accumulation of lipid droplets in the cytoplasm; the cells show numerous finger-like projections of the cell membrane, typical for epithelioid cells; mesenterial lymph node, E 325/09, TEM. D: Remnants of collagen fibres in the centre of an extensive caseation focus; liver, E 110/09, Silver staining (GMA); bars in A = 1 mm, B and D = 100 µm.

The occurrence of caseation in fibrous foci (Fig. 15) was related to an infiltration with inflammatory cells, especially with epithelioid cells (Fig. 15 A). These cells could then undergo caseation (Fig. 15 B) with simultaneous lysis of collagen fibres (see 4.3.2.1.3.).
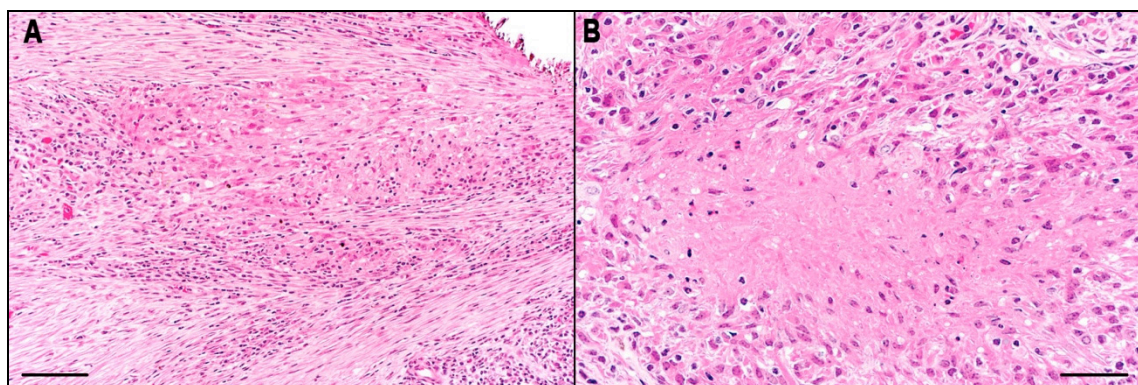
Figure 15. Caseation and calcification in bovine tuberculosis:

A: Infiltration of epithelioid cells and lymphocytes in an extensive fibrosis near a large tubercle (top right calcification); mesenterial lymph node, E 97/09, H&E (GMA). B: Caseation necrosis of the epithelioid cells in fibrous connective tissue; mesenterial lymph node, E 108/09, H&E (GMA); bars in A = 100 µm, B = 50 µm.

The acute inflammation of the lung (Fig. 16) was accompanied by a severe alveolar pulmonary oedema. Foci developed in this oedema that striked by their strong eosinophilia (Fig. 16 A and B). There were only a few inflammatory cells at the beginning; later the infiltration with neutrophils and epithelioid cells appeared, followed by an encapsulation by fibrous connective tissue. In addition to the oedema, fibrin is presumably also involved (Fig. 16 B) in the development of this caseation form. The degree of lung parenchyma destruction was more obvious in Silver staining (Fig. 16 C and D).
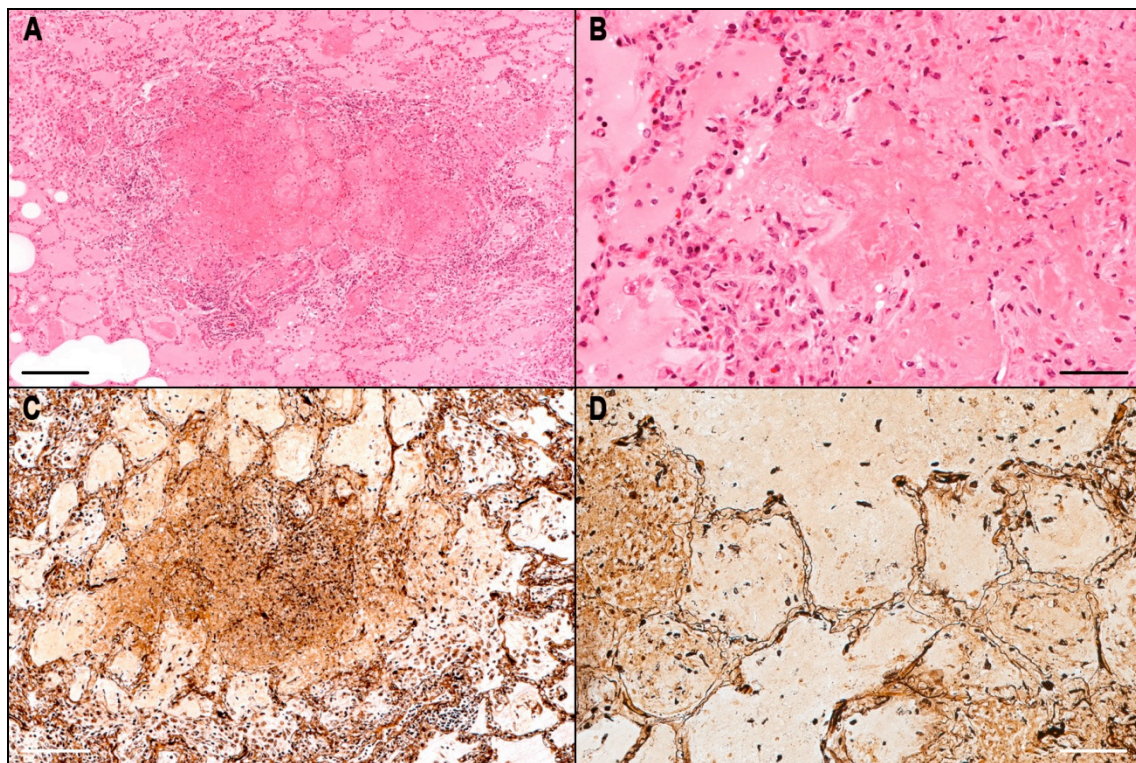
Figure 16. Caseation and calcification in bovine tuberculosis:
A: Acute tuberculous inflammation of the lung, there is a focal necrosis within a severe alveolar pulmonary oedema, the focal necrosis is characterised by its amorphousness and a severe eosinophilia; lung, E 322/09, H&E (GMA). B: At the high magnification, an indistinct layering of the caseation is visible, which possibly develops through deposition of fibrin; the number of inflammatory cells is still few in this early stage; lung, E 322 /09, H&E (GMA). C: The destruction of the lung parenchyma is obvious in the Silver staining; lung, E 322/09, Silver staining (GMA). D: Degeneration of oedematous alveolar septa develops at the borders of the focal necrosis; lung, E 322/09, Silver staining (GMA); bars in A = 200 µm, B and D = 50 µm, C = 100 µm.

In addition to the caseation, calcification (Fig. 17) is also a characteristic process in bovine tuberculosis. Calcification was and is an important diagnostic indication of the presence of

tuberculosis in cattle and man. Foci of calcification occurred within the caseation of tubercles (Fig. 17 A) and in the caseation of the epithelioid cell granulomatous inflammation (Fig. 17 B). The calcifications were often found nearby the tubercle centre. In the epithelioid cell granulomatous inflammation, the calcification developed in the caseation as well (Fig. 17 C), but occasionally the epithelioid cells showed direct calcification (Fig. 17 D) without previous caseation.
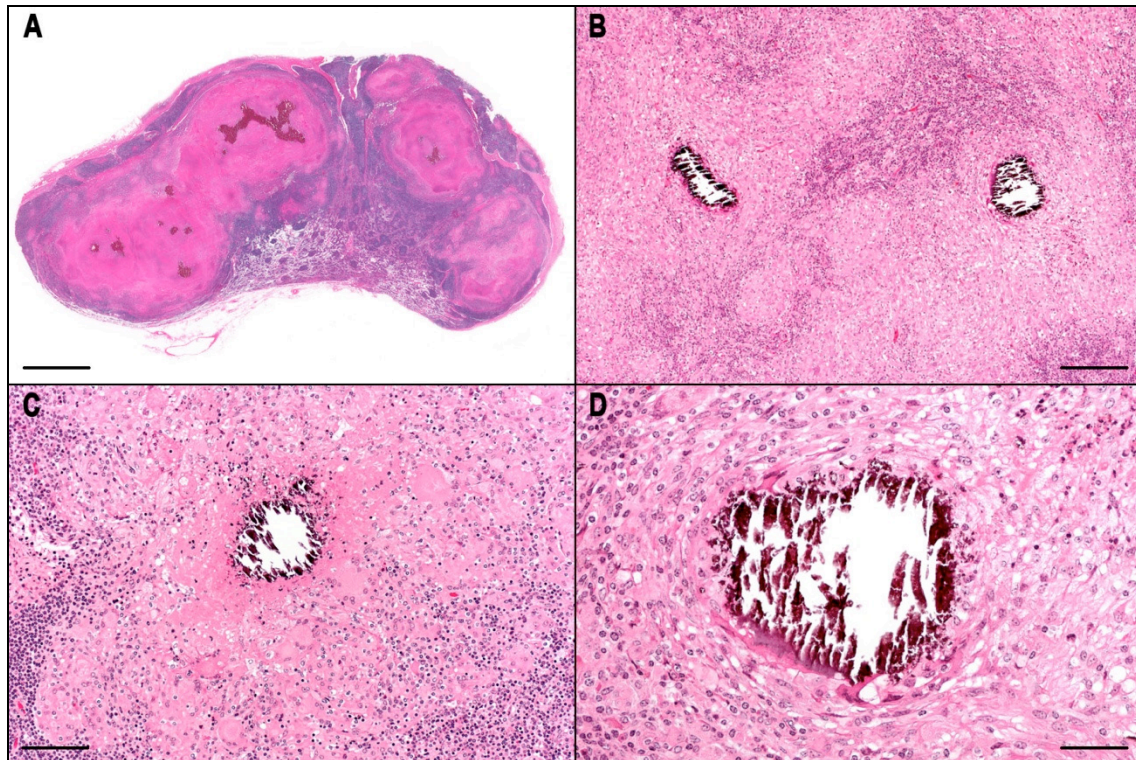
Figure 17. Caseation and calcification in bovine tuberculosis:
A: Several typical tubercles in a lymph node with extensive caseation; the calcificated foci are irregularly formed and are found in the centre of the caseation; mesenterial lymph node, E 113/09, H&E (Paraffin). B: Foci of epithelioid cell granulomatous inflammation with central foci of calcification; the plastic embedded tissue is not decalcified, therefore calcification frequently breaks out during cutting; mesenterial lymph node, S 413/14, H&E (GMA). C: Focal epithelioid cell granulomatous inflammation with caseation and central calcification; mesenterial lymph node, S 602/14, H&E (GMA). D: Focus of epithelioid cell granulomatous inflammation with a direct central calcification of degenerated cells without visible caseation; mesenterial lymph node, S 413/14, H&E (GMA); bars in A = 2 mm, B = 200 μm, C = 100 μm, D = 50 μm.

4.3.2.1.2. Inflammatory Cells

4.3.2.1.2.1. Epithelioid Cells and Multinucleated Giant Cells

Epithelioid cells and multinucleated giant cells are components of the mononuclear phagocyte system (MPS). They are the crucial cells for the classification of an inflammation into the group of granulomatous inflammations.

In tuberculous lesions in cattle, epithelioid cells appeared in two different arrangements. That could be as a component of a classic granulomatous inflammation, in a tubercle (Fig. 18 A and B) or as the predominant participant of the epithelioid cellular granulomatous inflammation (Fig. 18 C and D). Dendritic cells were another relevant cell type for the tuberculous inflammation, but they could not be identified through routine staining.
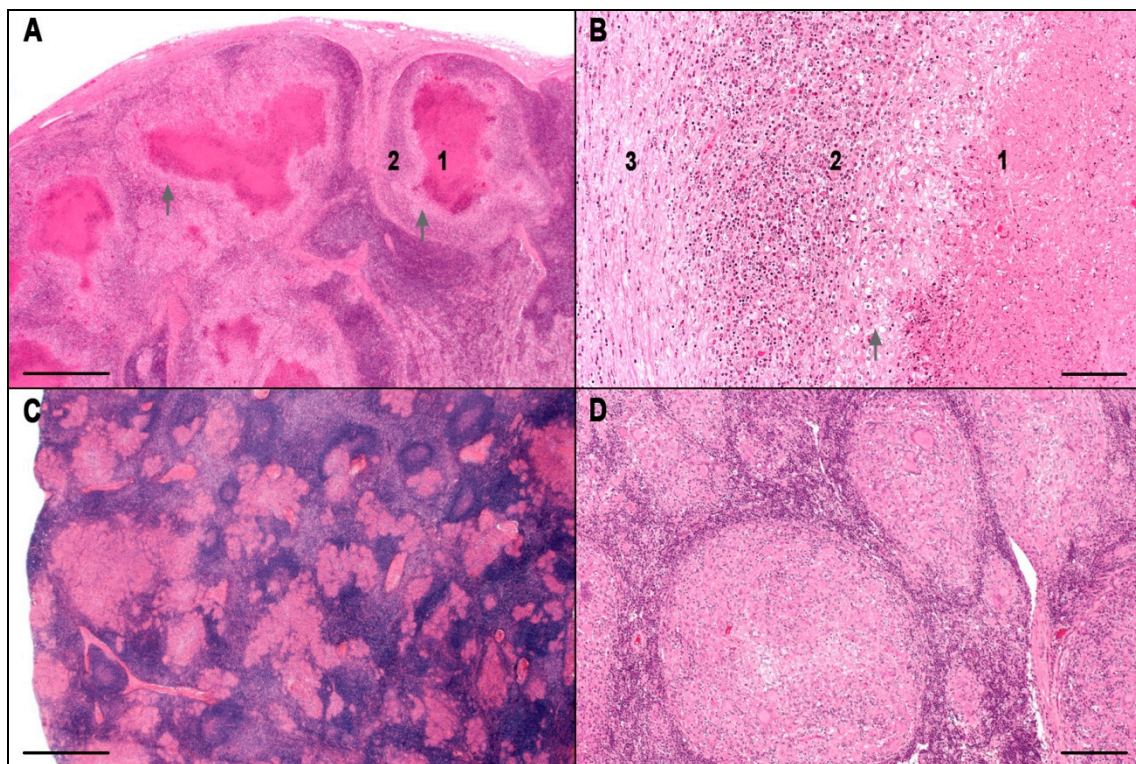
Figure 18. Cytology of epithelioid and multinucleated giant cells in bovine tuberculosis:
A: Epithelioid cells are located in the typical tubercle in a narrow, light zone (arrows) between the central caseation (1) and the zone with lymphocytes (2); mesenterial lymph node, S 598/14, H&E (GMA). B: Epithelioid cells form a narrow, eosinophilic band (arrow) between caseation (1) and the zone with lymphocytes (2); a vacuolisation of the cells is recognizable; adjacent is a fibrous capsule (3); mesenterial lymph node, S 598/14, H&E (GMA). C: Overview of a lymph node with numerous foci of epithelioid cell granulomatous inflammation; the foci are irregularly formed and have different sizes; mesenterial lymph node, S 594/14, H&E (Paraffin). D: Multiple foci with epithelioid cell granulomatous inflammation; the foci are almost homogenously organised, consist exclusively of cells, show no layering and have no central caseation; mesenterial lymph node, S 413/14, H&E (GMA); bars in A, C = 1 mm, B = 100 μm, D = 200 μm.

Epithelioid cells were usually located in a small zone between the central caseous necrosis and the lymphocytic inflammatory zone in a tubercle (Fig. 18 A and B). At the lower

magnification in the H&E staining, this zone was mostly recognized as a light coloured margin around the caseous necrosis (Fig. 18 A).

At the higher magnification, these cells appeared in a typical epithelioid cell morphology (see below) (Fig. 19 A and B) or they were vacuolated (Fig. 19 C and D), especially in close neighbourhood to the caseation. In semi-thin sections stained with Toluidine blue-safranin, the stored material within the vacuoles appeared as lipids (Fig. 19 E).
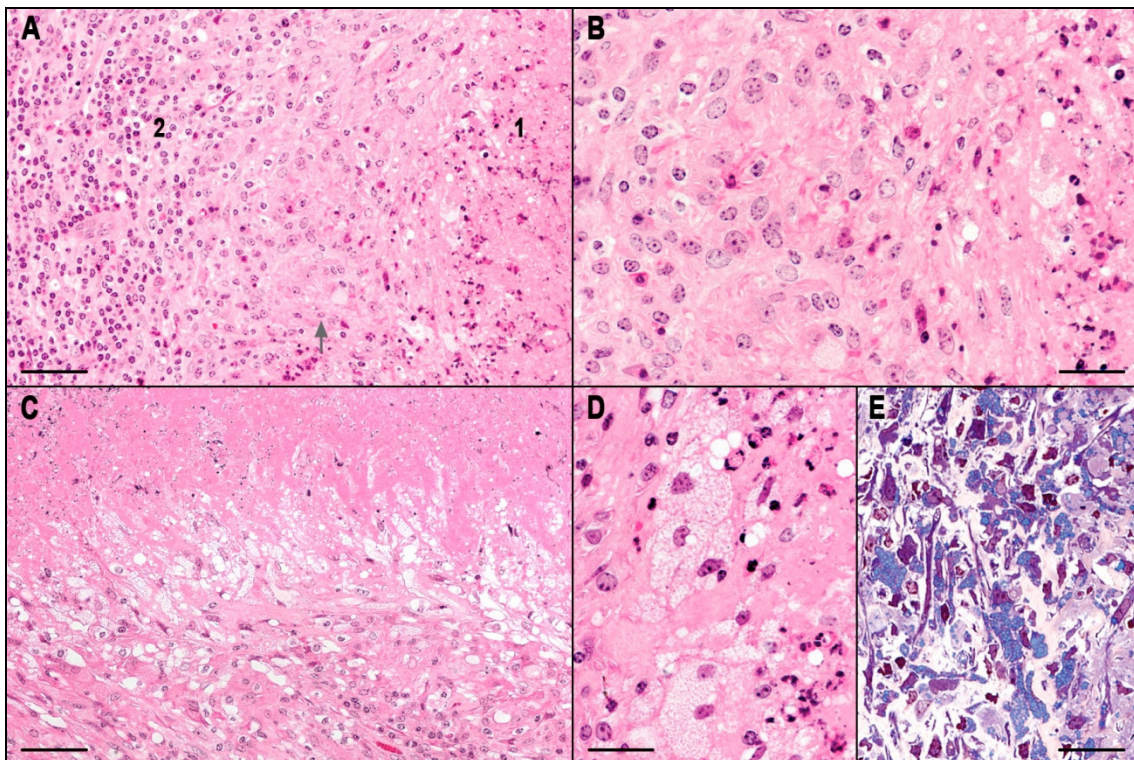
Figure 19. Cytology of epithelioid and multinucleated giant cells in bovine tuberculosis:
A: Zone with epithelioid cells (arrow) between caseation (1) and the zone with lymphocytes (2); retropharyngeal lymph node, S 409/14, H&E (GMA). B: The picture shows predominantly epithelioid cells with an extensive, eosinophilic cytoplasm; cell borders are not visible; the nucleus is lightly coloured, rich of euchromatin and has numerous small nucleoli; there are interspersed lymphocytes and single neutrophils; at the right border of the picture beginning caseation; retropharyngeal lymph node, S 409/14, H&E (GMA). C: Severe vacuolisation of epithelioid cells adjacent to the caseation; mesenterial lymph node, S 413/14, H&E (GMA). D: Vacuolisation of numerous epithelioid cells, in addition neutrophils and lymphocytes; retropharyngeal lymph node, S 409/14, H&E (GMA). E: Numerous intracytoplasmic blue coloured fat droplets are recognisable in the semi-thin section stained with Toluidine blue-safranin; mesenterial lymph node, E 325/09, TEM, (TEM No: 4938/3), bars in A, C = 50 µm, B, D, E = 25 µm.

The epithelioid cell granulomatous inflammation occurred in various extensions: from individual cells, which were clearly visible especially in lymph nodes, to extensive cell accumulations (Fig.18 D). The quantity of foci with epithelioid cells was also variable (Fig.18

C). The characteristic features of epithelioid cell granulomatous inflammation, in contrast to the tubercles, were the lack of layering of the cells, the irregular form of the foci, and the predominance of the epithelioid cells within the foci (Fig. 20 A and B). It has already been mentioned that the epithelioid cell granulomatous inflammation was frequently surrounded by lymphocytes easily recognizable in the lung (Fig. 20 B). The possibility of caseation within an epithelioid cell granulomatous inflammation is described in Chapter 4.3.2.1.1.
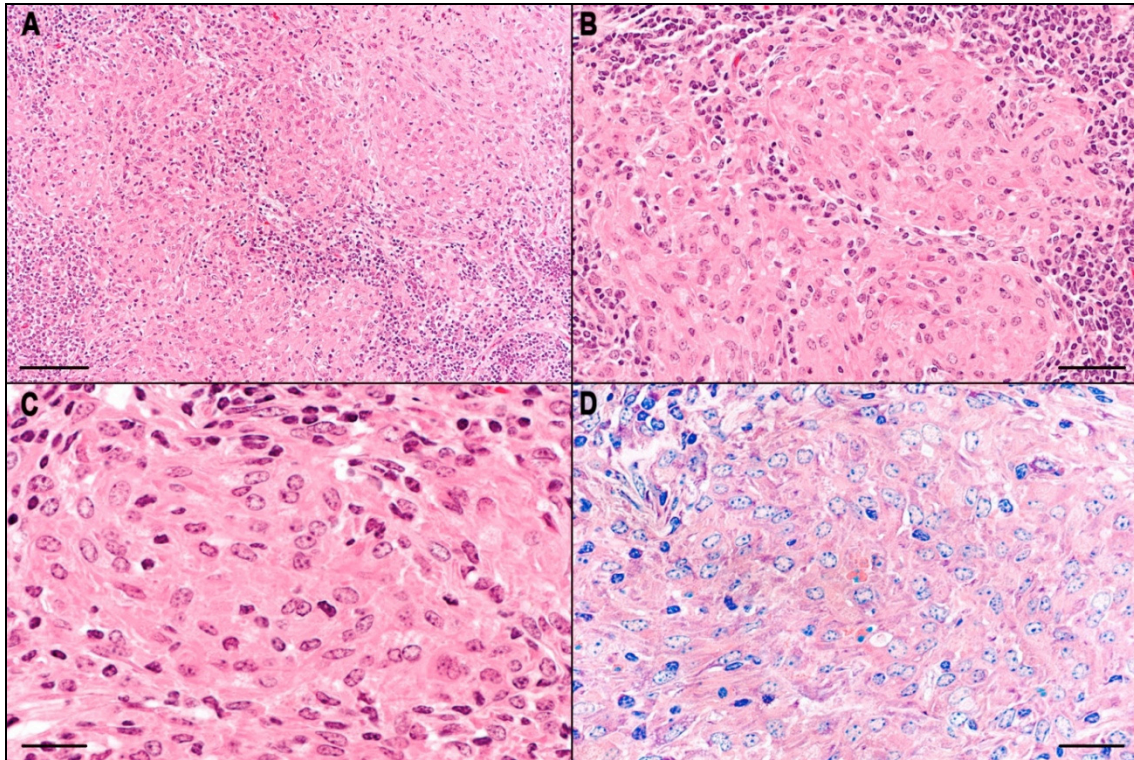
Figure 20. Cytology of epithelioid and multinucleated giant cells in bovine tuberculosis:
A: Overview of an epithelioid cell granulomatous inflammation, the roundish foci are homogenously organised and surrounded by a margin of lymphocytes; lung, E 322/09, H&E (GMA). B: Coalescent foci of epithelioid cell granulomatous inflammation, surrounded by lymphocytes; lung, E 322/09, H&E (GMA). C: Typical epithelioid cells with extensive eosinophilic cytoplasm, indistinct cell borders, elongated and partly indented, bright, vesicular nuclei with numerous small nucleoli; in the edge regions lymphocytes; lung, E 322/09, H&E (GMA). D: Specially the numerous small nucleoli within the vesicular nucleus are obvious in the Giemsa staining; lung, E 322/09, Giemsa (GMA); bars in A = 100 µm, B = 50 µm, C, D = 25 µm.

The epithelioid cells were large cells with abundant, eosinophilic cytoplasm in H&E stainings (Fig. 20 C). The cell borders of the epithelioid cells were indistinct. The nucleus was large, had an elongated, often shoe soles like shape or was occasionally deeply indented; the nucleus was pale and vesicular (rich in euchromatin). The nucleoli were numerous (up to eight per nucleus), small and usually located near the nuclear wall which was clearly seen especially in the Giemsa stained slides (Fig. 20 D). Ultrastructural, mitochondria and a distinct rough

endoplasmic reticulum dominated (Fig. 21 A). Nucleus and nucleoli correlated to the light microscopical description. The surface of the epithelioid cells was irregularly formed.
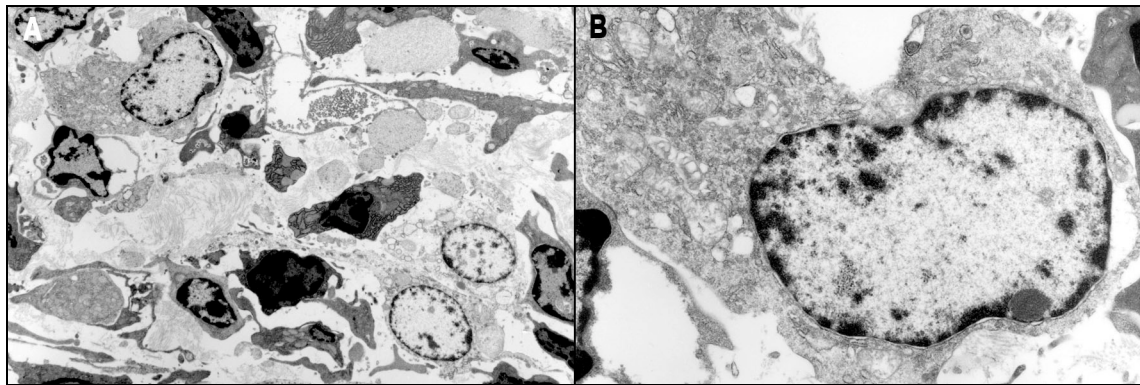
Figure 21. Cytology of epithelioid and multinucleated giant cells in bovine tuberculosis:
A: Overview of the ultrastructure of epithelioid cells; they possess extensive cytoplasm, which contains numerous organelles, the surface of the cells is pleomorphic; there are mainly lymphocytes beside the epithelioid cells. B: A high magnification of A; the extensive cytoplasm contains numerous mitochondria and a well formed endoplasmic reticulum; the nucleus has scant heterochromatin, which is located predominantly at the nuclear wall; mesenterial lymph node, E 325/09, TEM.

Multinucleated giant cells occurred, just as the epithelioid cells, in two localisations: in the epithelioid cell granulomatous inflammation (Fig. 22 A) or within the tubercle in the neighbourhood to central caseation (Fig. 22 B). Individual cells could be found among the autochthonous lymphocytes of the altered lymph nodes. In these two localisations, they were lacking (Fig. 20 B), occurred in small amounts (Fig. 22 C) or large amounts, so that they were the predominant cell type (Fig. 22 D).
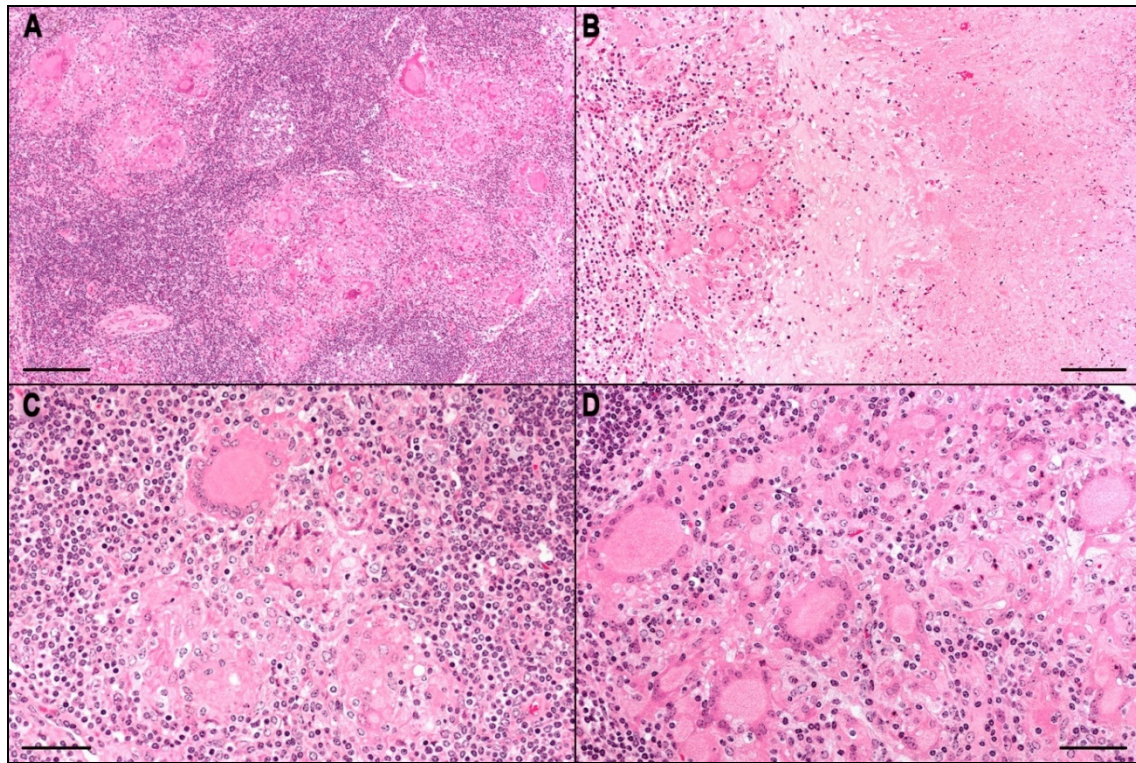
Figure 22. Cytology of epithelioid and multinucleated giant cells in bovine tuberculosis:
A: Foci with epithelioid cell granulomatous inflammation with a higher content of multinucleated giant cells in a lymph node; mesenterial lymph node, S 414/14, H&E (GMA). B: Tubercle with numerous multinucleated giant cells in the epithelioid cell zone adjacent to the central caseation; mesenterial lymph node, S 594/14, H&E (GMA). C: Epithelioid cell granulomatous inflammation with a single multinucleated giant cell; mesenterial lymph node, S 606/14, H&E (GMA). D: Epithelioid cell granulomatous inflammation consisting predominantly of multinucleated giant cells; mesenterial lymph node, S 612/14, H&E (GMA); bars in A = 200 µm, B =100 µm, C, D = 50 µm.

Langhans-type giant cell was the typical multinucleated cell for the tuberculosis. The diameter of the roundish giant cell was up to 120 µm. Elongated cells could reach a length of 160 µm. The Langhans-type multinucleated giant cells had lower numbers of nuclei (up to 30 in a section) in comparison to foreign body-type multinucleated giant cells. The nuclei had a typical horse-shoe or circular arrangement at the periphery (Fig. 23 A to C). The nuclei had a very similar morphology among each other and had similarity with the nuclei of the epithelioid cells (abundant euchromatin, numerous small nucleoli). The cytoplasm was eosinophilic and mostly homogeneous. But there were also multinucleated giant cells with a mild to severe degree of vacuolisation at the periphery of the cell (Fig. 23 D and E), up to the presence of Touton-type giant cells (Fig. 23 F) with centrally located nuclei and a high degree of vacuolisation at the periphery of the cell.

A frequently observed phenomenon was emperipolesis, in which a viable cell penetrated into another living cell. These penetrating cells could be neutrophils or lymphocytes (Fig. 23 G to I).
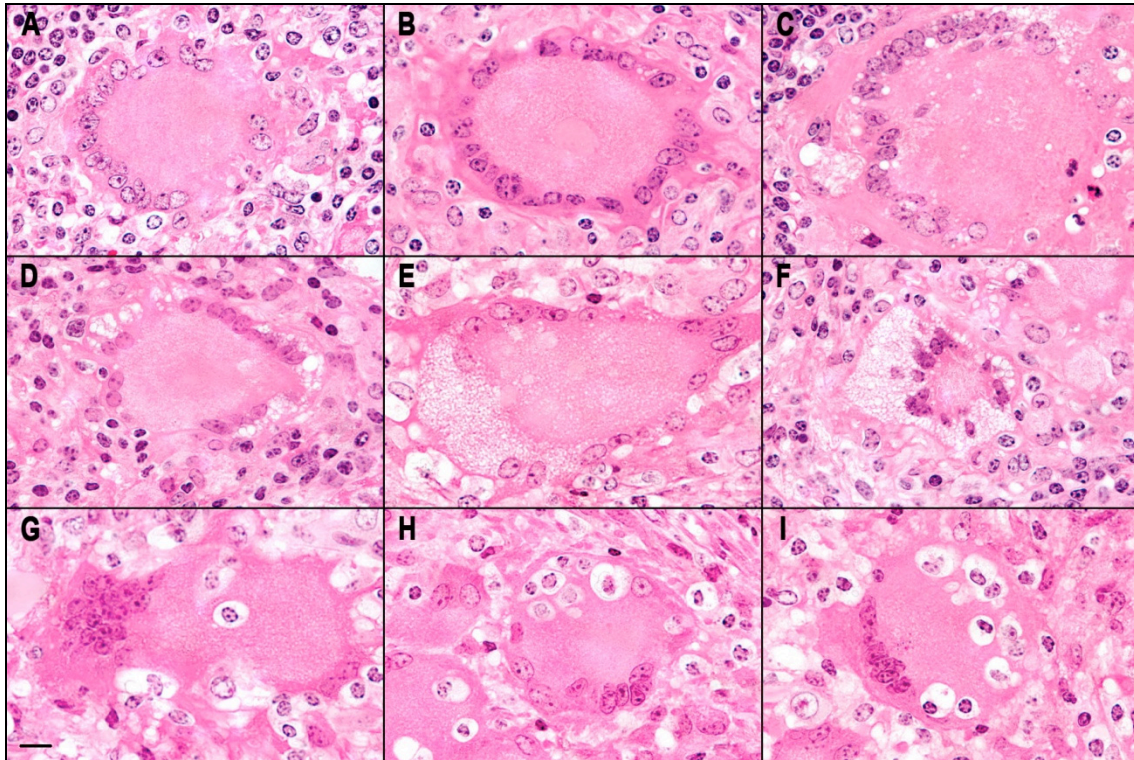
Figure 23. Cytology of epithelioid and multinucleated giant cells in bovine tuberculosis:
A-C: Typical Langhans-type multinucleated giant cells with horse shoe-shaped (A, C) or annular (B) arranged nuclei; the cytoplasm is homogenous and eosinophilic; the nuclei are mainly monomorphic. D-F: Vacuolisation of the giant cell at the periphery of the cytoplasm, mild (D), moderate (E) and severe (F); the cell in F is a Touton-type giant cell with annular vacuolisation of the cytoplasm at the periphery and centrally arranged nuclei. G-I: Different grades of emperipolesis, mainly with lymphocytes, in C a single neutrophil; mesenterial lymph node, S 606/14, S 602/14, 598/14, H&E (GMA); bar for A-I = 10 μm.

Lysozyme and the antibody against the myelomonocytic antigen calprotectin (MAC387) were suitable as immunohistochemical markers for cells of the mononuclear phagocyte system (MPS). It has been shown that lysozyme reacts only with cells of the MPS. The MAC387 antibody detected mainly neutrophilic granulocytes, but the recognition of MPS-cells is difficult.

Epithelioid cells in the epithelioid cell granulomatous inflammation and in tubercles showed a positive reaction with the antibody against lysozyme (Fig. 24). The positive reaction was present in the cytoplasm of the cells. The volume of the cells and the cell borders are distinctly visible due to the positive reaction. The nucleus was usually located eccentrical

(Fig. 24 A, B, D, and G); the positive reaction product was commonly not clearly related to the cell nucleus (Fig. 24 C). The intensity of the positive reaction in the cells was seen in varying degrees (Fig. 24 A versus F). The reaction product was partly homogenous and partly granular (Fig. 24 C and G).
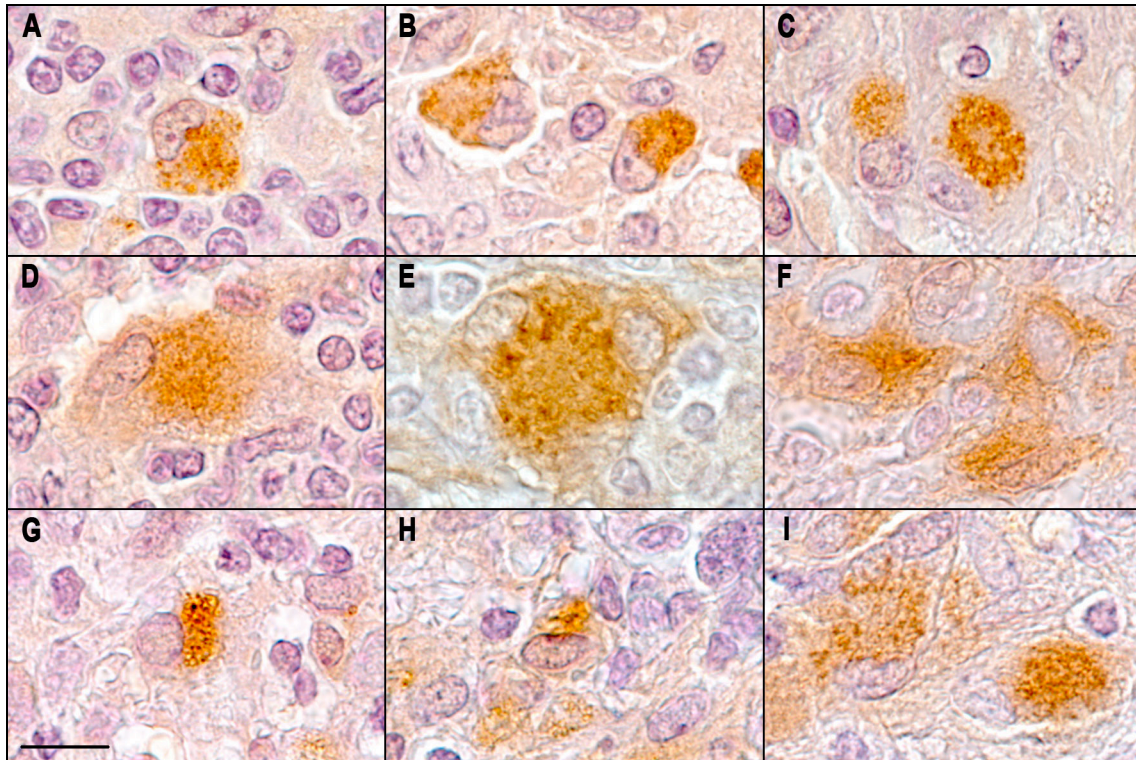
Figure 24. Cytology of epithelioid and multinucleated giant cells in bovine tuberculosis:
A-I: Immunohistochemical detection of lysozyme in epithelioid cells. The cytoplasms of the cells react strongly positive; the circumference of the cells and the cell borders are clearly visible. The nucleus is most commonly eccentrical (A, B, D). The strength of the reaction occurs in different intensities (A to H); the reaction product can be homogenous (D, F, I) or granular (A, C, G). The antibody reacts positive only with a part of the epithelioid cells; lung S 1256/12, mesenterial lymph node, S 1257/12, retropharyngeal lymph node S 1259/12, mesenterial lymph node, S 1260/12; bar for A-I = 10 μm.

The reaction of the multinucleated giant cells with the antibody against lysozyme (Fig. 25) was weaker than the reaction of epithelioid cells. The reaction product was found in the voluminous cytoplasm within the cell centre. The positive reaction was found either in the whole cytoplasm (Fig. 25 A and G) or annular within the cytoplasm (Fig. 25 B and H). The reaction product was partly homogenous (Fig. 25 E) and partly granular (Fig. 25 B) as seen in the epithelioid cells. Completely negative giant cells occurred occasionally (Fig. 25 I).
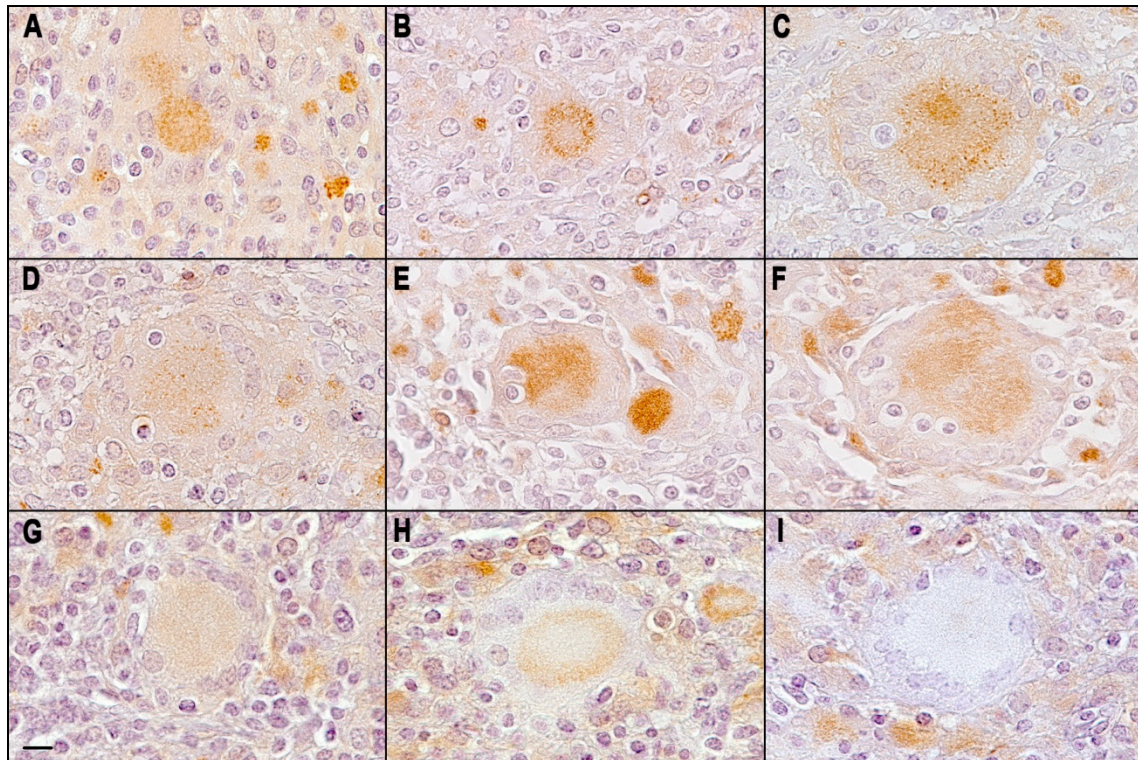
Figure 25. Cytology of epithelioid and multinucleated giant cells in bovine tuberculosis:
A: Immunohistochemical detection of lysozyme in Langhans-type giant cells; the cytoplasm in the centre of the cells reacts in varying degrees positively; the reaction product is partly fine granular (B, C); in addition to a homogenous reaction, there is also an annular positivity (B, H); completely negative single giant cells (I); mesenterial lymph node, S 1258/12, retropharyngeal lymph node, S 1259/12, mesenterial lymph node, S 1260/12; bar for A-I = 10 μm.

The immnohistochemical detection of the myelomonocytic antigen calprotectin (MAC387) (Fig. 26) revealed only a weak reaction in epithelioid and in giant cells. In contrast, neutrophils showed a strong positive reaction (Fig. 26 C) so that it was often difficult to discern the multilobulated nuclei.
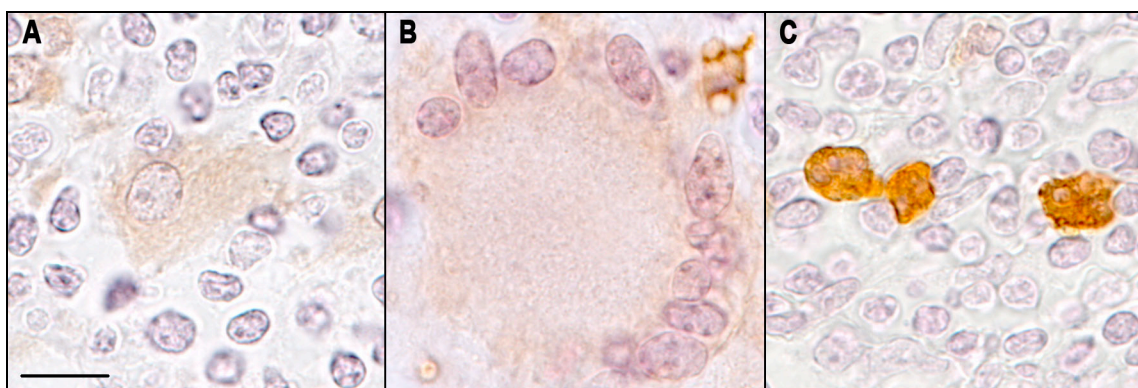
Figure 26. Cytology of epithelioid and multinucleated giant cells in bovine tuberculosis:
A-C: Immunohistochemical detection of calprotectin (MAC387). The reaction is weak in epithelioid cells (A) and in multinucleated giant cells (B). Contrary to that, neutrophils react strong. The

recognition of the lobulated nucleus is difficult; mesenterial lymph node, S 1258/12; bar for A-C = 10 µm.

For the relations between epithelioid and multinucleated giant cells and the other inflammatory cells in the tuberculous inflammation see in Chapter 4.3.2.1..

4.3.2.1.2.2. Polymorphonuclear Leukocytes

Polymorphonuclear leukocytes were observed in varying amounts within all different forms of the tuberculous inflammation. The cells either appeared morphologically intact or they were in different stages of disintegration. The intact neutrophils were recognized by their multilobulated nuclei and a homogenous and eosinophilic cytoplasm in H&E staining (Fig. 27 A). However, they were easier recognizable in Giemsa staining by their purple granules, a pale pink cytoplasm, and deep blue-violet nucleus. The disintegrated neutrophils consisted of the accumulations of nuclear debris (leukocytoclasia) (Fig. 27 C); the recognition of these remnants as neutrophils was possible only by an infiltration of intact neutrophils in the neighborhood (Fig. 28 A) or by a typical spatial arrangement within the inflammation (Fig. 29 A).

By immunohistochemistry neutrophils were significantly positive for the myelomonocytic antigen MAC387 (calprotectin). The differentiation between neutrophils and epithelioid cells might often be difficult (Fig. 27 B).
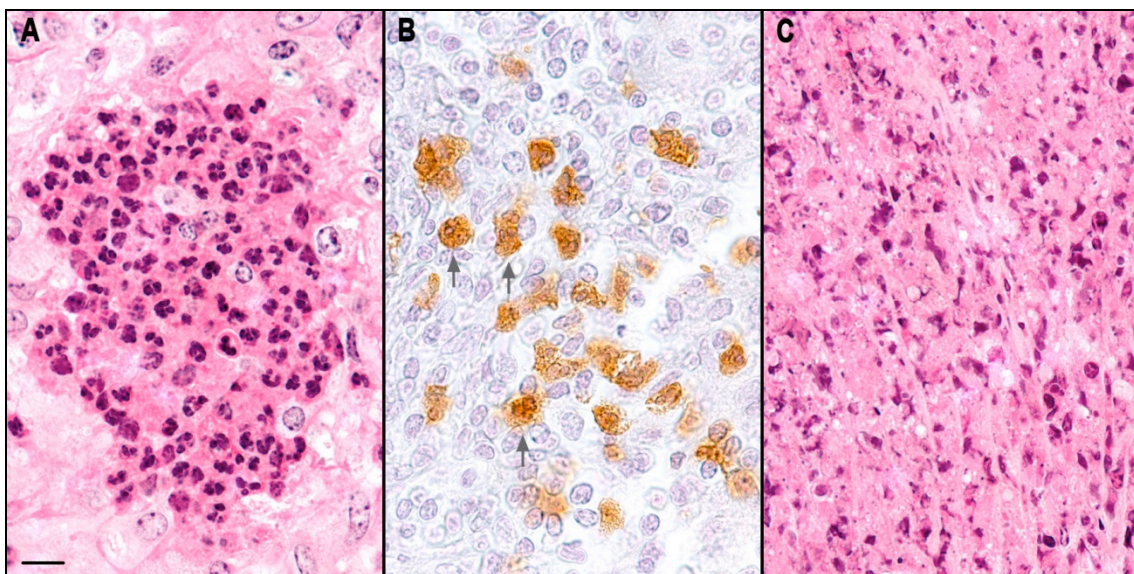
Figure 27. Cytology of neutrophils in bovine tuberculosis:

A: Cluster of intact neutrophils in a granuloma with the typical nuclear morphology and cytoplasmic staining; mesenterial lymph node, S 612/14, H&E (GMA). B: Immunohistochemical demonstration of MAC387 (calprotectin), strong positivity in neutrophils (arrows); retropharyngeal lymph node, S 1259/12, IHC (Paraffin). C: Accumulation of necrotic neutrophils in a caseous necrosis (leukocytoclasia); retropharyngeal lymph node, S 409/14, H&E (GMA); bar for A-C = 10 μm.

Neutrophils occurred in small numbers and scattered in many locations of the tuberculous inflammation. Localizations, where they were found in larger amounts, are: a) in the inner inflammatory zone around larger caseous necrosis (focal or band-like arranged) (Fig. 28 A), b) in the satellite granulomas within the inflammatory zone of larger caseating necrosis (Fig. 28 B), c) within epithelioid cell granulomatous inflammation in varying amounts (Fig. 28 C and D), d) within large foci of caseous necrosis (Fig. 29 A), e) in the acute tuberculous inflammation of the lung (Fig. 29 B), f) in the area of intrusions of tuberculous inflammation into bronchi/bronchioli (Fig. 29 C), g) in the inner zone of tuberculous cavitating lesions (Fig. 29 D). Here only the typical localizations of neutrophils are listed, the relations to the other cells of the tuberculous granulomatous inflammation are given in Chapter 4.3.2.1..
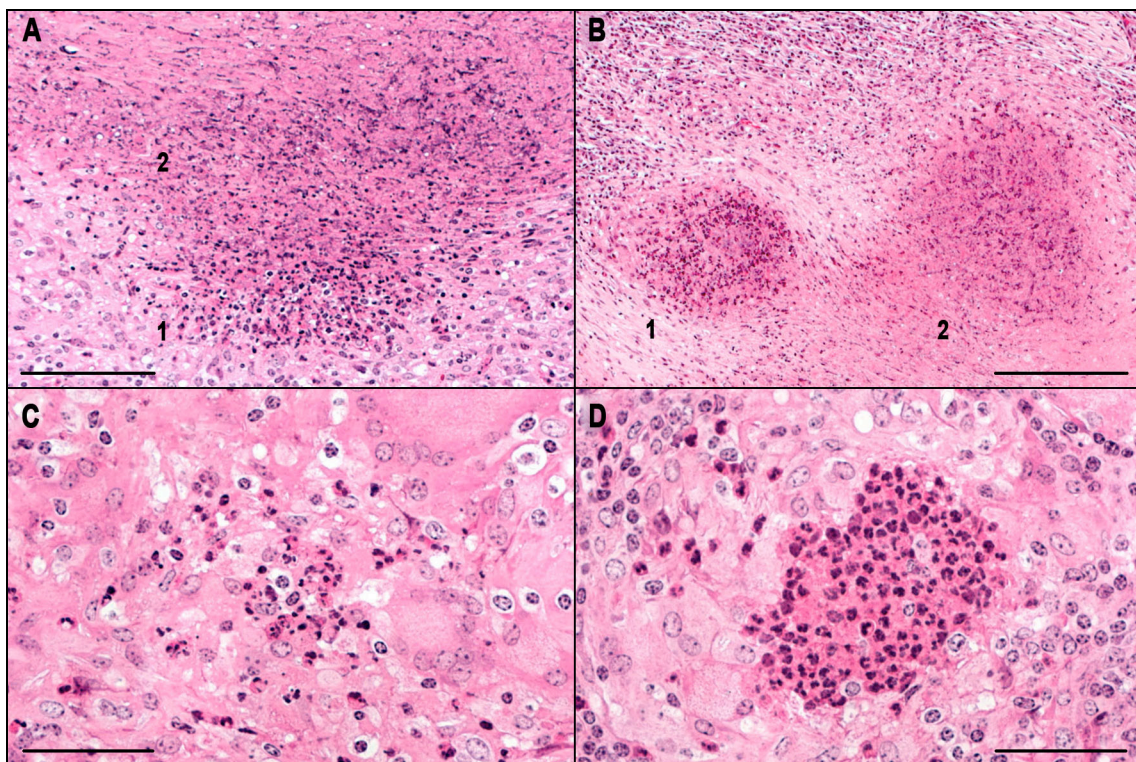
Figure 28. Distribution of neutrophils in bovine tuberculosis:
A: Inner zone of a large caseous necrosis (Macro-pattern I), the neutrophils at the periphery are still intact (1), the degree of disintegration increases with the transition into the caseating necrosis (2); retropharyngeal lymph node, S 409/14, H&E (GMA). B: Infiltration of neutrophils in satellite granulomas within the inflammatory/fibrous zone of a large granuloma (Macro-pattern I), the left focus shows intact neutrophils (1) and the right one already disintegrated cells (2); liver, E 110/09, H&E (GMA). C: Epithelioid cell granulomatous inflammation with a low number of intact neutrophils

between epithelioid and multinucleated giant cells; mesenterial lymph node, S 602/14, H&E (GMA).
D: Epithelioid cell granulomatous inflammation with numerous intact neutrophils in the center, where epithelioid cells are already destroyed; mesenterial lymph node, S 602/14, H&E (GMA); bars in A = 100 µm, in B = 200 µm, in C and D = 50 µm.
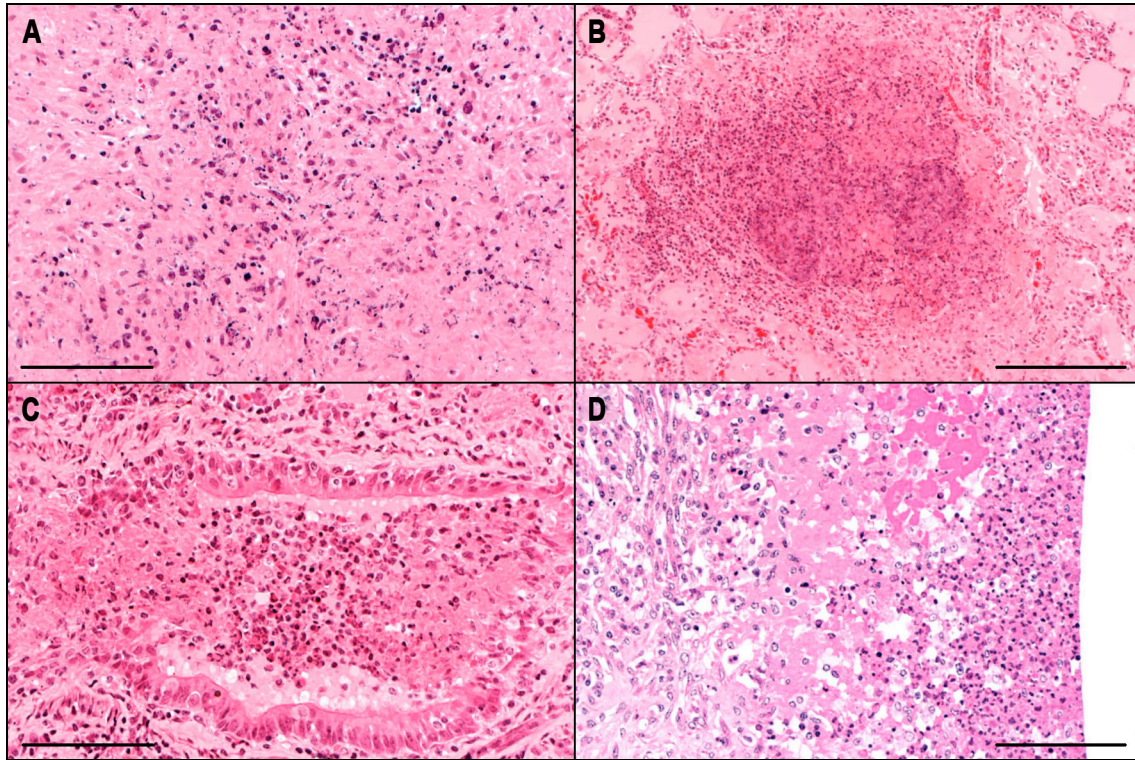
Figure 29. Distribution of neutrophils in bovine tuberculosis:
A: Centre of a large caseous necrosis (Macro-pattern I) with numerous disintegrated neutrophils; lung, E 322/09, H&E (GMA). B: Acute inflammation of lung, alveolar lung oedema with severe focal infiltration of neutrophils; lung, E 322/09, H&E (GMA). C: Lung with an intrusion of tuberculous inflammation into a bronchiole; lung, E 322/09, H&E (GMA). D: Bordering zone of a cavitating lesion of the lung; lung, S 770/13, H&E (GMA); bars in A, C and D = 100 µm, in B = 200 µm.

4.3.2.1.2.3. Lymphocytes and Plasma Cells

It was easily possible to determine the amount of lymphoid cells involved in the tuberculous inflammation in alterations of non-lymphoid organs, such as lung (Fig. 30 A) or liver (Fig. 30 C). On the contrary, the presence of autochthonous lymphocytes and the impossibility to differentiate them from inflammatory lymphoid infiltrates made it nearly impossible to estimate the quantity of these cells within lymph nodes.

Large infiltrates of lymphoid cells occurred in two forms in tuberculous inflammation: on the one hand as concentric accumulations around large caseous necrosis (Fig. 30 A and C) and epithelioid cell granulomatous inflammation (Fig. 30 B); on the other hand, as irregularly

formed, large aggregates of lymphocytes between epithelioid cell granulomatous inflammation (Fig. 30 B).

The concentric arrangements were frequently supported by concentric layered collagen fibres (Fig. 30 D).
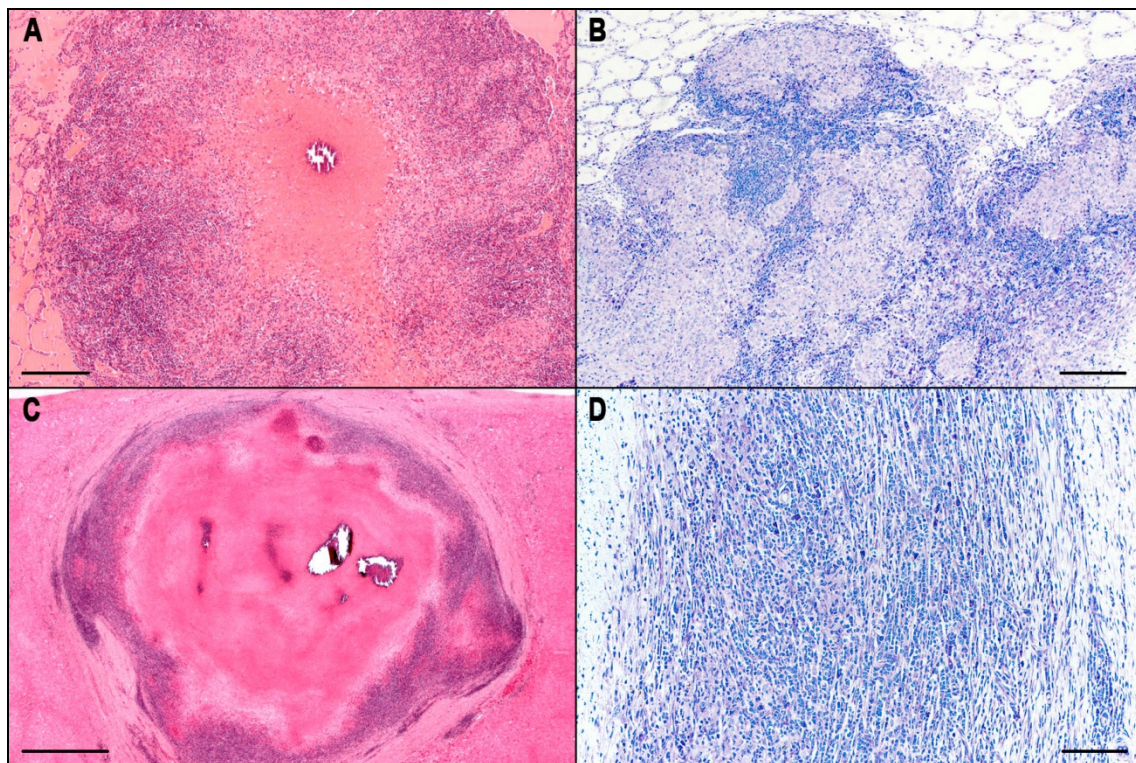
Figure 30. Cytology of lymphocytes and plasma cells in bovine tuberculosis:
A: Large tuberculous granuloma in the lung with a broad zone of lymphocytes around the central caseation with calcification; lung, S 1256/12, H&E (Paraffin). B: Multiple foci of epithelioid cell granulomatous inflammation in the lung; the lymphocytes are found concentrically around the foci or as irregularly formed foci; lung, E 322/09, Giemsa (GMA). C: Large tuberculous granuloma in the liver with a broad zone of lymphocytes around a central caseation with calcification; liver, H&E (GMA). D: Lymphocytes at the periphery of a caseation; lymphocytes are supported by concentrically arranged collagen fibres (pale eosinophilic); liver, E 110/09, Giemsa (GMA); bars in A and B = 200 µm, in C = 1 mm, in D = 100 µm.

Cytologically, lymphocytic infiltrates consisted predominantly of small lymphocytes, most obvious in larger aggregates (Fig. 31 A). Lymphoblasts occurred uncommonly and immunoblastic cells rarely (Fig. 31 C). Multifocally there were scattered plasma cells (Fig. 31 B). Lymphoblasts had more abundant cytoplasm and finer chromatin in the nucleus when compared to lymphocytes. Immunoblasts within the granuloma could be activated B or T cells. They were large, round lymphocytes with large, distinctive light-stained nucleus, a large nucleolus and an intensely basophilic cytoplasm. On the other hand, small lymphocytes had

small amount of weakly basophilic cytoplasm and a round, dark-stained nucleus. The plasma cells were distinguished from lymphocytes by their high amount of cytoplasm and their eccentric, compact dark nucleus. Between larger lymphocytic infiltrates there occurred regularly single cells with a large vesicular nucleus and a faintly coloured cytoplasm (Fig. 31 D).

Immunohistochemically, CD3 T-lymphocytes dominated (Fig. 31 E). B-lymphocytes (CD20) occurred as aggregates, which can be occasionally extensive (Fig. 31 F). T-lymphocytes usually approximated to the caseation zone, while infiltration with CD 20-positive B-lymphocytes started in a greater distance to the caseation zone. Strong CD 79a- positive B-lymphocytes (Fig. 31 G) occurred only sporadically, usually in form of blastic cells or with plasma cell morphology.

The relationships between lymphocytes and other inflammatory cells are presented in Chapter 4.3.2.1..
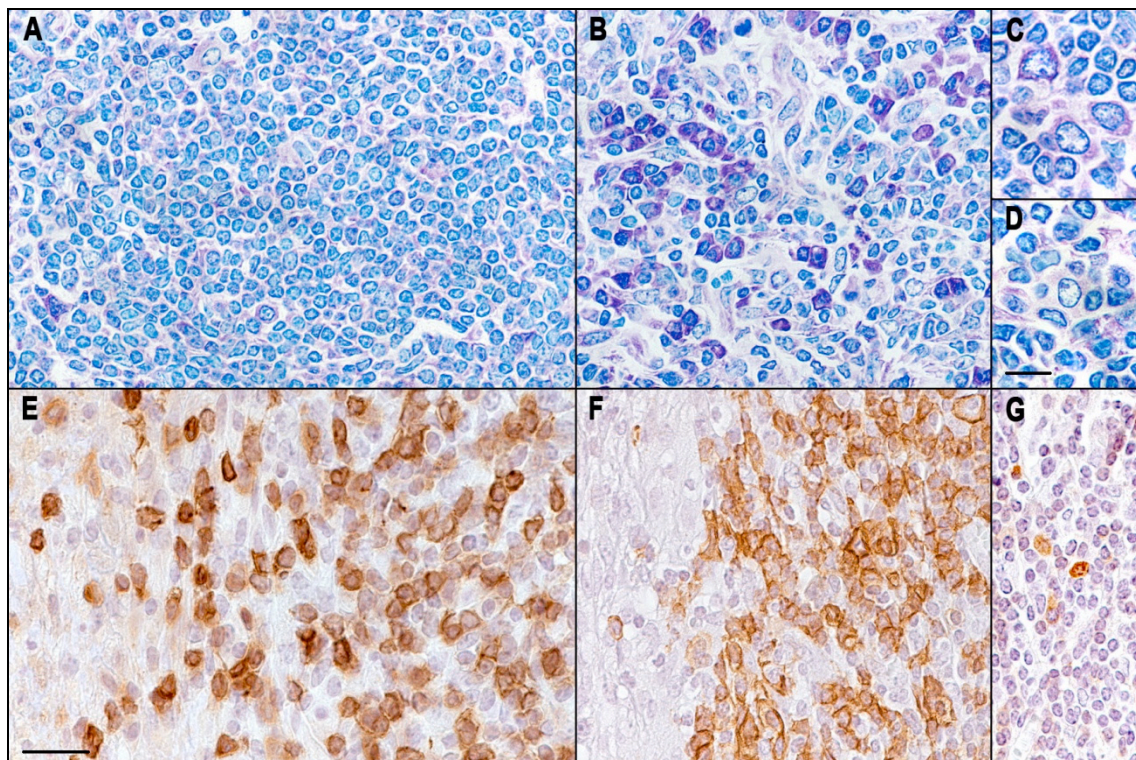
Figure 31. Cytology of lymphocytes and plasma cells in bovine tuberculosis:
A: A focal extensive aggregate of predominantly small lymphocytes in the lung; lung, E 322/09, Giemsa (GMA). B: Typical plasma cells scattered between lymphocytes; E 322/09, Giemsa (GMA). C: Few immunoblastic/ lymphoblastic lymphocytes; lung, E 322/09, Giemsa (GMA). D: Commonly found single large cells with large vesicular nucleus and poorly stained cytoplasm; lung, E 322/09, Giemsa (GMA). E: CD3-positive T-lymphocytes at the periphery of a caseation zone; mesenterial

lymph node, S 1257/12, IHC CD3. F: Infiltration with CD20-positive B-lymphocytes at the periphery of a caseation zone; the cells approximate not to the caseation zone; mesenterial lymph node, S 1257/12, IHC CD20. G: Few CD79a-positive lymphocytes, interspersed between numerous small lymphocytes; mesenterial lymph node, S 1257/12, IHC CD79a; bars in E for A, B, E, F, G = 25 µm and bar in D for C and D = 10 µm.

4.3.2.1.2.4. Mast Cells and Eosinophilic Granulocytes

Mast cells and eosinophilic granulocytes could only be recognized in Giemsa stained sections. Mast cells occurred in low amounts in the fibrous capsule and in the lymphocytic zone of the tubercle (Fig. 32). On the contrary, they were rare both in the epithelioid cell zone and nearby the caseation (Fig. 32 A). The mast cells showed typical metachromatic granules, the form of these cells were spindle-shaped. Rare eosinophilic granulocytes also occurred in the same localisations as mast cells (Fig. 32 B).
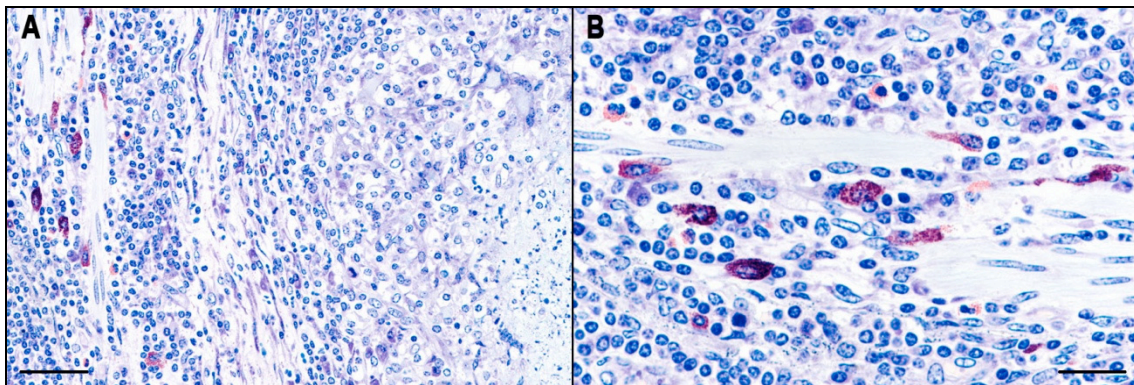
Figure 32. Cytology of mast cells and eosinophilic granulocytes in bovine tuberculosis:
A: Mast cells play a minor role in the tuberculous inflammation. They occur in the fibrous capsule and in the lymphocytic zone of the tubercle. They are rarely found both in the epithelioid cell zone and nearby the caseation (the right side of the picture); portal lymph node, E 325/09, Giemsa (GMA). B: Eosinophilic granulocytes occur nearby the mast cells. Their nucleus is two-lobed; the granules are orange in colour after Giemsa staining; portal lymph node, E 325/09, Giemsa (GMA); bars in A = 50 µm, B = 25 µm.

4.3.2.1.3. Fibrous Connective Tissue

The fibrous connective tissue was recognized as bundles of spindle-shaped cells in H&E staining with their central, oval, and hyperchromatic nucleus (fibroblasts and fibrocytes). They were admixed with collagen fibres and could be detected in varying arrangements and amounts within the tuberculous inflammation. The histological evaluation of the fibrous connective tissue reaction in the tuberculous inflammation was more reliably by using Silver staining of the collagen fibres (Fig. 33 to 36). It was shown that the amount and the

arrangement of the fibrous connective tissue were influenced by numerous factors. Thus, there was an association between the macroscopic pattern, the histological type of the inflammation and the affected organ as well as with the chronicity of the inflammation.

The dependency on the macroscopic pattern of the tuberculous inflammation was obvious. In pattern I and II (Fig. 33), completely developed typical tubercles, a distinct fibre-rich capsule developed (Fig. 33 A).
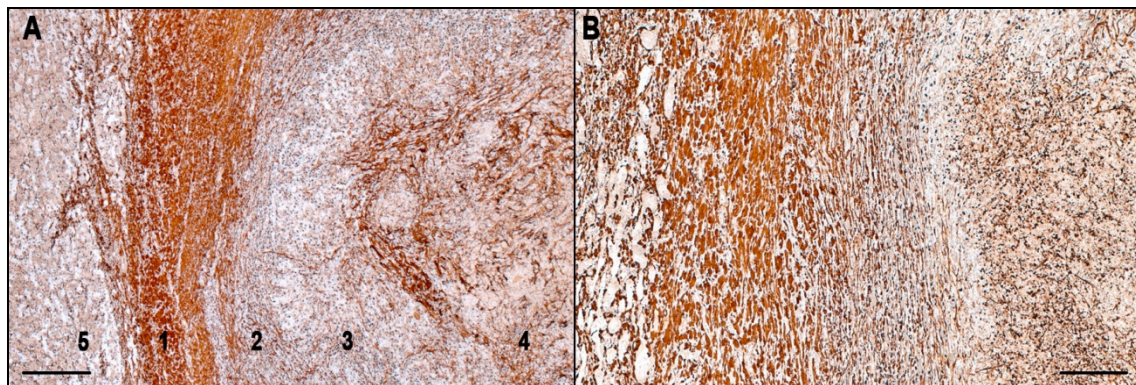
Figure 33. Fibrous connective tissue in bovine tuberculosis:
A: Demonstration of collagen fibres in the overview of a classic tubercle with a distinct connective tissue capsule (1), the lymphocytic zone (2) as well as epithelioid cells (3), the central caseation (4) and adjacent liver tissue (5); liver, E 110/09, Silver staining (GMA). B: Detail of Fig. A, the concentrically arranged collagen fibres in the capsule and in the lymphocytic zone are clearly visible as well as the different density and thickness of the fibres in both zones; remnant of fibres in the caseation are detectable; liver, E 110/09, Silver staining (GMA); bars in A = 200 µm, B = 100 µm.

However, loosely arranged collagen fibres were also found in the lymphocytic zone (Fig. 33 B). Similarly as in the capsule, the collagen fibres were arranged around the central caseation. The occurrence of the fibres within the caseation is described in Chapter 4.3.2.1.1.

In the macroscopic pattern III, in which the different components of the inflammation were arranged completely irregular, there was a similar disarranged pattern of the collagen fibres (Fig. 34). Irregularly arranged foci of inflammation and caseation were interspersed with dense fibre bundles and the remnants of the local tissue (Fig. 34 A). At higher magnification, it was apparent that the inflammation and the caseation were adapted to the arrangement of the collagen fibres (Fig. 34 B), suggesting that the reactively formed collagen fibre-rich connective tissue could be subjected to an acute inflammation and caseation process again.
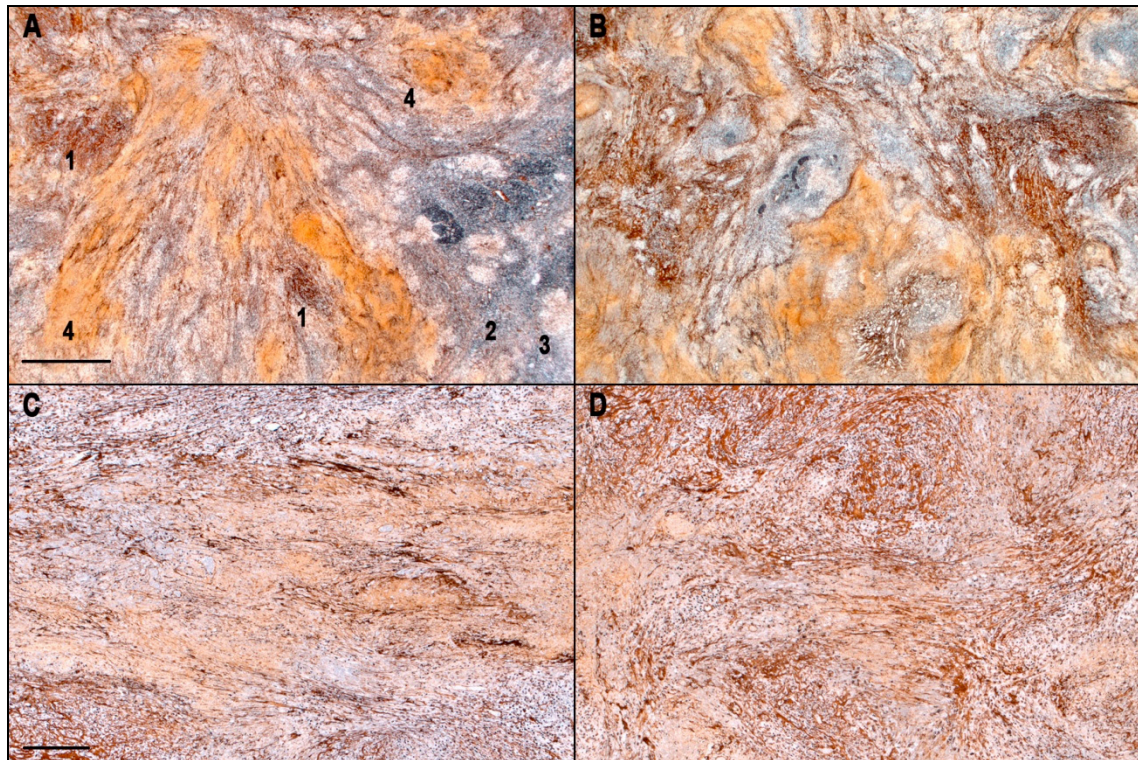
Figure 34. Fibrous connective tissue in bovine tuberculosis:
A: Demonstration of the collagen fibres in lymph nodes with macroscopic pattern III (see 4.3.1.1.3.); there is a disarranged side by side of collagen fibres (1), local lymph node tissue (2) with foci of epithelioid cell granulomatous inflammation (3) and longitudinal foci of caseous necrosis (4); mediastinal lymph node, E 108/09, Silver staining (GMA). B: An analogue picture in the lymph node of another animal with a higher amount of collagen fibres; mediastinal lymph node, E 322/09, Silver staining (GMA). C: It is recognizable at the higher magnification, that the reactively formed collagen fibres are subjected to a caseation again and that the caseation aligns the orientation of the fibres; mediastinal lymph node, E 108/09, Silver staining (GMA). D: Another part of the same lymph node with a higher proportion of collagen fibres, which are also subjected to a beginning caseation; mediastinal lymph node, E 108/09, Silver staining (GMA); bars in A for A and B = 1 mm, in C for C and D = 200 µm.

The side by side arrangement of chronic-reactive fibrosis and acute inflammation with caseation resulted in the completely disorganized picture of macroscopic pattern III, and it also explained the difference in the form of the foci, namely roundish in patterns I and II (see above).

The two previously described patterns of fibrosis occurred in chronic inflammatory processes. Young tuberculous inflammations were either the epithelioid cell granulomatous inflammation or younger tubercles (Fig. 35). Only a few collagen fibres within the foci and at the periphery of the foci were detecable in the epithelioid cell granulomatous inflammation (Fig. 35 A and C), there was no distinctive arrangement of the fibres.
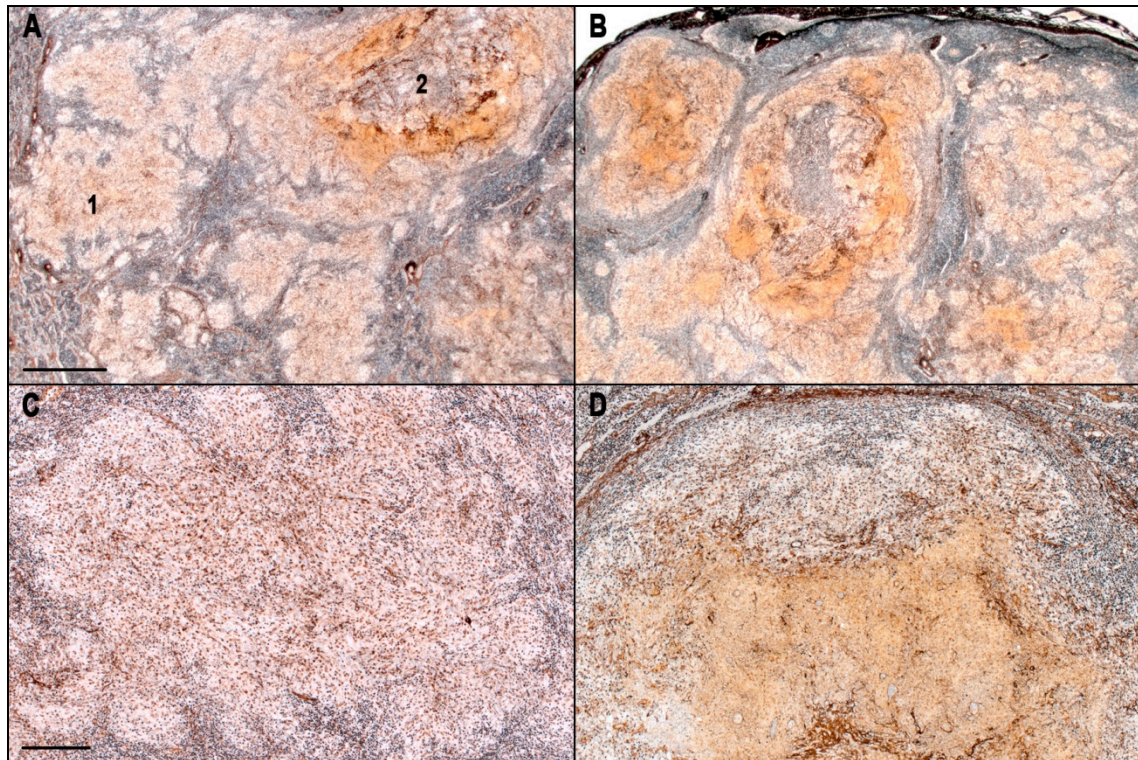
Figure 35. Fibrous connective tissue in bovine tuberculosis:
A: Demonstration of collagen fibres in a young tuberculous inflammation, with foci of epithelioid cell granulomatous inflammation (1) and beginning tubercle formation with caseation (2); mesenterial lymph node, E 108/09, Silver staining (GMA). B: Another area of the same lymph node with numerous young tubercles; mesenterial lymph node, E 108/09, Silver staining (GMA). C: Epithelioid cell granulomatous inflammation with a low amount of collagen fibres at the periphery of the foci; mesenterial lymph node, E 108/09, Silver staining (GMA). D: Young tubercle, which develops in a focus with epithelioid cell granulomatous inflammation; there is also a low amount of collagen fibres, the formation of a capsule is only indistinctive; mesenterial lymph node, E 108/09, Silver staining (GMA); bars in A for A and B = 1 mm, in C for C and D = 200 µm.

The amount of collagen fibers is low also in young tubercles with initiating caseation (Fig. 35 B and D). There was no distinct capsule formation (Fig. 35 D).

The tuberculosis of the lung differed from the tuberculosis of other organs by the occurrence of an acute inflammation with extensive oedema (Fig. 36). The earliest alteration was a roundish destruction of the lung parenchyma with severe neutrophilic infiltration (Fig. 36 A). A mild collagen fibre proliferation occurred at the periphery of these foci (Fig. 36 B). Another early encountered alteration was the epithelioid cell granulomatous inflammation (Fig. 36 C), where a mild formation of collagen fibres exists (Fig. 36 D). Young tubercles with beginning caseation were also accompanied by a mild to moderate deposition of collagen fibres (Fig. 36 E and F), like young tubercles in the other organs.
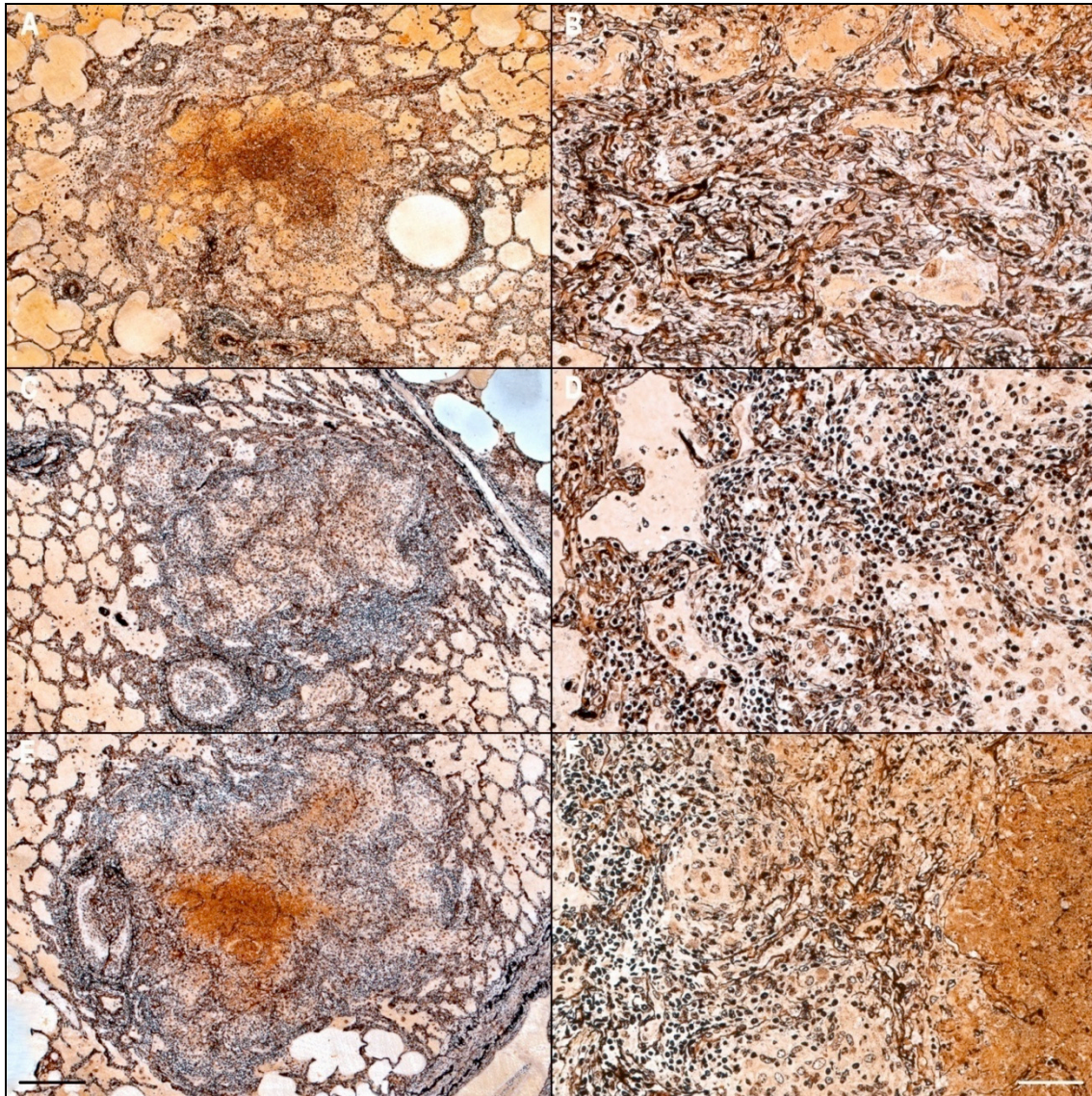
Figure 36. Fibrous connective tissue in bovine tuberculosis:
Demonstration of collagen fibres in different stages of the acute tuberculous inflammation in the lung:
A and B: A focus of acute degeneration of severely oedematous lung parenchyma and aggregates of
neutrophils in the centre of the focus; a beginning of deposition of collagen fibres at the periphery of
the foci is visible in (B). C and D: Focus with epithelioid cell granulomatous inflammation; a mild
deposition of collagen fibres is also detectable. E and F: Beginning tubercle formation in a focus with
epithelioid cell granlomatous inflammation; the accumulation of collagen fibres is more obvious (F),
but overall mild; a capsule formation is not visible; lung, E 322/09, Silver staining (GMA); bars in E
for A, C, and E = 200 µm, in F for B, D, and F = 50 µm.

4.3.2.2. The Types of Histological Alterations

Histologically, tuberculous inflammation in cattle could be divided into four types. Besides
the obligatory existence of epithelioid cells and a different amount of multinucleated giant
cells, the major determinants were the amount of necrosis (caseation) and fibrosis, as well as
the arrangement of these components.

Besides that, the lung lesions showed additional features, which were characteristic for pulmonary tuberculosis. These distinct features of the lung were evaluated separately in the organ description part (see 4.3.3.1.).

4.3.2.2.1. Histo-type 1

The type 1 was predominantly characterised by the presence of epithelioid cells. It could be divided into two subtypes.

4.3.2.2.1.1. Subtype 1a

This subtype (Fig. 37) predominantly consisted of epithelioid cells. The epithelioid cell aggregates varied in their size from areas consisting of a few cells (Fig. 37 A) to extensive infiltrations (Fig. 37 B). The foci occurred solitary (Fig. 37 A) or in form of numerous foci in different sizes side by side (Fig. 37 C and D). In addition to the epithelioid cells, multinucleated giant cells appeared in variable amounts. This subtype could reveal small foci of caseation (Fig. 37 D) up to necrosis occupying almost the entire focus. Neutrophils appeared in variable amounts, too. A thin layer of fibrous encapsulation might occur.
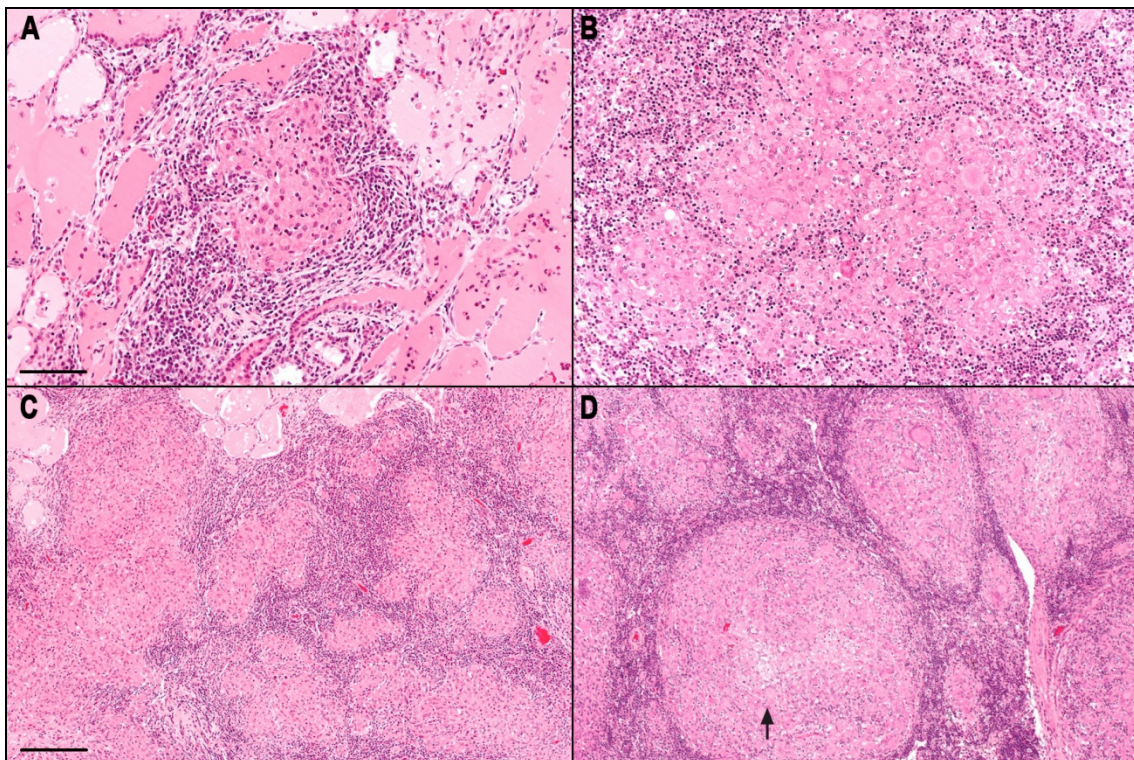
Figure 37. Histo-types in bovine tuberculosis:

A: Histo-type 1, subtype 1a is characterised by focal aggregates of epithelioid cells, which can be located solitary as small foci in the tissue; lung, E 322/09 H&E, (GMA). B: Large aggregate of epithelioid cells surrounded by original lymph node tissue; mesenterial lymph node, S 602/14, H&E (GMA). C: Several foci of epithelioid cells of variable size in the lung, surrounded by numerous lymphocytes; lung, E 322/09, H&E (GMA). D: Large foci of epithelioid cells and few multinucleated giant cells, caseation (arrow) begins in some foci; mesenterial lymph node, S 413/14, H&E (GMA); bars in A and B = 100 µm, C and D = 200 µm.

4.3.2.2.1.2. Subtype 1b

This subtype predominantly consisted of epithelioid cells, too (Fig. 38). The foci were usually located solitary in the inflammatory reaction zone of larger tubercles (satellite foci) (Fig. 38 B). The foci of variable size could be found in the lymphocytic zone (Fig. 38 B) or in the fibrosis (Fig. 38 C). These foci could increase in size, succumb to central caseation and they might finally coalesce with the central caseation of the tubercle thereby contributing its growth.
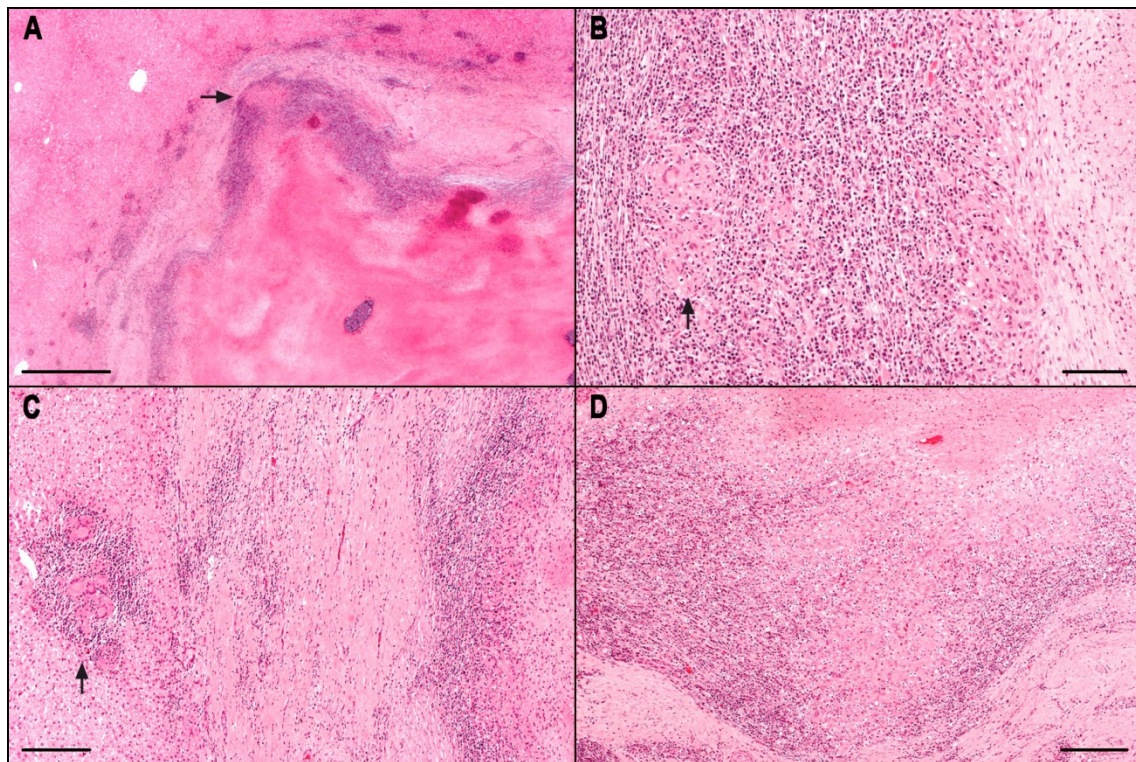
Figure 38. Histo-types in bovine tuberculosis:
A: Histo-type 1, subtype 1b is similar organised as the subtype 1a; essential difference is its location within the reaction zone of a larger tubercle (arrow); liver, E 110/09, H&E (GMA). B: Single epithelioid and giant cells in the lymphocytic zone (arrow), the central caseation of the tubercle at the right side of the picture; liver, E 110/09, H&E (GMA). C: Focus of epithelioid and giant cells near the fibrous capsule (arrow), the central caseation at the right side of the picture; liver, E 110/09, H&E (GMA). D: Large focus of epithelioid cells, which is in connection with the central caseation at one side; furthermore, the focus is surrounded by lymphocytes and the fibrous capsule of the tubercle; liver, E 110/09, H&E (GMA); bars in   A = 1 mm, B = 100 µm, C and D = 200 µm.

4.3.2.2.2. Histo-type 2

Type 2 was the classical tubercle (Fig. 39) with its onionskin-like layering. The caseous necrosis was found in the centre with or without a variable number of calcified foci (Fig. 39 A). The necrosis was followed by a reaction zone with several layers. The innermost layer adjacent to the caseation consisted of epithelioid cells and multinucleated giant cells, which became fatty degenerated first, then became necrotic and finally became part of the caseation. The subsequent zone consisted of lymphocytes and is variably thick. The outer layer was built by a fibrous capsule. Satellite foci with epithelioid cells occurred in lymphocytic zone and in the fibrosis (Histo-subtype 1b). They could caseate and coalesce with the central caseation (Fig. 39 A). According to the macro-patterns I and II, the tubercles occurred solitary (Fig. 39 A) or smaller foci were found side by side (Fig. 39 B).
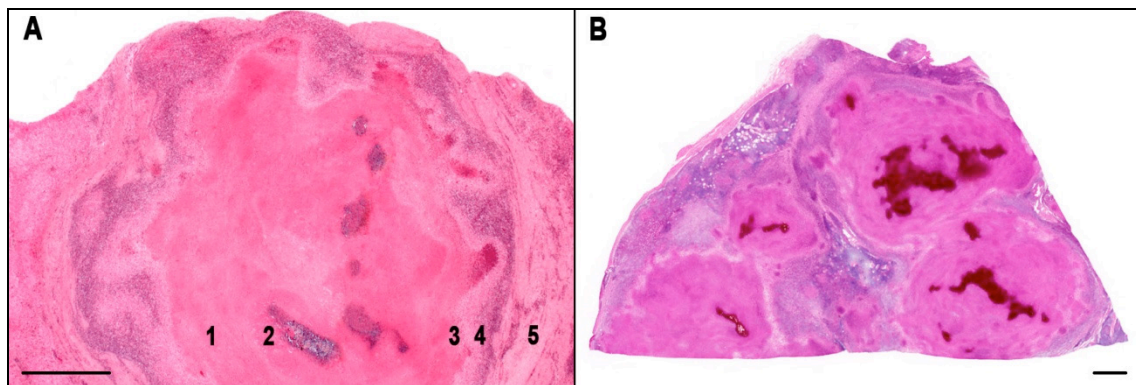
Figure 39. Histo-types in bovine tuberculosis:
A: Histo-type 2 is the classical tubercle with its onionskin-like layering, the central caseation (1) with calcification (2), the different layers of the reaction zone with the inner zone of epithelioid cells (3) and the lymphocytic zone (4) as well as the outer fibrous capsule (5). This solitary tubercle corresponds to the macro-pattern I; liver, E 110/09, H&E (GMA). B: Also numerous small tubercles with the same structure as the solitary tubercle can be found side by side corresponding to the macro-pattern II; portal lymph node, E 110/09, H&E (GMA); bars in A = 1 mm, B = 2 mm.

4.3.2.2.3. Histo-type 3

Histo-types 3 and 4 were characterised by a completely disordered structure, which was clearly visible even at the macro-pattern (Pattern III and IV).

The irregular structure of this type could best be seen at the lower magnification (Fig. 40 A and B). Details were visible only at the higher magnification. The typical component of histo-type 3 was the fibre-rich fibrous connective tissue, which crossed the inflammation in

irregular streams (Fig. 40 C). The arrangement of the fibrous connective tissue suggested reparative processes in terms of scarring. There were focal aggregates of epithelioid cells, which again could undergo caseation (Fig. 40 D). Lymphocytes and neutrophils also occurred. Calcification was rare in comparison with histo-type 4.
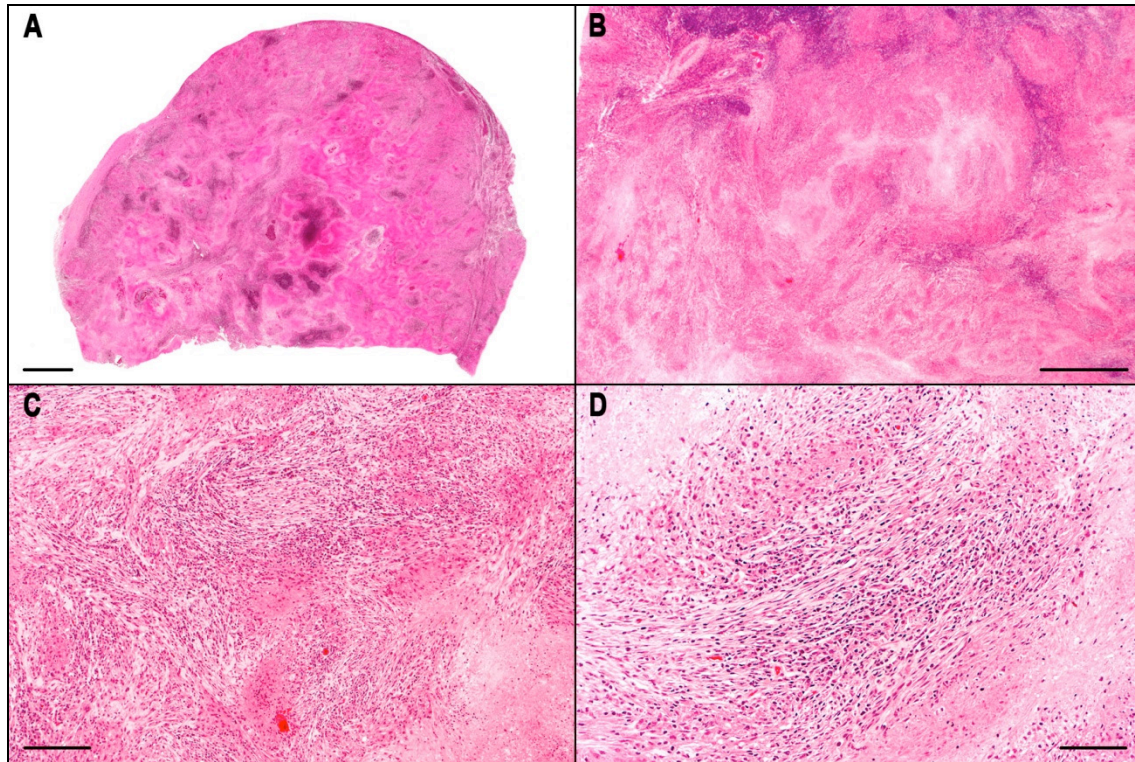
Figure 40. Histo-types in bovine tuberculosis:
A: Histo-type 3 presents a completely disordered composition in the overview. This histological picture corresponds to the macro-pattern III; mediastinal lymph node, E322/09, H&E (GMA). B: The individual components also are not visible at the lower magnification; mesenterial lymph node; E 108/09, H&E (GMA). C: At the higher magnification, the large portion of fibrous connective tissue is visible, which is arranged in thick bundles; the fibrous tissue is intermingled with foci of epithelioid cells and caseation; mesenterial lymph node; E 108/09, H&E (GMA). D: Cell- and fibre-rich fibrous connective tissue with small foci of epithelioid cell, surrounded by foci of caseation; mesenterial lymph node; E 108/09, H&E (GMA); bars in A = 2 mm, B = 1 mm, C = 200 µm, D = 100 µm.

4.3.2.2.4. Histo-type 4

Type 4 was also irregularly arranged like histo-type 3 (Fig. 41 A). Its crucial component was the extensive, irregularly formed areas of caseation (Fig. 41 B), which underwent extensive, also irregularly formed calcification. The arrangement of the epithelioid cells was apparently looser than in histo-type 2 (Fig. 41 C). Remnants of the original tissue were often found in the extensive caseation (Fig. 41 D). Paler areas in the caseation could be an indication of oedema

(Fig. 41 D). Extension and arrangement of the caseation might point to an acute progressive destruction of the tissue (acute exudative phase).
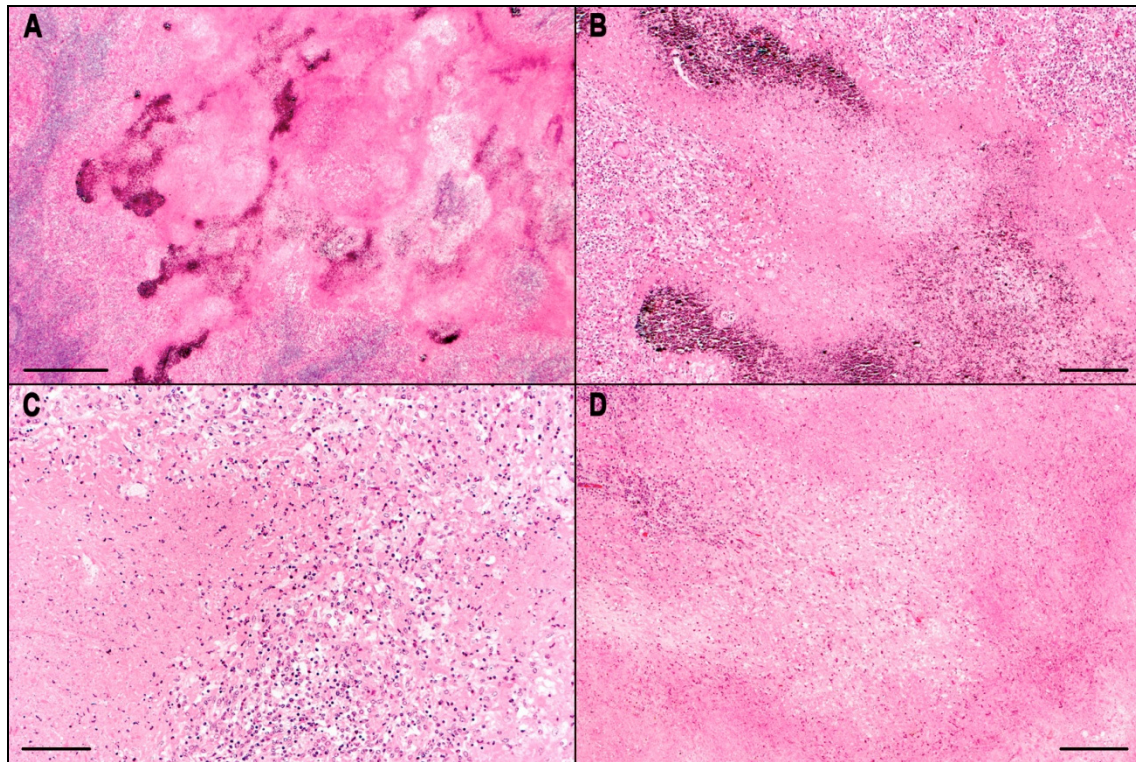
Figure 41. Histo-types in bovine tuberculosis:
A: Histo-type 4 is also completely disordered; calcification is striking, which is also extremely variable in shape. This histological picture presents the macro-pattern IV; mesenterial lymph node, S 785/13, H&E (GMA). B: Extensive, irregularly formed calcification is visible at the higher magnification; mesenterial lymph node, S 785/13, H&E (GMA). C: The caseation is not surrounded by a distinct reaction zone, epithelioid cells and lymphocytes are loosely arranged; mesenterial lymph node, S 785/13, H&E (GMA). D: Remnants of the original tissue are found in the very large foci with caseation, the pale areas display areas with oedema; mesenterial lymph node, S 612/14, H&E (GMA); bars in A = 1 mm, B and D = 200 µm, C = 100 µm.

4.3.2.3. Quantification of Histology Types

A total of 238 paraffin tissue sections from affected organs were examined for the histological diagnosis of bovine tuberculosis and also regarding the histological typing of the tuberculous inflammation.

The different histological types were present occasionally as individual types but often in a combination within an affected tissue. The occurrence of satellite epithelioid cell granulomatous inflammation (Histo-subtype 1b) together with type 2 was the most common combination type. As seen in Table 7, the most common types were subtype 1a and histo-type

2 (143/238 tissue sections). On the contrary, histo-type 4 was seen less common (41/238 tissue sections). Histological types 3 and type 4 were common especially within the mesenterial lymph nodes. On the other hand, these two types were not present in liver and intestine; in addition, histo-type 4 was also not present in the retropharyngeal lymph node. Furthermore, subtype 1a was not observed in the liver and the intestine.

Table 7. Quantification of the four histo-types of the tuberculous inflammation in individual organs.

Organ	Subtype 1a	Subtype 1b	Type 2	Type 3	Type 4
Lung	11	9	21	3	2
Mediastinal lymph node	19	11	29	15	1
Small intestine	-	1	1	-	-
Mesenterial lymph node	100	33	61	40	36
Liver	-	5	7	-	1
Portal lymph node	8	6	11	5	1
Retropharyngeal lymph node	5	3	13	6	-

4.3.2.4. Development of the Granulomatous Inflammation in Tuberculosis

The findings of the histological examinations reveal different possible developmental stages of the granulomatous inflammation. Depending on the organs involved, two major initial alterations exist.

The basic phenomenon of the granulomatous inflammation in bovine tuberculosis is the accumulation of epithelioid cells and/or multinucleated giant cells. As a second step commonly a central area of caseating necrosis develops often associated with neutrophils. Neutrophils might be a component in the development of caseous necrosis, but caseation without neutrophils also occurs. The caseation often underlies calcification. Thereafter, lymphocytes accumulate and formation of fibrous tissue takes place at the periphery of the tuberculous inflammation, thus forming a classical tubercle (Fig. 42 and 43).
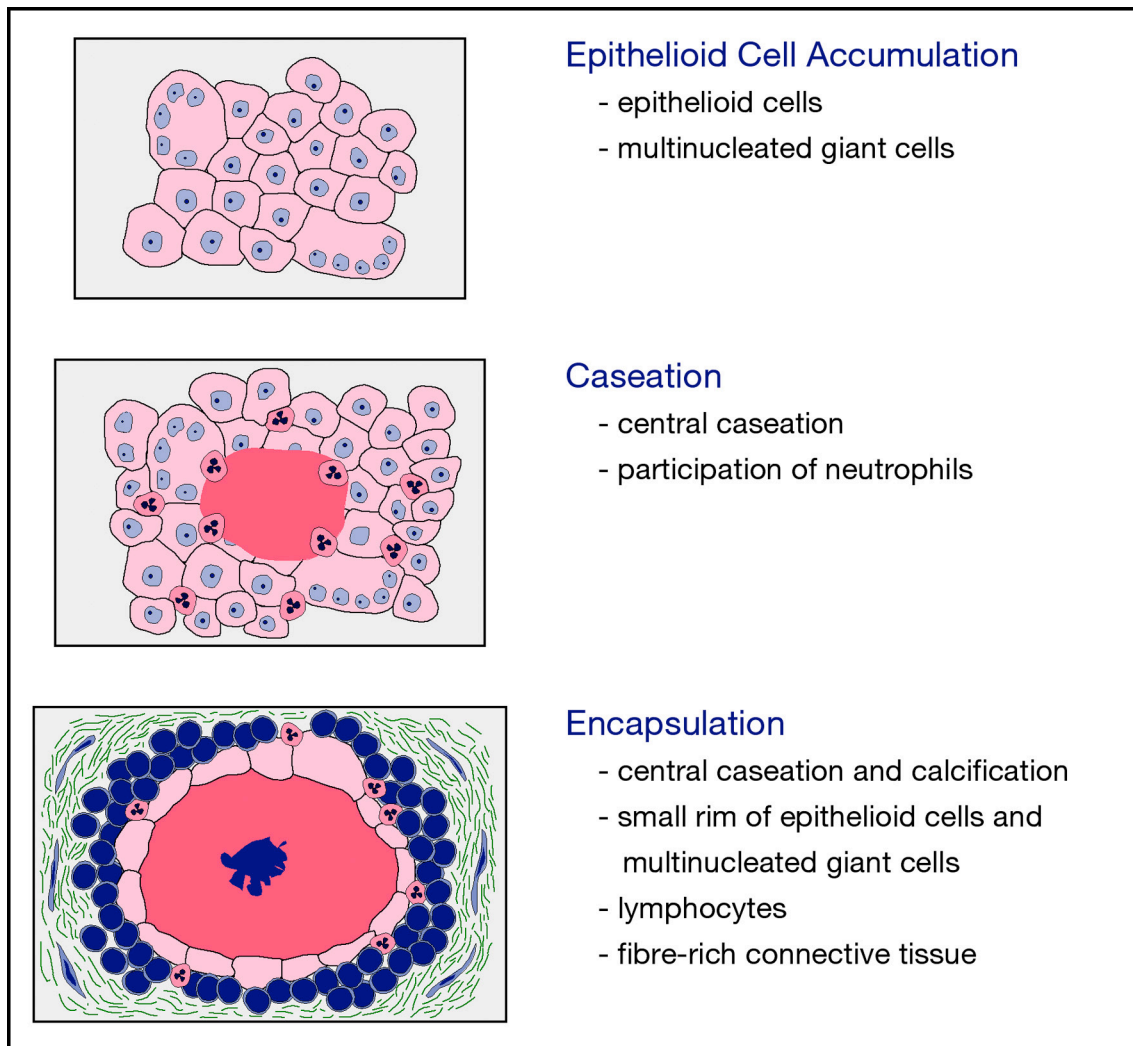
Figure 42. Representative scheme for the initial stages of tubercle in bovine tuberculosis:
First step is an epithelioid cell granulomatous inflammation, followed by the development of a central caseating necrosis often with neutrophil infiltration. Accumalation of lymphocytes and encapsulation by fibrous connective tissue is the last stage.
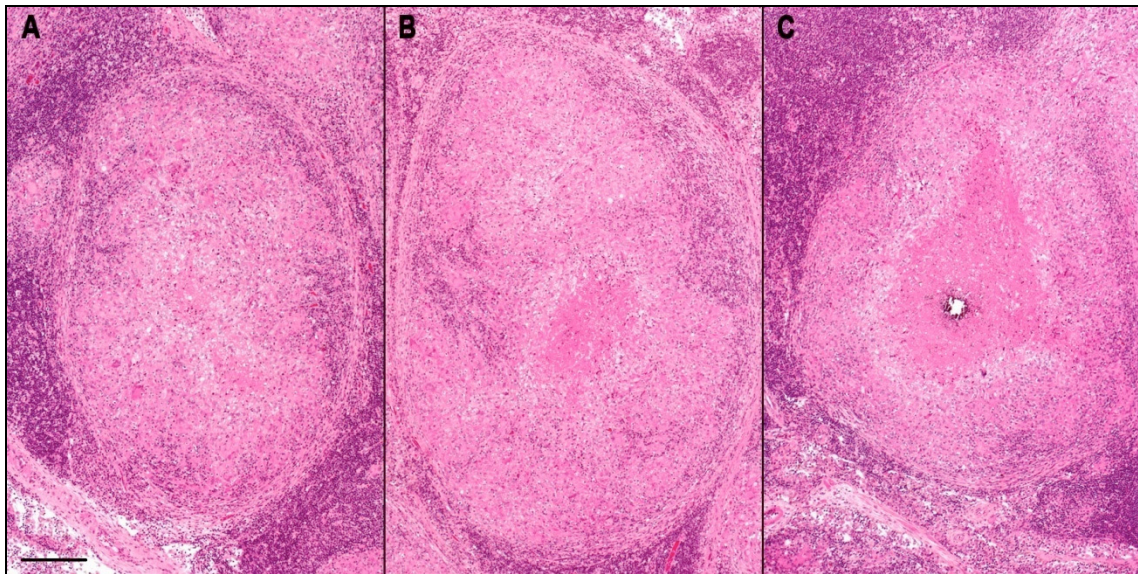
Figure 43. Initial stages in bovine tuberculosis:
Representative tissue sections to demonstrate the development of a tubercle. A: Infiltration of epithelioid cells and MNGCs. B: The beginning of caseous necrosis with neutrophil infiltration. C: The lymphocyte infiltration, beginning of fibrous encapsulation and calcification within the caseation; mesenterial lymph node, S 413/14, H&E (GMA); bar in A for A - C = 200 µm.

In the lung tuberculosis can start with a second, totally diffent initial lesion, the primary exudative-inflammatory reaction (according to PALLASKE, 1961), possibly due to the loose organization of lung tissue (Fig. 44). This picture is compatible with the macro-pattern VI.

The exudative-inflammatory reaction is characterised by an extensive alveolar oedema, local deposition of fibrin going along with necrosis of alveolar tissue leading to caseation, too. This is followed by the accumulations of the inflammatory cells, first epithelioid cells later lymphocytes and connective tissue (see also Fig. 44).

Normal Lung Tissue
loosely arranged

Exudativ-Inflammatory
Reaction (Pallaske)
- highgrade alveolar oedema
- deposition of fibrin
- necrosis of alveolar septae
  with caseation

Productive Reaction
- accumulation of epithelioid
  cells, lymphocytes, connective
  tissue in the periphery
- risk of intrusion into bronchioles
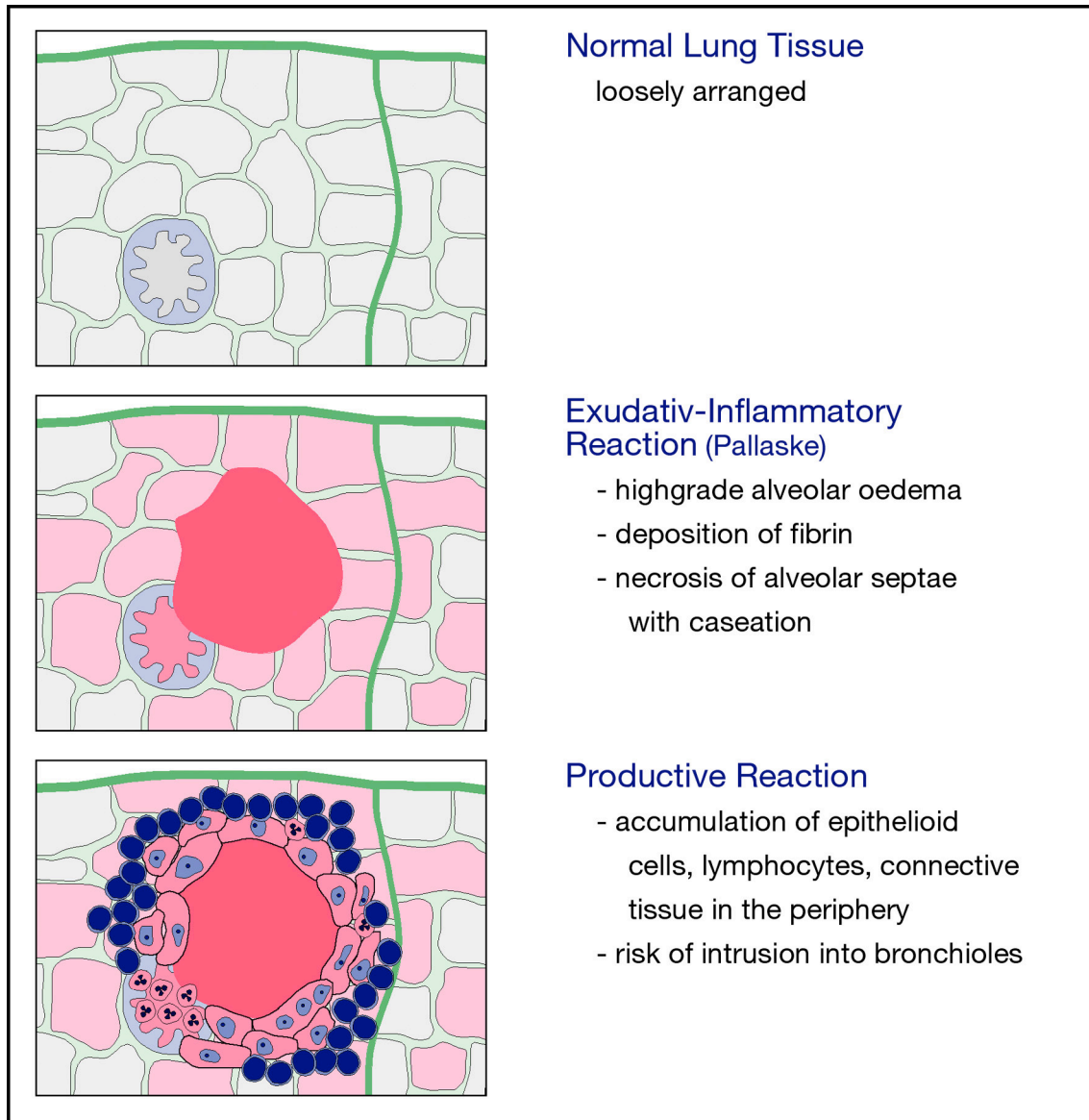
Figure 44. Development of the exudative tuberculous inflammation of the lung in bovine tuberculosis.

Accumulations of epithelioid cells and/or giant cells can develop in different localisations. A. The foci of macro-pattern I and II as classical tubercles, which correspond to histo-type 2, described above arise in the non-altered tissue. B. At the periphery of the larger tubercle as so-called satellite epithelioid cell granulomatous inflammation (see below), which corresponds to the histo-type 1b. C. Within the reparatively built fibre-rich connective tissue, this then leads to macro-pattern III and histo-type 3 as well.

According to macro-patterns I and presumably II the growth of tubercles can occur appositionally by means of satellite granulomas (histo-type 1b) (see below).

Accumulations of epithelioid cells and multinuclear giant cells within larger masses of reparatively built fibre-rich connective tissue may indicate a protracted-recurrent growth, according to macro-pattern III and histo-type 3 (see Figs. 8, 9 and 40).

Besides that, there are also extensive, rapidly growing foci of caseation with indistinct cellular demarcation, a rapidly progressive growth according to macro-pattern IV and histo-type 4 (see Figs. 10 and 41).

As described above, the growth in larger tubercles can take place appositionally. The appositional growth is characterised by an accumulation of the epithelioid cells and/or MNGCs, satellite epithelioid cell granulomatous inflammation (Histo-subtype 1b), within the inflammatory zone or fibrous capsule of the tubercle. Subsequently caseous necrosis occurs in the centre of this satellite epithelioid cell granulomatous inflammation, often accompanied by infiltration with neutrophils. This caseous necrosis extends and becomes integrated into the caseous necrosis of the large tubercle (Figs. 45 and 46).
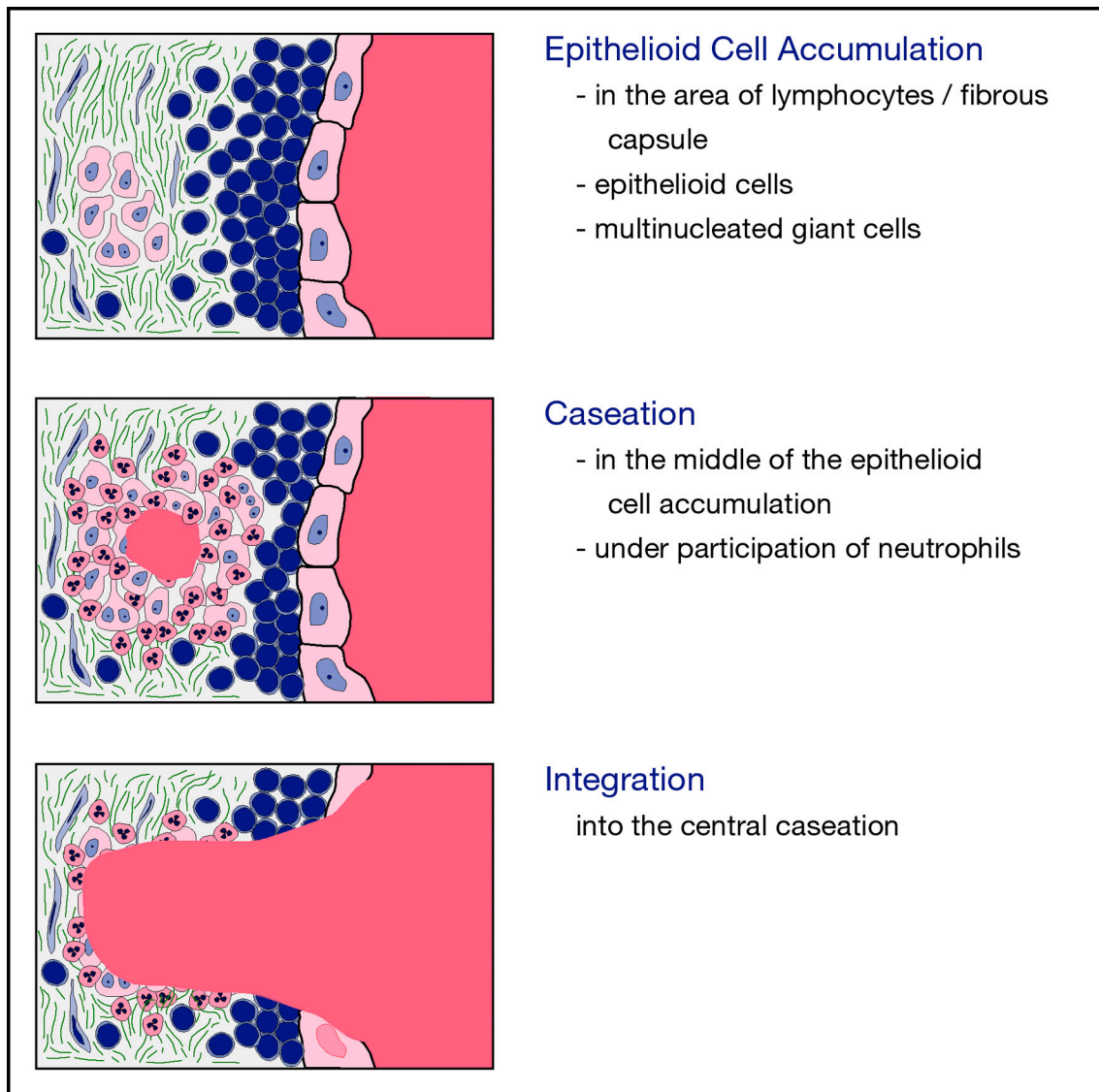
Figure 45. Scheme of the appositional growth of the tuberculous inflammation in larger tubercles:
Top: Occurrence of epithelioid cell granulomatous inflammation within the inflammatory zone of the
large tubercle; middle: Beginning of the caseous necrosis following neutrophil accumulation; bottom:
Integration into the caseation of the large tubercle.
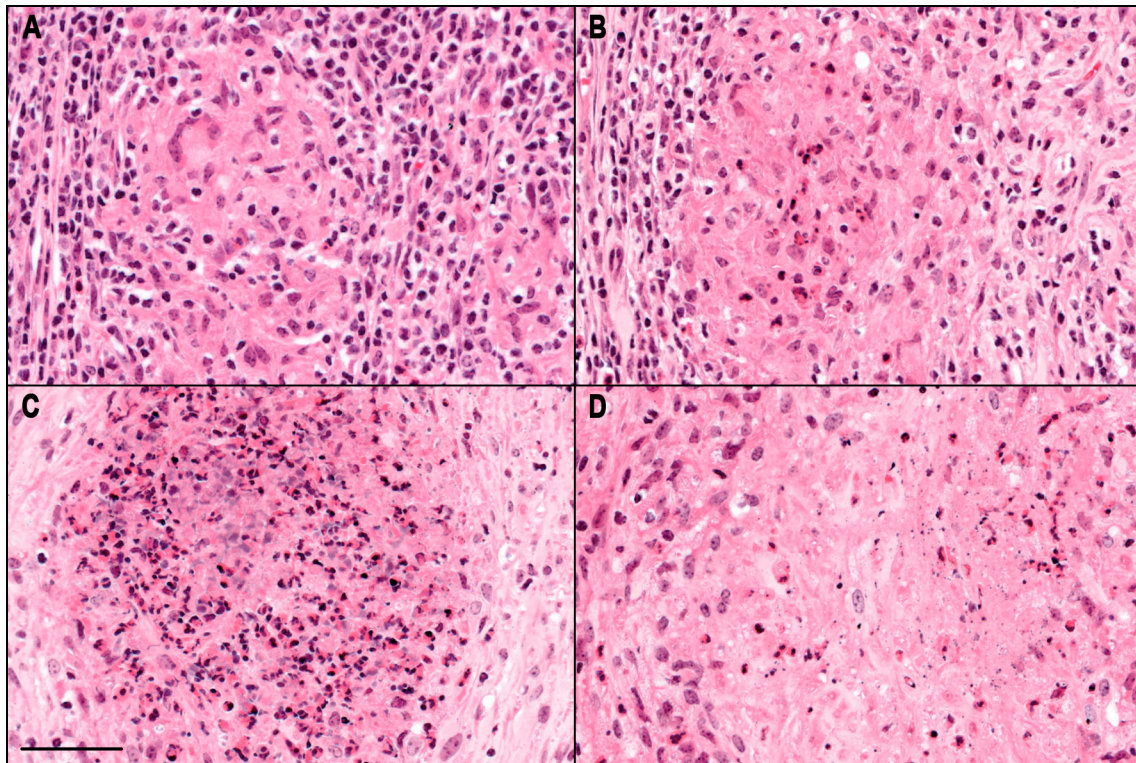
Figure 46. Appositional growth of the tuberculous inflammation in larger tubercles:
A: Accumulation of epithelioid cells and multinucleated giant cells in the inflammatory zone consisting mainly of lymphocytes (satellite focus). B: Beginning infiltration of a satellite focus by neutrophils. C: Massive infiltration by neutrophils with destruction of epithelioid cells and giant cells. D: Caseation of the focus, epithelioid cells are not longer detectable, neutrophils only as clastic cell remnants, the caseation has become contact with the central caseation in the large tubercle on the right side; liver, E 110/09, H&E (GMA), bar in C for A-D = 50µm.

In addition to the local growth of the tuberculous foci (see above), a dissemination of the tuberculosis can also occur in the body. This dissemination can occur through lympho-haematogenous way according to the macro-pattern II, for example in the regional lymph node, or in the lung following intrusion in the bronchioles also through canalicular way (see Fig. 47 und 52).

4.3.3. Tuberculous Alterations of Individual Organs

4.3.3.1. Lung

Lung samples from 11 cattle showed tuberculous alterations. All macro-patterns described in Chapter 4.3.1.1 were found (Fig. 47 und 48). In addition, there was an acute inflammatory type of tuberculosis in the lung, the so-called exudative reaction type, which was

macroscopically characterised by a brownish colour, by a high water content and by pale foci of caseation (Fig. 47 A, see also Fig. 12 A).
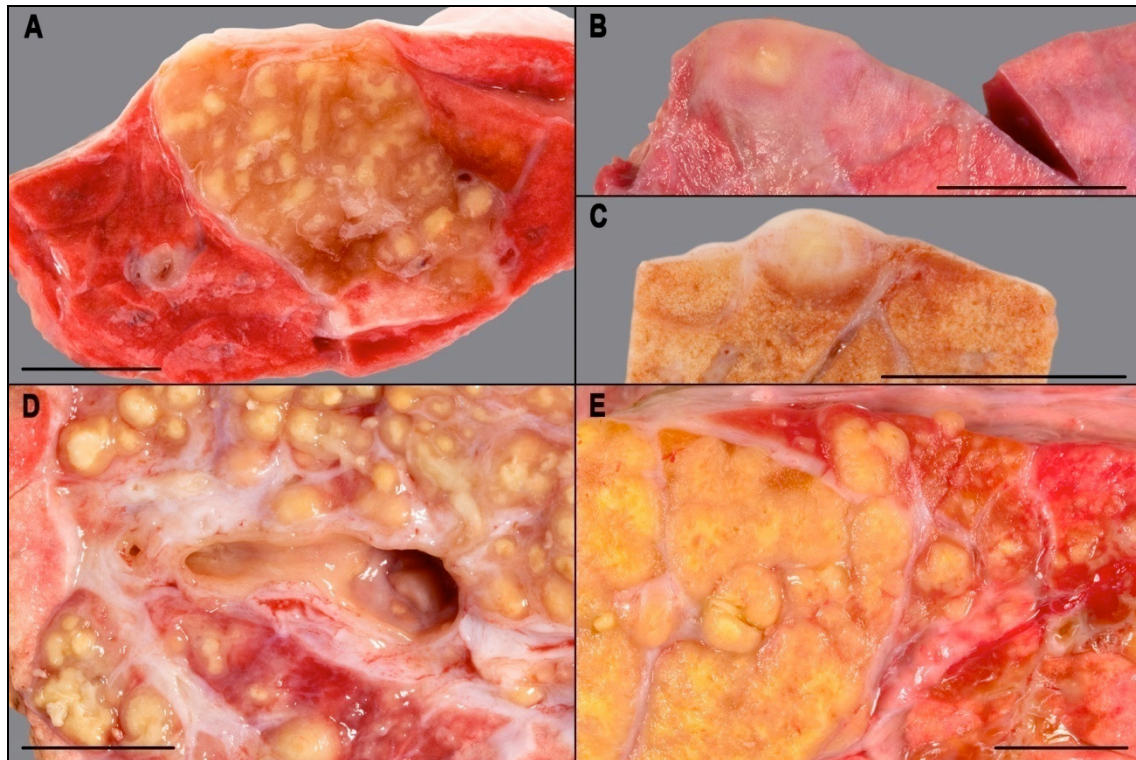
Figure 47. Macroscopic lung alterations in bovine tuberculosis:
A: Focal acute exudative reaction with oedema and irregularly shaped foci of caseating necrosis; lung, S 1256/12. B: Solitary tubercle, view on the lung surface, the diameter of the focus is approximately 4 mm; lung. C: Cut surface of the same focus as in B, an indistinctive layering is visible (Macro-pattern I); lung. D: Multiple tubercles with a small diameter, the layering can be seen partly (Macro-pattern II), an intrusion of the tuberculous inflammation in the small bronchus can be seen; lung, S 605/13. E: Large focus of a disarranged tuberculous inflamed tissue, compatible with macro-pattern III; lung, E 322/09; bars in A-E = 1 cm (specimens fixed in Klotz´s solution).

On the cut surface, occasional intrusions of the tuberculous inflammation into the conducting airways could be found (Fig. 47 D). Another typical finding for the lung was the occurrence of melting cavities, the so-called cavitating tuberculosis (Fig. 48). Cavities were found either in the centre of tubercles (Fig. 48 A) or they incorporated areas with a size of a whole lung lobule (Fig. 48 B).
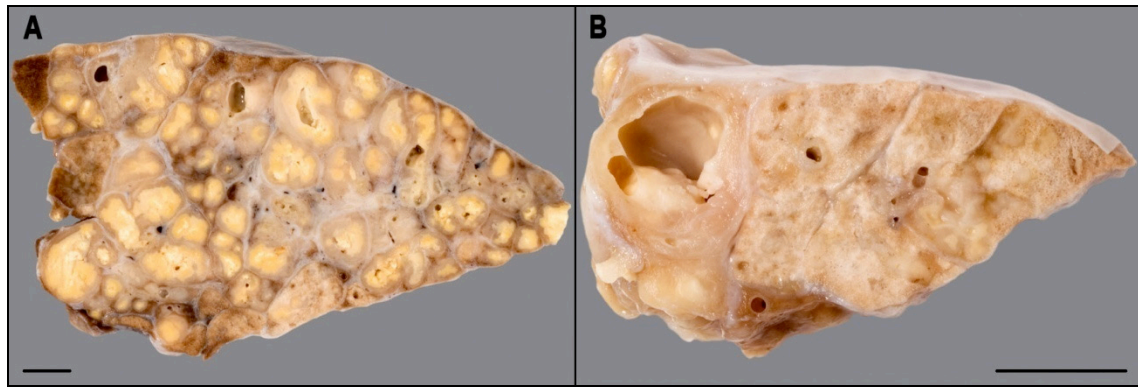
Figure 48. Macroscopic lung alterations in bovine tuberculosis:
A: Multiple tubercles with distinctive layering comprising the entire cut surface of the lung lobe (Macro-pattern I), cavities are visible in several tubercles; lung, S 422/14. B: Large focus with a cavitating tuberculosis; lung, S 600/14; bars in A and B = 1 cm. (specimens fixed in formalin).

Histologically, all four in Chapter 4.3.2.2. described histo-types could be found in the lung (Figs. 49 to 51). The most encountered histological granulomatous inflammation type was histo-type 2 (see Table 7 and Fig. 49).
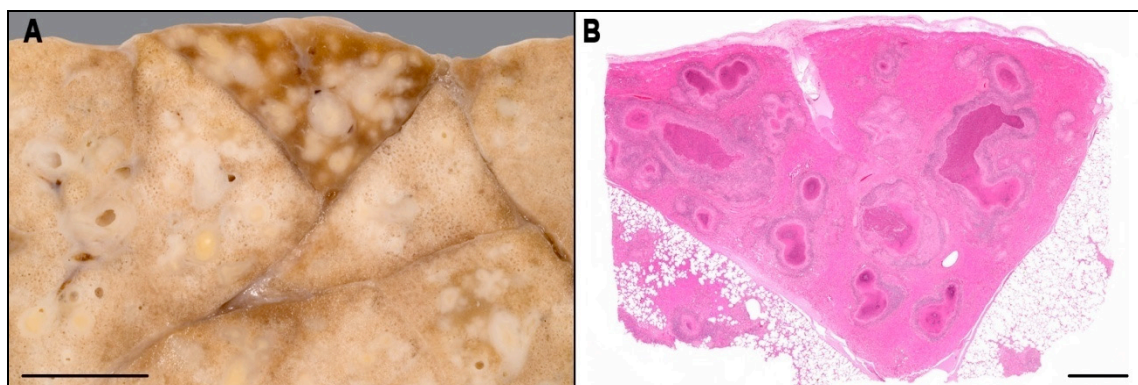
Figure 49. Lung alterations in bovine tuberculosis:
A: Single lung lobule with multiple small tubercles, accordant with macro-pattern II, lung, S 770/13. B: The same lung lobule as in A, numerous layered tubercles are visible (histo-type 2); lung, S 770/13, H&E (GMA); bars in A = 1 cm, B = 2 mm.

Histo-type 2 resulted from solitary or satellite foci of epithelioid cell granulomatous inflammation (Histo-subtypes 1a and 1b) (Fig. 50). The epithelioid cell granulomatous inflammation underwent caseation in variable extent (Fig. 50 C and D). Furthermore, alterations of histo-types 1 and 2 occurred side by side.
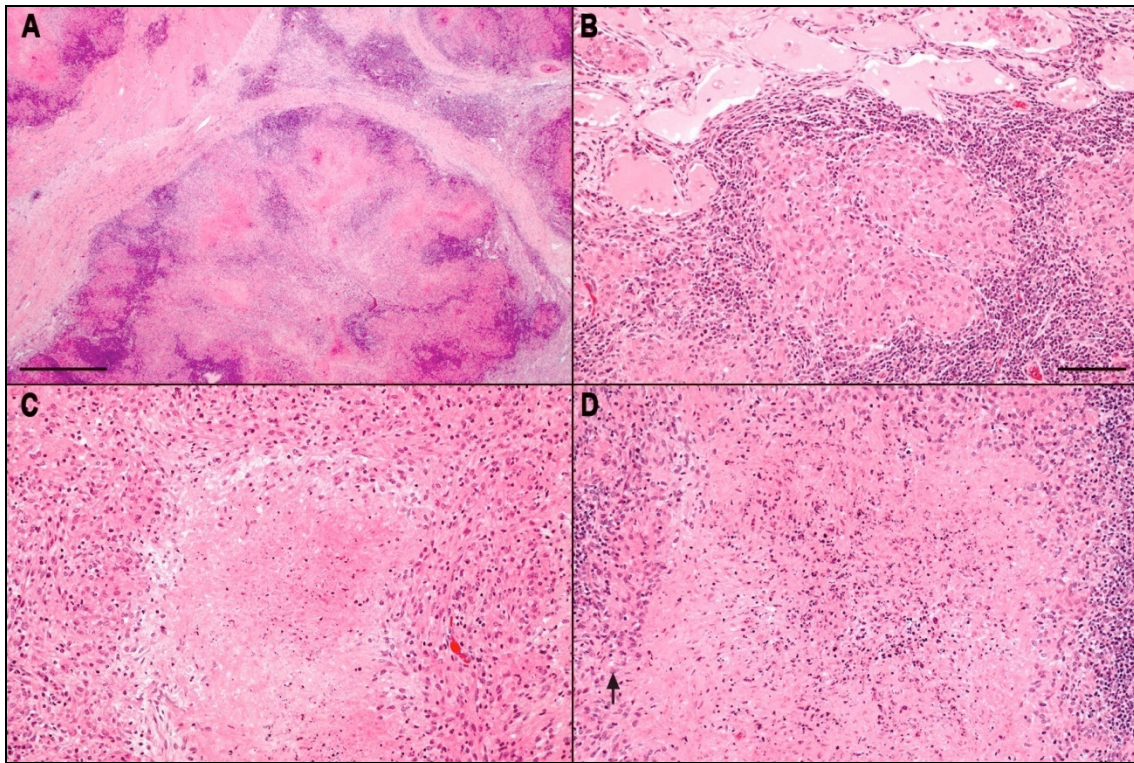
Figure 50. Lung alterations in bovine tuberculosis:
A: Large focus with epithelioid cell granulomatous inflammation (Histo-subtype 1a); lung, E 322/09, H&E (GMA). B: Solitary focus of an epithelioid cell granulomatous inflammation, surrounded by lymphocytes, a caseation is not visible; pulmonary alveolar oedema at the top of the picture; lung, E 322/09, H&E (GMA). C: Focal epithelioid cell granulomatous inflammation with central caseating necrosis; lung, E 322/09, H&E (GMA). D: Focal epithelioid cell granulomatous inflammation with extensive caseation, a few epithelioid cells (arrow) in the periphery; lung, E 322/09, H&E (GMA); bars in A = 1 mm, in B for B, C and D = 100 µm.

Besides the reaction types described above, an additional type was observed in the lung - the exudative reaction type (Fig. 51). The characteristic findings were an extensive amorphous, lightly eosinophilic alveolar oedema with occasionally foamy alveolar macrophages and hyperaemic alveolar capillaries. Therein lay small highly eosinophilic foci with necrosis of the alveolar septa and deposition of small irregular fibrils (fibrin) (Fig. 51 B). Other foci contained a high number of neutrophils (Fig. 51 C) or epithelioid cells surrounded by lymphocytes (Fig. 51 D).
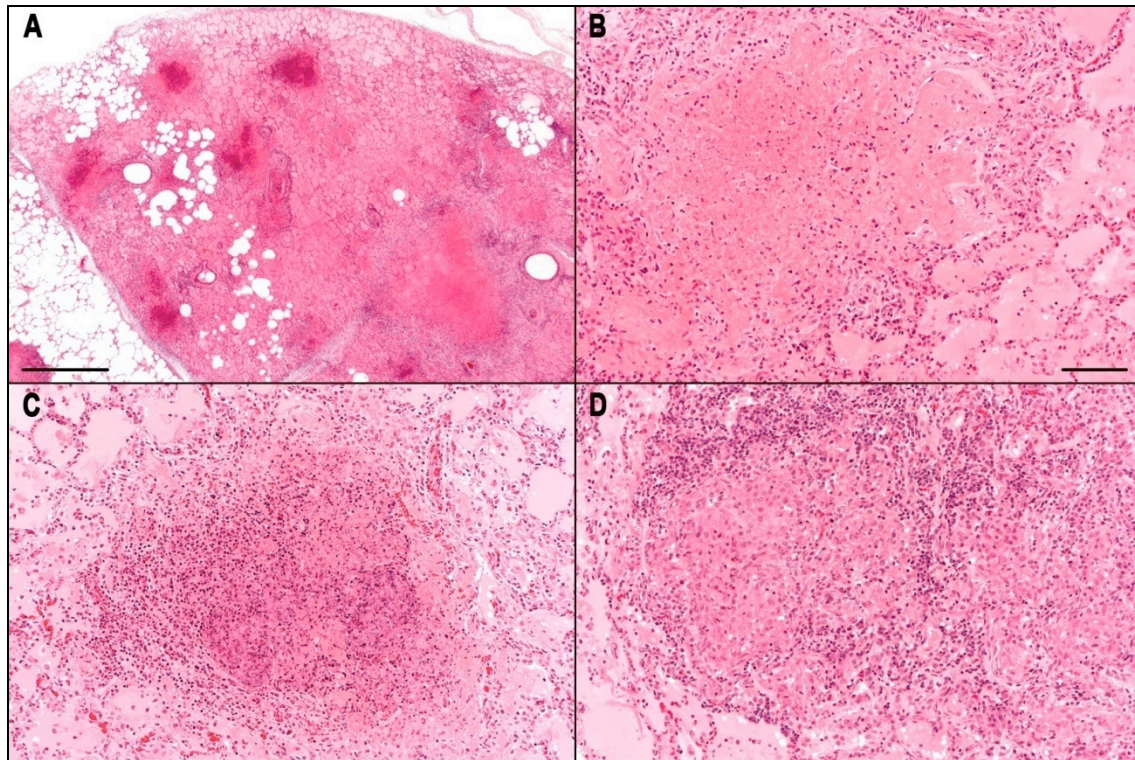
Figure 51. Lung alterations in bovine tuberculosis:
A: Acute exudative reaction of the lung, an overview with an extensive pulmonary alveolar oedema and numerous fresh foci with a beginning caseation; lung, E 322/09, H&E (GMA). B: Fresh focus with fibrin deposition within the oedema fluid and necrosis of alveolar septae; inflammatory cells are sparsely detectable; lung, E 322/09, H&E (GMA). C: Fresh focus with necrosis of alveolar septae and extensive aggregates of neutrophils; lung, E 322/09, H&E (GMA). D: Focus, which predominantly consists of epithelioid cell and is surrounded by lymphocytes, in the immediate vicinity of fresh caseous foci; lung, E 322/09, H&E (GMA); bars in A = 1 mm, in B for B, C and D = 100 μm.

Another typical form of the tuberculous inflammation of the lung was the inflammatory intrusion into the airways (Fig. 52). The destructed bronchi and bronchioles were characterised by the absence of smooth muscle, cartilage (in bronchus) and the loss of the lining columnar epithelium. These structures were replaced by an amorphous, eosinophilic material consisting of destroyed cells, oedema, fibrin and intact as well as disintegrated neutrophils (Fig. 52 B and C). In some cases, the inflammation was of the acute type (Fig. 52 B) in others of an older one (Fig. 52 C). Sometimes small accumulations of epithelioid cells within alveolar lumina occurred (Fig. 52 D).
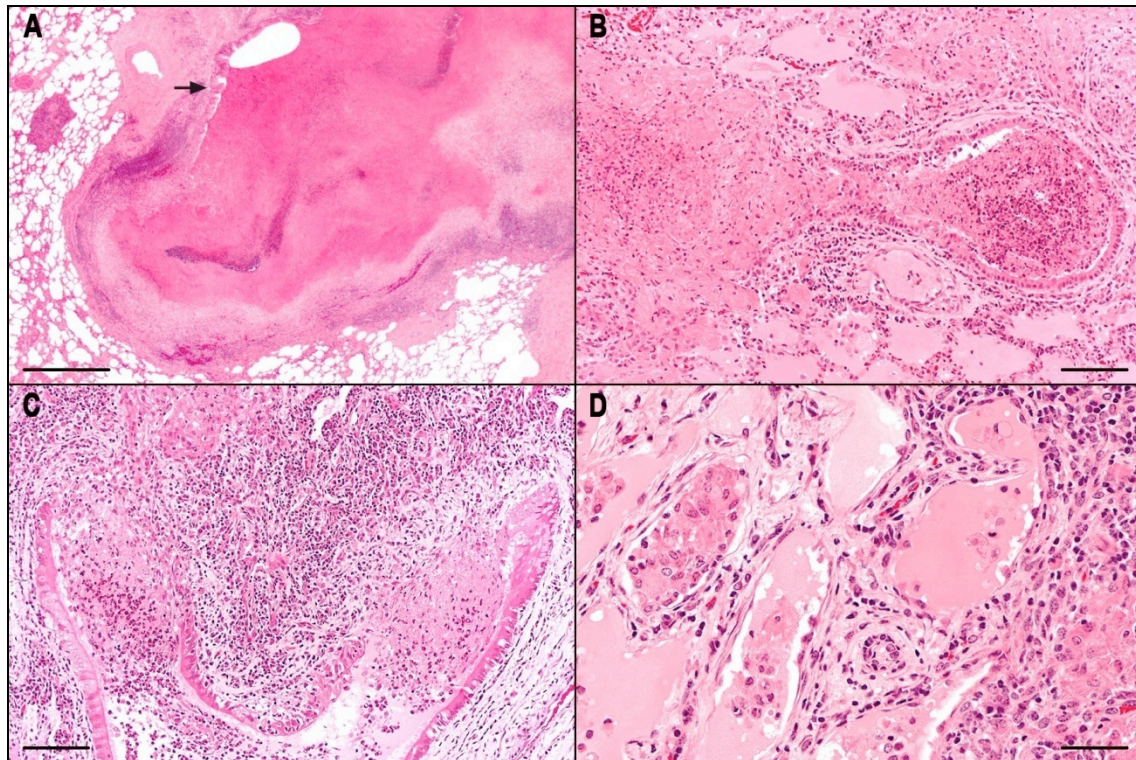
Figure 52. Lung alterations in bovine tuberculosis:
A: Intrusion of the tuberculous inflammation into the airways, small bronchus, extensive caseous necrosis of the bronchus wall, there are only remnants of the original epithelium left (arrow); lung, E 322/09, H&E (GMA). B: Intrusion of an acute exudative inflammation in a bronchiole with destruction of its wall; lung, E 322/09, H&E (GMA). C: Chronic tuberculous inflammation, which invades a bronchiole; lung, E 322/09, H&E (GMA). D: Aggregates of epithelioid cells in the lumen of an alveole adjacent to a tuberculous inflammation (right side of the picture); lung, E 322/09, H&E (GMA); bars in A = 1 mm, B and C = 100 µm, D = 50 µm.

An additional typical tuberculous lesion of the lung was the liquefaction of tissue that underwent caseous necrosis leading to a cavitating tuberculosis (Fig. 53). Macroscopically, the roundish cavities were found in the centre of larger tubercles (Fig. 53 A). Histologically the cavities were lined by intact and disintegrated neutrophils intermingled with fibrin, followed by epithelioid cells and occasionally multinucleated giant cells, lymphocytes and plasma cells, the outer layer was the fibrous capsule (Fig. 53 B to D).
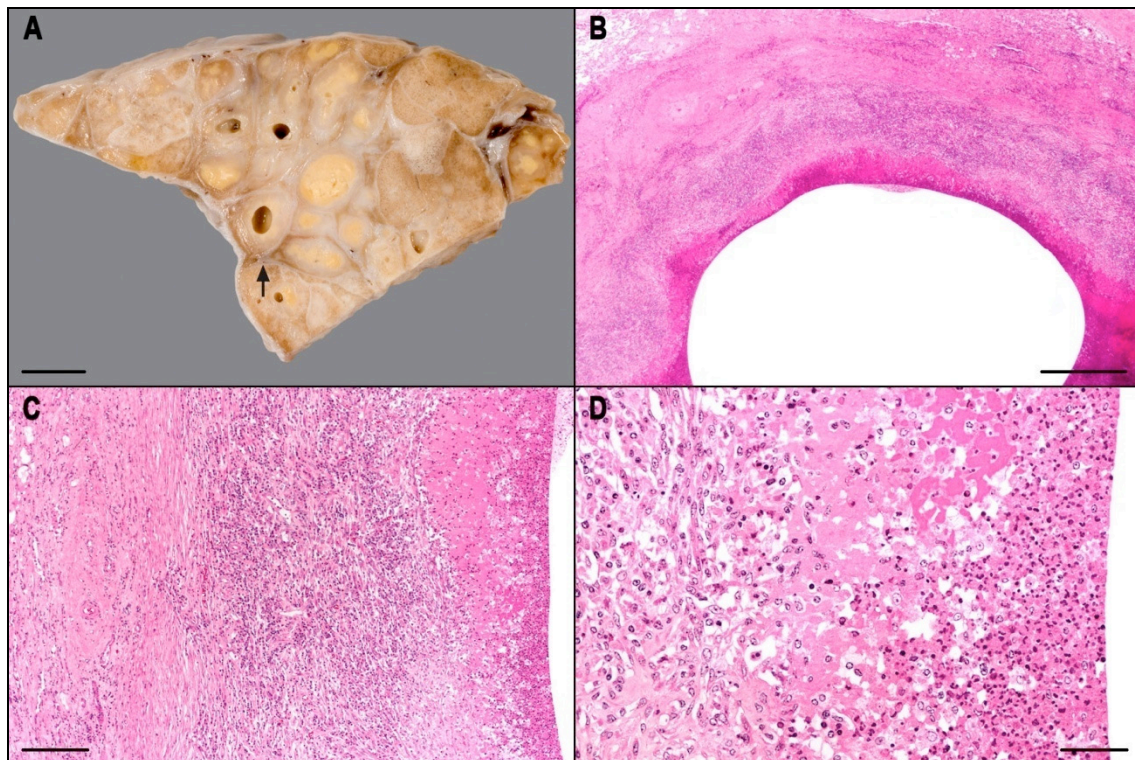
Figure 53. Lung alterations in bovine tuberculosis:
A: Liquefaction of the caseous necrosis of tubercles as a first step in the formation of a cavitating tuberculous pneumonia, macroscopic picture with multiple cavities (arrow); lung, S 770/13. B: Overview of the border of a liquefied focus of caseous necrosis; lung, S 770/13, H&E (GMA). C: The demarcation of the cavity consists of neutrophils, fibrin and necrotic cells, followed by lymphocytes and fibroblasts with few collagen fibres as well as an outer fibrous capsule (left side of the picture); lung, S 770/13, H&E (GMA). D: At high magnification, the inner side of the border with neutrophils and fibrin, followed by lymphocytes and fibroblasts (left side of the picture); lung, S 770/13, H&E (GMA); bars in A = 1 cm, B = 1 mm, C = 200 µm, D = 50 µm.

4.3.3.2. Serosa

The classical tuberculous alteration of serous membranes is the pearl disease. It could be seen in the thoracic cavity of one cow (Fig. 54). Nodular alterations from 5 mm to maximal 20 mm in a diameter occurred focally on the pulmonary pleura (Fig. 54 A) and on the parietal pleura of the diaphragm. Their cut surface corresponded predominantly to the nodules of macro-pattern I and occasionally also the foci of the macro-pattern III (Fig. 54 B and C). At the lung, the nodules were not only directly on the pleura (Fig. 53 A), but also formed lobulated annexes (Fig. 54 B). Their histology corresponded to the macroscopical picture, the classic tubercle predominated (Histo-subtype 1a) (Fig. 54 D), foci with a disordered structure of the tuberculous tissue could also occasionally be found (Macro pattern III).
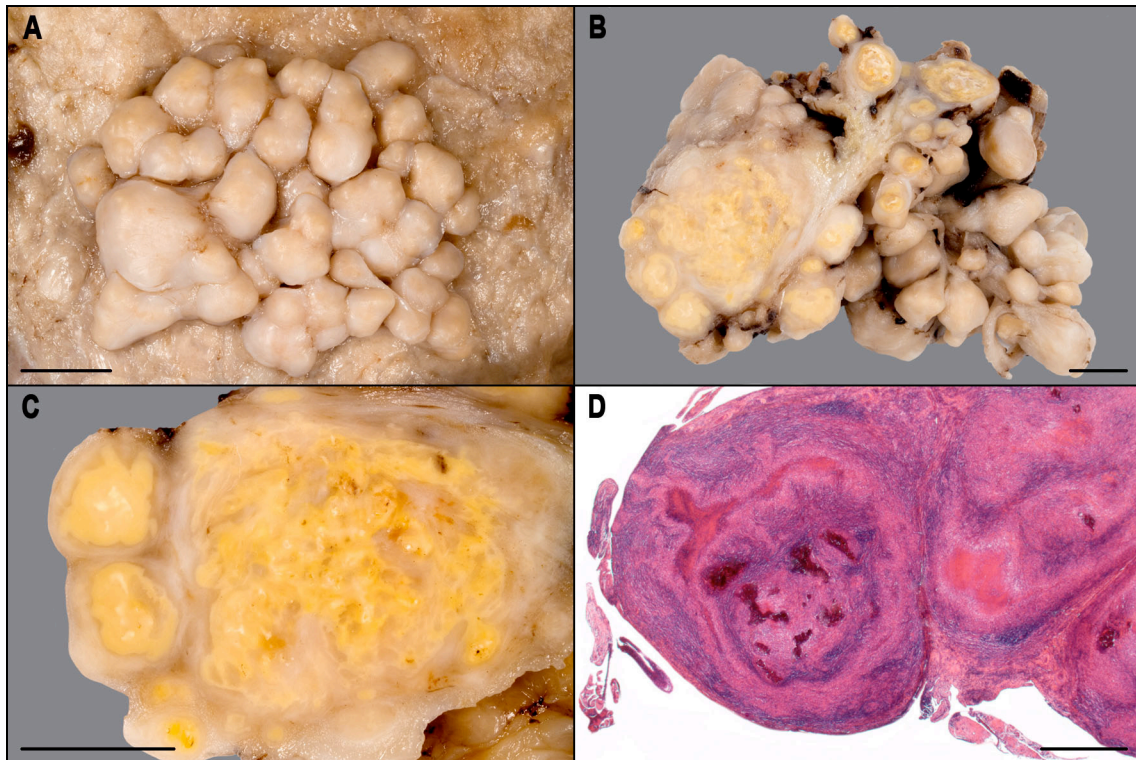
Figure 54. The classic picture of pearl disease, only found in one animal:
A: Numerous spherical structures on the pulmonary pleura; lung, S 770/13. B: The cut surface of the foci showed a distinct caseation; lung, S 770/13. C: Cut surface at higher magnification, besides the roundish foci with layering structure (tubercle, left side of the picture), there were also alterations of macro-pattern III with a disordered structure of the tuberculous tissues (middle of the picture); lung, S 770/13. D: The individual foci of the pearl disease showed predominantly layering structure of the classical tubercle (Histo-subtype 1a); pleura, S 770/13, H&E (Paraffin); bars in A, B and C = 1 cm, D = 1 mm.

4.3.3.3. Small Intestine

Only one tuberculous lesion in one animal could be found in the small intestine (Fig. 55). It was a small, roundish focus with a diameter of approximately 4 mm (Fig. 55 A). On the cut surface (Fig. 55 B), caseation and calcification were visible in the centre of the focus, compatible with the macro-pattern I. Histologically, there was a focal, roundish lesion within the mucosa and the sub-mucosa at the edge of a Peyer´s patch (Fig. 55 C). The tuberculous granuloma was compatible with the criteria described as histo-type 2 and subtype 1b. No severe destruction of villus epithelium and moderate numbers of macrophages, lymphocytes in the lamina propria were observed. The number of acid-fast bacteria that could be demonstrated within the lesion was very low, only single bacteria within an epithelioid cell (Fig. 55 D).
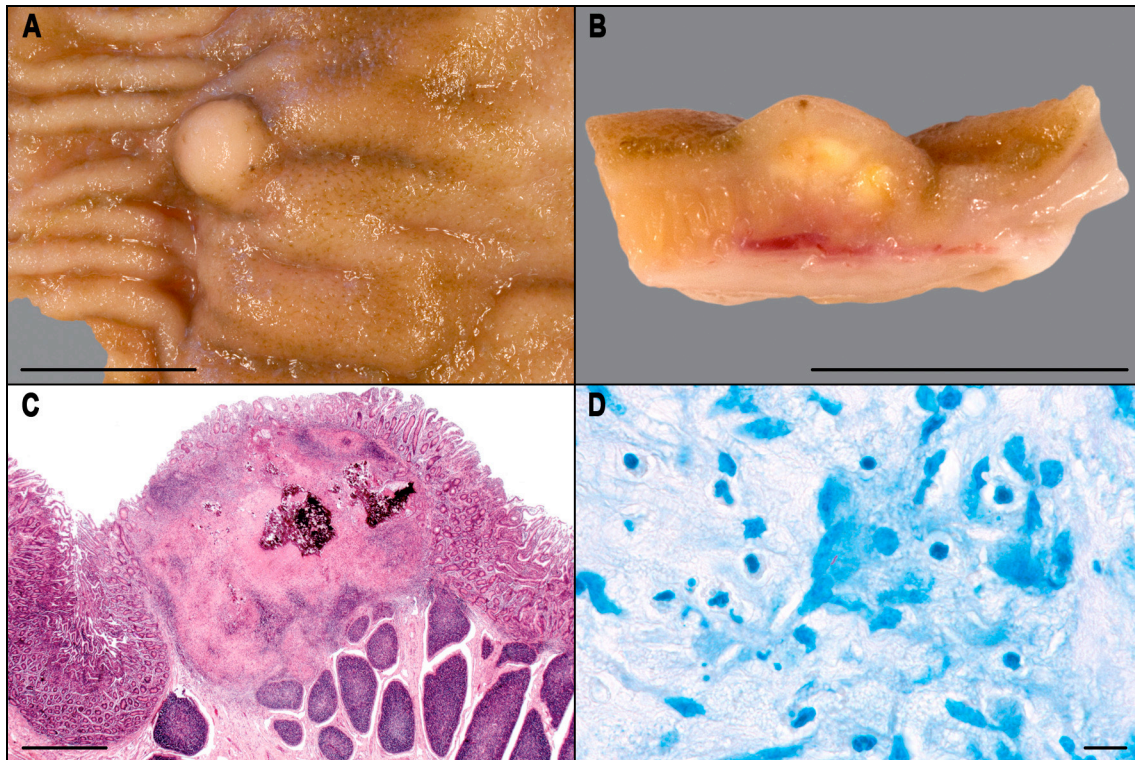
Figure 55. Small intestine alterations in bovine tuberculosis:
A: A single tuberculous focus in small intestine, its diameter is approximately 4 mm. The spherical covering mucous membrane is intact; small intestine, E 102/09. B: Cut surface of the same focus as in A, caseation and calcification can be seen in its centre; small intestine, E 102/09. C: The histological overview shows a typical tubercle with central caseation and calcification, a clear capsule is not visible; the mucous membrane is intact; the focus is found at the edge of a Peyer's patch (bottom right); small intestine, E 102/09, H&E (Paraffin). D: The numbers of acid-fast bacilli, which are found in this focus, are extremely low. In the picture, an acid-fast bacillus in the cytoplasm of an epithelioid cell; small intestine, E 102/09, FF staining (Paraffin); bars in A, B = 1 cm, C = 1 mm, D = 10 μm.

4.3.3.4. Liver

Tuberculous alterations in the liver could be found in a total of 5 animals (Fig. 56). All of them consisted of typical tubercles, which were associated with macro-pattern I. The foci were well visible layered (Fig. 56 A), with caseation and calcification in the centre, the pale brown reaction-zone with inflammatory cells and a well visible fibrous capsule. The foci were in variable in their size (Fig. 56 B), up to 2 foci per liver could be found.

Histologically, the foci showed also a distinctive concentrically layered structure, they were compatible with histo-type 2 and subtype 1b.
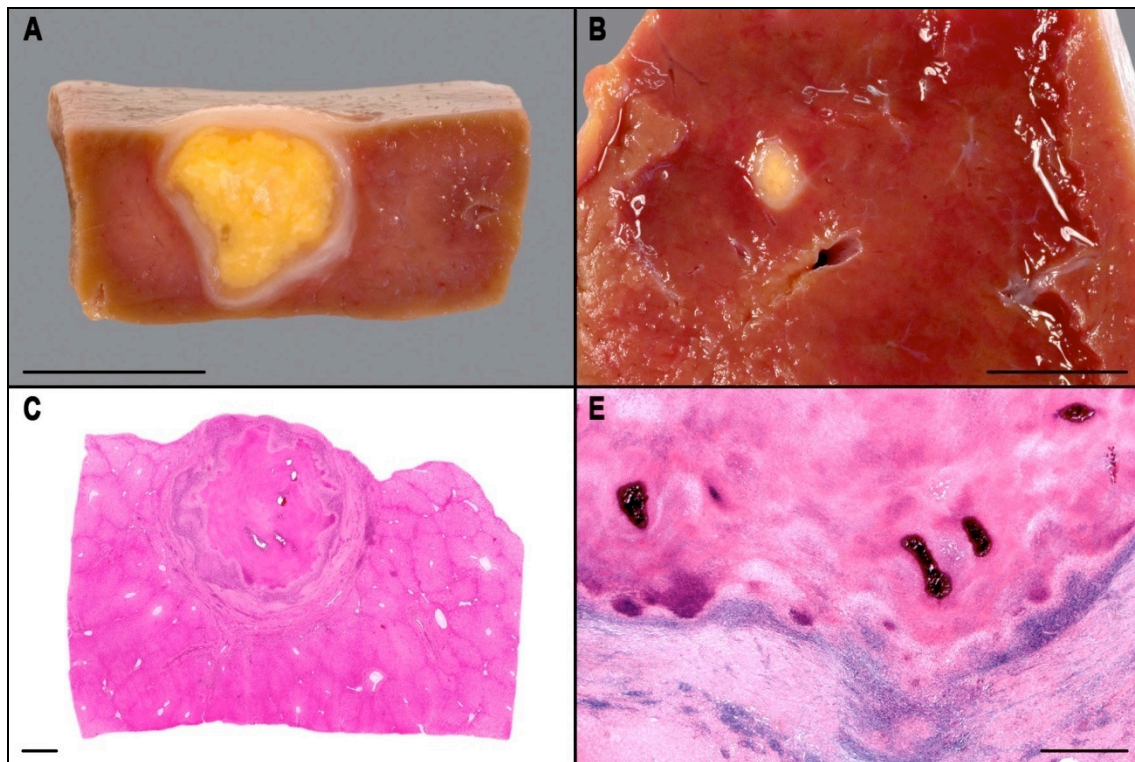
Figure 56. Liver alterations in bovine tuberculosis:
A: Tuberculous foci in the liver were only compatible with macro-pattern I, large foci with an onionskin-like structure. There is yellowish, dry caseation with whitish foci of calcification in the centre, which is surrounded by the reaction zone, predominantly consisting of epithelioid cells, lymphocytes and the fibrous capsule at the outer as well; liver, E 110/09 (the organ was fixed in Klotz´s solution). B: The foci in the liver are in different sizes, a small focus is found in the liver of this animal; liver, E 322/09 (the organ was fixed in Klotz´s solution). C: Histological overview of a typical tuberculous focus (tubercle) in the liver, with its layering structure; liver, E 110/09, H&E (GMA). D: Higher magnification of the focus with central caseation and calcification, the light zone of epithelioid cells, the lymphocytic zone and at the outer fibrous capsule, the typical structure of a tubercle; liver, E 110/09, H&E (Paraffin); bars in A and B = 1 cm, C = 2 mm, D = 1 mm.

4.3.3.5. Lymph Nodes

Paraffin and GMA tissue sections from mesenterial (132), mediastinal (40), portal (14) and retropharyngeal (14) lymph nodes were examined from 81 cattle. All five macro-patterns (see 4.3.1.1.) occurred in the lymph nodes (Fig. 57). Also all four different histo-types of the granulomatous inflammation occurred in the lymph nodes (except histo-type 4 in the retropharyngeal lymph nodes).
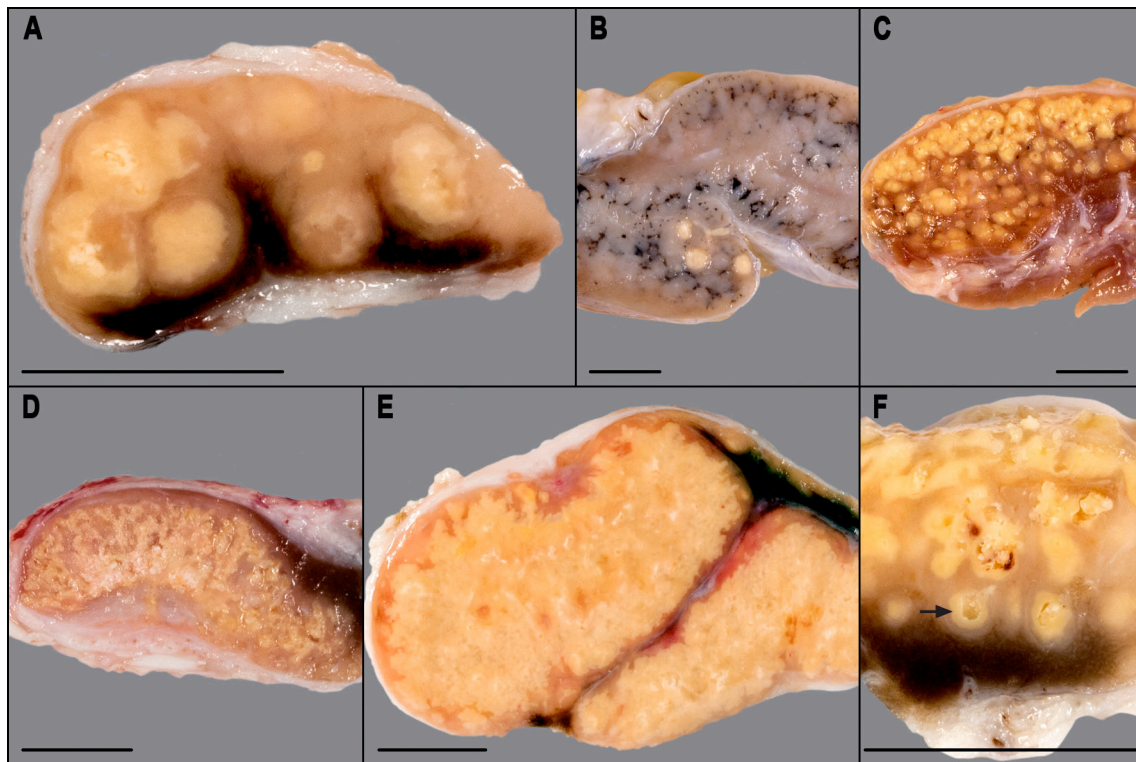
Figure 57: Lymph node alterations in bovine tuberculosis. All five macro-patterns occurred in lymph nodes:
A: Macro-pattern I with large roundish foci with a distinct cup shaped structure; mesenterial lymph node, E 113/09. B and C: Macro-pattern II with only a few or numerous small roundish foci, the layering structure can macroscopically not easily be recognized; mediastinal lymph node, S 1256/12. D: Macro-pattern III with an irregular and not circular arranged tuberculous tissue; mesenterial lymph node, E 97/09. E: Macro-pattern IV shows caseation in the larger part of the tissue section; mesenterial lymph node, E 110/09. F: Macro-pattern V with cavity formation (arrow); mesenterial lymph node, S 412/14; bar for A - F = 1 cm.

4.3.4. Detection of Mycobacteria and Mycobacterial Antigens

4.3.4.1. Acid-fast Staining Modified According to Fite-Faraco (FF Staining)

Acid-fast bacilli were detected in at least one organ of 70 out of the 84 cattle with tuberculous lesions comprising 163 out of the 238 investigated tissue sections (see also RIESEBERG, 2016). They appeared as lightly curved or rod-shaped. Except for a few cases, only sparse acid-fast bacilli were found in the granulomatous lesions, as described in detail in the study of RIESEBERG (2016).

Bacteria were most frequently found in the caseation (Fig. 58 A to C), including the calcification (Fig. 58 D). Often several bacteria in the positive cases could easily be found in both localisations, wherein the bacteria were then often agglomerated in foci.
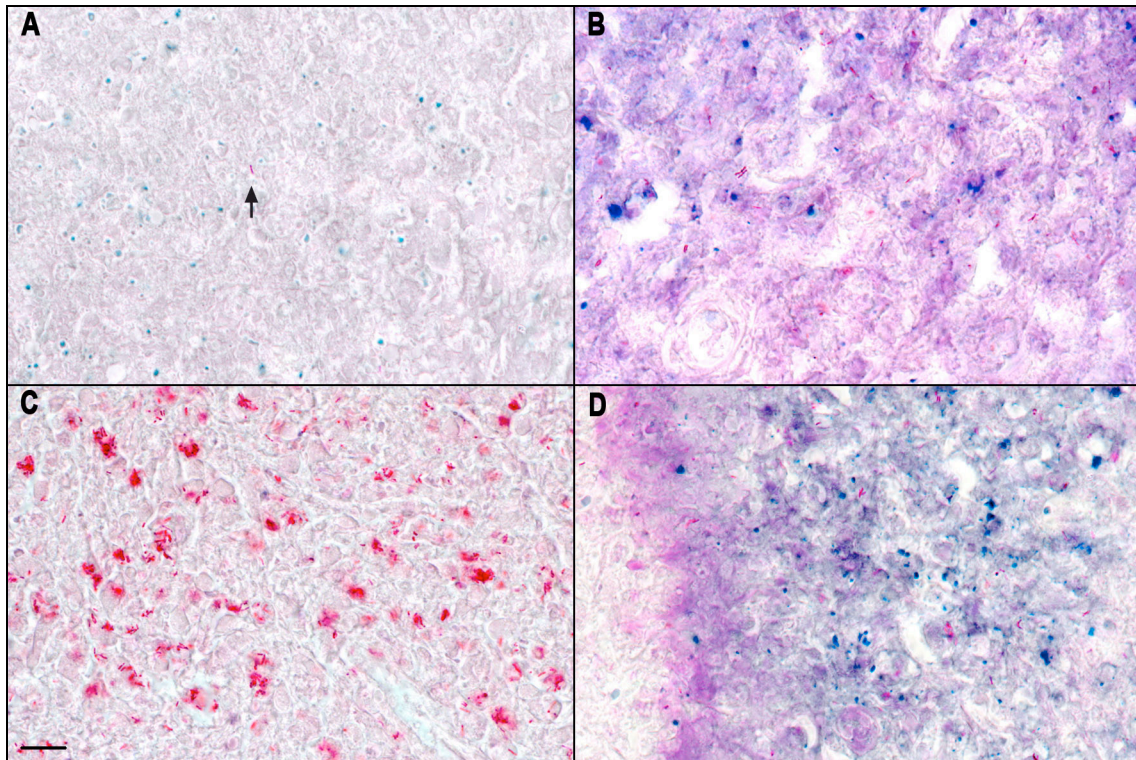
Figure 58. Demonstration of acid-fast bacteria in bovine tuberculosis:
A: Bacteria within the caseous necrosis, a single bacterium (arrow); mesenterial lymph node, S 128/13, FF (Paraffin). B: Medium amount of bacteria; mesenterial lymph node, S 179/13 FF (Paraffin). C: The single tissue with a high bacterial load; mesenterial lymph node, E 102/09, FF (Paraffin). D: Bacteria within the calcified area of a caseous necrosis; mesenterial lymph node S 179/13, FF (Paraffin), acid-fast staining; bar in C for A-D = 10 µm.

Predominantly single or rarely more bacteria could be observed in the cytoplasma of epithelioid cells (Fig. 59 A), on the other hand much more single bacteria in the cytoplasm of multinucleated giant cells (Fig. 59 B). Infrequently, remnants of bacteria appeared in the cytoplasm of degenerated neutrophils (Fig. 59 C). Bacteria were found at the border of viable epithelioid cells and the central caseation (Fig. 59 D). Low numbers of acid-fast bacilli were also detected in the high-grade alveolar oedema of the lung. Bacteria could never be found in the zone with lymphocytes or the fibrous capsule.
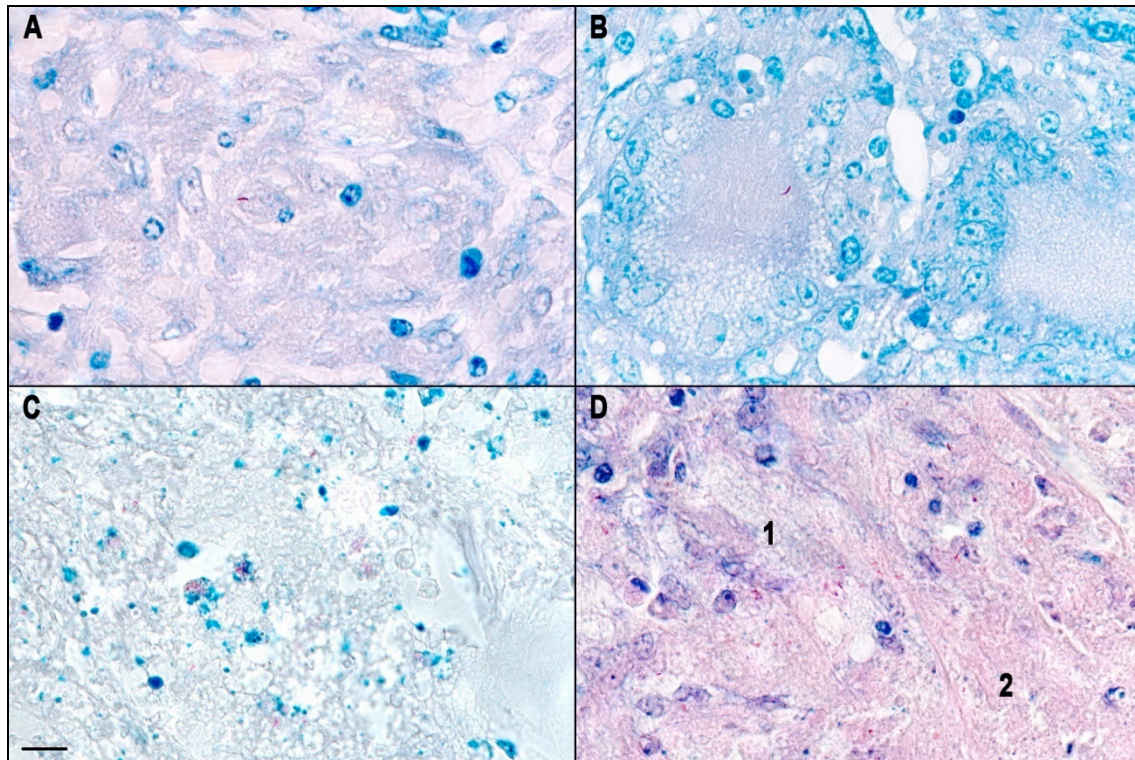
Figure 59. Demonstration of acid-fast bacteria in bovine tuberculosis:
A: Single bacterium in the cytoplasm of an epithelioid cell; liver, E 324/09, FF (Paraffin). B: Single bacterium in the cytoplasm of a multinucleated giant cell; mesenterial lymph node, S 415/14, FF (Paraffin). C: Remnants of bacteria in the cytoplasm of degenerating neutrophils; lung, E 323/09, FF (Paraffin). D: Bacteria at the border between viable epitheliod cell (1) and the area with caseating necrosis (2); mesenterial lymph node, S 179/13, FF, acid-fast staining; bar in C for A-D = 10 µm.

4.3.4.2. Immunohistochemical (IHC) Demonstration of Mycobacterial Antigens

The immunohistochemical investigations were performed on tissue sections from 232 paraffin blocks using a polyclonal rabbit anti-*M. tuberculosis* complex (Rb x Tbc) antibody and a polyclonal rabbit anti-*M. bovis* antibody on some selected sections. The positive reaction occurred as amorphous or fine granular light to dark brown colour. Samples were evaluated according to the localisation and the strength of positive reaction. Embedded cultured bacteria served as a positive control (see 4.2.).

4.3.4.2.1. Comparison of Anti Mycobacterial Antibodies

During the IHC investigations with polyclonal rabbit anti-*M. tuberculosis* complex antibody (Rb x Tbc) positive reaction was controlled using the positive control sections in each run Sensitivity and specificity of the polyclonal rabbit anti-*M. tuberculosis* complex (Rb x Tbc) antibody were compared with the polyclonal rabbit anti-*M. bovis* (Rb x *M. bovis*) antibody on

selected tissue sections. The positive reaction within the necrotic zone was similar for both antibodies, but the strength of the positive reaction obtained by the antibody against *M. tuberculosis* complex was stronger than of the antibody against *M. bovis*. Furthermore, the *M. tuberculosis* complex antibody showed a positive reaction intracellular in the cytoplasm of epithelioid cells and part of the multinucleated giant cells, while the *M. bovis* antibody gave only a weak positive reaction in these cells. On the basis of these results, *M. tuberculosis* complex antibody was more sensitive as compared with the *M. bovis* antibody.

4.3.4.2.2. Distribution of the Mycobacterial Antigen

An amorphous or fine granular brown positive reaction product could be observed in different areas of the tuberculous lesions (Figs. 60 and 61), thus areas of the granulomatous inflammation were divided into three groups for the evaluation of a positive reaction (Fig. 62). Zone 1 was the necrotic centre of the granulomatous inflammation. Positive reaction occurred in 149 out of the 232 tissue sections in this zone. The strength of the positive reaction was in 31/149 strong (+++), in 30/149 tissue samples moderate (++), and in 89/149 tissue samples weak (+). The inflammatory zone adjacent to the caseaous necrosis was termed as zone 2, which showed the positive reaction intracellular in the cytoplasm of the epithelioid cells (Fig. 60 B and D) and MNGCs (Fig. 60 A) in 142 out of the 232 tissue sections. The strength of the positive reaction was strong in 21/142, moderate in 46/142 and weak in 75/142. Zone 3 presented the outer zone of the granulomatous inflammation, mainly the area with lymphocytes, and the positive signal was detected intracellular in single large cells with a large pale nucleus (Fig. 61 C and D) in 154 out of the 232 tissue sections. The strength of the positive reaction was in 21/154 (strong), in 44/154 moderate and in 91/154 weak positive reaction. Bacterial antigen could also be demonstrated in cells of the epithelioid cell granulomatous inflammation, this means in epitheliod cells (Fig. 61 A) and in MNGCs (Fig. 61 B). In some cases, cells carrying bacterial antigen occurred in sinus of lymph nodes with a tuberculous inflammation (Fig. 61 E).

The distribution of the mycobacterial antigens within the tissue sections and the strength of the reaction are depicted in the Fig. 62 and Table 8.
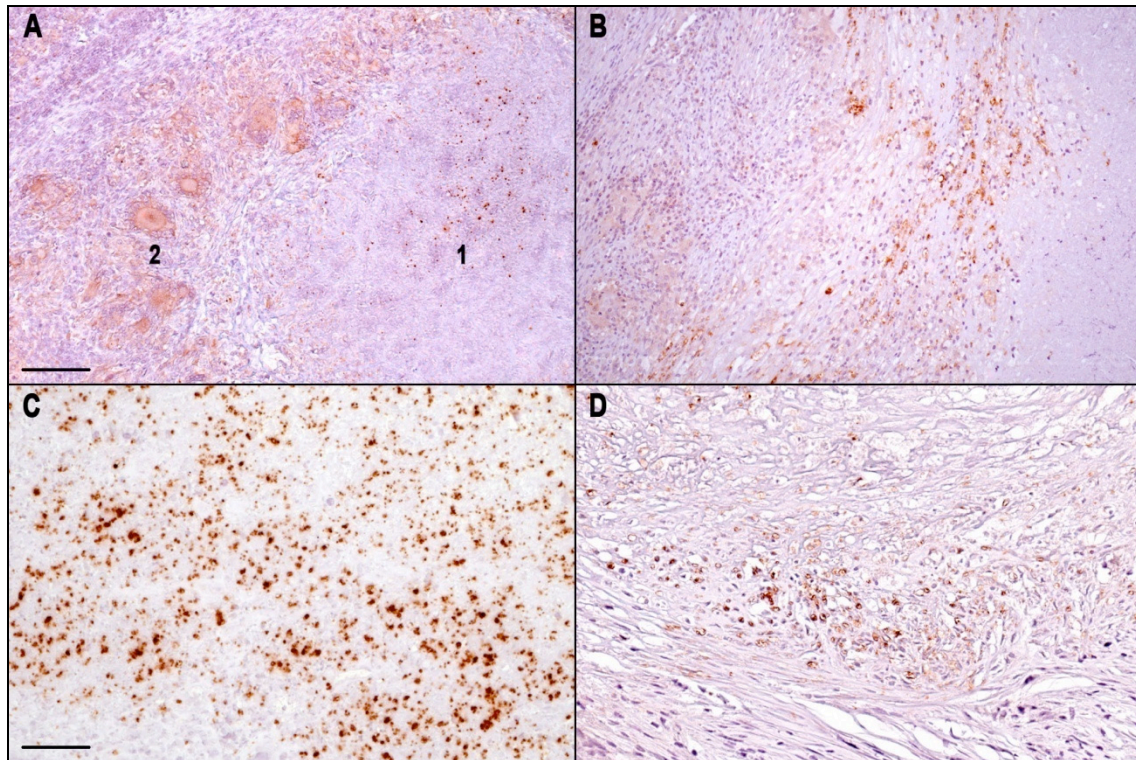
Figure 60. Immunohistochemical demonstration of mycobacterial antigen:
A: Overview over a tubercle, antigen is visible in the caseous necrosis (1) and in the zone of inflammatory cells, escpecially within multinucleated giant cells (2); mesenterial lymph node, S 415/14, IPO. B: Overview over a tubercle, antigen can be demonstrated mainly in epithelioid cells in the inner zone of inflammatory cells; mediastinal lymph node, E 321/09, IPO. C: Large amount of bacterial antigen in the caseous necrosis (strong reaction); mesenterial lymph node, E 102/09, IPO. D: Mycobacterial antigen in epithelioid cells in the immediate vicinity to the caseous necrosis; mesenterial lymph node, E 97/09, IPO; bars in A for A and B = 100 µm, in C for C and D = 50 µm.
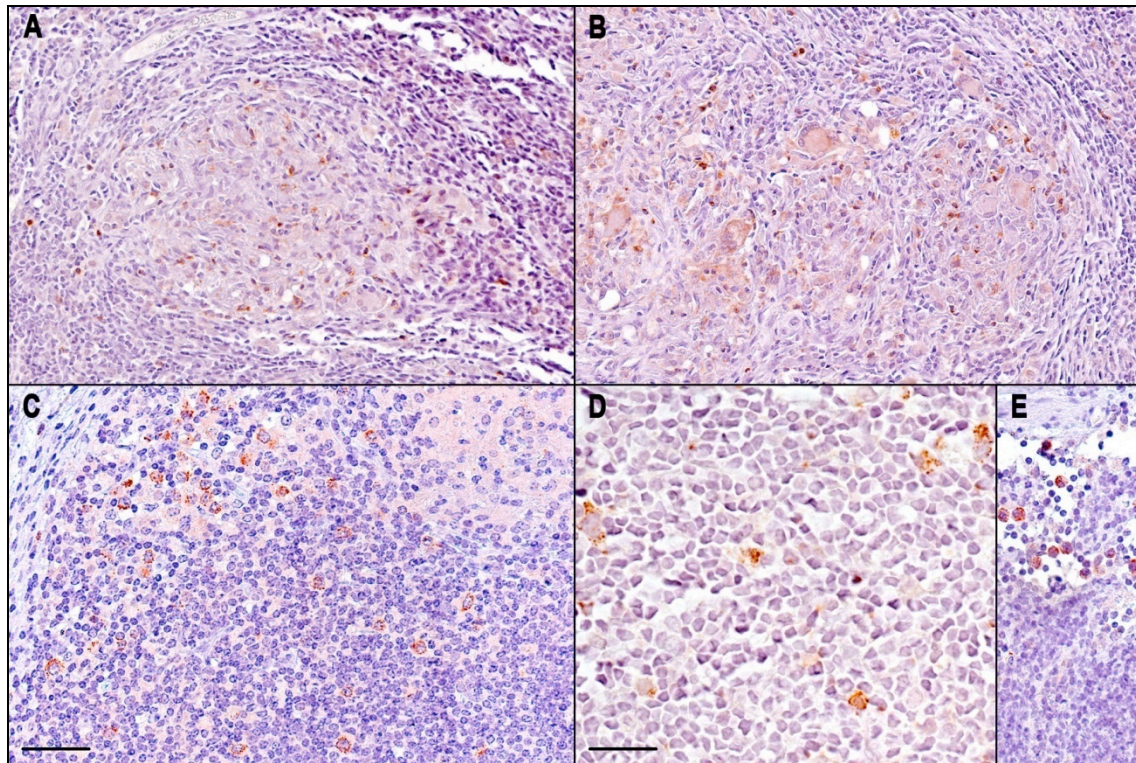
Figure 61. Immunohistochemical demonstration of mycobacterial antigen:
A: Epithelioid cell granulomatous inflammation with bacterial antigen in several epithelioid cells; mesenterial lymph node, E 320/09, IPO. B: Epithelioid cell granulomatous inflammation with a weak positive reaction in multinucleated giant cells and a strong reaction in epithelioid cells; mesenterial lymph node, E 320/09, IPO. C: Strongly granular positive cells scattered between lymphocytes in the outer inflammatory zone; mesenterial lymph node, S 1258/12, IPO. D: Higher magnification of a corresponding location as in (C) with single cells showing a marked granular positive reaction in their cytoplasm; mesenterial lymph node, E 108/09, IPO. E: clearly positive cells in a sinus of a lymph node with tuberculous inflammation; mesenterial lymph node, S 1258/09; bars in C for A, B, C, E = 50 µm, D = 25 µm.
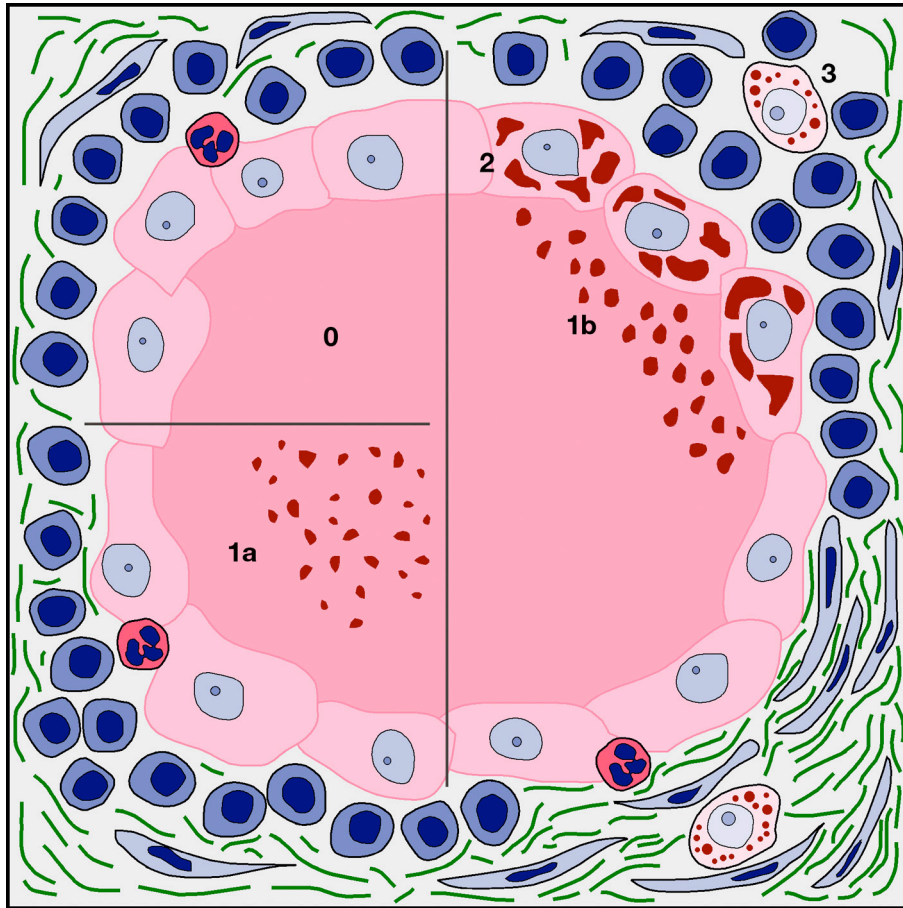
Figure 62. Immunohistochemistry (anti-*M. tuberculosis* complex antibody):
0: not detectable (Zone 1) Mycobacterial antigen is detectable a) within the centre of caseous necrosis (Zone 1a); b) in the periphery of the necrosis (Zone 1b); c) intracellular in cells of the inflammatory mantle zone (Zone 2); d) in single cells of the outer zone (Zone 3).

Table 8. The localisation of the mycobacterial antigens within the tissue and the strength of the positive reaction.

The localisation of the bacilli	Numbers of the tissue sections	Strong reaction	Moderate reaction	Weak reaction
First zone (1)	149	31	30	89
Second zone (2)	142	21	46	75
Third zone (3)	154	21	44	91
Total number	232	73	120	255

4.3.4.2.3. Quantification of the Immunohistochemistry Results

A total of 209 out of the 232 (90%) investigated tissue sections gave positive reaction with the polyclonal rabbit anti-*M. tuberculosis* complex (Rb xTbc) antibody. The number of the positive tissue sections of the different organs is given in Table 9.

Table 9. Number of immunohistochemically positive tissue sections and organ distribution of mycobacterial antigens.

Organ	Number of investigated sections	Number of positive sections
Lung	28	22
Mediastinal lymph node	37	32
Small intestine	1	1
Mesenterial lymph node	131	125
Liver	8	5
Portal lymph node	14	14
Retropharyngeal lymph node	12	12

4.3.4.3. Comparative Analyses of Fite-Faraco (FF) Staining and Immunohistochemistry (IHC)

The detection of mycobacteria or bacterial antigen was performed in 232 out of the 238 paraffin tissue sections for both FF staining and IHC. Out of the 232 paraffin tissue sections 151 were positive in both methods and 11 were negative in both methods. Furthermore, 60 tissue sections were detected positive in IHC, but were negative in FF staining. Eleven tissue sections were positive in FF staining, but there was no reaction in the IHC. The detailed list is given in Appendix 9.1.2. Tab. 11.

4.3.4.4. In Situ Investigations (ISH)

A light purple reaction was obtained in the positive control slides using a cocktail of the *M. tuberculosis* complex-oligonucleatid DNA probes (MTB187, MTB226, MTB770). The method was performed on several tissue sections (S 183/13, S 179/13, S 409/14, S 413/14, S

415/14), which had a lot of acid fast bacilli in the FF staining and had moderate to strong positive reaction (++/+++) with rabbit anti-*M. tuberculosis* complex antibody in immunohistochemstry. Different alternative ISH methods were tested to obtain a positive reaction in the tissue sections (listed in Materials and Methods 3.2.1.1.6.2.), but the positive reaction product was not as clear as in positive control slides. Similarly, the positive control slides gave a positive reaction with the EU bacteria-oligonucleatid DNA probes, but it failed in the investigated tuberculous tissue sections.

4.3.4.5. Investigations by Transmission Electron Microscopy (TEM)

4.3.4.5.1. Semi-thin Sections

A total of 294 semi-thin tissue sections out of the 404 epoxy resin blocks were evaluated using toluidine blue-safranin staining. The histological findings of the tissue sections included only necrotic zone with or without calcification, necrotic and non-necrotic granulomatous inflammations and also non-altered tissue samples. The different granulomatous inflammation types in toluidine blue-safranin staining were similar as that in H&E staining.

The screening of the semi-thin sections served also to select tissue blocks for the further immunohistological investigations. A total of 157 out of the 294 tissue sections were found appropriate for IHC investigations. They showed granulomatous inflammation with necrotic and non-necrotic zones, and included the different tissue components, such as fibrous tissue, capillaries or lymphatic vessels.

Postembedding immunohistochemistry was performed on these 157 selected tissue sections using the primary Rb x Tbc antibody (Fig. 63). Embedded cultured bacteria served as positive control (see 4.2.). A dark to light brown positive reaction occurred in 50 out of the 157 semi-thin sections (Fig. 63). The distribution of mycobacterial antigen was principally the same as in the paraffin sections. A positive reaction was observed in 24/50 tissue sections in the caseous necrosis zone and in 39/50 in the inflammatory zone as well as in the outer zone of the granulomatous inflammation. Appropriate tissue sections for the transmission electron microscopical investigations were 7 out of the 50 positive semi-thin sections.

Semi-thin sections showing a positive immunohistochemical reaction at definitive, easily retrievable tissue components were preferred for the TEM investigations (Fig. 63). These definitive components in the semi-thin sections guided to find the immunolabeled structures in the TEM.

4.3.4.5.2. Ultra-thin Sections

Seven ultra-thin sections were examined using TEM. The corresponding immunolabeled areas and cells were searched for the demonstration of mycobacteria in the TEM. The definitive tissue components guided to find the required areas and cells. Extracellular bacteria were determined in 2/7 mesenterial lymph node tissue samples (Fig. 63 C). Longitudinal and cross sections of mycobacteria were found at the same localisation of the positive reaction seen in the semi-thin slide with IHC. Morphologically, the bacterial cell wall appeared densely and the innerpart contained lipid vacuoles (Fig. 63 D). Only in one case, an intracellular bacillus was detected in the cytoplasm of a macrophage in the mesenterial lymph node. Bacterial antigen within the single cells in the outer inflammatory zone could not be detected in immunohistochemistry on semi-thin sections, so the nature of the positive reaction product in the immunohistochemistry on paraffin sections could not be elucidated.
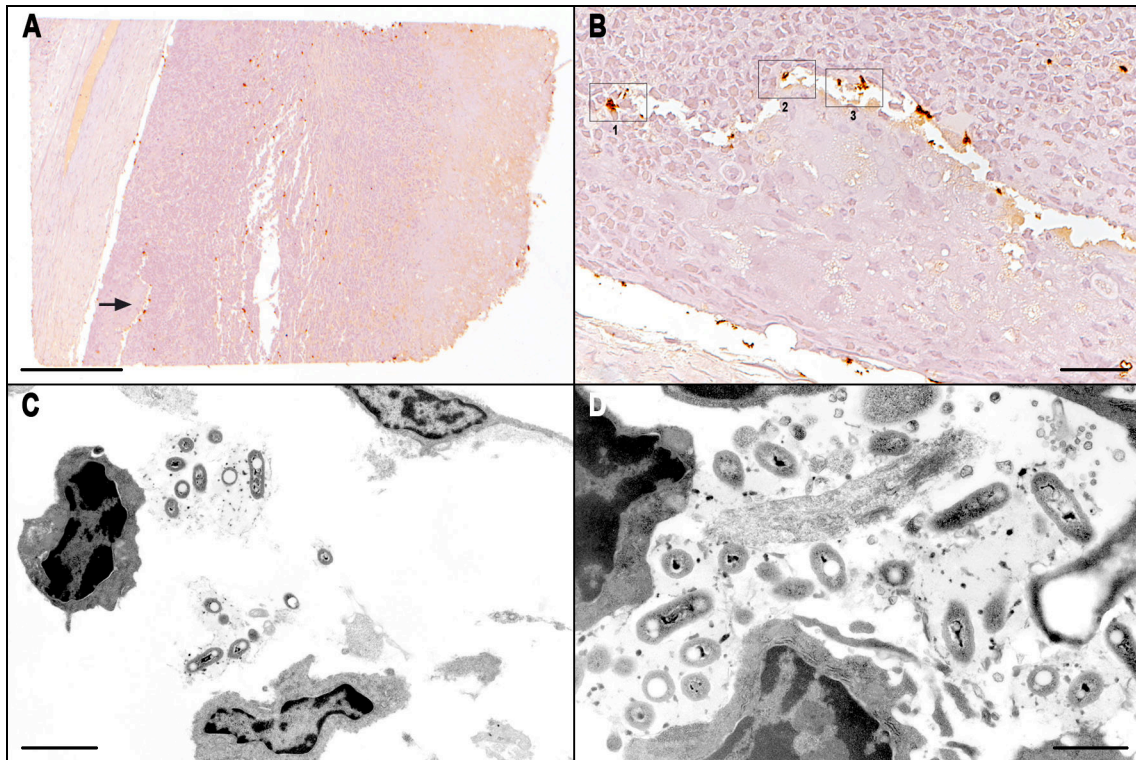
Figure 63. Transmission electron microscopical investigations in bovine tuberculosis:
A: Semi-thin section with disseminated spot-like dark-brown positive reaction products; mesenterial lymph node. B: High-power magnification of A (indicated by an arrow), single positive regions are marked (1 - 3), regions that were examined ultrastructurally; mesenterial lymph node, E 325/09, postembedding immunohistochemistry on semi-thin sections with anti-*Mycobacterium tuberculosis* complex antibody. C: extracellularly laying bacteria; mesenterial lymph node, E 325/09, TEM. D: bacteria with the phenotype of mycobacteria at a higher magnification; mesenterial lymph node, E 325/09, TEM; bars in A = 200 µm, B = 25 µm, C = 2 µm, D = 1 µm.

5. DISCUSSION

Bovine tuberculosis is still an important disease for cattle in Germany although Germany is regarded as tuberculosis free. The number of outbreaks has increased in Allgäu, Bavaria since 2008. The major relevant etiologic agent has been detected as *M. caprae* (LGL, 2014), which causes tuberculous inflammation. The diagnosis of tuberculous granulomatous inflammation and detection of acid-fast bacilli are possible using a light microscopy or an electron microscopy. However, special methods are required for the determination of mycobacteria, mycobacterial antigen or mycobacterial DNA.

The present study was performed on 84 cattle with bovine tuberculosis derived from several herds in Bavaria. The aim of the study was to determine the possible routes of infection, to investigate the macroscopical and histological alterations and development of tuberculous inflammation, to demonstrate the morphology of the tuberculous inflammation and to demonstrate the localisation and distribution of the mycobacteria within the tuberculous inflammation.

5.1. Interpretation of Possible Routes of Infection and Lesion Distribution

Bavaria has recently been reported to have bovine tuberculosis prevalence rate of 0.91% in cattle and in red deer (GERSTMAIER, 2011). Subsequently, the prevalence of *M. caprae* has been investigated in Austria and Alpine countries, including Bavaria. The pastures of these regions, shared by the same cattle and deer populations, are estimated as a possible reason for the transmission of the tuberculous infection from the infected deer to cattle (SCHOEPF et al., 2012). This assumption could also be associated with the samples in the present study by alimentary or aerogenous route of infection. The highest percentage (63%) of the lesions was detected in gastrointestinal tract, contrary to the previous studies (WHIPPLE et al., 1996; LIEBANA et al., 2008). Thus, the alimentary route was regarded as the first route of infection in the present study. But contrary to that, the aerogenous route has previously been considered to be the most important route of infection (PRITCHARD, 1988; NEILL et al., 2001). The second most common route of infection was the aerogenous route (19%) in the present study. Lesions were commonly found in the mediastinal lymph nodes, in the lung parenchyma and also on the pleura. There were also cases with concurrent alimentary and respiratory lesions

(13%). These lesions were found either in the respiratory and gastrointestinal tract side by side, or only in retropharyngeal lymph node. It has been described that retropharyngeal lymph nodes are more frequently associated with lung and mediastinal lymph node lesions than with mesenterial lymph node lesions (STAMP, 1944). However, retropharyngeal lymph node alterations could be related to both the alimentary and the aerogenous routes of infections in the present study.

5.2. Interpretation of Macroscopic Findings

Lung, mediastinal lymph node, liver, portal lymph node, small intestine, mesenterial lymph node and retropharyngeal lymph node from 84 cattle showed typical macroscopic findings of tuberculosis consisting of yellowish, caseified and mostly calcified nodules at the post-mortal examination. The lesions were compatible with primary tuberculous inflammation and comprised both as complete or in-complete primary complexes, as described by NIEBERLE (1938). The incomplete complexes were especially found in the mesenterial lymph nodes, followed by the mediastinal lymph nodes and portal lymph nodes. Chronic organ tuberculosis and post primary tuberculosis were not detected.

Macroscopic lesions were found in five macro-patterns, as described by RIESEBERG (2016). In the present study, these five macro-patterns were re-evaluated and compared with their histological counterparts. The results of this comparative study were considered highly convincing, 80% concordance between macroscopic and histologic findings. The characteristics defined for macro-patterns I and II showed typical tuberculous inflammation with a regular layered structure, which is the distinctive feature for the differentiation from other patterns. The lesions in macro-pattern II had foci with smaller diameters, which were verified by measured analysis, and were present in a greater number than macro-pattern I. The occurrence of the tuberculous foci in different diameters has also been used by STAMP (1948) for the interpretation of pulmonary tuberculosis in cattle. However, the histological overviews of both macro-patterns I and II were identical, consisting of a regular layered structure of the tuberculous inflammation (Histo-type 2). On the contrary, macro-pattern III displayed extremely disarranged structure. All the cut surface of the affected organ was altered in this macro-pattern. The histological overview was also identical whereby showing irregular composition of inflammatory cells and fibrous tissue (Histo-type 3). Like macro-pattern III, macro-pattern IV also showed extensive alterations in the affected organs in

comparison with macro-patterns I and II. Especially, large caseous necrosis and thin layer of fibrous tissue were distinctive on the cut surface of the affected organ. The histology showed a small zone of inflammatory cells and a thin layer of fibrous tissue around the caseous necrosis (Histo-type 4). The features and differences of the histological types of tuberculous inflammation are interpreted below (5.3.). Macro-pattern V presented cavitating tuberculosis in this study. This macro-pattern was most frequently accompanied by another macro-pattern and was found in the lung and lymph nodes. In addition to five macro-patterns, exudative pulmonary tuberculosis was also found in some lung samples, macro-pattern VI. But, pulmonary cavitating tuberculosis and macro-pattern VI are discussed below (see 5.4.)

5.3. Interpretation of Histological Findings

The results of the histological examination in the present study revealed that the main components of the tuberculous inflammation were caseous necrosis, neutrophils, epithelioid cells and Langhans-type giant cells, lymphocytes and fibrous connective tissue. However, mast cells and eosinophil granulocytes might also have a small role in tuberculous inflammation.

It is supposed that the central caseous necrosis is a result of the delayed type hypersensitivity to limit the mycobacterial growth, because they cannot multiply in the necrosis (DANNENBERG, 1991). It has already been indicated that caseous necrosis can liquefy or calcify (JUBB & KENNEDY, 1963). In the present study, caseous necrosis was commonly accompanied by variable amounts of calcification foci. Both of the caseous necrosis and calcification have been seen as common features for the tuberculous inflammation (LIEBANA et al., 2008).

Epithelioid cells and Langhans-type multinucleated giant cells, the cells of the mononuclear phagocyte system (MPS), played the principal role in the tuberculous inflammation. In the present study, they were arranged either in individual epithelioid cell granulomatous inflammation (Histo-type 1) or in the classical tubercles (Histo-type 2). Contrary to other studies (WANGOO et al., 2005; LIEBANA et al., 2008), epithelioid cell granulomatous inflammations also comprised caseous necrosis with or without calcification. It was assumed that fatty degenerated epithelioid cells underwent caseation. In addition, some epithelioid cell granulomatous inflammations demonstrated a focus of central calcification without any

indication of former caseation. In a tubercle (Histo-type 2), epithelioid and Langhans-type giant cells were found in the inner layer of the inflammatory zone, as described in other studies in men and cattle (ULRICHS et al., 2005; PALMER et al., 2007). Immunohistochemically, these cells could be determined by lysozyme and calprotectin (MAC387). The positive reaction obtained by lysozyme was more distinct than those by calprotectin (MAC387).

Intact and disintegrated neutrophils were found scattered or in aggregates in different localisations. Most commonly, they were detected in the caseous necrosis or around the caseous necrosis in combination with epithelioid cells and giant cells. These findings were compatible with a previous experimental study with calves (CASSIDY et al., 1999). Indeed, the role of the neutrophils in the pathogenesis of the tuberculous granulomatous inflammation in the early stage of infection has already been shown in an experimental study (PEDROSA et al., 2000). The participation of the neutrophils in the epithelioid cell granulomatous inflammation might be a trigger mechanism for the beginning of the caseous necrosis (TURNER et al., 2003). They also have a striking role in the regulation of the young granuloma formations in the chronic phases of infection (SEILER et al., 2003). In the present study, neutrophils are also involved in the acute lung tuberculous inflammation, which is discussed below (see 5.4.)

In addition to the neutrophils and macrophages (epithelioid cells), the cell mediated immune response is required to control and eliminate the mycobacteria, and it causes the development of the tuberculous inflammation (FLYNN & CHAN, 2001). In the present study, lymphocytes participated in the early and also later stages of the tuberculous inflammation. In agreement with a previous study (ULRICHS et al., 2005), the inflammatory zone was characterised by massive lymphocyte infiltration, which was rich in T and B lymphocytes. In accordance with the study of WANGOO and coworkers (2005), the majority of lymphocytes were CD3 T cells. They were seen throughout the inflammation. On the other hand, the aggregates of B lymphocytes were most prominent at the periphery of the inflammation.

The most prominent role seen for the fibrous tissue is the encapsulation of the tuberculous inflammation and the restriction of the progression of the inflammation. In the present study, the fibrous tissue encapsulation was clearly seen as a grey band in macro-patterns I and II, and as a thin layer in macro-pattern IV. Histological demonstration was performed by Masson´s

trichrome and Silvering stainings. The different amounts of fibrous connective tissue displayed regular and irregular arrangements and that could be related to the chronicity of the tuberculous inflammation. New collagen-fibre has also been shown in different stages of the tuberculous inflammation. It has been concluded that the increased degree of new collagen formation indicates the advancement of the lesion development (WANGOO et al., 2005).

Regardless of the composition of these components, tuberculous inflammation was evaluated on the basis of four different histo-types and also on an additional acute exudative type of pulmonary tuberculous inflammation. These four histo-types could be related to the sequential alterations in the development of tuberculous inflammation.

Histo-type 1 showed epithelioid cell granulomatous inflammation and was divided into two subtypes depending on the localisations. Histo-subtype 1a presented solitary epithelioid cell granulomatous inflammation, while histo-subtype 1b occurred as satellite epithelioid cell granulomatous inflammation within the inflammatory or fibrous zone of the tuberculous inflammation. It was assumed that the development of a tuberculous inflammation could start with an accumulation of the MPS cells, from an individual cell to extensive cell accumulations. The development of such an epithelioid cell granulomatous inflammation has been demonstrated by the maturation of monocytes into macrophages and then into epithelioid cells (ADAM, 1974). Thus, histo-subtype 1a corresponded to the initial stage of tuberculous inflammation in the present study. It might progress to the histo-type 2 after the development of both caseating necrosis and fibrous tissue. Histo-type 2 was characterised by a central caseous necrosis, which was surrounded by concentric layers of inflammatory cells and fibrosis. All of these components showed distinctive layers, as onionskin-like structure. This histo-type represents the classical tuberculous granuloma (MARIANO, 1995). Histo-type 3 could develop later than histo-types 1 and 2. This type showed especially proliferative and disordered fibrous tissue. Inflammatory cells also displayed disordered arrangement in combination with fibrous tissue. Although caseation and calcification were seen in this type, they were not as severe as seen in histo-type 4. Thus, histo-type 4 could be evaluated as the latest stage due to the thin layer of fibrous tissue encapsulation and large caseous necrosis and calcification as well. Caseation and calcification have also been demonstrated as the latest stages in an experimental study (WANGOO et al., 2005).

It was concluded that a tuberculous inflammation could progress appositionally either in an organ, or could disseminate by lympho-haematogenously to the other organs, or intra-canaliculary in the air ways of the lung (see 5.4.). Appositional growth was characterised by an epithelioid cell granulomatous inflammation, which could arise as a satellite granuloma (Histo-subtype 1b) within the inflammatory zone of a large tubercle. Thereafter, central caseation necrosis could occur in histo-subtype 1b and it could integrate into the large caseous necrosis of the large tubercle (Histo-type 2).

5.4. Pulmonary Tuberculosis

In the present study, tuberculous lesions of the respiratory tract were commonly found both in lung and in the regional mediastinal lymph nodes, in form of complete or incomplete primary complexes, as described previously (NIEBERLE, 1938; STAMP, 1944). Primary lung foci were detected in different macro-patterns. Previously, the macroscopic alterations of pulmonary primary foci have also been classified by Stamp. In that study, most of the primary lesions were found encapsulated, large, caseous and calcified, in many cases reaching up to 5 or 6 cm in diameter, mostly with cavity formations (STAMP, 1948). These characteristics showed similarity to the lung samples with macro-pattern I and II, and also those in a combination with pattern V. However, in the present study, the diameter in macro-pattern I reached a maximum of 2.4 cm. Furthermore, they comprised oedema with fibrin, disintegrated and intact neutrophils and also lymphocytes. They could be a sign for progressive pulmonary tuberculous inflammation. AUERBACH (1959) also describes that progressive primary complexes have the tendency to liquefaction and cavity formation.

STAMP (1944) referred that pleural involvement of the tuberculous inflammation can occur after a primary lung infection by direct lymphatic drainage from the lesion to the pleura. Lymphogenous spread could also be the cause of the pleural lesions in case number S 770/13, because there were no other findings indicating a haematogenous spread in that case.

Histological findings were compatible with their macro-patterns. Epithelioid cell granulomatous inflammations (Histo-subtypes 1a - 1b) and also classic tubercle granulomas (Histo-type 2) were the most common findings. They were also compatible with the productive type of tuberculous inflammation described by NIEBERLE (1938) and PALLASKE (1961). Furthermore, distinctive findings were bronchial wall necrosis and air-

way intrusions. The extension of caseous necrosis could cause the necrosis of bronchial walls and the loss of lining columnar epithelium. Thereafter, oedema with fibrin, degenerated columnar epithelial cells and disintegrated and intact neutrophils could replace the destructed bronchial walls.

Exudative alterations could also be detected in the lung in the present case. It was assumed that the development of these lesions could start at first with an acinar necrosis with an alveolar pulmonary oedema at the periphery of the necrosis, followed by the appearance of inflammatory cells, described by PALLASKE (1961). In addition, PALLASKE also mentioned that no bacilli are found in the alveolar pulmonary oedema. Contrary to that, a few numbers of acid-fast bacilli were found in the alveolar pulmonary oedema in the lung sections with FF staining.

5.5. Detection Methods

The detection of the mycobacteria was performed by different methods. While using FF staining and IHC bacteria and their antigenic fragments were detectable, ISH failed to give any positive reaction in the material from cattle. FF staining has already been considered as highly specific but less sensitive for the detection of acid-fast bacilli (WATRELOT-VIRIEUX et al., 2006). In the present study, a high percentage of the cases (83%) were detected FF positive, which could be interpreted as high specificity and sensitivity (RIESEBERG, 2016).

The specificity of the immunohistochemistry against mycobacteria has already been controversially discussed (HUMPHREY & WEINER, 1987; CASSIDY et al., 1999; WATRELOT-VIRIEUX et al., 2006; PUROHIT et al., 2007). However, it has been indicated that the use of monoclonal antibodies might be more specific than the use of polyclonal antibodies (CORNER et al., 1988).

The immunohistochemistry has been considered as a sensitive method for the determination of the mycobacterial antigens in the tuberculous inflammation (PUROHIT et al., 2007). In the present study, high percentage of the cases (90%) was obtained positive by polyclonal rabbit anti-*M. tuberculosis* complex primary antibody. Furthermore, the sensitivity was controlled by comparative study using polyclonal rabbit anti-*M. bovis* primary antibody and revealed that *M. tuberculosis* complex primary antibody works more sensitively than *M. bovis* primary

antibody. In addition, mycobacteria were also detected by TEM in the areas which were positive in IHC, but it still remained unclear due to the low number of cases.

The mycobacterial antigen was detected throughout the inflammation and also in the non-altered areas. Positive signals were detected most commonly in the caseation necrosis (Zone 1). Large amounts of positive signal were found intracellular in the epithelioid and Langhans-type giant cells in the inflammatory zone (Zone 2). That could be an indication for high phagocytic activity of these cells. On the other hand, the positive reaction was also detected intracellularly in large cells, which were outside the tuberculous inflammation (Zone 3). This situation has also been described previously in humans with pulmonary tuberculosis, and has been considered that mycobacteria could not only be found within the granulomatous inflammation, but also distant parts of the lung (ULRICHS et al., 2005).

Although there was a positive correlation between FF staining and IHC results, more positive localisations (Zones 1, 2, 3) were obtained by IHC. Contrary to that, the correlation between IHC results and TEM investigations was not identical. Although there were numerous positive extracellular areas and positive epithelioid cells in the semi-thin sections, only few mycobacteria could be found in the TEM investigations.

5.6. Conclusion

In conclusion, this study showed possible routes of infection for bovine tuberculosis and also revealed different macro-patterns and histo-types of tuberculous inflammation in the affected cattle. This classification of the macroscopic and histological findings, the predicted development and growth of the tuberculous inflammation and the evaluation of the components involved in the tuberculous inflammation could serve to further studies for a better understanding of the pathogenesis of bovine tuberculosis.

Furthermore, the detection of mycobacteria was performed using a light microscopy and TEM. Different detection methods were performed for this aim. It was assumed that only few numbers of mycobacteria could be found in the tuberculous inflammation, and FF staining could be the most sensitive method for the detection of mycobacteria. Due to the unclear sensitivity of IHC, this method could be an alternative method for FF staining.

6. SUMMARY

Several outbreaks of bovine tuberculosis, caused by *M. caprae,* occurred in the years between 2009 and 2014 in some cattle herds of Bavaria, Germany. The suspected cattle were investigated in context of the regulations of Germany. Following the culling, tissue samples including lung, liver, small intestine, their regional lymph nodes, and retropharyngeal lymph node were collected from 84 cattle for the further bacteriological and pathomorphological investigations.

The organs were evaluated macroscopically and light-microscopically. Furthermore, mycobacteria and mycobacterial antigens were demonstrated using acid-fast staining and immunohistochemistry, respectively. The ultrastructural demonstration of bacteria was carried out using semi-thin sections, in which the mycobacterial antigens were demonstrated by postembedding-immunohistochemistry.

Macroscopic alterations were associated with five patterns. Pattern I were typical layered tubercles with a larger diameter (up to 2.4 cm), they appeared single or in low numbers. Pattern II showed numerous small (up to 0.5 cm) layered tubercles. Pattern III had no clearly discernible structure and pattern IV consisted of extensive caseous necrosis. Pattern V were cavities emerging from liquefaction of caseous necrosis, especially in the lung; exclusively to the lung an additional acute exudative type of inflammation was observed.

The histological alterations were divided into four types. Type 1 predominantly consisted of non-layered accumulations of epithelioid cells and multinucleated giant cells. The type 2 corresponded to the classical layered tubercle and therefore paralleled the macroscopic patterns I and II. Type 3 showed disordered collections of fibre-rich fibrous tissue, foci with epithelioid cells, and with caseation necrosis, according to the pattern III. The type 4 had extensive, poorly restricted caseous foci analogous to pattern IV.

The distribution of the tuberculous lesions in the different organs and lymph nodes revealed that the most important route of infection was the alimentary tract (68%), followed by the aerogenous infection (19%). A combination of both routes of infection was present in 13% of the cases.

The acid-fast staining revealed that the numbers of detectable bacteria in the most of the infectious foci was very low. Caseation and calcification showed the highest amounts; single acid-fast bacteria regularly occurred in the multinucleated giant cells, and only sporadically in epithelioid cells. No bacteria could be detected outside of the inner inflammatory zone of the tubercles.

The immuohistochemical demonstration of mycobacterial antigens was positive in caseous foci, in epithelioid and multinucleated cells as well as in cells, which were found in the tubercles individually lying between the lymphocytes in the outside areas.

Mycobacteria could be demonstrated by transmission electron microscopy. The reliable detection of mycobacterial DNA by in situ hybridization failed.

7. ZUSAMMENFASSUNG

Mehrere Ausbrüche von Rindertuberkulose, verursacht durch *M. caprae,* traten in den Jahren 2009 bis 2014 in bayerischen Rinderbeständen auf. Die verdächtigen Tiere fielen im Rahmen der Schlachtung auf. Bei der nachfolgenden Keulung wurden für die vorliegende Studie von 84 Rindern Proben aus Lunge, Leber, Dünndarm und den regionären Lymphknoten sowie Retropharyngeallymphknoten für pathomorphologische und bakteriologische Untersuchungen gewonnen.

Die Organe wurden makroskopisch und lichtmikroskopisch beurteilt. Ferner wurden Mykobakterien mittels säurefester Färbung und mykobakterielle Antigene immunhistochemisch nachgewiesen. Der ultrastrukturelle Nachweis von Bakterien erfolgt anhand von Semidünnschnitten, in denen zuvor bakterielles Antigen durch postembedding-Immunhistochemie nachgewiesen worden war.

Die makroskopischen Veränderungen konnten fünf Mustern zugeordnet werden. Muster I waren typische geschichtete Tuberkel mit einem größeren Durchmesser (bis 2,4 cm), die einzeln oder in geringer Anzahl vorlagen. Muster II zeigte zahlreiche kleinere (bis 0,5 cm) geschichtete Tuberkel. Muster III wies keine klar erkennbare Strukturierung auf und Muster IV bestand aus umfangreichen Verkäsungsherden. Muster V waren Einschmelzungskavernen, vor allem in der Lunge; ausschließlich an der Lunge konnte zusätzlich eine akut-exsudative Entzündung nachgewiesen werden.

Die histologischen Veränderungen wurden in vier Typen eingeteilt. Typ 1 bestanden überwiegend aus ungeschichteten Ansammlungen von Epitheloidzellen und mehrkernigen Riesenzellen. Der Typ 2 entsprach dem klassischen geschichteten Tuberkel und somit den makroskopischen Mustern I und II. Typ 3 zeigte eine ungeordnete Ansammlung von faserreichem Bindegewebe, Herden mit Epitheloidzellen und Verkäsungsherden, entsprechend dem Muster III. Der Typ 4 wies umfangreiche, schlecht begrenzte Verkäsungsherde analog zum Muster IV auf, die histologisch schlecht begrenzt waren.

Die Verteilung der tuberkulösen Läsionen in den verschiedenen Organen und Lymphknoten ergab, dass der wichtigste Infektionsweg die älimentare Infektion (68%) war, gefolgt von der aerogenen (19%). In 13 % der Fälle lag eine Kombination beider Infektionswege vor.

Die säurefeste Färbung zeigte insbesondere, dass die Anzahl nachweisbarer Bakterien in den meisten Entzündungsherden sehr gering war. Die höchsten Gehalte wiesen Verkäsung und Verkalkung auf; in den mehrkernigen Riesenzellen traten regelmäßig einzelne säurefeste Stäbchen auf, selten dagegen in Epitheloidzellen. Außerhalb der entzündlichen Innenzone konnten keine Bakterien in den Tuberkeln nachgewiesen werden.

Der immunhistochemische Nachweis von mykobakteriellem Antigen war positiv in Verkäsungsherden, in Epitheloidzellen und mehrkernigen Riesenzellen sowie Zellen, die sich in Tuberkeln einzeln zwischen den im Außenbereich liegenden Lymphozyten fanden.

Mykobakterien konnten transmissionselektronenmikroskopisch nachgewiesen werden. Es gelang hingegen nicht, mykobakterielle DNA verläßlich durch in Situ Hybridisierung zu detektieren.

8. REFERENCES

Adam DO, 1974, The Structure of Mononuclear Phagocytes Differentiating <u>In Vivo</u> *I. Sequential Fine and Histologic Studies of the Effect of Bacillus Calmette Guerin* (BCG). American Journal of Pathology; 76: 17-48.

Adam DO, 1975, The Structure of Mononuclear Phagocytes Differentiating *In Vivo*. II. The Effect of *Mycobacterium tuberculosis*. American Journal of Pathology; 80: 101-13.

Amand ALS, Frank DN, De Groote MA, Basaraba RJ, Orme IM, Pace NR, 2005, Use of Specific rRNA Oligonucleotide Probes for Microscopic Detection of *Mycobacterium tuberculosis* in Culture and Tissue Specimens. Journal of Clinical Microbiology; 43: 5369-71.

Ameni G, Aseffa A, Engers H, Young D, Gordon S, Hewinson G, Vordermeier M, 2007, High Prevalence and Increased Severity of Pathology of Bovine Tuberculosis in Holsteins Compared to Zebu Breeds Under Field Cattle Husbandry in Central Ethiopia. Clinical and Vaccine Immunology; 14: 1356-61.

Aranaz A, Liebana E, Mateos A, Dominguez L, Vidal D, Domingo M, Gonzolez O, Rodriguez-Ferri EF, Bunschoten AE, Van Embden JD, Cousins D, 1996, Spacer Oligonucleotide Typing of *Mycobacterium bovis* Strains from Cattle and Other Animals: a Tool for Studying Epidemiology of Tuberculosis. Journal of Clinical Microbiology; 34: 2734-40.

Aranaz A, Liebana E, Mateos A, Dominguez L, Cousins D, 1998, Restriction Fragment Length Polymorphism and Spacer Oligonucleotide Typing: a Comparative Analysis of Fingerprinting Strategies for *Mycobacterium bovis*. Veterinary Microbiology; 61: 311-24.

Aranaz A, Liebana E, Gomez-Mampaso E, Galan JC, Cousins D, Ortega A, Blazquez J, Baquero F, Mateos A, Suarez G, Dominguez L, 1999, *Mycobacterium tuberculosis* subsp. *caprae* subsp. nov.: a Taxonomic Study of a New Member of the

Mycobacterium tuberculosis Complex Isolated from Goats in Spain. International Journal of Systematic Bacteriology; 49: 1263-73.

Aranaz A, Cousins D, Mateos A, Dominguez L, 2003, Elevation of *Mycobacterium tuberculosis* subsp. *caprae* Aranaz et al. 1999 to Species Rank as *Mycobacterium caprae* comb. nov., sp. nov. International Journal of Systematic and Evolutionary Microbiology; 53: 1785-9.

Artois M, Blancou J, Dupeyroux O, Gilot-Fromont E, 2011, Sustainable Control of Zoonotic Pathogens in Wildlife: How to Be Fair to Wild Animals? Revue Scientifique Et Technique-Office International Des Epizooties; 30: 733-43.

Asselineau J, Lederer E, 1950, Structure of the Mycolic Acids of Mycobacteria. Nature; 166: 782-3.

Auerbach O, 1959, The Natural History of the Tuberculous Pulmonary Lesion. The Medical Clinics of North America: 239-51.

Azuma I, Kimura H, Yamamura Y, 1968, Chemical and Immunological Properties of Polysaccharides of Wax D Extracted from *Mycobacterium tuberculosis* Strain Aoyama B. Journal of Bacteriology; 96: 567-68.

Azuma I, Thomas DW, Adam A, Ghuysen JM, Bonaly R, Petit JF, Lederer E, 1970, Occurrence of N-glycolylmuramic Acid in Bacterial Cell Walls: a Preliminary Survey. Biochimica Et Biophysica Acta; 208: 444-51.

Banchereau J, Steinman RM, 1998, Dendritic Cells and the Control of Immunity. Nature; 392: 245-52.

Barbolini G, Bisetti A, Colizzi V, Damiani G, Migaldi M, Vismara D, 1989, Immunohistologic Analysis of Mycobacterial Antigens by Monoclonal Antibodies in Tuberculosis and Mycobacteriosis. Human Pathology; 20: 1078-83.

Barksdale L, Kim KS, 1977, Mycobacterium. Bacteriological Reviews; 41: 217-72.

Besra GS, Khoo KH, McNeil MR, Dell A, Morris HR, Brennan PJ, 1995, A New Interpretation of the Structure of the Mycolyl-arabinogalactan Complex of *Mycobacterium tuberculosis* as Revealed Through Characterization of Oligoglycosylalditol Fragments by Fast-atom Bombardment Mass Spectrometry and 1H Nuclear Magnetic Resonance Spectroscopy. Biochemistry; 34: 4257-66.

Bloch H, 1950, Studies on the Virulence of Tubercle Bacilli; Isolation and Biological Properties of a Constituent of Virulent Organisms. Journal of Experimental Medecine; 91: 197-218.

Blomgran R, Ernst JD, 2011, Lung Neutrophils Facilitate Activation of Naive Antigen-Specific CD4(+) T Cells during *Mycobacterium tuberculosis* Infection. Journal of Immunology; 186: 7110-9.

Boddinghaus B, Rogall T, Flohr T, Blocker H, Bottger EC, 1990, Detection and Identification of Mycobacteria by Amplification of rRNA. Journal of Clinical Microbiology; 28: 1751-9.

Bonenberger TE, Ihrke PJ, Naydan DK, Affolter VK, 2001, Rapid Identification of Tissue Micro-Organisms in Skin Biopsy Specimens from Domestic Animals Using Polyclonal BCG Antibody. Veterinary Dermatology; 12: 41-7.

Brennan PJ, Nikaido H, 1995, The Envelope of Mycobacteria. Annual Review of Biochemistry; 64: 29-63.

Brosch R, Gordon SV, Marmiesse M, Brodin P, Buchrieser C, Eiglmeier K, Garnier T, Gutierrez C, Hewinson G, Kremer K, Parsons LM, Pym AS, Samper S, van Soolingen D, Cole ST, 2002, A New Evolutionary Scenario for the *Mycobacterium tuberculosis* Complex. Proceedings of the National Academy of Sciences of the United States of America; 99: 3684-9.

Buddle BM, Delisle GW, Pfeffer A, Aldwell FE, 1995, Immunological Responses and Protection Against *Mycobacterium bovis* in Calves Vaccinated with a Low Dose of BCG. Vaccine; 13: 1123-30.

Buddle BM, Wards BJ, Aldwell FE, Collins DM, de Lisle GW, 2002, Influence of Sensitisation to Environmental Mycobacteria on Subsequent Vaccination Against Bovine Tuberculosis. Vaccine; 20: 1126-33.

Buddle BM, Wedlock DN, Denis M, Vordermeier HM, Hewinson RG, 2011, Update on Vaccination of Cattle and Wildlife Populations Tuberculosis. Veterinary Microbiology; 151: 14-22.

Buelens C, Verhasselt V, DeGroote D, Thielemans K, Goldman M, Willems F, 1997, Human Dendritic Cell Responses to Lipopolysaccharide and CD40 Ligation are Differentially Regulated by Interleukin-10. European Journal of Immunology; 27: 1848-52.

Buergelt CD, 1978, Pathological Evaluation of Paratuberculosis in Naturally Infected Cattle. Veterinary Pathology; 15: 196-207.

Burrell R, 1991, Microbiological Agents as Health Risks in Door Air. Environmental Health Perspectives; 95: 29-34.

Calmette A, 1931, Preventive Vaccination Against Tuberculosis with BCG. Proceedings of the Royal Society of Medicine; 24: 1481-90.

Cancela MMG, Marin JFG, 1993, Comparison of Ziehl-Neelsen Staining and Immunohistochemistry for the Detection of *Mycobacterium bovis* Bovine and Caprine Tuberculous Lesions. Journal of Comparative Pathology; 109: 361-70.

Caruso AM, Serbina N, Klein E, Triebold K, Bloom BR, Flynn JL, 1999, Mice deficient in CD4 T Cells Have Only Transiently Diminished Levels of IFN-γ, Yet Succumb to Tuberculosis. Journal of Immunology; 162: 5407-16.

Cassidy JP, Bryson DG, Pollock JM, Evans RT, Forster F, Neill SD, 1999, Lesions in Cattle Exposed to *Mycobacterium bovis*-inoculated Calves. Journal of Comparative Pathology; 121: 321-37.

Cassidy JP, Bryson DG, Cancela MMG, Forster F, Pollock JM, Neill SD, 2001, Lymphocyte Subtypes in Experimentally Induced Early-stage Bovine Tuberculous Lesions. Journal of Comparative Pathology; 124: 46-51.

Chan J, Fan X, Hunter SW, Brennan PJ, Bloom BR, 1991, Lipoarabinomannan, a Possible Virulence Factor Involved in Persistence of *Mycobacterium tuberculosis* within Macrophages. Infection and Immunity; 59: 1755-61.

Chatterjee D, Hunter SW, McNeil M, Brennan PJ, 1992a, Lipoarabinomannan. Multiglycosylated form of the Mycobacterial Mannosphosphatidylinositol. Journal of Biological Chemistry; 267: 6228-33.

Chatterjee D, Lowell K, Rivoire B, McNeil MR, Brennan PJ, 1992b, Lipoarabinomannan of *Mycobacterium tuberculosis* Capping with Mannoosyl Residues in Some Strains Journal of Biologic Chemistry; 267: 6234-9.

Chatterjee D, 1997, The Mycobacterial Cell Wall: Structure, Biosynthesis and Sites of Drug Action. Current Opinion in Chemical Biology; 1: 579-88.

Collins DM, Stephens DM, 1991, Identification of an Insertion Sequence, IS1081, in Mycobacterium bovis. FEMS Microbiology Letters; 67: 11-6.

Commission Decision of 17 December 1996 Lying Down the Methods of Control for Maintaining the Officially Free Status of Bovine Herds in Certain Member States and Regionsof Member States.

Commission Decision of 15 July 1999 Establishing the Officially Free Status of Bovine Herds of Certain Member States or Regions of Member States and Repealling Decision 97/76/EC.

Commission Regulation (EC) No 1226/2002 of 8 July 2002 Amending Annex B to Council Directive 64/432/EEC.

Commission Decision of 23 June 2003 Establishing the Official Tuberculosis, Brucellosis, and Enzootic Bovine Leukosis Free Status of Certain Member States and regions of Member States as Regards Bovine Herds.

Council Directive 97/12/EC of 17 March 1997 Amending and Updating Directive 64/432/EEC on Health Problems Affecting Intra-Community Trade in Bovine Animals and Swine.

Corner LA, John M, Bundesen PG, Wood PR, 1988, Identification of *Mycobacterium bovis* Isolates Using a Monoclonal Antibody. Veterinary Microbiology; 18: 191-6.

Corner LA, 1994, Post-mortem Diagnosis of *Mycobacterium bovis* Infection in Cattle. Veterinary Microbiology; 40: 53-63.

Cousins DV, Francis BR, Gow BL, 1989, Advantages of a New Agar Medium in the Primary Isolation of *Myobacterium bovis*. Veterinary Microbiology; 20: 89-95.

Cousins DV, Wilton SD, Francis BR, 1991, Use of DNA Amplification for the Rapid Identification of *Mycobacterium bovis*. Veterinary Microbiology; 27: 187-95.

Cousins DV, Bastida R, Cataldi A, Quse V, Redrobe S, Dow S, Duignan P, Murray A, Dupont C, Ahmed N, Collins DM, Butler WR, Dawson D, Rodriguez D, Loureiro J, Romano MI, Alito A, Zumarraga M, Bernardelli A, 2003, Tuberculosis in Seals Caused by a Novel Member of the *Mycobacterium tuberculosis* Complex: *Mycobacterium pinnipedii* sp. nov. International Journal of Systematic and Evolutionary Microbiology; 53: 1305-14.

Cvetnic Z, Spicic S, Katalinic-Jankovic V, Marjanovic S, Obrovac M, Benic M, Mitak M, Pavlik I, 2006, *Mycobacterium caprae* Infection in Cattle and Pigs on One Family Farm in Croatia: a Case Report. Veterinarni Medicina; 51: 523-31.

Cvetnic Z, Katalinic-Jankovic V, Sostaric B, Spicic S, Obrovac M, Marjanovic S, Benic M, Kirin BK, Vickovic I, 2007, *Mycobacterium caprae* in Cattle and Humans in Croatia. International Journal of Tuberculosis and Lung Disease; 11: 652-8.

Daffe M, Brennan PJ, McNeil M, 1990, Predominant Structural Features of the Cell Wall Arabinogalactan of Mycobacterium tuberculosis as Revealed Through Characterization of Oligoglycosyl Alditol Fragments by Gas Chromatography/Mass Spectrometry and by 1H and 13C NMR Analyses. Journal of Biological Chemistry; 265: 6734-43.

Dalton DK, Pittsmeek S, Keshav S, Figari IS, Bradley A, Stewart TA, 1993, Multiple Defects of Immune Cell Function in Mice with Disrupted Interferon- γ Genes. Science; 259: 1739-42.

Dannenberg AM, 1991, Delayed-type Hypersensitivity and Cell-mediated Immunity in the Pathogenesis of Tuberculosis. Immunology Today; 12: 228-33.

Dannenberg AM, 1993, Immunopathogenesis of Pulmonary Tuberculosis. Hospital Practice; 28: 51-8.

Dao DN, Kremer L, Guerardel Y, Molano A, Jacobs WR, Porcelli SA, Briken V, 2004, *Mycobacterium tuberculosis* Lipomannan Induces Apoptosis and Interleukin-12 Production in Macrophages. Infection and Immunity; 72: 2067-74.

De la Rua-Domenech R, Goodchild AT, Vordermeier HM, Hewinson RG, Christiansen KH, Clifton-Hadley RS, 2006, Ante Mortem Diagnosis of Tuberculosis in Cattle: a Review of the Tuberculin Tests, Gamma-Interferon Assay and Other Ancillary Diagnostic Techniques. Research in Veterinary Science; 81: 190-210.

Demangel C, Bean AGD, Martin E, Feng CG, Kamath AT, Britton WJ, 1999, Protection Against Aerosol *Mycobacterium tuberculosis* Infection Using *Mycobacterium bovis* Bacillus Calmette Guerin-infected Dendritic Cells. European Journal of Immunology; 29: 1972-79.

Demangel C, Bertolino P, Britton WJ, 2002, Autocrine IL-10 Impairs Dendritic Cell (DC)- derived Immune Responses to Mycobacterial Infection by Suppressing DC Trafficking to Draining Lymph Nodes and Local IL-12 Production. European Journal of Immunology; 32: 994-1002.

De Smedt T, VanMechelen M, DeBecker G, Urbain J, Leo O, Moser M, 1997, Effect of Interleukin-10 on Dendritic Cell Maturation and Function. European Journal of Immunology; 27: 1229-35.

Doherty ML, Monaghan ML, Bassett HF, Quinn PJ, Davis WC, 1996, Effect of Dietary Restriction on Cell-mediated Immune Responses in Cattle Infected with *Mycobacterium bovis*. Veterinary Immunology and Immunopathology; 49: 307-20.

Domingo M, Vidal E, Marco A, 2014, Pathology of Bovine Tuberculosis. Research in Veterinary Science; 97: S20-S9.

EFSA, 2015, Scientific Report of EFSA and ECDC - The European Union Summary Report on Trends and Sources of Zoonoses, Zoonotic Agents and Food Borne Outbreaks in 2013 - European Food Safety Authority European Centre for Disease Prevention and Control. EFSA Journal: 1-162.

Eisenstein BI, 1990, The Polymerase Chain Reaction. A New Method of Using Molecular Genetics for Medical Diagnosis. New England Journal of Medicine; 322: 178-83.

Erler W, Martin G, Sachse K, Naumann L, Kahlau D, Beer J, Bartos M, Nagy G, Cvetnic Z, Zolnir-Dovc M, Pavlik I, 2004, Molecular Fingerprinting of *Mycobacterium bovis* subsp *caprae* Isolates from Central Europe. Journal of Clinical Microbiology; 42: 2234-38.

Ehrlich P, 1882, Aus dem Verein fur innere Medicin zu Berlin - Sitzung vom 1 Mai. Deutsche Medizinische Wochenschrift, 8: 269-70.

Eruslanov EB, Lyadova IV, Kondratieva TK, Majorov KB, Scheglov IV, Orlova MO, Apt AS, 2005, Neutrophil Responses to *Mycobacterium tuberculosis* Infection in Genetically Susceptible and Resistant Mice. Infection and Immunity; 73: 1744-53.

Feizabadi MM, Robertson ID, Cousins DV, Hampson DJ, 1996, Genomic Analysis of *Mycobacterium bovis* and Other Members of the *Mycobacterium tuberculosis* complex

by Isoenzyme Analysis and Pulsed-field Gel Electrophoresis. Journal of Clinical Microbiology; 34: 1136-42.

Fenhalls G, Stevens L, Moses L, Bezuidenhout J, Betts JC, van Helden P, Lukey PT, Duncan K, 2002a, In Situ Detection of *Mycobacterium tuberculosis* Transcripts in Human Lung Granulomas Reveals Differential Gene Expression in Necrotic Lesions. Infection and Immunity; 70: 6330-8.

Fenhalls G, Stevens-Muller L, Warren R, Carroll N, Bezuidenhout J, Van Helden P, Bardin P, 2002b, Localisation of Mycobacterial DNA and mRNA in Human Tuberculous Granulomas. Journal of Microbiological Methods; 51: 197-208.

Fifis T, Costopoulos C, Radford AJ, Bacic A, Wood PR, 1991, Purification and Characterization of Major Antigens from a *Mycobacterium bovis* Culture Filtrate. Infection and Immunity; 59: 800-7.

Fifis T, Corner LA, Rothel JS, Wood PR, 1994, Cellular and Humoral Immune Responses of Cattle to Purified *Mycobacterium bovis* Antigens. Scandinavian Journal of Immunology; 39: 267-74.

Fine PEM, 1995, Variation in Protection by BCG: Implications of and for Heterologous immunity. Lancet; 346: 1339-45.

FLI, 2012, Jahresbericht. Friedrich-Loffler-Institut, Bundesforschungsinstitut für Tiergesundheit; 1-149.

Flynn JL, Chan J, Triebold KJ, Dalton DK, Stewart TA, Bloom BR, 1993, An Essential Role for Interferon- γ in Resistance to *Mycobacterium tuberculosis* Infection. Journal of Experimental Medicine; 178: 2249-54.

Flynn JL, Chan J, 2001, Immunology of Tuberculosis. Annual Review of Immunology; 19: 93-129.

Francis J, 1971, Susceptibility to Tuberculosis and the Route of Infection. Australian Veterinary Journal; 47: 414.

Fratti RA, Backer JM, Gruenberg J, Corvera S, Deretic V, 2001, Role of Phosphatidylinositol 3-kinase and Rab5 Effectors in Phagosomal Biogenesis and Mycobacterial Phagosome Maturation Arrest. Journal of Cell Biology; 154: 631-44.

Fratti RA, Chua J, Vergne I, Deretic V, 2003, *Mycobacterium tuberculosis* Glycosylated Phosphatidylinositol Causes Phagosome Maturation Arrest. Proceedings of the National Academy of Sciences of the United States of America; 100: 5437-42.

Frothingham R, Hills HG, Wilson KH, 1994, Extensive DNA Sequence Conservation Throughout the *Mycobacterium tuberculosis* Complex. Journal of Clinical Microbiology; 32: 1639-43.

Gallagher J, Horwill DM, 1977, A Selective Oleic Acid Albumin Agar Medium for the Cultivation of *Mycobacterium bovis*. Journal of Hygiene; 79: 155-60.

Gavier-Widen D, Chambers MA, Palmer N, Newell DG, Hewinson RG, 2001, Pathology of Natural *Mycobacterium bovis* Infection in European Badgers (Meles meles) and Its Relationship with Bacterial Excretion. Veterinary Record; 148: 299-304.

Gerstmaier E, 2011, Validierung molekularbiologischer und immunologischer Nachweisverfahren für die Tuberkulose bei Rindern und Tuberkulosemonitoring beim Rotwild. Universitätsbibliothek der Ludwig-Maximilians-Universität, München.

Ghuysen JM, 1968, Use of Bacteriolytic Enzymes in Determination of Wall Structure and Their Role in Cell Metabolism. Bacteriological Reviews; 32: 425-64.

Gilleron M, Ronet C, Mempel M, Monsarrat B, Gachelin G, Puzo G, 2001, Acylation State of the Phosphatidylinositol Mannosides from *Mycobacterium bovis* Bacillus Calmette Guerin and Ability to Induce Granuloma and Recruit Natural Killer T Cells. Journal of Biological Chemistry; 276: 34896-904.

Gortazar C, Vicente J, Samper S, Garrido JM, Fernandez-De-Mera IG, Gavin P, Juste RA, Martin C, Acevedo P, De La Puente M, Hofle U, 2005, Molecular Characterization of *Mycobacterium tuberculosis* Complex Isolates from Wild Ungulates in South-central Spain. Vet Res; 36: 43-52.

Grange JM, Yates MD, 1994, Zoonotic Aspects of *Mycobacterium bovis* Infection. Veterinary Microbiology; 40: 137-51.

Griffin JM, Hahesy T, Lynch K, Salman MD, McCarthy J, Hurley T, 1993, The Association of Cattle Husbandry Practices, Environmental Factors and Farmer Characteristics with the Occurence of Chronic Bovine Tuberculosis in Dairy Herds in the Republic of Ireland. Preventive Veterinary Medicine; 17: 145-60.

Gutierrez M, Samper S, Gavigan JA, Marin JFG, Martin C, 1995, Differentiation by Molecular Typing of *Mycobacterium bovis* Strains Causing Tuberculosis in Cattle and Goats. Journal of Clinical Microbiology; 33: 2953-6.

Gutierrez M, Samper S, Jimenez MS, van Embden JDA, Marin JFG, Martin C, 1997, Identification by Spoligotyping of a Caprine Genotype in *Mycobacterium bovis* Strains Causing Human Tuberculosis. Journal of Clinical Microbiology; 35: 3328-30.

Haddad N, Ostyn A, Karoui C, Masselot M, Thorel MF, Hughes SL, Inwald J, Hewinson RG, Durand B, 2001, Spoligotype Diversity of *Mycobacterium bovis* Strains Isolated in France from 1979 to 2000. Journal of Clinical Microbiology; 39: 3623-32.

Harboe M, Wiker HG, Duncan JR, Garcia MM, Dukes TW, Brooks BW, Turcotte C, Nagai S, 1990, Protein G-based Enzyme-linked Immunosorbent Assay for Anti-MPB70 Antibodies in Bovine Tuberculosis. Journal of Clinical Microbiology; 28: 913-21.

Henderson RA, Watkins SC, Flynn JAL, 1997, Activation of Human Dendritic Cells Following Infection with *Mycobacterium tuberculosis*. Journal of Immunology; 159: 635-43.

Hermans PWM, Vansoolingen D, Bik EM, Dehaas PEW, Dale JW, Vanembden JDA, 1991, Insertion Element IS*987* from *Mycobacterium bovis* BCG is Located in a Hot-spot Integration Region for Insertion Elements in *Mycobacterium tuberculosis* Complex Strains. Infection and Immunity; 59: 2695-705.

Hickman SP, Chan J, Salgame P, 2002, *Mycobacterium tuberculosis* Induces Differential Cytokine Production from Dendritic Cells and Macrophages with Divergent Effects on Naive T Cell Polarization. Journal of Immunology; 168: 4636-42.

Huard RC, Lazzarini LCD, Butler WR, van Soolingen D, Ho JL, 2003, PCR-based Method to Differentiate the Subspecies of the *Mycobacterium tuberculosis* Complex on the Basis of Genomic Deletions. Journal of Clinical Microbiology; 41: 1637-50.

Humphrey DM, Weiner MH, 1987, Mycobacterial Antigen Detection by Using Immunohistochemistry in Pulmonary Tuberculosis. Human Pathology; 18: 701-8.

Hunter SW, Brennan PJ, 1990, Evidence for the Presence of a Phosphatidylinositol Anchor on the Lipoarabinomannan and Lipomannan of Mycobacterium tuberculosis. Journal of Biological Chemistry; 265: 9272-9.

Hutchings MR, Harris S, 1997, Effects of Farm Management Practices on Cattle Grazing Behaviour and the Potential for Transmission of Bovine Tuberculosis from Badgers to Cattle. Veterinary Journal; 153: 149-62.

Jubb KVF, Kennedy PC, 1963, Pathology of Domestic Animals. Academic Press, New York and London; 1: 176-91.

Kamerbeek J, Schouls L, Kolk A, van Agterveld M, van Soolingen D, Kuijper S, Bunschoten A, Molhuizen H, Shaw R, Goyal M, van Embden J, 1997, Simultaneous Detection and Strain Differentiation of *Mycobacterium tuberculosis* for Diagnosis and Epidemiology. Journal of Clinical Microbiology; 35: 907-14.

Kanetsuna F, 1968, Chemical Analyses of Mycobacterial Cell Walls. Biochimica Et Biophysica Acta; 158: 130-43.

Karlson AG, Lessel EF, 1970, Mycobacterium bovis nom. nov. International Journal of Systematic Bacteriology; 20: 272-82.

Kasai H, Ezaki T, Harayama S, 2000, Differentiation of Phylogenetically Related Slowly Growing Mycobacteria by Their *gyrB* Sequences. Journal of Clinical Microbiology; 38: 301-8.

Kaufmann SHE, 1988, CD8+ T Lymphocytes in Intracellular Microbial Infections. Immunology Today; 9: 168-74.

Keane J, Remold HG, Kornfeld H, 2000, Virulent *Mycobacterium tuberculosis* Strains Evade Apoptosis of Infected Alveolar Macrophages. Journal of Immunology; 164: 2016-20.

Kirschner P, Springer B, Vogel U, Meier A, Wrede A, Kiekenbeck M, Bange FC, Bottger EC, 1993, Genotypic Identification of Mycobacteria by Nucleic Acid Sequence Determination: Report of a 2 Year Experience in a Clinical Laboratory. Journal of Clinical Microbiology; 31: 2882-9.

Koch R, 1882, Die Ätiologie der Tuberkulose. Berliner Klinische Wochenschrift; 19: 221-30.

Kopp E, Medzhitov R, 2003, Recognition of Microbial Infection by Toll-like Receptors. Current Opinion in Immunology; 15: 396-401.

Krebs JR, 1997, Bovine Tuberclosis in Cattle and Badgers. Report to the Rt Hon Dr Jack Cunningham MP, Ministry of Agriculture, Fisheries and Food, London.

Kubica T, Rusch-Gerdes S, Niemann S, 2003, *Mycobacterium bovis* subsp caprae Caused One-third of Human *M. bovis*-associated Tuberculosis Cases Reported in Germany between 1999 and 2001. Journal of Clinical Microbiology; 41: 3070-7.

Langmuir AD, 1961, Epidemiology of Airborne Infection. Bacteriological Reviews; 25: 173-81.

Lederer E, Adam A, Ciorbaru R, Petit JF, Wietzerbin J, 1975, Cell Walls of Mycobacteria and Related Organisms Chemistry and Immunostimulant Properties. Molecular and Cellular Biochemistry; 7: 87-104.

Lehmann KB, Neumann RO, 1896, Atlas und Grundriss der Bakteriologie und Lehrbuch der speciellen bakteriologischen Diagnostik. Lehmann, Munich.

Leipig M, Naumann L, Schramme C, Hermanns W, 2009, Ausbruch boviner Tuberkulose verursacht durch *Mycobacterium caprae* im Unterallgäu. Sonderdruck Amtstierärztlicher Dienst und Lebensmittelkontrolle; 16: 1-4.

Lesslie IW, 1959, A Comparison of Biological and Some Cultural Methods for the Primary Isolation of *Mycobacterium tuberculosis*. Journal of Comparative Pathology; 69: 1-9.

Levy-Frebault VV, Portaels F, 1992, Proposed Minimal Standards for the Genus *Mycobacterium* and for Description of New Slowly Growing *Mycobacterium* Species. International Journal of Systematic Bacteriology; 42: 315-23.

LGL Jahresbericht, 2014, Bayerisches Landesamt für Gesundheit und Lebensmittelsicherheit;175.

Liebana E, Aranaz A, Francis B, Cousins D, 1996, Assessment of Genetic Markers for Species Differentiation within the *Mycobacterium tuberculosis* Complex. Journal of Clinical Microbiology; 34: 933-8.

Liebana E, Aranaz A, Aldwell FE, McNair J, Neill SD, Smyth AJ, Pollock JM, 2000, Cellular Interactions in Bovine Tuberculosis: Release of Active Mycobacteria from Infected Macrophages by Antigen-stimulated T Cells. Immunology; 99: 23-9.

Liebana E, Johnson L, Gough J, Durr P, Jahans K, Clifton-Hadley R, Spencer Y, Hewinson RG, Downs SH, 2008, Pathology of Naturally Occurring Bovine Tuberculosis in England and Wales. Veterinary Journal; 176: 354-60.

Liebana E, Aranaz A, Dominguez L, Mateos A, González-Llamazares O, Rodriguez-Ferri EF, Domingo M, Vidal D, Cousins D, 1997, The Insertion Element IS*6110* is a Useful Tool for DNA Fingerprinting of *Mycobacterium bovis* Isolates from Cattle and Goats in Spain. Veterinary Microbiology; 54: 223-33.

Lyashchenko KP, Pollock JM, Colangeli R, Gennaro ML, 1998, Diversity of Antigen Recognition by Serum Antibodies in Experimental Bovine Tuberculosis. Infection and Immunity; 66: 5344-9.

Maclennan AP, Randall HM, Smith DW, 1961, The Occurence of Methyl Ethers of Rhamnose and Fucose in Specific Glycolipids of Certain Mycobacteria. Biochemical Journal; 80: 309-18.

Maddock ECG, 1933, Studies on the Survival Time of the Bovine Tubercle Bacillus in Soil, Soil and Dung, in Dung and on Grass, with Experiments on the Preliminary Treatment of Infected Organic Matter and the Cultivation of the Organism. Journal of Hygiene; 33: 103-17.

Maddock ECG, 1934, Further Studies on the Survival Time of the Bovine Tubercle Bacillus in Soil, Soil and Dung, in Dung and on Grass, with Experiments on Feeding Guinea Pigs and Calves on Grass Artificially Infected with Bovine Tubercle Bacilli. Journal of Hygiene; 34: 372-9.

Madkour MM, Al Saif A, Al Shahed M, Al Moutaery KR, Al Kudwah A, 2004,Tuberculosis. Springer, Berlin Heidelberg;1: 23.

Maglione PJ, Xu JY, Chan J, 2007, B Cells Moderate Inflammatory Progression and Enhance Bacterial Containment upon Pulmonary Challenge with *Mycobacterium tuberculosis.* Journal of Immunology; 178: 7222-34.

Mangiapan G, Vokurka M, Shouls L, Cadranel J, Lecossier D, vanEmbden J, Hance AJ, 1996, Sequence Capture-PCR Improves Detection of Mycobacterial DNA in Clinical Specimens. Journal of Clinical Microbiology; 34: 1209-15.

Mariano M, 1995, The Experimental Granuloma. A Hypothesis to Explain the Persistence of the Lesion. Revista do Instituto de Medicina Tropical de São Paulo; 37: 161-76.

McKenzie RA, Donald BA, 1979, Lymphadenitis in Cattle Associated with *Corynebacterium equi*: a Problem in Bovine Tuberculosis Diagnosis. Journal of Comparative Pathology; 89: 31-8.

Menzies FD, Neill SD, 2000, Cattle-to-Cattle Transmission of Bovine Tuberculosis. Veterinary Journal; 160: 92-106.

Monaghan ML, Doherty ML, Collins JD, Kazda JF, Quinn PJ, 1994, The Tuberculin Test. Veterinary Microbiology; 40: 111-24.

Mostowy S, Cousins D, Brinkman J, Aranaz A, Behr MA, 2002, Genomic Deletions Suggest a Phylogeny for the *Mycobacterium tuberculosis* Complex. Journal of Infectious Diseases; 186: 74-80.

Mote RF, Muhm RL, Gigstad GC, 1975, A Staining Method Using Acridine Orange and Auramine O for Fungi and Mycobacteria in Bovine Tissue. Biotechnic & Histochemistry; 50: 5-9.

Mustafa T, Wiker HG, Mfinanga SGM, Morkve O, Sviland L, 2006, Immunohistochemistry Using a *Mycobacterium tuberculosis* Complex Specific Antibody for Improved Diagnosis of Tuberculous Lymphadenitis. Modern Pathology; 19: 1606-14.

Neill SD, Pollock JM, Bryson DB, Hanna J, 1994, Pathogenesis of *Mycobacterium bovis* Infection in Cattle. Veterinary Microbiology; 40: 41-52.

Neill SD, Bryson DG, Pollock JM, 2001, Pathogenesis of Tuberculosis in Cattle. Tuberculosis; 81: 79-86.

Nieberle K, 1938, Tuberkulose und Fleischhygiene. Stuttgart: G. Fischer Verlag.

Niemann S, Harmsen D, Rusch-Gerdes S, Richter E, 2000a, Differentiation of Clinical *Mycobacterium tuberculosis* Complex Isolates by *gyrB* DNA Sequence Polymorphism Analysis. Journal of Clinical Microbiology; 38: 3231-4.

Niemann S, Richter E, Rusch-Gerdes S, 2000b, Differentiation among Members of the *Mycobacterium tuberculosis* Complex by Molecular and Biochemical Features: Evidence for Two Pyrazinamide-Susceptible Subtypes of *M. bovis*. Journal of Clinical Microbiology; 38: 152-7.

Niemann S, Richter E, Rusch-Gerdes S, 2002, Biochemical and Genetic Evidence for the transfer of *Mycobacterium tuberculosis* subsp *caprae* Aranaz et al. 1999 to the Species *Mycobacterium bovis* Karlson and Lessel 1970 (Approved Lists 1980) as *Mycobacterium bovis* subsp *caprae* comb. nov. International Journal of Systematic and Evolutionary Microbiology; 52: 433-6.

Nikaido H, Kim SH, Rosenberg EY, 1993, Physical Organization of Lipids in the Cell Wall of *Mycobacterium chelonae*. Molecular Microbiology; 8: 1025-30.

Norby B, Bartlett PC, Fitzgerald SD, Granger LM, Bruning-Fann CS, Whipple DL, Payeur JB, 2004, The Sensitivity of Gross Necropsy, Caudal Fold and Comparative Cervical Tests for the Diagnosis of Bovine Tuberculosis. Journal of Veterinary Diagnostic Investigation; 16: 126-31.

Orme IM, Cooper AM, 1999, Cytokine/Chemokine Cascades in Immunity to Tuberculosis. Immunology Today; 20: 307-12.

Pallaske G, 1961, Pathologische Anatomie und Pathogenese der spontanen Tuberkulose der Tiere. Stuttgart: G. Fischer Verlag.

Palmer MV, Whipple DL, Olsen SC, 1999, Development of a Model of Natural Infection with *Mycobacterium bovis* in White-tailed Deer. Journal of Wildlife Diseases; 35: 450-7.

Palmer MV, Whipple DL, Waters WR, 2001, Experimental Deer-to-Deer Transmission of *Mycobacterium bovis*. American Journal of Veterinary Research; 62: 692-6.

Palmer MV, Waters WR, Whipple DL, 2004, Investigation of the Transmission of *Mycobacterium bovis* from Deer to Cattle through Indirect Contact. American Journal of Veterinary Research; 65: 1483-9.

Palmer MV, Waters WR, Thacker TC, 2007, Lesion Development and Immunohistochemical Changes in Granulomas from Cattle Experimentally Infected with *Mycobacterium bovis*. Veterinary Pathology; 44: 863-74.

Pate M, Svara T, Gombac M, Paller T, Zolnir-Dovc M, Emersic I, Prodinger WM, Bartos M, Zdovc I, Krt B, Pavlik I, Cvetnic Z, Pogacnik M, Ocepek M, 2006, Outbreak of Tuberculosis Caused by *Mycobacterium caprae* in a Zoological Garden. Journal of Veterinary Medicine Series B-Infectious Diseases and Veterinary Public Health; 53: 387-92.

Pavlik I, Dvorska L, Bartos M, Parmova I, Melicharek I, Jesenska A, Havelkova M, Slosarek M, Putova I, Martin G, Erler W, Kremer K, Van Soolingen D, 2002a, Molecular Epidemiology of Bovine Tuberculosis in the Czech Republic and Slovakia in the Period 1965-2001 Studied by Spoligotyping. Veterinarni Medicina; 47: 181-94.

Pavlik I, Dvorska L, Matlova L, Svastova P, Parmova I, Bazant J, Veleba J, 2002b, Mycobacterial Infections in Cattle in the Czech Republic During 1990-1999. Veterinarni Medicina; 47: 241-50.

Pavlik I, 2006, The Experience of New European Union Member States Concerning the Control of Bovine Tuberculosis. Veterinary Microbiology; 112: 221-30.

Pedrosa J, Saunders BM, Appelberg R, Orme IM, Silva MT, Cooper AM, 2000, Neutrophils Play a Protective Nonphagocytic Role in Systemic *Mycobacterium tuberculosis* Infection of Mice. Infection and Immunity; 68: 577-83.

Peters W, Ernst JD, 2003, Mechanisms of Cell Recruitment in the Immune Response to *Mycobacterium tuberculosis*. Microbes and Infection; 5: 151-8.

Pollock JM, Pollock DA, Campbell DG, Girvin RM, Crockard AD, Neill SD, Mackie DP, 1996, Dynamic Changes in Circulating and Antigen-responsive T-cell Subpopulations Post-*Mycobacterium bovis* Infection in Cattle. Immunology; 87: 236-41.

Pollock, JM, Welsh, MD, McNair, J, 2005, Immune responses in bovine tuberculosis: Towards new strategies for the diagnosis and control of disease. Veterinary and Immunopathology; 108: 37-43.

Prescott JF, 1991, *Rhodococcus equi*: an Animal and Human Pathogen. Clinical Microbiology Reviews; 4: 20-34.

Pritchard DG, 1988, A Century of Bovine Tuberculosis 1888-1988: Conquest and Controversy Journal of Comparative Pathology; 99: 357-99.

Prodinger WM, Eigentler A, Allerberger F, Schonbauer M, Glawischnig W, 2002, Infection of Red Deer, Cattle, and Humans with *Mycobacterium bovis* subsp *caprae* in Western Austria. Journal of Clinical Microbiology; 40: 2270-2.

Prodinger WM, Brandstatter A, Naumann L, Pacciarini M, Kubica T, Boschiroli ML, Aranaz A, Nagy G, Cvetnic Z, Ocepek M, Skrypnyk A, Erler W, Niemann S, Pavlik I, Moser I, 2005, Characterization of *Mycobacterium caprae* Isolates from Europe by Mycobacterial Interspersed Repetitive Unit Genotyping. Journal of Clinical Microbiology; 43: 4984-92.

Pucken VB, Götz F, Mansfeld R, Moder S, Sauter-Louis C, Straubinger RK, Knubben-Schweizer G, 2015, The Intra-dermal Tuberculin Test: Literature, Directive and Implementation in Practice. Tierarztliche Praxis. Ausgabe G, Grosstiere/Nutztiere; 43: 197-206.

Purohit MR, Mustafa T, Wiker HG, Morkve O, Sviland L, 2007, Immunohistochemical Diagnosis of Abdominal and Lymph Node Tuberculosis by Detecting *Mycobacterium tuberculosis* Complex Specific Antigen MPT64. Diagnostic Pathology; 2: 1-9.

Radford AJ, Wood PR, Billmanjacobe H, Geysen HM, Mason TJ, Tribbick G, 1990, Epitope Mapping of the *Mycobacterium bovis* Secretory Protein MPB70 Using Overlapping Peptide Analysis. Journal of General Microbiology; 136: 265-72.

Rescigno M, Martino M, Sutherland CL, Gold MR, Ricciardi-Castagnoli P, 1998, Dendritic Cell Survival and Maturation are Regulated by Different Signaling Pathways. Journal of Experimental Medicine; 188: 2175-80.

Rhoades ER, Frank AA, Orme IM, 1997, Progression of Chronic Pulmonary Tuberculosis in Mice Aerogenically Infected with Virulent *Mycobacterium tuberculosis*. Tubercle and Lung Disease; 78: 57-66.

Rieseberg B, 2016, Tuberkulose bei Rindern (*M. caprae*) aus den Jahren 2009-2014 Untersuchungen zur Verteilung säurefester Bakterien im Gewebe und Beschreibungen morphologischer Veränderungen. Universitätsbibliothek der Ludwig-Maximilians-Universität, München.

Ritacco V, Dekantor IN, Barrera L, Nader A, Bernardelli A, Torrea G, Errico F, Fliess E, 1987, Assessment of the Sensitivity and Specificity of Enzyme Linked Immunosorbent Assay (ELISA) for the Detection of Mycobacterial Antibodies in Bovine Tuberculosis. Journal of Veterinary Medicine Series B-Zentralblatt Fur Veterinarmedizin Reihe B-Infectious Diseases and Veterinary Public Health; 34: 119-25.

Ritacco V, Lopez B, Barrera L, Nader A, Fliess E, Dekantor IN, 1990, Further Evaluation of an Indirect Enzym Linked Immunosorbent Assay for the Diagnosis of Bovine Tuberculosis. Journal of Veterinary Medicine Series B-Zentralblatt Fur Veterinarmedizin Reihe B-Infectious Diseases and Veterinary Public Health; 37: 19-27.

Ritacco V, Lopez B, De Kantor IN, Barrera L, Errico F, Nader A, 1991, Reciprocal Cellular and Humoral Immune Responses in Bovine Tuberculosis. Research in Veterinary Science; 50: 365-7.

Rojas M, Garcia LF, Nigou J, Puzo G, Olivier M, 2000, Mannosylated Lipoarabinomannan Antagonizes *Mycobacterium tuberculosis*-induced Macrophage Apoptosis by Altering Ca+2-dependent Cell Signaling. Journal of Infectious Diseases; 182: 240-51.

Ross BC, Raios K, Jackson K, Dwyer B, 1992, Molecular Cloning of a Highly Repeated DNA Element from *Mycobacterium tuberculosis* and Its Use as an Epidemiological Tool. Journal of Clinical Microbiology; 30: 942-6.

Runyon EH, 1959, Anonymous Mycobacteria in Pulmonary Disease. Medical Clinics of North America; 43: 273-90.

Schmitt SM, Fitzgerald SD, Cooley TM, BruningFann CS, Sullivan L, Berry D, Carlson T, Minnis RB, Payeur JB, Sikarskie J, 1997, Bovine Tuberculosis in Free-ranging White-tailed Deer from Michigan. Journal of Wildlife Diseases; 33: 749-58.

Schoepf K, Prodinger WM, Glawischnig W, Hofer E, Revilla-Fernandez S, Hofrichter J, Fritz J, Kofer J, Schmoll F, 2012, A Two Years' Survey on the Prevalence of Tuberculosis Caused by *Mycobacterium caprae* in Red Deer (Cervus elaphus) in the Tyrol, Austria. International Scholarly Research Network Veterinary Science; 2012: 1-7.

Seiler P, Aichele P, Bandermann S, Hauser AE, Lu B, Gerard NP, Gerard C, Ehlers S, Mollenkopf HJ, Kaufmann SHE, 2003, Early Granuloma Formation After Aerosol *Mycobacterium tuberculosis* Infection is Regulated by Neutrophils via CXCR3-signaling Chemokines. European Journal of Immunology; 33: 2676-86.

Shinnick TM, Good RC, 1994, Mycobacterial Taxonomy. European Journal of Clinical Microbiology & Infectious Diseases; 13: 884-901.

Silva MT, Nazare M, Silva T, Appelberg R, 1989, Neutrophil Macrophage Cooperation in the Host Defense Against Mycobacterial Infections. Microbial Pathogenesis; 6: 369-80.

Smith RMM, Drobniewski F, Gibson A, Montague JDE, Logan MN, Hunt D, Hewinson G, Salmon RL, O'Neill B, 2004, *Mycobacterium bovis* Infection, United Kingdom. Emerging Infectious Diseases; 10: 539-41.

Stamp JT, 1944, A Review of the Pathogenesis and Pathology of Bovine Tuberculosis with Special Reference to Practical Problems. Veterinary Record; 56: 443-6.

Stamp JT, 1948, Bovine Pulmonary Tuberculosis. Journal of Comparative Pathology and Therapeutics; 58: 9-23.

Stender H, Lund K, Petersen KH, Rasmussen OF, Hongmanee P, Miorner H, Godtfredsen SE, 1999a, Fluorescence In Situ Hybridization Assay Using Peptide Nucleic Acid Probes for Differentiation between Tuberculous and Nontuberculous Mycobacterium Species in Smears of Mycobacterium Cultures. Journal of Clinical Microbiology; 37: 2760-5.

Stender H, Mollerup TA, Lund K, Petersen KH, Hongmanee P, Godtfredsen SE, 1999b, Direct Detection and Identification of *Mycobacterium tuberculosis* in Smear-positive Sputum Samples by Fluorescence In Situ Hybridization (FISH) Using Peptide Nucleic Acid (PNA) Probes. International Journal of Tuberculosis and Lung Disease; 3: 830-7.

Thierry D, Brisson-Noel A, Vincent-Levy-Frebault V, Nguyen S, Guesdon JL, Gicquel B, 1990, Characterization of a *Mycobacterium tuberculosis* Insertion Sequence, IS*6110*, and Its Application in Diagnosis. Journal of Clinical Microbiology; 28: 2668-73.

Thoen CO, Jarnagin JL, Muscoplat CC, Cram LS, Johnson DW, Harrington R, 1980, Potential Use of Lymphocyte Blastogenic Responses in Diagnosis of Bovine Tuberculosis. Comparative Immunology Microbiology and Infectious Diseases; 3: 355-61.

Thoma-Uszynski S, Kiertscher SM, Ochoa MT, Bouis DA, Norgard MV, Miyake K, Godowski PJ, Roth MD, Modlin RL, 2000, Activation of Toll-like Receptor 2 on Human Dendritic Cells Triggers Induction of IL-12, But Not IL-10. Journal of Immunology; 165: 3804-10.

Trinchieri G, 1993, Interleukin-12 and Its role in the Generation of Th1 Cells. Immunology Today; 14: 335-8.

Tuberkulose- Verordnung, 2014, Verordnung zum Schutz gegen die Tuberkulose des Rindes.

Turner OC, Basaraba RJ, Orme IM, 2003, Immunopathogenesis of Pulmonary Granulomas in the Guinea Pig After Infection with *Mycobacterium tuberculosis*. Infection and Immunity; 71: 864-71.

Tuyttens FAM, Delahay RJ, MacDonald DW, Cheeseman CL, Long B, Donnelly CA, 2000, Spatial Perturbation Caused by a Badger (Meles meles) Culling Operation: Implications for the Function of Territoriality and the Control of Bovine Tuberculosis (*Mycobacterium bovis*). Journal of Animal Ecology; 69: 815-28.

Ulrichs T, Lefmann K, Reich M, Morawietz L, Roth A, Brinkmann V, Kosmiadi GA, Seiler P, Aichele P, Hahn H, Krenn V, Gobel UB, Kaufmann SH, 2005, Modified Immunohistological Staining Allows Detection of Ziehl-Neelsen-negative *Mycobacterium tuberculosis* Organisms and Their Precise Localization in Human Tissue. Journal of Pathology; 205: 633-40.

Umemura M, Yahagi A, Hamada S, Begum MD, Watanabe H, Kawakami K, Suda T, Sudo K, Nakae S, Iwakura Y, Matsuzaki G, 2007, IL-17-mediated Regulation of Innate and Acquired Immune Response Against Pulmonary *Mycobacterium bovis* Bacille Calmette Guerin Infection. Journal of Immunology; 178: 3786-96.

Underhill DM, Ozinsky A, Smith KD, Aderem A, 1999, Toll-like Receptor 2 Mediates Mycobacteria-induced Proinflammatory Signaling in Macrophages. Proceedings of the National Academy of Sciences of the United States of America; 96: 14459-63.

Vanembden JDA, Cave MD, Crawford JT, Dale JW, Eisenach KD, Gicquel B, Hermans P, Martin C, McAdam R, Shinnick TM, Small PM, 1993, Strain Identification of *Mycobacterium tuberculosis* by DNA Fingerprinting: Recommendations for a Standart Methodology. Journal of Clinical Microbiology; 31: 406-9.

Varello K, Pezzolato M, Mascarino D, Ingravalle F, Caramelli M, Bozzetta E, 2008, Comparison of Histologic Techniques for the Diagnosis of Bovine Tuberculosis in the Framework of Eradication Programs. Journal of Veterinary Diagnostic Investigation; 20: 164-9.

Vitale F, Capra G, Maxia L, Reale S, Vesco G, Caracappa S, 1998, Detection of *Mycobacterium tuberculosis* Complex in Cattle by PCR Using Milk, Lymph Node Aspirates, and Nasal Swabs. Journal of Clinical Microbiology; 36: 1050-5.

Vordermeier HM, Chambers MA, Cockle PJ, Whelan AO, Simmons J, Hewinson RG, 2002, Correlation of ESAT-6-specific Gamma Interferon Production with Pathology in Cattle Following *Mycobacterium bovis* BCG Vaccination Against Experimental Bovine Tuberculosis. Infection and Immunity; 70: 3026-32.

Wang J, Zhou XM, Pan B, Yang LF, Yin XM, Xu BR, Zhao DM, 2013, Investigation of the Effect of *Mycobacterium bovis* Infection on Bovine Neutrophils Functions. Tuberculosis; 93: 675-87.

Wangoo A, Johnson L, Gough J, Ackbar R, Inglut S, Hicks D, Spencer Y, Hewinson G, Vordermeier M, 2005, Advanced Granulomatous Lesions in *Mycobacterium bovis*-infected Cattle are Associated with Increased Expression of Type I Procollagen, γ δ (WC1+) T Cells and CD 68+ Cells. Journal of Comparative Pathology; 133: 223-34.

Warren RM, Gey van Pittius NC, Barnard M, Hesseling A, Engelke E, de Kock M, Gutierrez MC, Chege GK, Victor TC, Hoal EG, van Helden PD, 2006, Differentiation of *Mycobacterium tuberculosis* Complex by PCR Amplification of Genomic Regions of Difference. International Journal of Tuberculosis and Lung Disease; 10: 818-22.

Waters WR, Palmer MV, Pesch BA, Olsen SC, Wannemuehler MJ, Whipple DL, 2000, Lymphocyte Subset Proliferative Responses of *Mycobacterium bovis*-infected Cattle to Purified Protein Derivative. Veterinary Immunology and Immunopathology; 77: 257-73.

Watrelot-Virieux D, Drevon-Gaillot E, Toussaint Y, Belli P, 2006, Comparison of Three Diagnostic Detection Methods for Tuberculosis in French Cattle. Journal of Veterinary Medicine Series B-Infectious Diseases and Veterinary Public Health; 53: 321-5.

Wayne LG, Kubica GP, 1986, The Mycobacteria. P. H. A. Sneath and J. G. Holt. BAltimore: Williams & Wilkins. Bergey's Manual of Systematic Bacteriology; 2: 1435-57.

Wedlock DN, Denis M, Skinner MA, Koach J, de Lisle GW, Vordermeier HM, Hewinson RG, den Hurk SVL, Babiuk LA, Hecker R, Buddle BM, 2005, Vaccination of Cattle with a CpG Oligodeoxynucleotide-formulated Mycobacterial Protein Vaccine and *Mycobacterium bovis* BCG Induces Levels of Protection Against Bovine Tuberculosis Superior to Those Induced by Vaccination with BCG Alone. Infect Immun; 73: 3540-6.

Welsh MD, Cunningham RT, Corbett DM, Girvin RM, McNair J, Skuce RA, Bryson DG, Pollock JM, 2005, Influence of Pathological Progression on the Balance between Cellular and Humoral Immune Responses in Bovine Tuberculosis. Immunology; 114: 101-11.

Whipple DL, Bolin CA, Miller JM, 1996, Distribution of Lesions in Cattle Infected with Mycobacterium bovis. Journal of Veterinary Diagnostic Investigation; 8: 351-4.

Whitlock RH, Buergelt C, 1996, Preclinical and Clinical Manifestations of Paratuberculosis (Including Pathology). Veterinary Clinics of North America: Food Animal Practice; 12: 345-56.

WHO, 2015, Global Tuberculosis Report. World Health Organization: 1-204.

Williams RS, Hoy WA, 1930, The Viability of B.Tuberculosis (Bovinus) on Pasture Land, in Stored Faeces and in Liquid Manure. Journal of Hygiene; 30: 413-9.

Wood PR, Rothel JS, 1994, In Vitro Immunodiagnostic Assays for Bovine Tuberculosis. Veterinary Microbiology; 40: 125-35.

Ziehl F, 1882, Zur Färbung des Tuberkelbacillus. Deutsche Medizinische Wochenschrift; 8: 451-3.

9. APPENDIX

9.1. Tables

9.1.1. Table 10. Macro-pattern distribution of individual organs.
Abbreviations: Animal No.: animal number LN: lymph node.

Animal No.	Organ	Macro-pattern
E 96/09	Mesenterial LN	-
E 97/09	Mesenterial LN	III
E 98/09	Mesenterial LN	III
E 100/09	Mediastinal LN	-
	Portal LN	-
E 102/09	Small intestine	I
	Mesenterial LN	IV
E 106/09	Mesenterial LN	III – IV
E 107/09	Mediastinal LN	III
E 108/09	Mediastinal LN	III
	Mesenterial LN	III
E 110/09	Liver	I
	Portal LN	I – III
	Mediastinal LN	I
	Lung	-
	Mesenterial LN	IV
E 112/09	Mesenterial LN	I
	Portal LN	-
E 113/09	Mesenterial LN	I
E 114/09	Mesenterial LN	III
E 312/09	Mesenterial LN	-
E 313/09	Portal LN	-
	Mesenterial LN	-
E 316/09	Mesenterial LN	-
E 317/09	Portal LN	-
	Lung	I
	Mediastinal LN	II –III
	Liver	-
	Mesenterial LN	-
E 320/09	Mesenterial LN	-
E 321/09	Mediastinal LN	-
E 322/09	Lung	II

Animal No.	Organ	Macro-pattern
	Mediastinal LN	III
	Mesenterial LN	-
	Portal LN	-
	Liver	I
E 323/09	Lung	II
	Mesenterial LN	-
E 324/09	Liver / Peritoneum	-
E 325/09	Portal LN	-
	Liver	-
E 325/09	Mesenterial LN	-
E 326/09	Mesenterial LN	-
S 1224/12	Lung	-
S 1256/12	Mediastinal LN	II
	Lung	III
S 1257/12	Mesenterial LN	III
S 1258/12	Mesenterial LN	III
S 1259/12	Retropharyngeal LN	II
S 1260/12	Mesenterial LN	I
S 126/13	Mediastinal LN	III
S 127/13	Mediastinal LN	II
S 128/13	Mesenterial LN	III
S 173/13	Mediastinal LN	-
S 175/13	Retropharyngeal LN	I
S 179/13	Mesenterial LN	III
S 183/13	Portal LN	I
	Mesenterial LN	I – III
S 292/13	Mesenterial LN	I
S 293/13	Portal LN	I
S 294/13	Portal LN	III
	Mesenterial LN	II – III – IV
S 295/13	Portal LN	-
	Mesenterial LN	III
S 298/13	Mesenterial LN	II
S 299/13	Retropharyngeal LN	I – IV
	Mesenterial LN	III
S 300/13	Mesenterial LN	I – III
S 605 /13	Mediastinal LN	I – II
	Lung	II
S 607/13	Lung	-

Animal No.	Organ	Macro-pattern
	Mediastinal LN	III
S 770/13	Mesenterial LN	III
	Lung	I –V
	Mediastinal LN	-
S 776/13	Mesenterial LN	-
	Retropharyngeal LN	-
S 778/13	Mesenterial LN	-
S 778/13	Retropharyngeal LN	-
S 779/13	Mediastinal LN	-
S 780/13	Mediastinal LN	-
S 782/13	Mediastinal LN	-
S 783/13	Mesenterial LN	-
S 785/13	Mesenterial LN	-
S 789/13	Mediastinal LN	I – V
S 1200/13	Mediastinal LN	III
S 1202/13	Mediastinal LN	III
S 1204/13	Mesenterial LN	III
S 1205/13	Mesenterial LN	IV
S 1207/13	Mesenterial LN	II
S 409/14	Retropharyngeal LN	II
S 410/14	Mesenterial LN	-
S 411/14	Mesenterial LN	-
S 412/14	Mesenterial LN	I – III – V
S 413/14	Mesenterial LN	II – III
S 414/14	Mesenterial LN	III
S 415/14	Mesenterial LN	III
S 416/14	Mesenterial LN	III
S 418/14	Mesenterial LN	-
S 419/14	Mesenterial LN	I – III
S 422/14	Lung	I – V
S 423/14	Mesenterial LN	III
S 425/14	Mesenterial LN	III
S 426/14	Mesenterial LN	III
S 594/14	Mesenterial LN	III
S 598/14	Mesenterial LN	II
S 599/14	Mesenterial LN	III
S 600/14	Mesenterial LN	-
	Lung	I –V
S 602/14	Mesenterial LN	III

Animal No.	Organ	Macro-pattern
S 606/14	Mesenterial LN	III
S 607/14	Mesenterial LN	III
S 611/14	Mesenterial LN	III
S 612/14	Mesenterial LN	III
S 1067/14	Mesenterial LN	I
S 1068/14	Mesenterial LN	III

9.1.2. Table 11. Histological examination of the tissue samples.
Abbreviations: Animal No.: animal number; LN: lymph node; NI: not investigated; FF: Fite-Faraco staining; IHC: immunohistochemistry, 1: necrotic zone, 2: inflammatory zone, 3: outer zone; +++: strong positive immune reaction, ++: moderate positive immune reaction, +: weak positive immune reaction with the polyclonal rabbit anti-*M. tuberculosis* (Rb x Tbc).

Animal No.	Organ	Histo-type	FF	IHC
E 96/09	Mesenterial LN	1a – 2	+	2, 3 +
E 97/09	Mesenterial LN	3	+	1, 2, 3 +
E 98/09	Mesenterial LN	1a – 2 – 3	+	2 +
E 100/09	Mediastinal LN	2	+	1, 2, 3 +
	Portal LN	3	+	2, 3 +
E 102/09	Small intestine	1b – 2	+	1 +++, 2 +, 3 ++
	Mesenterial LN 1	3	+	1, 2 +
	Mesenterial LN 2	1a – 1b – 2	-	1 +
E 106/09	Mesenterial LN	3	+	1, 2, 3 +
E 107/09	Mediastinal LN	1a – 1b – 2 – 3	+	1, 2 +
E 108/09	Mediastinal LN 1	1b – 4	+	-
	Mediastinal LN 2	1a – 3	+	-
	Mediastinal LN 3	3	+	-
	Mesenterial LN 1	1a – 1b – 2 – 4	+	1, 2 +
	Mesenterial LN 2	1a – 1b – 4	-	1, 2, 3 +
	Mesenterial LN 3	1a – 1b – 4	+	-
	Mesenterial LN 4	1a – 3	+	2, 3 +

Animal No.	Organ	Histo-type	FF	IHC
	Mesenterial LN 5	1a – 2 – 4	-	-
E 110/09	Liver 1	1b – 2	-	-
	Liver 2	1b – 2	-	1 +
	Liver 3	1b – 2	+	1 +
	Liver 4	1b – 2	-	1 ++
	Portal LN 1	3	+	1, 2, 3 +
	Portal LN 2	1b – 2	+	1, 2, 3 +
	Portal LN 3	1b – 2	+	1, 2, 3 +
E 110/09	Portal LN 4	1b – 2	-	1, 2, 3 +
	Mediastinal LN 1	1b – 2	+	1 +, 2+
	Mediastinal LN 2	1b – 2	+	3 +
	Lung	1b – 2	-	1 +++, 2 ++, 3 +
	Mesenterial LN 1	2	+	1 ++, 2, 3 +++
	Mesenterial LN 2	2	-	1 +
E 112/09	Mesenterial LN 1	2 – 4	+	2 +
	Mesenterial LN 2	1a – 1b – 2 – 4	+	2 +
	Portal LN	1b – 2	+	1 +
E 113/09	Mesenterial LN	2	+	1 +
E 114/09	Mesenterial LN 1	1a – 3	-	NI
	Mesenterial LN 2	1a – 3	-	1 +
	Mesenterial LN 3	1a – 3	-	1 ++
E 312/09	Mesenterial LN	3	+	1, 2, 3 +
E 313/09	Portal LN	1b – 2	+	2, 3 +
	Mesenterial LN	1b – 2 – 3	-	1, 2, 3 +
E 316/09	Mesenterial LN	1b – 2	+	1, 2, 3 +
E 317/09	Portal LN	1a – 1b – 2	+	1, 2, 3 +

Animal No.	Organ	Histo-type	FF	IHC
	Lung	1a	-	2 +
	Mediastinal LN	1b – 2	+	1, 2, 3 +
	Liver	2	-	-
	Mesenterial LN 1	1a – 1b – 2	+	1 +
	Mesenterial LN 2	1a – 1b – 3	+	1 +
E 320/09	Mesenterial LN 1	1a – 2	-	2, 3 +
	Mesenterial LN 2	1a – 2 – 4	+	1, 2, 3 +
E 321/09	Mediastinal LN	1b – 2	+	1, 2, 3 +
E 322/09	Lung 1	2	-	1+
	Lung 2	2	+	1+
	Lung 3	4	+	1+
	Lung 4	4	-	-
	Mediastinal LN	3	+	1 +
	Mesenterial LN 1	1a – 4	+	1 +++, 2, 3 ++
	Mesenterial LN 2	1a	+	3 +
	Mesenterial LN 3	1a – 4	+	1, 2, 3 +
	Mesenterial LN 4	4	+	1, 2, 3 +
	Mesenterial LN 5	4	-	3 +
	Mesenterial LN 6	1a – 4	+	2 +
	Mesenterial LN 7	1a – 4	+	2, 3 +
	Portal LN	1a – 4	+	1 +
	Liver	2	-	-
E 323/09	Lung	1a – 1b – 2	+	NI
	Mesenterial LN	3	+	1 +++, 2 ++, 3 +
E 324/09	Liver / Peritoneum	1a	+	2, 3 +
E 325/09	Portal LN	2	-	1 +++, 2, 3 ++

Animal No.	Organ	Histo-type	FF	IHC
	Liver	2	+	1 +
	Mesenterial LN	1a – 1b – 2 - 4	+	1 ++, 2, 3 +++
E 326/09	Mesenterial LN	1a – 2 – 3 – 4	+	1, 2, 3 +++
S 1224/12	Lung	1a – 1b – 2	+	-
S 1256/12	Mediastinal LN 1	1a – 1b – 2	+	3 +
	Mediastinal LN 2	1a – 1b – 2	+	3 +
	Mediastinal LN 3	2	+	1 +
S 1256/12	Lung 1	1a – 2	+	2 +
	Lung 2	1a – 1b – 2	+	2 +
S 1257/12	Mesenterial LN	1a – 2 – 4	+	1 ++, 2, 3 +
S 1258/12	Mesenterial LN	1a – 3	+	1, 2, 3 +++
S 1259/12	Retropharyngeal LN	1a – 2	+	1, 3 +
S 1260/12	Mesenterial LN	1a – 1b – 2	+	1, 2, 3 +++
S 126/13	Mediastinal LN 1	1a	+	3 +
	Mediastinal LN 2	1a	+	3 +
	Mediastinal LN 3	3	+	NI
S 127/13	Mediastinal LN	2	+	1, 2, 3 ++
S 128/13	Mesenterial LN	1a – 4	+	3 +
S 173/13	Mediastinal LN	1a	+	3 +
S 175/13	Retropharyngeal LN 1	2 – 3	-	3 +
	Retropharyngeal LN 2	2 – 3	+	1 +, 2, 3 ++
S 179/13	Mesenterial LN 1	1a – 4	+	1 ++, 3 +
	Mesenterial LN 2	1a – 4	+	1, 3 +
S 183/13	Portal LN	1a – 2	-	3 +
	Mesenterial LN 1	1a – 1b – 2	+	3 +
	Mesenterial LN 2	1a – 1b – 2	+	2 +

Animal No.	Organ	Histo-type	FF	IHC
	Mesenterial LN 3	1a – 1b – 2	+	1, 3 +
S 292/13	Mesenterial LN 1	2	+	1, 2, 3 ++
	Mesenterial LN 2	2 – 3	+	1 ++
S 293/13	Portal LN	2 – 3	+	1, 2, 3 ++
S 294/13	Portal LN	1a – 2 – 3	+	3 +
	Mesenterial LN 1	1a – 3	+	1 +
	Mesenterial LN 2	1a – 2 – 3	+	2 +
S 294/13	Mesenterial LN 3	1a – 2 – 3	+	1, 2 +
	Mesenterial LN 4	1a – 2 – 3	+	2 +
	Mesenterial LN 5	1a – 2 – 3	+	1 +, 2 +
S 295/13	Portal LN	1a – 2 – 3	-	3 +
	Mesenterial LN 1	1a – 2	-	2, 3 +
	Mesenterial LN 2	3	+	1, 2, 3 +
	Mesenterial LN 3	1a – 3	+	1, 3 ++
	Mesenterial LN 4	1a – 3	+	1 ++
S 298/13	Mesenterial LN 1	1a – 2	-	-
	Mesenterial LN 2	1a – 2	-	-
S 299/13	Retropharyngeal LN 1	1a – 1b – 2	+	1, 2, 3 +
	Retropharyngeal LN 2	1a – 2 – 3	+	1 ++, 2, 3 +
	Retropharyngeal LN 3	1b – 2 – 3	+	1 +
	Mesenterial LN 1	2 – 3	+	1 +, 2, 3 ++
	Mesenterial LN 2	1a – 2 – 3	+	2, 3 +
S 300/13	Mesenterial LN 1	1a – 2 – 3	+	3 +
	Mesenterial LN 2	1a – 3	+	1, 2 ++
	Mesenterial LN 3	3	+	1, 2 ++
	Mesenterial LN 4	1a – 2 – 3	+	1, 2 +++

Animal No.	Organ	Histo-type	FF	IHC
S 605 /13	Mediastinal LN 1	A: 1b - 2 / B: 2	A: + / B: +	A:1 +++ / B: 1, 2 ++
	Mediastinal LN 2	A: 1a – 1b – 2 / B: 1a – 2	A: +/ B:+	A: 1 +++ / B: 1, 2, 3 +++
	Mediastinal LN 3	2	+	2, 3 +
	Mediastinal LN 4	2	+	1 +++
	Lung 1	A: 1a – 2 / B: 1a – 2	A: + / B: +	A 2 + / B -
	Lung 2	2	-	-
	Lung 3	A: 2 / B: 2	A:+ / B: +	A:1 +++ / B: 1 ++, 2 +
S 607/13	Lung	1a	+	1 +++, 3 +
	Mediastinal LN	1b – 2	+	1 +
S 770/13	Mesenterial LN 1	A: 1a – 2 – 3 / B: 1b – 2	A:+ / B: +	A: 1 +++ / B: 1, 2 +++
	Mesenterial LN 2	2 – 3	+	1, 2 +++
	Lung 1	3	+	1, 2 +
	Lung-Pleura 2	2	+	-
	Lung-Pleura 3	3	+	-
	Mediastinal LN 1	2	+	-
	Mediastinal LN 2	2 – 3	+	3 +
	Mediastinal LN 3	3	+	2, 3 +
S 776/13	Mesenterial LN	2	-	NI
	Retropharyngeal LN 1	3	-	NI
	Retropharyngeal LN 2	1a – 2 – 3	-	NI
S 778/13	Mesenterial LN 1	1b – 2	+	2, 3 +++
	Mesenterial LN 2	1a – 1b – 2	-	1 +, 2, 3 +++
	Mesenterial LN 3	1a – 1b – 2	+	-
	Retropharyngeal LN 1	1a – 2	-	1 ++
	Retropharyngeal LN 2	1b – 2	+	3 +
S 779/13	Mediastinal LN 1	1a – 2 – 3	-	1, 3 +

Animal No.	Organ	Histo-type	FF	IHC
	Mediastinal LN 2	1a – 2 – 3	+	3 +
S 780/13	Mediastinal LN 1	1a – 2 – 3	-	-
	Mediastinal LN 2	1a – 2 – 3	-	1 ++
S 782/13	Mediastinal LN	1a	+	3 +
S 783/13	Mesenterial LN	1a – 4	+	1 +
S 785/13	Mesenterial LN 1	1a – 4	+	1 +++
	Mesenterial LN 2	1a – 4	+	-
S 789/13	Mediastinal LN 1	1b – 2 – 3	-	-
	Mediastinal LN 2	1a – 2	-	-
S 1200/13	Mediastinal LN 1	1a – 2 – 3	+	2, 3 ++
	Mediastinal LN 2	1a – 2	+	1 +, 2, 3 ++
	Mediastinal LN 3	1a – 2	+	1 +, 2, 3 ++
S 1202/13	Mediastinal LN 1	1a – 2 – 3	+	1 +, 2, 3 ++
	Mediastinal LN 2	3	+	1 +, 2, 3 ++
S 1204/13	Mesenterial LN 1	1a – 3 – 4	+	1 +, 2, 3 ++
	Mesenterial LN 2	1a – 4	+	1, 2, 3 +
S 1205/13	Mesenterial LN 1	3	+	1 +, 2, 3 ++
	Mesenterial LN 2	1a – 3	+	1, 2, 3 +
S 1207/13	Mesenterial LN	1a	-	3 +
S 409/14	Retropharyngeal LN 1	1a – 2	+	2, 3 +++
	Retropharyngeal LN 2	1a – 2	+	2, 3 ++
	Retropharyngeal LN 3	1a – 2	+	1 +, 2, 3 ++
	Retropharyngeal LN 4	1a – 2	+	1 +++, 3 +++
S 410/14	Mesenterial LN 1	1a – 2	-	1 +, 2, 3 +
	Mesenterial LN 2	1a – 2	-	1, 2 +, 3 ++
S 411/14	Mesenterial LN	1a – 2	-	2 +, 3 ++

Animal No.	Organ	Histo-type	FF	IHC
S 412/14	Mesenterial LN 1	1a – 1b – 2	-	1 +, 2, 3 ++
	Mesenterial LN 2	1a – 1b – 3	+	1 +, 2, 3 ++
	Mesenterial LN 3	1a – 2	-	1 +, 2, 3 +++
	Mesenterial LN 4	1a – 1b – 2 – 3	+	1 +, 2, 3 ++
S 413/14	Mesenterial LN 1	1a – 2	+	1, 2, 3 +
	Mesenterial LN 2	1a – 1b – 4	+	1, 2, 3 +
	Mesenterial LN 3	1a – 1b – 3	+	1 +++, 2, 3 ++
S 413/14	Mesenterial LN 4	1a – 1b – 4	-	1 +, 2, 3 ++
S 414/14	Mesenterial LN 1	1a – 1b – 2	-	1, 2, 3 ++
	Mesenterial LN 2	1a – 1b – 2	-	1 ++, 2, 3 +++
S 415/14	Mesenterial LN 1	1a – 4	+	1, 2, 3 +
	Mesenterial LN 2	1a – 2 – 4	+	1, 2, 3 +++
	Mesenterial LN 3	1a – 2	+	1, 2, 3 +++
S 416/14	Mesenterial LN 1	1a	-	3 ++
	Mesenterial LN 2	1a – 2 – 4	-	1, 2, 3 +++
	Mesenterial LN 3	1a – 4	-	1, 2, 3 ++
S 418/14	Mesenterial LN 1	1a – 1b – 2	+	1 ++, 2, 3 +
	Mesenterial LN 2	1a – 1b – 2	+	1, 2, 3 ++
S 419/14	Mesenterial LN 1	1a – 1b – 2	+	1, 2, 3 ++
	Mesenterial LN 2	1a – 1b – 4	+	1, 2, 3 +
	Mesenterial LN 3	1a – 1b – 2	-	1, 2, 3 +
S 422/14	Lung 1	2	-	1, 2, 3 +++
	Lung 2	1a – 1b – 2	-	2, 3 ++
	Lung 3	1b – 2	+	1, 2, 3 +++
	Lung 4	1b – 2	-	1, 2, 3 ++
	Lung 5	1a – 1b – 2	-	1, 2, 3 ++

Animal No.	Organ	Histo-type	FF	IHC
	Lung 6	1a – 1b – 2	-	2, 3 ++
S 423/14	Mesenterial LN 1	1a – 1b – 2	-	1, 2, 3 ++
	Mesenterial LN 2	1a – 1b – 2	-	1, 2, 3 ++
	Mesenterial LN 3	1b – 2	+	1 +, 2, 3 +
S 425/14	Mesenterial LN 1	1a – 4	+	1 +, 2, 3 +
	Mesenterial LN 2	1a	-	1 +, 2, 3 +
S 426/14	Mesenterial LN 1	1a – 2	+	1, 2, 3 ++
S 426/14	Mesenterial LN 2	1a – 2	+	1, 2, 3 +
S 594/14	Mesenterial LN 1	1a	-	3 +
S 598/14	Mesenterial LN 1	1a – 1b – 2	-	1 +, 2 ++, 3 +++
	Mesenterial LN 2	1a – 1b – 2	-	1 +, 2, 3 ++
	Mesenterial LN 3	1b – 2	-	2 +, 3 ++
S 599/14	Mesenterial LN 1	1a	+	1 +, 3 +
	Mesenterial LN 2	1a – 4	+	1, 2 +
S 600/14	Mesenterial LN	1a	-	3 ++
	Lung 1	2	-	1, 3 +++, 2 ++
	Lung 2	2	+	2, 3 +
	Lung 3	1a – 3	+	3 +
	Lung 4	2	+	1 +, 2, 3 ++
S 602/14	Mesenterial LN 1	1a	+	1 ++, 2, 3 +++
	Mesenterial LN 2	1a	-	3 ++
S 606/14	Mesenterial LN 1	1a – 3	+	1, 2, 3 +++
	Mesenterial LN 2	3	+	1 +, 2 ++
S 607/14	Mesenterial LN 1	1a	-	2, 3 ++
	Mesenterial LN 2	1a – 3	+	1 +++, 2, 3 ++
S 611/14	Mesenterial LN	3	+	1, 2, 3 +

Animal No.	Organ	Histo-type	FF	IHC
S 612/14	Mesenterial LN 1	1a – 4	+	1 ++, 2, 3 +
	Mesenterial LN 2	1a – 4	-	1 +++, 2 ++, 3 +
	Mesenterial LN 3	1a	-	2, 3 +
S 1067/14	Mesenterial LN 1	1a	-	3 +
	Mesenterial LN 2	1a	-	3 +
	Mesenterial LN 3	2	-	3 +
S 1068/14	Mesenterial LN 1	1a – 4	-	1 +++, 3 +
	Mesenterial LN 2	1a – 4	-	1 +++, 2, 3 +

9.2. Fixation Solutions

9.2.1. Formaldehyde Solution (4%)

- 1 l 37-40% formaldehyde (SAV Liquid Production, Flintsbach, No. FO-1000-37-1)
- 1 l phosphate buffer (Appendix 9.2.1.1.)
- 8 l aqua dest.

9.2.1.1. Phosphate Buffer

- 40 g sodium-dihydrogen-phosphate-monohydrate (Applichem, Darmstadt, No. A1372.1000)
- 65 g di-sodiumhydrogenphosphate (Applichem, Darmstadt, No. A1373.1000)
- 10 l aqua dest.

9.2.1.2. Klotz´s Solution

- 500 g sodium-chloride
- 1100 g sodium-sulphate
- 900 g sodium-carbonate
- 1000 g chloral-hydrate

- 1000 ml formaldehyde (40%)
- 90 l aqua dest.

9.3. Solution Solutions for the Staining of Paraffin Sections

9.3.1. Haemalaun Eosin Staining

9.3.1.1. Haemalaun Solution

- Mayer`s haemalaun solution (VWR, International GmbH, Darmstadt, No. 1.09249.2500)

9.3.1.2. HCl-alcohol Stock Solution

- 7000 ml 96% ethanol
- 100 ml 25% hydrochloric-acid (Roth, Karlsruhe, No. X8971)
- 2500 ml aqua dest.

9.3.1.3. HCl-alcohol-Ready to Use-Solution (0.5%)

- 100 ml HCl-alcohol stock solution (Appendix 9. 3.1.2.)
- 100 ml 70% ethanol

9.3.1.4. Eosin Solution (1%)

- 10 g eosin (Merck, Darmstadt, No. 1.15935.0100) solve in warm aqua dest., then cooling down
- 1.5 ml 96% acetic-acid
- 1000 ml aqua dest.

9.3.2. Giemsa Staining

9.3.2.1. Phosphate Buffer (0.1 M)

9.3.2.1.1. Solution A

- 13.61 g/l di-potassium-hydrogen-phosphate-anhydrous (Roth, Karlsruhe, Art.- No. P1949.1)
- 1000 ml aqua dest.

9.3.2.1.2. Solution B

- 3.55 g/l disodium-hydrogen-orthophosphate (Spicker, Baierbrunn, No. A2530)
- 250 ml aqua dest.

The solutions must be kept in the fridge.

9.3.2.2. Giemsa-Ready to Use-Solution

- 97.5 ml solution A
- 2.5 ml solution B

Mix and heat up app. 70-80˚C.

- 7 ml Giemsa stock solution (Merck, Darmstadt, No. 1.09204.1000)

Adjust solution to pH 5.0 and filter.

9.3.2.3. Acetic-acid (0.5%)

- 5 ml acetic acid (Applichem, Darmstadt, No. A3701.2500PE)
- 1000 ml aqua dest.

9.3.3. Masson´s Trichrome Stain

9.3.3.1. Weigert`s Iron Haematoxylin

9.3.3.1.1. Solution A

- 10 g haematoxylin crystallized (Merck, Darmstadt, No.1.04302.1000)
- 1000 ml aqua dest.

Leave the solution to cool down in a closed bottle.

9.3.3.1.2. Solution B

- 11.6 g iron(III)chloride (Merck, Darmstadt, No. 1.039430250)
- 980 ml aqua dest.
- 10 ml 25% hydrochloric-acid (Applichem, Darmstadt, No. A0658)

Mix the solutions A and B in ratio 1:1 before use.

9.3.3.2. Azophloxine Solution

- 1.25 g azophloxine (Chroma Gesellschaft Schmid GmbH, Köngen, No. 18050)
- 0.5 ml acetic-acid (Applichem, Darmstadt, No. A3701.2500PE)
- 250 ml aqua dest.

9.3.3.3. Red Color Stock Solution

9.3.3.3.1. Solution A

- 5 g acid fuchsine (Sigma, No. A2284)
- 5 ml acetic-acid (Applichem, Darmstadt, No. A3701.2500PE)
- 500 ml aqua dest.

9.3.3.3.2. Solution B

- 10 g xylidine-ponceau (RAL Diagnostic, Martillac, No. 223-178-3)
- 10 ml acetic-acid (Applichem, Darmstadt, No. A3701.2500PE)

- 1000 ml aqua dest.

9.3.3.4. Red Color-Ready to Use-Solution

- 20 ml solution A (Appendix 9.3.3.3.1.)
- 80 ml solution B (Appendix 9.3.3.3.2.)
- 20 ml azophloxine (Appendix 9.3.3.2.)

Filter them together.

9.3.3.5. Phosphotungstic Acid-orange G

- 15 g phosphotungstic-acid-hydrate (Merck, Darmstadt, No. 1.00583.0250)
- 10 g orange G (Merck, Darmstadt, No. 1.15925.0025)
- 500 ml aqua dest.

9.3.3.6. Aniline Blue

- 10 g aniline blue (Merck, Darmstadt, Art. - No.1279)
- 10 ml acetic-acid (Applichem, Darmstadt, No. A3701.2500PE)
- 1000 ml aqua dest

9.3.3.7. Acetic-acid (5%)

- 50 ml acetic-acid (Applichem, Darmstadt, No. A3701.2500PE)
- 10 000 ml aqua dest.

9.3.4. Acid-fast Staining according to Fite-Faraco

9.3.4.1. Xylol Paraffin Oil

- 300 ml paraffin oil (Roth, Karlsruhe, Art.- No. 9190.1)
- 600 ml xylol (SAV Liquid Production, Flintsbach, No. X TR-5000-97-1)

9.3.4.2. HCL-alcohol (1%) Stock Solution

- 7000 ml 96% ethanol (SAV Liquid Production, Flintsbach, No. ETO-30000-96-1)
- 2500 ml aqua dest.
- 100 ml 25% acetic-acid (Applichem, Darmstadt, No. A3701.2500PE)

9.4. Solutions of the GMA Embedding Technique

9.4.1. Rising Solution for GMA Embedding Machine

Preparation of Cacodylate Buffer (0.1 M)

- 16.5 g dimethylarsinic-acid-sodium-salt-trihydrate (Applichem, No. A2140)
- 6.23 ml 1 N hydrochloric-acid (Applichem, No. A1434)
- 105 g sucrose (Merck, Darmstadt, No. 1.07687.5000)
- 1.105 g potassium-chloride-dihydrate (Merck, Darmstadt, No. 2382)
- 1500 ml aqua dest.

Mix and adjust the pH value to 7.2.

9.4.2. Solution A

- 60 ml 2 hydroxethyl-methacrylate (Merck, Darmstadt, No. 800588)
- 20 ml methyl-methacrylate (Merck, Darmstadt, No. 800590)
- 16 ml ethylene-glycol-monobutyl-ether (Merck, Darmstadt, No. 801554)
- 2 ml polyethylene-glycol (Merck, Darmstadt, No. 817003)
- 388 mg benzoyl-peroxide (Merck, Darmstadt, No. 801641)

9.4.3. Solution B

- 50 ml solution A (Appendix 9.4.3.)
- 100 µl N,N-dimethylaniline (Merck, Darmstadt, No. 803060)

9.5. Staining Solutions of GMA Sections

9.5.1. Haematoxylin-Eosin-Phloxin Staining

9.5.1.1. HCL-alcohol (1%)

- 10 ml 25% hydrochloric-acid (Applichem, Darmstadt, No. A0658)
- 700 ml 96% ethanol (SAV Liquid Production, Flintsbach, No. ETO-30000-96-1)
- 250 ml aqua dest.

9.5.1.2. Stock Solutions

9.5.1.2.1. Eosin Stock Solution

- 1.0 g eosin (Applichem, No. A0822)
- 1000 ml aqua dest.

9.5.1.2.2. Phloxine Stock Solution

- 1.0 g phloxine B (Merck, Darmstadt, No. 15926)
- 1000 ml aqua dest.

9.5.1.3. Eosin-Phloxine-Ready to Use-Solution

- 468 ml 96% ethanol (SAV Liquid Production, Flintsbach, No. ETO-30000-96-1)
- 30 ml eosin stock solution (Appendix 9.5.1.2.1.)
- 3 ml phloxine stock solution (Appendix 9.5.1.2.2.)
- 2.4 ml 96% acetic-acid (Merck, Darmstadt, No. 1.00062.2500)

9.5.2. Giemsa Staining

9.5.2.1. Phosphate Buffer

- 200 ml potassium-dihydrogen-phosphate (Merck, Darmstadt, No. 1.04873.1000) 9,12 g/l
- 160 ml disodium-hydrogen-phosphate-dihydrate (Merck, Darmstadt, No. 1.06580.1000)

Adjust the pH value to 6.7.

9.5.2.2. Giemsa-Ready to Use-Solution

- 200 ml phosphate buffer (Appendix 9.5.2.1.)
- 14 ml Giemsa stock solution (Merck, Darmstadt, No. 9204)

Adjust the pH value to 6.7.

9.5.2.3. Acetic-acid (0.5%)

- 5 ml acetic-acid (Applichem, Darmstadt, N. A3701,2500PE)
- 1000 ml aqua dest.

9.5.3. Silver Staining

9.5.3.1. Methenamine Solution (3%)

- 2.16 g methenamine (Merck, Darmstadt, No. 1,04343,0500)
- 72 ml aqua dest.

9.5.3.2. Borax Solution (2%)

- 0.4 g disodium-tetraborate-decahydrate extra pure (EWG Merck, Darmstadt, No. 1.06303.1000)
- 20 ml aqua dest.

9.5.3.3. Silver-nitrate Solution

- 5 g silver-nitrate (Merck, Darmstadt, No. 1.01512.0100)
- 100 ml aqua dest.

9.5.3.4. Gold-chloride Solution

9.5.3.4.1. Gold-chloride Stock Solution

- 1g 99.5% tetrachloroauric(III)acid trihydrate
- 100ml aqua dest.

9.5.3.4.2. Gold-chloride-Ready to Use-Solution (0.1%)

- 10 ml gold-chloride stock solution (Appendix 9.5.3.4.1.)
- 90 ml aqua dest.

9.5.3.5. Periodic-acid Solution (0.1%)

- 10 g periodic-acid (Roth, Karlsruhe, No. 32572)
- 1000 ml aqua dest.

9.5.3.6. Sodium-thiosulphate Solution (2%)

- 20 g sodium-thiosulphate (Merck, Darmstadt, No. 6512.2500)
- 1000 ml aqua dest.

9.6. Solutions for Transmission Electron Microscopy

9.6.1. Solutions for Resin Embedding

9.6.1.1. Sørensen's Phosphate Buffer

9.6.1.1.1. Solution A

- 2.269 g potassium-hydrogen-phosphate (KH2PO4) (NeoLab Art., No. 2830)

- 250 ml aqua dest.

9.6.1.1.2. Solution B

- 11.876 g sodium-hydrogen-phosphate-dihydrate (Na2HPO4.2H2O) (NeoLab, Heidelberg, Art., No. 4820)
- 1000 ml aqua dest.

Mix 80.8 ml solution B and 19.2 ml solution A and adjust the pH value to 7.4.

9.6.1.2. Glutaraldehyde (6.25%)

- 25 ml 25 % glutaraldehyde solution in water (Serva, Heidelberg, No. 23115)
- 100 ml Sørensen's phosphate buffer (Appendix 9.6.1.1.)

9.6.1.3. Merthiolate Solution (1%)

- 0.1 g ethylmercurithiosalicylic-acid-sodium salt (Serva, Heidelberg, No. 11375)
- 10 ml aqua dest.

9.6.1.4. Rinse Solution

- 100 ml Sørensen's phosphate buffer (Appendix 9.6.1.1.)
- 6.84 g D(+)-sucrose (Roth, Kalsruhe, No. 4621.1)
- 1 or 2 drops of 1% merthiolate solution (Appendix 9.6.1.3.)

9.6.1.5. Osmium(VIII)oxide (OsO$_4$) (1%)

9.6.1.5.1. Osmium(VIII)oxide (2%)

- 1 g ampule osmium(VIII)oxide 99.9% (Chempur, Karlsruhe, Art. - No. 006051)
- 50 ml Aqua dest.

OsO$_4$ for Fixation-Ready to Use-Solution (1%)

- 0.45 g D(+)-sucrose (Roth, Kalsruhe, No. 4621.1)
- 1 ml aqua dest.
- 2 ml 0.1 N HCl (Roth, Kalsruhe, No. K0241.1)
- 2 ml veronal buffer (Morphisto, Frankfurt, No. 12321)
- 5 ml 2% osmium(VIII)oxide (Appendix 9.6.1.5.1.)

9.6.1.6. Epon Glycidyl Ether Mix

9.6.1.6.1. Solution A

- 38.32 g glycidyl-ether 100 (Serva, Heidelberg, No. 2104502)
- 45.30 g dodecenylsuccinic-acid-anhydride (DDSA) (Serva, Heidelberg, No.2075501)

9.6.1.6.2. Solution B

- 61.80 g glycidyl-ether 100 (Serva, Heidelberg, No. 2104502)
- 56.34 g methylanic-anhydride (MNA) (Serva, Heidelberg, No. 2945201)

Glycidyl Ether Mix-Ready to Use-Solution

- 41.20 g solution A (Appendix 9.6.1.6.1.)
- 75.00 g solution B (Appendix 9.6.1.6.2.)
- 1.5 ml 2,4,6-tris(dimethylaminomethyl)phenol (DMP 30) (Serva, Heidelberg, No. 3967501)

9.6.2. Staining Solutions of Semi-thin Sections

9.6.2.1. Toluidine Blue

- 0.8 g toluidine blue O (Roth, Karlsruhe, No. 0300.2)
- 1 g di sodium-tetraborate (Merck, Darmstadt, No. 6306)

- 100 ml aqua dest.

9.6.2.2. Safranin

- 1 g safranin O (Chroma-Waldeck GmbH, Münster, No. 1B463)
- 1 g di-sodium-tetraborate (Merck, Darmstadt, No. 6306)
- 40 g D(+)-sucrose (Neolab, Heidelberg, No. 5015)
- 2-3 drops formalin
- 100 ml aqua dest.

9.6.3. Contrasting of the Ultra-thin Sections

9.6.3.1. Uranyl-acetate (2%)

- 1 g uranyl-acetate (Agar Scientific, Stansted, England, No. R1260A)
- 50 ml aqua dest.

9.6.3.2. Lead-citrate

9.6.3.2.1. Solution A

- 1.655 g lead-nitrate (Merck, Darmstadt, No. 7398)
- 5 ml aqua dest.

9.6.3.2.2. Solution B

- 2.94 g sodium-citrate (Merck, Darmstadt, No. 6448)
- 10 ml aqua dest.

9.6.3.2.3. Solution C

- 1 g NaOH-pellets (Neolab, Heidelberg, No. 1087)
- 25 ml aqua dest.

Lead-citrate-Ready to Use-Solution

- 6 ml solution B
- 4 ml solution A (drop wise admitted)
- 8 ml solution C

Solve the mixed solution in 32 ml aqua dest. and then filtrate with a hard filter paper (Neolab, Heidelberg, No. H602)

9.7. Solutions for Immunohistochemistry

9.7.1. 0.5 M TBS (Tris Buffer Saline) pH 7.6

- 60.5 g tris (Applichem, Darmstadt, No. A2264.1000)
- 90 g NaCl (Applichem, Darmstadt, No. A1371.1000)
- 2 N HCl (Roth, Karlsruhe, No. X897.2)
- 700 ml aqua dest.

Solve the tris-hydroxymethyl-aminomethane in aqua dest. and adjust the pH value to 7.6. Fill up with the aqua dest. to 1000 ml and control the pH-value again. For the use solution, dilute with aqua dest. to a concentration of 1:10.

9.7.2. Tris/EDTA Buffer pH 9.0 for Microwave

- 2 ml 0.5M EDTA (Applichem, Darmstadt, No. A5097)
- 1.21 g tris (Applichem, Darmstadt, No. A2264.1000)

Adjust pH value to 9.0. Solve 0.5 M EDTA solution in 1000 ml aqua dest. and add 1,21 g tris.

9.7.3. Stock Solution A

- 21.01 g citric-acid-monohydrate (Merck, Darmstadt, No. 1.00244.1000)
- 1000 ml aqua dest.

9.7.4. Stock Solution B

- 29.41 g sodium-citrate (Merck, Darmstadt, 6448.1000)
- 1000 ml aqua dest.

9.7.5. 10mM Citrate Buffer with Tween 20

- 9 ml stock solution A (Appendix 9.7.3.)
- 41 ml stock solution B (Appendix 9.7.4.)
- 0.5 ml tween 20
- 450 ml aqua dest.

9.7.6. Hydrogen-peroxide (1%)

- 6 ml 30 % hydrogen-peroxide solution (Applichem, Darmstadt, No. A1134.1000)
- 174 ml aqua dest.

9.7.7. DAB-Ready to Use-Solution

- 10 mg 3,3'-diaminobenzidine-tetrahydrochloride-dihydrate (DAB) (tablets) (KEM-EN-TEC Dig. Toostrup, No. 4170)
- 10 ml aqua dest. (solve in dark place)

Before use; add 1 µl 30% hydrogen-peroxide (Applichem, Darmstadt, No. A1134.1000) to 1 ml DAB-solution.

9.7.8. Avidin-biotin Complex (ABC)

ABC (Vector Lab. Burlingame, PK 6100)

- 5 µl reagent A
- 5 µl reagent B
- 500 µl TBS pH 7.6 (Appendix 9.7.1.)

Mix 30 min before use.

9.7.9. Sodium-ethylate Solution

- 2 g sodium-hydroxide pellets (Roth, Karlsruhe, No. 6771.1)
- 100 ml 100 % ethanol (Roth, Karlsruhe, No. 9065.3)

Solve the sodium-hydroxide pellets in the ethanol and incubate the solution for 3 days. The solution can be used after it turns brown.

9.8. The Solutions for In Situ Hybridization

9.8.1. Diethylpyrocarbonate (DEPC)-water

- 9.1 ml DEPC (Applichem, Darmstadt, No. A0881)
- 1000 ml aqua dest. (0.1% DEPC)

Mix, let stand overnight, autoclave at 121˚C

9.8.2. SSC (Saline Sodium Citrate) (20 x)

- 175.30 g NaCl (3M) (Appendix 9.8.18.1.)
- 88.20 g Na-citrate-dihydrate (0,3 M) (Applichem, Darmstadt, No. A3597)

Solve in DEPC-water, adjust pH value to 7.0 (with 0.1 N HCl), add 1000 ml DEPC-water and autoclave.

9.8.3. SSC (2x)

- 100 ml SSC (20x) (Appendix 9.8.2.)
- 900 ml aqua dest.

Adjust pH value to 7 (with 0.1 N HCl), add 1000 ml DEPC-water and autoclave.

9.8.4. SSC (1x)

- 50 ml SSC (20x) (Appendix 9.8.2.)
- 950 ml aqua dest.

Adjust pH value to 7.0 (with 0.1 N HCl), add 1000 ml DEPC-water and autoclave.

9.8.5. SSC (0.1x)

- 5 ml SSC (20x) (Appendix 9.8.2.)
- 995 ml aqua dest.

Adjust pH value to 7.0 (with 0.1 N HCl), add 1000 ml DEPC-water and autoclave.

9.8.6. Herring sperm DNA

9.8.6.1. Stock Solution

- 250 mg herring sperm DNA (Invitrogen, Karlsruhe, No. 15634-017)
- 12.5 ml TE-buffer (1x) (Appendix 9.8.17.) pH 8.0

Heat to 50˚C, solve and freeze.

9.8.6.2. Ready to Use-Solution (50 µg/ml)

- 5 µl stock solution (Appendix 9.8.6.1.)
- 995 µl TE-buffer (1x) (Appendix 9.8.17.)

9.8.7. Deionized Formamide

- 50 ml formamide (Applichem, Darmstadt, No. A3606)
- 5 g mixed bed resin (BioRad, Munich, No. 1437424)

Mix for 30 min, filter 2 times and freeze at -20˚C.

9.8.8. Dextran-sulphate 50%

- 10 g dextran-sulphate (Applichem, Darmstadt, No. A4970)
- 20 ml DEPC-water (Appendix 9.8.1.)

Keep in the fridge.

9.8.9. Proteinase K Buffer

- 6 ml 0.5 M tris buffer pH 7.6 (Appendix 9.8.20.2.)
- 10 µl proteinase K (Applichem, Darmstadt, No. A4392)
- 54 ml aqua dest.

9.8.10. Solution I

For 1 ml:

- 50 µl herring sperm-DNA-Ready to use-solution (Appendix 9.8.6.2.)
- 70 µl formamid (Appendix 9.8.7.)
- 20 µl MTB187 (Eurofins, No. 018117652)
- 20 µl MTB770 (Eurofins, No. 018247388)
- 20 µl MTB226 (Eurofins, No. 018247389)

Mix solution and incubate at 95 ˚C in water bathtub, then on ice.

9.8.11. Solution II

- 430 µl formamide (Appendix 9.8.7.)
- 200 µl SSC (20x) (Appendix 9.8.2.)
- 20 µl Denhardt's solution (Eppendorf, No. U103479K)
- 100 µl dextran-sulphate (Appendix 9.8.8.)

- 110 µl aqua dest.

Mix solutions and keep in ice.

9.8.12. Buffer I

9.8.12.1. Buffer I (2x)

- 200 ml tris HCl (1 M), pH 7.5 (Appendix 9.8.20.1)
- 60 ml NaCl (5 M) (Appendix 9.8.18.2.)

Add 1000 ml DEPC-water (Appendix 9.8.1.) and autoclave.

9.8.12.2. Buffer I (1x)

- 100 ml buffer I (2x) (Appendix 9.8.12.1.)
- 100 ml aqua dest.

9.8.13. Buffer III pH 9.5

- 15.8 g (100mM) tris-HCl (Applichem, Darmstadt, No. A2267)
- 5.8 g (100mM) NaCl (Applichem, Darmstadt, No. A2942)
- 700-800 ml DEPC-water (Appendix 9.8.1) and adjust the pH value to 9.5.
- 4.75 g (50mM) $MgCl_2$ (Merck, Darmstadt, No. 2382)
- 1000 ml DEPC-water (Appendix 9.8.1)

9.8.14. Equilibration Buffer

For 1 ml:

- 500 µl buffer I (2x) (Appendix 9.8.12.1.)
- 50 µl normal goat serum (MP Biomedicals, Eschwege, No. 092939149)
- 30 µl triton-X 10% (Applichem, Darmstadt, No. A4975)

- 500 µl aqua dest.

9.8.15. Anti-digoxigenin Solution

- 1:100 equilibration buffer 60 min
- 1000 µl equilibration puffer (Appendix 9.8.14.)
- 10 µl anti-digoxigenin-AP-fab-fragment (Roche, Mannheim, No. 1093274)

9.8.16. NBT-BCIP Solution

- 1000 µl buffer III
- 4.5 µl nitro-blue-tetrazolium-chloride (NBT) (Roche, Mannheim No.14799527)
- 3.5 µl 5-bromo-4-chloro-3-indolyl-phosphate, toluidine salt (BCIP) (Roche, Mannheim No. 13513022)
- 2.5 µl levamisole (Appendix 9.8.19.)
- 9.8.17. TE Buffer pH 8.0

9.8.17.1. TE Buffer (1x) pH 8.0

- 1.58 g (10 mM) tris (Applichem, Darmstadt, No. A2267)
- 0.372 g (1 mM) EDTA (Applichem, Darmstadt, No. A5097)
- 1000 ml DEPC-water (Appendix 9.8.1.)

Adjust pH value to 8.0.

9.8.17.2. TE Buffer (10x) pH 8.0

- 15.76 g (100 mM) tris (Applichem, Darmstadt, No. A2267)
- 3.72 g (10 mM) EDTA (Applichem, Darmstadt, No. A5097)
- 1000 ml DEPC (Appendix 9.8.1.)

Adjust pH value to 8.0.

9.8.18. NaCl Solution

9.8.18.1. 3 M NaCl

- 17.53 g NaCl (Applichem, Darmstadt, No. A2942)
- 100 ml DEPC-water (Appendix 9.8.1.)

9.8.18.2. 5 M NaCl

- 146.1 g NaCl (Applichem, Darmstadt, No. A2942)
- 500 ml DEPC-water (Appendix 9.8.1.)

9.8.19. Levamisole

- 96 mg levamisole (Applichem, Darmstadt, No. 4341)
- 1 ml aqua dest

9.8.20. Tris-HCl Buffer

9.8.20.1. Tris-HCl Buffer (1 M)

- 121.0 g tris (Applichem, Darmstadt, No. A2264)
- 800 ml DEPC-water (Appendix 9.8.1.)

Adjust pH value to 7.6 using HCl and autoclave.

9.8.20.2. Tris-HCl Buffer (0.5 M)

- 60.5 g tris (Applichem, Darmstadt, No. A2264)
- 800 ml DEPC-water (Appendix 9.8.1.)

Adjust pH value to 7.6 using HCl and autoclave.

9.8.20.3. Tris-HCl Buffer (10 mM)

For 60 ml solution:

- 0.6 ml tris-HCl Buffer (1 M)
- 59.4 ml DEPC-water (Appendix 9.8.1.)

9.8.21. Citrate Buffer (1 mM)

- 0.1052 g citric-acid-monohydrate (Merck, Darmstadt, No. 100244.1000)
- 500 ml aqua dest.

9.8.22. Achromopeptidase Solving Solution

- 350 µl achromopeptidase (Sigma, Taufkirchen, No. A3547-100KU) (60 U/ml in the end solution)

Solve in 60 ml NaCl-tris HCl Buffer (0.01 M) (Appendix 9.8.22.1.)

9.8.22.1. NaCl-tris HCl Buffer (0.1 M)

- 1 ml NaCl (5 M) (Appendix 9.8.18.2.)
- 10 ml 0.5 M tris (Appendix 9.8.20.2.)

Add 489 ml DEPC-water (Appendix 9.1.) and adjust pH value to 8.0.

9.8.23. Lysozyme (10 mg/ml) Solving Solution

For 1 ml:

- 100 µl tris-EDTA buffer (10x) (Appendix 9.8.17.2)
- 100 µl lysozyme (Sigma, Taufkirchen, No. L1667-1G) (10 mg/ml in the end solution)
- 800 µl DEPC-water (Appendix 9.8.1.)

9.8.24. Achromopeptidase + Lysozyme Solving Solution

- 1.2 ml 0.5 M tris buffer (Appendix 9.8.20.2.)

- 58.8 ml DEPC (Appendix 9.8.1.)

- 175 µl achromopeptidase (30 U/ml in the end solution)

- 600 µl lysozyme (1 mg/ml in the end solution)

9.8.25. HCl Solution (0.01 M)

For 60 ml:

- 0.6 ml HCl

- 59.4 ml DEPC-water (Appendix 9.8.1.)